



WEATHER LORE VALIDATION TOOL USING FUZZY COGNITIVE MAPS BASED ON COMPUTER VISION

by

SOLOMON MWANJELE MWAGHA

Doctoral Thesis

Submitted in fulfilment of the requirements for the degree

Doctor of Philosophy

in the

Department of Information Technology

at the

CENTRAL UNIVERSITY OF TECHNOLOGY, FREE STATE

Supervisor: Dr Muthoni Masinde

Co-Supervisor: Dr TsegayeTadesse

August 2016

Copyright Notice

This doctoral thesis is to be used for only academic or non-commercial research purposes. The information contained in this thesis is to be published with acknowledgement of the source. The rights of this doctoral thesis are held by the author.

This doctoral thesis is published by the Central University of Technology, Free State, in terms of a non-exclusive licence granted to CUT by the author.

Disclaimer

The presentation of this thesis contains colour images meant to present visually the results in a more understandable form. While printing or viewing the thesis in grey scale (black and white) is possible, it is recommended that for clarity the thesis is viewed (or printed) in full-colour format.

Dedication

I wish to dedicate this thesis with my gratitude to all my family members for their kind support and assistance in the completion of this study.

God bless you all.

Declaration

This research as presented in this thesis is my original work, and has not been presented for any other university award. Knowledge derived from other sources has been clearly indicated, with acknowledgement and reference to the literature.

This study was completed under the guidance of Dr Muthoni Masinde, Department of Information Technology at the Central University of Technology, Free State.

Solomon Mwanjele Mwagha

Signature: _____

Date: _____

In our capacity as supervisors of this thesis, we certify that the above statements are true to the best of our knowledge

Dr Muthoni Masinde

Signature: _____

Date: _____

Dr Tsegaye Tadesse

Signature: _____

Date: _____

Acknowledgments

I would like to thank my supervisor, Dr Muthoni Masinde, who has devoted much time to my research and has always been very patient with my questions. I would also like to thank Dr Masinde for her assistance in the conceptualization of my research idea as well as for suggesting to me possible sources of literature and software that I used in my research.

The doctoral supervision co-supervisor, Dr Tsegaye Tadesse, at the University of Nebraska, Lincoln, has been helping me to stay focused on what was important in the project, so I did not get lost in small details.

Abstract

The creation of scientific weather forecasts is troubled by many technological challenges (Stern & Easterling, 1999) while their utilization is generally dismal. Consequently, the majority of small-scale farmers in Africa continue to consult some forms of weather lore to reach various cropping decisions (Baliscan, 2001). Weather lore is a body of informal folklore (Enock, 2013), associated with the prediction of the weather, and based on indigenous knowledge and human observation of the environment. As such, it tends to be more holistic, and more localized to the farmers' context. However, weather lore has limitations; for instance, it has an inability to offer forecasts beyond a season. Different types of weather lore exist, utilizing almost all available human senses (feel, smell, sight and hearing). Out of all the types of weather lore in existence, it is the visual or observed weather lore that is mostly used by indigenous societies, to come up with weather predictions.

On the other hand, meteorologists continue to treat this knowledge as superstition, partly because there is no means to scientifically evaluate and validate it. The visualization and characterization of visual sky objects (such as moon, clouds, stars, and rainbows) in forecasting weather are significant subjects of research. To realize the integration of visual weather lore in modern weather forecasting systems, there is a need to represent and scientifically substantiate this form of knowledge.

This research was aimed at developing a method for verifying visual weather lore that is used by traditional communities to predict weather conditions. To realize this verification, fuzzy cognitive mapping was used to model and represent causal relationships between selected visual weather lore concepts and weather conditions. The traditional knowledge used to produce these maps was attained through case studies of two communities (in Kenya and South Africa). These case studies were aimed at understanding the weather lore domain as well as the causal effects between metrological and visual weather lore. In this study, common astronomical weather lore factors related to cloud physics were identified as: bright stars, dispersed clouds, dry weather, dull stars, feathery clouds, gathering clouds, grey clouds, high clouds, layered clouds, low clouds, stars, medium clouds, and rounded clouds. Relationships between the concepts were also identified and formally represented using fuzzy cognitive maps.

On implementing the verification tool, machine vision was used to recognize sky objects captured using a sky camera, while pattern recognition was employed in benchmarking and scoring the objects. A wireless weather station was used to capture real-time weather parameters. The visualization tool was then designed and realized in a form of software artefact, which integrated both computer vision and fuzzy cognitive mapping for experimenting visual weather lore, and verification using various statistical forecast skills and metrics. The tool consists of four main sub-components: (1) Machine vision that recognizes sky objects using support vector machine classifiers using shape-based feature descriptors; (2) Pattern recognition—to benchmark and score objects using pixel orientations, Euclidean distance, canny and grey-level concurrence matrix; (3) Fuzzy cognitive mapping that was used to represent knowledge (i.e. active hebbian learning algorithm was used to learn until convergence); and (4) A statistical computing component was used for verifications and forecast skills including brier score and contingency tables for deterministic forecasts.

Rigorous evaluation of the verification tool was carried out using independent (not used in the training and testing phases) real-time images from Bloemfontein, South Africa, and Voi-Kenya. The real-time images were captured using a sky camera with GPS location services. The results of the implementation were tested for the selected weather conditions (for example, rain, heat, cold, and dry conditions), and found to be acceptable (the verified prediction accuracies were over 80%). The recommendation in this study is to apply the implemented method for processing tasks, towards verifying all other types of visual weather lore. In addition, the use of the method developed also requires the implementation of modules for processing and verifying other types of weather lore, such as sounds, and symbols of nature.

Extended Abstract

Since time immemorial, from Australia to Asia, Africa to Latin America, local communities have continued to rely on weather lore observations to predict seasonal weather as well as its effects on their livelihoods (Alcock, 2014). This is mainly based on many years of personal experiences in observing weather conditions. However, when it comes to predictions for longer lead-times (i.e. over a season), weather lore is uncertain (Hornidge & Antweiler, 2012). This uncertainty has partly contributed to the current status where meteorologists and other scientists continue to treat weather lore as superstition (United-Nations, 2004), and not capable of predicting weather.

One of the problems in testing the confidence in weather lore in predicting weather is due to wide varieties of weather lore that are found in the details of indigenous sayings, which are tightly coupled to locality and pattern variations (Oviedo et al., 2008). This traditional knowledge is entrenched within the day-to-day socio-economic activities of the communities using it and is not globally available for comparison and validation (Huntington, Callaghan, Fox, & Krupnik, 2004). Further, this knowledge is based on local experience that lacks benchmarking techniques; so that harmonizing and integrating it within the science-based weather forecasting systems is a daunting task (Hornidge & Antweiler, 2012). It is partly for this reason that the question of validation of weather lore has not yet been substantially investigated. Sufficient expanded processes of gathering weather observations, combined with comparison and validation, can produce some useful information. Since forecasting weather accurately is a challenge even with the latest supercomputers (BBC News Magazine, 2013), validated weather lore can be useful if it is incorporated into modern weather prediction systems.

Validation of traditional knowledge is a necessary step in the management of building integrated knowledge-based systems. Traditional knowledge incorporated into knowledge-based systems has to be verified for enhancing systems' reliability. Weather lore knowledge exists in different forms as identified by traditional communities; hence it needs to be tied together for comparison and validation. The development of a weather lore validation tool that can integrate a framework for acquiring weather data and methods of representing the weather lore in verifiable forms can be a significant step in the validation of weather lore against actual weather records using conventional weather-observing instruments. The success of validating weather lore could stimulate the opportunity for integrating acceptable weather lore with modern systems of weather

prediction to improve actionable information for decision making that relies on seasonal weather prediction.

In this study a hybrid method is developed that includes computer vision and fuzzy cognitive mapping techniques for verifying visual weather lore. The verification tool was designed with forecasting based on mimicking visual perception, and fuzzy thinking based on the cognitive knowledge of humans. The method provides meaning to humanly perceivable sky objects so that computers can understand, interpret, and approximate visual weather outcomes.

Questionnaires were administered in two case study locations (KwaZulu-Natal province in South Africa, and Taita-Taveta County in Kenya), between the months of March and July 2015. The two case studies were conducted by interviewing respondents on how visual astronomical and meteorological weather concepts cause weather outcomes. The two case studies were used to identify causal effects of visual astronomical and meteorological objects to weather conditions. This was followed by finding variations and comparisons, between the visual weather lore knowledge in the two case studies. The results from the two case studies were aggregated in terms of seasonal knowledge. The causal links between visual weather concepts were investigated using these two case studies; results were compared and aggregated to build up common knowledge. The joint averages of the majority of responses from the case studies were determined for each set of interacting concepts.

The modelling of the weather lore verification tool consists of input, processing components and output. The input data to the system are sky image scenes and actual weather observations from wireless weather sensors. The image recognition component performs three sub-tasks, including: detection of objects (concepts) from image scenes, extraction of detected objects, and approximation of the presence of the concepts by comparing extracted objects to ideal objects. The prediction process involves the use of approximated concepts generated in the recognition component to simulate scenarios using the knowledge represented in the fuzzy cognitive maps. The verification component evaluates the variation between the predictions and actual weather observations to determine prediction errors and accuracy.

To evaluate the tool, daily system simulations were run to predict and record probabilities of weather outcomes (i.e. rain, heat index/hotness, dry, cold index). Weather observations were captured periodically using a wireless weather station. This process was repeated several times

until there was sufficient data to use for the verification process. To match the range of the predicted weather outcomes, the actual weather observations (measurement) were transformed and normalized to a range [0, 1]. In the verification process, comparisons were made between the actual observations and weather outcome prediction values by computing residuals (error values) from the observations. The error values and the squared error were used to compute the Mean Squared Error (MSE), and the Root Mean Squared Error (RMSE), for each predicted weather outcome.

Finally, the validity of the visual weather lore verification model was assessed using data from a different geographical location. Actual data in the form of daily sky scenes and weather parameters were acquired from Voi, Kenya, from December 2015 to January 2016. The results on the use of hybrid techniques for verification of weather lore is expected to provide an incentive in integrating indigenous knowledge on weather with modern numerical weather prediction systems for accurate and downscaled weather forecasts.

List of Acronyms

ASAL – Arid and Semi-Arid Lands

BBC –British Broadcasting Corporation

BoF – Bag of Features

BoP – Bag of Points

BoW – Bag of Words

CSI – Critical Success Index

CUT – Central University of Technology, Free State

DBC – Differential Box Counting

DWT – Discrete Wavelet Transform

FCM – Fuzzy Cognitive Mapping

GBCM – Grid-Based Colour Moments

GLCM – Grey Level Concurrence Matrix

HOG – Histogram of Oriented Gradients

ICT – Information Communication Technology

IK – Indigenous Knowledge

IT – Information Technology

LBP – Local Binary Patterns

LDA – Linear Discriminate Analysis

LoG – Laplacian of Gaussian

MAE – Mean Absolute Error

MAPE – Mean Absolute Percentage Error

ME – Mean Error

MSE – Mean Squared Error

NESW – North East South West

PCA – Principal Component Analysis

RGB – Red Green Blue

RMSE – Root Mean Squared Error

ROI – Region of Interest

SCF – Seasonal Climate Forecasts

SIFT – Scale Invariant Feature Transform

SPSS – Statistical Package for Social Sciences

SSIM – Structural Similarity Index

SURF – Speeded-Up Robust Features

TK – Traditional Knowledge

TS – Threat Score

UK – United Kingdom

UN – United Nations

UNEP – United Nations Environmental Programme

UNL – University Of Nebraska Lincoln

USA – United States of America

WMO – World Meteorological Organization

XML – Extensive Mark-up Language

Table of Contents

COPYRIGHT NOTICE	II
DISCLAIMER	III
DEDICATION	IV
DECLARATION	V
ACKNOWLEDGMENTS	VI
ABSTRACT	VII
EXTENDED ABSTRACT	IX
LIST OF ACRONYMS	XII
TABLE OF CONTENTS	XIV
LIST OF FIGURES	XVI
LIST OF TABLES	XVIII
RESEARCH PUBLICATIONS	XX
CHAPTER ONE: INTRODUCTION AND BACKGROUND INFORMATION	1
1.1 INTRODUCTION	1
1.2 STATEMENT OF THE PROBLEM	3
1.3 MOTIVATION AND JUSTIFICATION	4
1.4 RESEARCH QUESTIONS AND OBJECTIVES.....	4
1.5 RESEARCH HYPOTHESIS	5
1.6 THE SOLUTION APPROACH	6
1.7 SCOPE AND LIMITATION OF THE RESEARCH	6
1.8 SIGNIFICANCE, ACHIEVEMENTS AND CONTRIBUTION	7
1.9 EVALUATION CRITERIA	9
1.10 STRUCTURE OF THESIS	9
CHAPTER TWO: LITERATURE REVIEW AND BACKGROUND WORK	12
2.1 INTRODUCTION	12
2.2 COMPARISON BETWEEN WEATHER LORE AND SCIENCE	12
2.3 THE CONCEPT OF WEATHER FORECASTING	15
2.4 FUZZY COGNITIVE MAPS METHODS FOR HUMAN KNOWLEDGE REPRESENTATION	18
2.5 COMPUTER VISION FOR MIMICKING HUMAN VISUAL PERCEPTION	28
2.6 THE ROLE OF COMPUTING IN TRADITIONAL WEATHER FORECASTS VERIFICATION	47
CHAPTER THREE: RESEARCH METHODOLOGY	54
3.1 INTRODUCTION	54
3.2 RESEARCH DESIGN	56
3.3 USE OF CASE STUDIES	60
3.4 SOLUTION DESIGN PROCESS	62
3.5 EXPERIMENTATION PROCESS	68
3.6 VERIFICATION PROCEDURE.....	69

3.7	EVALUATION PROCEDURES.....	69
CHAPTER FOUR: WEATHER LORE INVESTIGATION AND VERIFICATION TOOL DESIGN.....		70
4.1	INTRODUCTION	70
4.2	IDENTIFICATION OF CONCEPTS AND THEIR RELATIONS IN THE VISUAL WEATHER LORE DOMAIN	70
4.3	CAUSAL EFFECTS OF VISUAL ASTRONOMICAL & METEOROLOGICAL CONCEPTS.....	74
4.5	FORMAL REPRESENTATIONS OF VISUAL WEATHER LORE KNOWLEDGE	96
4.6	THE BLUEPRINT OF WEATHER LORE VERIFICATION TOOL.....	102
4.6.1	OBJECT RECOGNITION IN VISUAL SKY SCENES USING MACHINE LEARNING.....	104
4.7	FUZZY COGNITIVE MAPPING TECHNIQUE FOR WEATHER OUTCOME SCENARIOS PROCESSING	109
4.8	DETERMINATION OF FORECAST SKILLS FOR VERIFICATION OF VISUAL WEATHER LORE.....	118
CHAPTER FIVE: IMPLEMENTATION OF VISUAL WEATHER LORE VERIFICATION TOOL		122
5.1	OVERVIEW OF THE TOOL	122
5.2	DETECTION OF SKY OBJECTS	123
5.3	SIMULATION OF WEATHER OUTCOMES THROUGH FUZZY COGNITIVE MAPS SIMULATIONS.....	156
5.4	COMPILATION OF ACTUAL WEATHER OBSERVATIONS USING WIRELESS SENSORS	172
5.5	VISUAL WEATHER LORE VERIFICATION USING FORECAST SKILLS	176
CHAPTER SIX: PERFORMANCE EVALUATION, DISCUSSION AND CONCLUSIONS.....		187
6.1	INTRODUCTION	187
6.2	EVALUATION OF RESEARCH OBJECTIVES.....	187
6.3	INNOVATIVE ASPECTS OF THE RESEARCH.....	195
6.4	RECOMMENDATIONS FOR FUTURE DEVELOPMENTS	196
REFERENCES.....		198
A. APPENDIX OF TABLES		225
C. APPENDIX OF FIGURES		246
APPENDIX: PHASE I DATA COLLECTION INSTRUMENTS.....		246
APPENDIX: PHASE II DATA COLLECTION INSTRUMENTS.....		264

List of Figures

Figure 2-1 : Depiction of an FCM.....	20
Figure 2-2: An FCM showing influence between IK concepts.....	20
Figure 2-3: Fuzzy Inference process (source: Mathworks, 2015).....	28
Figure 2-4: Approaches for shape representation. (Source: D. Zhang, G. Lu, 2004).....	40
Figure 2-5: GIST feature extraction. (Source Li-Jia L, etal., 2009)	41
Figure 2-6; Extracted feature from Zebra Image using Gabor filter. (Source: V. Shiv Naga Prasad, 2005) 42	
Figure 2-7; Grey Level Co-Occurrence Matrix (GLCM) feature extraction process.....	42
Figure 2-8: Image matching using Scale Invariant Feature Transform (SIFT) (David Lowe, 2004).....	44
Figure 2-9: Speeded Up Robust Features (SURF) features on an image (source: Mathworks, 2015).....	45
Figure 2-10: Histogram of Oriented Gradients (HOG) image features (source: Mathworks, 2015)	46
Figure 2-11: Bag of Visual Words (source: Mathworks, 2015).....	46
Figure 2-12: Forecast Skill Scores as Measure of Forecasts Quality (Source: Christoph Frei, 2014).....	52
Figure 3-1: Soutlion Design Process	62
Figure 4-1 Analysis and Design Procedure.....	70
Figure 4-2: Location of KwaZulu-Natal in South Africa.....	75
Figure 4-3: Data Collection Points at KwaZulu-Natal	76
Figure 4-4: Location of Taita-Taveta County in Kenya.....	80
Figure 4-5: Data Collection Points in Taita-Taveta County of Kenya.....	80
Figure 4-6: Trends of Knowledge of Weather in Kenya and South Africa	84
Figure 4-7: Comparison of Modal Causal Effects between Kenya and South Africa.....	87
Figure 4-8: Comparison of Mean Causal Effects between Kenya and South Africa.....	87
Figure 4-9: Modal Causal Effect in Kenya and South Africa Winter	89
Figure 4-10: Modal Causal Effect in Kenya and South Africa Summer.....	89
Figure 4-11: Modal Causal Effect in Kenya and South Africa Autumn	89
Figure 4-12: Modal Causal Effect in Kenya and South Africa Spring	89
Figure 4-13: Comparison of Mean and Modal Aggregated Knowledge	90
Figure 4-14: Trend of Aggregated Mean and Mode for the Winter Season.....	93
Figure 4-15: Trend of Aggregated Mean and Mode for the Summer Season	93
Figure 4-16: Trend of Aggregated Mean and Mode for the Autumn Season	93
Figure 4-17: Trend of Aggregated Mean and Mode for the Spring Season.....	94
Figure 4-18: FCM for the Spring Season	101
Figure 4-19: Architecture of the Visual Weather Lore Verification Method	103
Figure 4-20: Use Case Diagram for the Weather Lore Verification Tool	104
Figure 4-22: Process of Preparing Image Sets for Detector Training	105
Figure 4-21: The Object Recognition Process	105
Figure 4-23: Flow Chart for Training Detectors.....	106
Figure 4-24: Object Detection and Extraction Process.....	107
Figure 4-25: Similarity Check between Detected and True Objects.....	107
Figure 4-26: Estimating the Presence Concepts from Detected Objects	108
Figure 4-27: Process Flow of Generating Number and Probability of Nodes in FCM	109

Figure 4-28: Flowchart for Selection of Weather Seasons	111
Figure 4-29: The Overlapping Nature of the Weather Seasons	112
Figure 4-30: Flowchart for Activation of New Concepts states	113
Figure 4-31: Process Flow in Predictions Transformation and Normalization.....	114
Figure 4-32: Flowchart for Transforming Concepts.....	115
Figure 4-33: Learning Process in FCM	116
Figure 4-34: Sample Network Graph Depicting Connection in Concepts.....	117
Figure 4-35: Process for Verification of Forecast Skill	119
Figure 4-36: Flowchart for Computing Verification Statistics.....	120
Figure 5-1: Object Time and Date Meta-Data	124
Figure 5-2: GPS Meta-Data	124
Figure 5-3: Samples of Similar Sky Objects	130
Figure 5-4: Example of some manipulated sky objects	131
Figure 5-5: Segment of XML Representation of Detectors.....	138
Figure 5-6: Multiple Bounding Boxes (selection) Around detected Objects	140
Figure 5-7: Effect of Merge Threshold (Mathworks 2014 Software was used)	142
Figure 5-8: Independent Extracted Object	143
Figure 5-9: Graphical Depiction of Prediction Inputs and Outputs	158
Figure 5-10: Prediction Steps	160
Figure 5-11: Iterative Predictions Convergence Graph	165
Figure 5-12: Depiction of Prediction Location in Map.....	166
Figure 5-13: Snapshot of Major Predicted Outcomes	168
Figure 5-14: Graphical depiction of the Summer Weather Season.....	169
Figure 5-15: Oregon Scientific Weather Station	174
Figure 5-16: Section of Predictions/Observation Data Sets.....	177
Figure 5-17: Graphs of Predictions Vs Observations	178
Figure 5-18: Snapshot of Error Metrics	181
Figure 5-19: snapshot of Contingency Tables	185
Figure 6-1: Graphs of Prediction/Observation Categorical Values	192
Figure 6-2: Graphs of MSE/MAE	193
Figure 6-3: Snapshot of Contingency Tables.....	194
Figure C-1: Mean Causal Effect in Kenya and South Africa Winter	246
Figure C-2: Mean Causal Effect in Kenya and South Africa Summer.....	246
Figure C-3: Mean Causal Effect in Kenya and South Africa Autumn	246
Figure C-4: Mean Causal Effect in Kenya and South Africa Spring.....	246

List of Tables

Table 4—1: Collection of Visual Weather Indicators.....	72
Table 4—2: Grouping of Clouds by levels.....	73
Table 4—3: Characteristics of Weather Seasons in KwaZulu-Natal.....	78
Table 4—4: Characteristics of Weather Seasons in Taita-Taveta, Kenya.....	83
Table 4—5: Comparison of Mode and Mean Knowledge for the Relations in Weather Concepts.....	86
Table 4—6: Summary of Modal Seasonal Causal effects in Kenya and South Africa.....	88
Table 4—7: Aggregated Mode and Mean Knowledge on Concepts.....	91
Table 4—8: Aggregated Mode and Mean Knowledge for the Various Weather Seasons.....	92
Table 4—9: Aggregated Causal Effect (Kenya and South Africa).....	95
Table 4—10: Kenya and South Africa Aggregated Seasonal Causal Effects.....	96
Table 4—11: Final Fuzzy Cognitive Map for Winter Season.....	99
Table 4—12: Final Fuzzy Cognitive Map for Summer Season.....	100
Table 4—13: Analysis of the Importance of Nodes (Concepts) for Spring Season.....	101
Table 4—14: Transformation Values for Human Weather Descriptions.....	118
Table 4—15: Representation of Observations and Predictions Summary.....	118
Table 5—1: Comparison of Features Descriptors in Sky Objects.....	127
Table 5—2: Sample Variation of Sky Objects.....	129
Table 5—3: The Ground Truths for Visual Sky Objects.....	132
Table 5—4 : Evaluation of the Training Factors for Sky Objects Detectors.....	135
Table 5—5: Evaluation of Feature Models for Sky Objects Detectors.....	136
Table 5—6: Determination of Optimal Merge Thresholds for Sky Object Detectors.....	141
Table 5—7: Performance of Measures for Benchmarking Negative Instances to Ground Truths.....	151
Table 5—8: Performance of Measures for Benchmarking Negative Instances to Ground Truths.....	152
Table 5—9: Description of Concepts.....	157
Table 5—10: Concepts Values at Various Iterations.....	164
Table 5—11: Summer Season Dynamics.....	171
Table 5—12: Autumn Season Dynamics.....	171
Table 5—13: Winter Season Dynamics.....	171
Table 5—14: Spring Season Dynamics.....	171
Table 5—15: Seasonal FCM Dynamics.....	172
Table 5—16: Weather Parameters Recorded.....	175
Table 5—17: General Contingency Table.....	182
Table 5—18: Contingency Table (Rain).....	183
Table 5—19: Contingency Table (Dry).....	184
Table 5—20: Contingency Table (Heat).....	184
Table 5—21: Contingency Table (Cold).....	184
Table 6—1: List of astronomical and meteorological aspects.....	188
Table 6—2: Results of analysis of the importance of concepts.....	190
Table A—1: Summary of Causal effects on Weather Outcomes.....	225
Table A—2: Relations between Visual Weather Concepts.....	229

Table A—3: Causal Effects of Weather Concepts to Weather Outcomes during Winter Season.....	230
Table A—4: Causal Effects of Weather Concepts to Weather Outcomes during Summer Season	231
Table A—5: Causal Effects of Weather Concepts to Weather Outcomes during Autumn Season.....	232
Table A—6: Causal Effects of Weather Concepts to Weather Outcomes during Spring Season.....	233
Table A—7: Relations between Weather Concepts	234
Table A—8: Causal Effects of Weather Concepts during the Winter Season	235
Table A—9: Causal Effects of Weather Concepts during the Summer Season.....	236
Table A—10: Causal Effects of Weather Concepts during the Autumn Season	237
Table A—11: Causal Effects of Weather Concepts during the Spring Season	238
Table A—12: Representation of Knowledge for Kenya Winter	239
Table A—13: Representation of Knowledge for South Africa Winter	239
Table A—14: Representation of Knowledge for Kenya Summer	240
Table A—15: representation of knowledge for south africa winter	240
Table A—16: Representation of Knowledge for Kenya Autumn.....	241
Table A—17: Representation of Knowledge for South African Autumn	241
Table A—18: Representation of Knowledge for Kenya Spring	242
Table A—19: Representation of Knowledge for South Africa Spring.....	242
Table A—20 Summary of Mean Seasonal Causal effects in Kenya and South Africa.....	243
Table A—21: Final Fuzzy Cognitive Map for Autumn Season	244
Table A—22: Final Fuzzy Cognitive Map for Spring Season.....	245

Research Publications

[1] S.M. Mwagha and M. Masinde, “Scientific Verification of Weather Lore for Drought Forecasting – The Role of Fuzzy Cognitive Mapping,” IST-Africa 2015 Conference Proceedings, P.C.A.M.C. (Eds), ed., Lilongwe, Malawi: IIMC International Information Management Corporation, 2015, pp. 1-13.

[2] S.M. Mwagha and M. Masinde. A Sensor-based Weather Forecasting System using Weather Lore. 7th EAI International Conference on e-Infrastructure and e-Services for Developing Countries, December 15–16, 2015, Cotonou, Benin

Chapter One: Introduction and Background Information

1.1 Introduction

In the older lifestyles of the past, the scientific (especially Seasonal Climate Forecasts (SCFs)) weather forecasting methodologies in use today were not available (Anandaraja & Rathakrishnan, 2008; Chagonda et al., 2015); people observed their environment to determine weather patterns (Alcock, 2014; Cannell, 1933). Clues to future weather patterns were realized by looking at the skies, using the behaviour of animals, birds as well as plants; it was also based on beliefs (Anandaraja & Rathakrishnan, 2008) and myths (Suter, 2013). Among these indicators, it is the observation of the sky (Narasimhan & Nayar, 2002) that played the greatest role as a weather prediction method. For example, a red sky at sunset indicated dry weather conditions while red sky at sunrise meant moisture/rain was expected. It has been demonstrated that cloud patterns can be used as accurate weather predictors (Calbo & Sabburg, 2008). Rainbows have also been an indicator of weather, as it refracts the light and breaks it down into colours; for instance, a rainbow in the morning to the west usually indicates approaching rains. The visualization of weather lore is made possible by the human visual cognitive system (Hullman, Krupka, & Adar, 2015) that has an extraordinary capability of distinguishing a wide variety of visual objects in different appearances. The visual recognition process occurs with little effort due to the brilliant structure of the human brain (Xue, 2014) and its capacity for quick parallel processing. In the modern world, computer vision researchers aim to understand human perception and model automatic visual recognition systems.

Weather lore can be defined as the body of informal folklore, associated with the prediction of the weather based on indigenous knowledge (IK) and human observation of the environment. A great number of researchers have been directing efforts towards promoting weather lore especially on disaster management and how to integrate them to the SCFs (Baliscan, 2001; Goodchild & Glennon, 2010; Okonya & Kroschel, 2013). This is driven by the realization that SCFs and weather lore complement each other and that the rich weather lore could help in making the forecasts more relevant to the local people's context. Though having generated promising results, such integration initiatives still face many challenges (Nakashima & McLean, 2012). For instance, the initiatives tend to take the approach of using the weather lore to enrich the SCFs and hence losing most of the weather lore's richness especially the more sustainable

indigenous drought mitigation strategies (Mwagha, Waiganjo, Moturi, & Masinde, 2014; Oviedo et al., 2008). Weather lore is holistic (Enock, 2013); it describes the effects of the forecast on the people's way of life. It gives the details of the rainy season in terms of its onset, cessation, general distribution (for instance, determining if there are dry spells in-between), and suitability for different crops, among other effects. The weather forecast further gives decision support information such as when to start and stop planting, how many times planting should be done, what to plant, how to plant and even where to plant. Weather lore is very dynamic (Warren, 1998). For example, in the short-term (up to 24 hours), it gives very accurate information on rainfall timings, including the nature (such as hail) and direction of the rain. Trying to represent these aspects using conventional systems would yield an incomprehensibly complex system (Mwagha & Masinde, 2015).

On the other hand, fuzzy cognitive mapping (FCM), which is a combination of fuzzy logic and cognitive mapping, can be used to model imprecise data and nonlinear functions of arbitrary complexity; this makes it an appropriate vessel for modelling and representation of weather lore knowledge as used in weather forecasting. Knowledge in systems that are characterized by uncertainty and complex (Obiedat, 1994) processes can be represented using fuzzy cognitive mapping. Fuzzy logic (Aguilar, 2004) is derived from fuzzy set theory dealing with reasoning that is approximate rather than precisely deducible from classical predicated logic. A cognitive map (Nasserzadeh, Jafarzadeh, Mansouri, & Sohrabi, 2008) is a representation and reasoning model on causal knowledge in the form of a directed, labelled and cyclic graph whose nodes represent causes or effects and whose arcs represent causal relations between these nodes. Cognitive maps represent beliefs (knowledge), which are laid out about a given domain of interest and are useful as a means of decision support. Fuzzy cognitive mapping has proven efficient for solving problems comprising a number of decisions involving uncontrollable variables that are causally interrelated. FCM is a 'powerful tool in decision making' (Gulati, 2014) which aims at capturing the functioning of a complex system based on human understanding. FCMs are made up of signed diagraphs with feedback that describes the causal links between concepts (Dissanayake & AbouRizk, 2007; Maitra & Banerjee, 2014). To come up with common FCM, knowledge from different experts can be accumulated through combining several FCMs into a big FCM by merging same concepts (Stach, Kurgan, & Pedrycz, 2007).

Fuzzy cognitive maps can be used to represent the causal knowledge (Hossein, Zarandi, Khademian, & Minaei-bidgoli, 2012) and experience, accumulated over a certain period on a complex phenomenon; this makes them a good candidate for modelling and representing weather lore. In this case, an FCM can be developed using human IK experts who know the operation of system and its behaviour in different circumstances. Weather lore is scarcely documented; however, it is orally passed on from one generation to the next. In the face of events such as industrialization and modernization, much weather lore has been lost. The ability of FCMs to work efficiently with missing data; in modelling systems with nonlinearities and surrounding uncertainty can help represent traditional knowledge. The ability of FCMs can be facilitated by the use of artificial neural networks techniques that incorporate ideas from fuzzy logic to integrate the information into decision support systems.

1.2 Statement of the Problem

As a consequence lack of confidence by traditional people in scientific weather prediction systems and many years' experience in observation of weather conditions, many traditional communities have been using visual weather lore observations in predicting weather and its effect on their livelihoods (Boven & Morohashi, 2002). With the need to make longer lead-times (over a season) for weather predictions, visual weather lore is at most considered to be doubtful (Nakashima & McLean, 2012). Meteorologists using modern instruments, such as satellites and weather-observing stations (Goswami, 1997), to predict weather still dispute whether any type of weather lore can be applied in predicting weather or should be considered as superstition (United-Nations, 2004). One aspect of the problem is that, even though there is some predictive quality (Zuma-netshiukhwi, Stigter, & Walker, 2013) in visual weather lore, there is no established technique yet that can be applied to verify and evaluate its validity. This is because validation is the basis of scientific process – but not all forms of weather lore can meet scientific thresholds (Nakashima & McLean, 2012). In addition, most of the different types of weather lore are identified and used in traditional communities to support livelihoods and therefore are not globally available for comparison and validation. Further, the weather lore knowledge applied in predictions is based on local experience (Okonya & Kroschel, 2013) and therefore lacks benchmarking techniques. This poses a significant challenge in the efforts towards harmonizing and integrating valuable visual weather lore knowledge into the conventional forecasting systems.

1.3 Motivation and Justification

Weather lore data may be available in different forms (Hornidge & Antweiler, 2012) as identified by traditional communities and needs to be harnessed, compared and validated. One possible practical approach is the use of actual weather data for matching weather images and conditions related to visual weather lore. For this approach, a considerable investigation of visual weather lore is required to compare and validate (Friederichs & Thorarinsdottir, 2012). Sufficient expanded process of analyzing traditional weather observations, combined with comparison and validation, can produce useful information (Oviedo et al., 2008). Since forecasting weather accurately is a challenge (BBC News Magazine, 2013), even with the latest supercomputers (Simeonov, Kilifarev, & Ilarionov, 2006), validating weather lore can help to integrate it into modern weather prediction systems.

Computer modelling has been applied to model and simulate complex phenomenon such as the visual weather lore (Mwagha & Masinde, 2015). After modelling, the resulting model outputs can further be verified with real-world knowledge. A computational model (Jones, 2010) can help in the integration of visual cognition methods together with knowledge representation and statistical methods to allow experimentation and verification. In this study, computer vision (Zhang J, 2006) techniques can be employed to detect and recognize sky weather images. The output of this can be passed through the fuzzy cognitive mapping system to predict weather outcomes which can further be scientifically verified using actual weather records.

1.4 Research Questions and Objectives

This research aimed at answering the following overarching research question:

Can weather lore be scientifically verified to provide useful climate information and be integrated with modern forecasting techniques to improve prediction and help in decision making?

This was answered through the following sub-questions:

- a) Which astronomical and meteorological visual aspects and techniques are commonly used in the context of traditional weather forecasting?
- b) What are the causal effects between visual astronomical and metrological phenomena for weather outcomes?

- c) Can computer vision techniques and fuzzy cognitive mapping be useful in representing visual weather lore in identifying weather concepts and verifying them?
- d) Can the development of a tool combining the methods in sub-questions (a) and (b) listed above be useful in predicting weather outcomes based on visual weather lore?
- e) To what degree of accuracy can the application of the tool in sub-question (d) above be useful in verifying visual weather lore?

By addressing the above research questions, the main objective of this research was to develop a visual weather lore verification tool that combines the techniques of computer vision and fuzzy cognitive mapping. The sub-objectives in this research include:

- a) identifying astronomical and meteorological visual aspects and techniques commonly used for weather forecasting in traditional communities;
- b) determining the existence of causal effects between visual astronomical and meteorological aspects and weather outcomes;
- c) applying the techniques of fuzzy cognitive mapping for efficient representation of the relationships between visual astronomical and meteorological aspects to weather outcomes;
- d) using computer vision techniques to recognize visual weather concepts that symbolize human visualized weather lore concepts;
- e) developing a tool combining the two methods listed in (c) and (d) above (i.e. fuzzy cognitive mapping and computer vision techniques) for predicting weather outcomes based on symbolized visual weather lore; and
- f) verifying the weather predictions from the combined tool (listed in (e) above) using observed weather to compute its forecast skills.

1.5 Research Hypothesis

The design of a visual weather lore verification tool (with forecast skill verification metrics) integrating computer vision (for visual sky objects recognition), fuzzy cognitive mapping techniques (for representing and predicting visual weather lore knowledge), and wireless sensor weather station (for acquiring actual weather observations) can efficiently be used to validate visual weather lore.

1.6 The Solution Approach

The research problem was addressed by using case study approach (Sunny, Mike, Bing, & Daying, 2012) to investigate the visual weather lore domain. This was followed by the design of a visual weather lore verification model that had three sub-components for handling detection, prediction and verification. The detection component was realized, using computer vision methods (Elissa, Mariya, Abhinav, Xinlei, & Ishan, 2015) of object recognition and approximation of the presence of visual objects in sky scenes. The second component was based on fuzzy cognitive mapping techniques (Steven et al., 2015), that was used to represent tacit knowledge on visual weather and to predict weather outcomes based on visual concepts. The third component is a verification module that compares system predictions to actual weather observations from a wireless weather station (Xiaojun Wang, Pan, & Weihong, 2015). The verification component is used in computing various forecast skills metrics (Hamill, 2006). The solution was tested and validated using actual weather data acquired from both South Africa and Kenya.

1.7 Scope and Limitation of the Research

This research reveals a method of successfully verifying traditional visual knowledge that is useful for weather prediction. Experts could refine the seasonal knowledge matrices to fill in gaps using new knowledge from their indigenous locations before simulating weather outcomes. The model was verified using the identified concepts with the recommendation that detectors for additional visual concepts be trained and tested before introducing additional concepts in the connection matrices.

This research assumed that not all visual weather lore can be acquired, hence making it impossible to characterize all forms of visual weather lore. Another assumption was that it was not possible to incorporate visual weather lore from all communities within the time frame of this study. Thus, only two communities (one in Kenya and one in South Africa) were investigated as case studies.

Image processing techniques were applied to pre-process weather images and conditions for characterization of visual weather lore, hence significant quantities of subsets of weather images to identify weather conditions were pre-processed for investigation in this research.

The pre-processing procedure guaranteed a sufficiently representative subset of characterized visual weather lore for testing performance of the visual weather lore verification tool.

The process of acquiring visual sky images from various formats could lead to incompatibility of the input images. Such incompatibility constraints were overcome by performing transformations of the images from the various formats independently and then to a jpeg image format. Furthermore, constraints for image data sources to use variable file format such as in jpg and jpeg images were implemented. In the case studies, modes of traditional knowledge estimates were used to handle missing data and hence could influence visual weather lore knowledge representation and prediction results. A substantial number of sky images were used to train and test the visual sky objects detectors, hence minimal discrepancies were assumed. To address the issue of weather complexity, the relationships between weather lore to weather images and weather data were confined to common and more general weather outcomes (rain/wet conditions, cold conditions, heat levels, dry conditions).

A considerable variety of weather lore (such as observation of clouds and visual astronomical signs of nature) was not incorporated in this research. This was because the research aimed at recognizing the scientific insight on using visual weather lore for weather prediction. The unverified weather lore such as behaviour of animals and signs of nature (Acharya, 2011b; Okonya & Kroschel, 2013) can be considered where methods to verify specific weather lore categories need to be developed.

1.8 Significance, Achievements and Contribution

Successful validation of weather lore stimulates the opportunity for integrating consistent visual weather lore with modern systems of weather prediction to enhance their applications in providing climate information for decision support systems. This research has made a significant contribution to the scientific community (and the society in general) because of its unique attempt to scientifically verify weather lore and integrate it with modern forecasting systems.

Specifically, this research is unique since it involves hybrid technique that combines computer vision (Aguilar, 2005) and fuzzy cognitive mapping to verify visual weather lore. In addition, this study used fuzzy cognitive mapping techniques in establishing relationships between visual weather lore and weather outcomes as well as predicting and verifying visual weather lore against actual (observed) weather records. The examination of computational applicability in

mimicking human sense and decision-making by understanding the relations between visual weather concepts and actual weather phenomena was achieved.

Information from literature and case studies was combined; to statistically explore knowledge in the visual weather lore domain, to develop a visual weather lore verification tool. A formulation was achieved for the definition of requirements, outputs and definition of mathematical logic that entails the design of a visual weather lore verification tool. In summary, this research uniquely contributed to the information technology and environmental science domains in the following ways:

- a) Through utilization of hybrid techniques that integrated computer vision, wireless weather sensors and fuzzy cognitive mapping to verify visual weather lore. Case studies were used to characterize visual weather lore to associated weather conditions. This also contributed to environmental-science research through integrating case study methods to investigate causal effects of traditional weather knowledge and computational methods to verify visual weather lore phenomenon.
- b) Applying computer vision methods to detect multiple sky objects in sky scenes that are observed by humans as traditional visual weather concepts. The sky objects detection component used input from sky scenes, and detected sky objects by successively extracting and representing them as sky concepts. The detected sky objects were symbolically represented as visual weather concepts.
- c) By effectively using fuzzy cognitive mapping techniques for representing links between visual weather lore and weather outcomes. In this, an investigation of the causal links between visual weather concepts was achieved using two case studies in which results were compared and aggregated to build up common knowledge. The results of statistical knowledge were used to represent seasonal weather knowledge using fuzzy cognitive maps in the form of connection matrices.
- d) A network of wireless weather stations was used for gathering actual weather observations. The sensors were setup to log weather parameters that were used to represent the verifiable weather observations. A statistical evaluation of the visual weather lore-based weather predictions was achieved by comparing the predicted weather outcomes to wireless weather sensor observations. Statistical evaluation was undertaken using daily inputs of weather outcomes predicted against the observed meteorological parameters. The results of

verification experiments revealed that the visual weather lore-based predicted outcomes were close to the actual weather outcomes observed using the wireless weather stations (over 80% accuracy).

- e) The designed visual weather lore verification tool automatically analyzes visual weather data that could complement modern satellite data and weather models. The links between the visual weather lore and modern scientific weather models were used to determine the accuracy of traditional weather knowledge.

1.9 Evaluation Criteria

To evaluate this research, each objective was tested against the research outcomes. Two case studies were used to come up with comparative studies and to ensure conformance of results from different study locations. Case studies were used to identify astronomical and meteorological visual aspects and techniques commonly used for weather forecasting in traditional communities. Statistical techniques were used to identify the existence of causal effects between visual astronomical and meteorological aspects and weather outcomes. A hybrid tool combining computer vision and fuzzy cognitive mapping for predicting weather outcomes based on symbolized visual weather lore was designed and tested. The computer vision components (for representation of visual sky objects) were tested using various features and the best features selected. The fuzzy cognitive mapping component was tested against various seasons and various dynamics of the seasonal FCMs represented. The prediction of weather outcomes was tested against actual observations of weather records.

1.10 Structure of Thesis

The thesis is divided into six chapters. In Chapter One, an overview of the weather lore domain and its significance on human life is provided, followed by the explanation of the implication of computing methods in addressing the weather lore verification problem. An overview of study approach and methods for verifying weather lore, as well as research evaluation criteria are briefly described.

Chapter Two explains the concept of weather lore and its role in adapting climate variability across the traditional communities. The use of visual astronomical and meteorological weather indicators by traditional communities for adapting climate change is discussed. This is followed by a discussion of the concept of weather forecasting and the role of seasonal climate forecasts in

comparison to traditional forecasts. Fuzzy cognitive mapping as a means of representing knowledge is explained in terms of the modelling, applications, designing and fuzzy inference mechanisms. The concept of using computer vision for visual object recognition is discussed in detail as a means of modelling the human way of observing the weather to make forecasts. A review on the strategies of verifying weather forecasts together with crowdsourcing as a method of gathering ground truth using human computation and mobile sensing is discussed. The chapter concludes by discussing some of the strategies that can be used to assess the accuracy of weather forecast skills through statistical and diagnostic approaches.

Chapter Three presents the procedures undertaken and techniques used for verification of visual weather lore. The main aim of this chapter is to explain the methodologies and how they have been applied. In the first section the methods for preliminary studies and understanding of the weather lore domain are explained. The use of case study methods to determine the existence of causal effects between meteorological and visual weather lore are presented. This is followed by the methods for analyzing case study results to come up with knowledge representations in the form of fuzzy cognitive maps. Finally, the methods used for implementing the software artefact for experimenting visual weather lore verification using hybrid techniques and metrics are presented. The research design and specific methodologies used in this research to examine the application of visual weather lore by traditional communities for predicting weather outcomes are also presented.

Chapter Four investigates knowledge in the visual weather lore domain followed by a description of a visual weather lore verification tool. The preliminary task was to recognize the visual weather lore domain through statistical analysis of interview responses of traditional knowledge on visual weather aspects. After identifying the domain, the next steps were to formulate the definition of requirements, outputs and definition of mathematical logic that comprise the visual weather lore verification tool.

Chapter Five presents the operation and results of the visual weather lore verification tool that is realized through experiments in a series of sub-components and presenting of results.

Chapter Six presents an evaluation of this research. In this chapter, a discussion of the verification of the results from the weather lore verification tool is presented, followed by

evaluation of the objectives of this research. Finally, the contributions of this research and recommendations for future work and conclusions are discussed.

Chapter Two: Literature Review and Background Work

2.1 Introduction

This chapter provides the concept of weather lore and its role in adapting to climate variability in the traditional communities; in particular, the use of visual astronomical and meteorological weather indicators by traditional communities for adapting to climate change is discussed. This is followed by a discussion of the concept of weather forecasting and the role of seasonal climate forecasts (SCFs) in comparison to traditional forecasts. Fuzzy cognitive mapping as a means of representing knowledge is explained in terms of the modelling, applications, designing and fuzzy inference mechanisms. The concept of using computer vision for visual object recognition is discussed in detail as a means of modelling the human way of observing the weather to make forecasts. A review on the strategies of verifying weather forecasts together with crowdsourcing as a method of gathering ground truth using human computation and mobile sensing is discussed. The chapter ends by discussing some of the strategies that can be used to assess the accuracy of weather forecast skills through statistical and diagnostic approaches.

2.2 Comparison between Weather Lore and Science

Traditional ways of weather forecasting existed before modern science, as weather changes have affected traditional peoples' livelihood since time immemorial (Baliscan, 2001; Enock, 2013). Traditional farmers, for instance, observed environment as guidance for timing agricultural activities (Baliscan, 2001; Zuma-netshiukhwi, Stigter, & Walker, 2013). Research indicates the need to document, integrate and validate traditional methods used for forecasting weather (Abdulrashid, 2013; Acharya, 2011b; Enock, 2013), but a major challenge is that the world's socio-political and cultural dimensions makes grave disputes to traditional beliefs and practices universally (Chiwanza, Musingafi, & Mupa, 2013; Ngara & Mangizvo, 2013). Further, the documentation and validation of traditional knowledge is facing vulnerabilities from climate change, population growth and urbanization (Masinde & Bagula, 2012).

The natural value of traditional knowledge (Huntington, Callaghan, Fox, & Krupnik, 2004) makes it a useful complement to conventional and scientific research (Abdulrashid, 2013; Huntington, Callaghan, Fox, & Krupnik, 2004; Muguti & Maposa, 2012). A major correspondence between traditional knowledge and science is the idea of observation and

replication (Huntington, Callaghan, Fox, & Krupnik, 2004). As science ventures in testing results with variable data, traditional knowledge is preserved to allow humans to thrive in changing environment (Huntington, Callaghan, Fox, & Krupnik, 2004). Current research aims at observing and testing knowledge to allow human survival in changing environments (Zuma-netshiukhwi, Stigter, & Walker, 2013). The disparity between traditional knowledge and scientific knowledge is that the former is very localized and adapted to the immediate environment (Masinde & Bagula, 2012). To reduce dissimilarities, simulation results from scientific weather experiments can be tested against traditional knowledge to increase confidence in scientific weather forecasts to traditional people (Green, Billy, & Tapim, 2010).

“Traditional knowledge is a systematic body of knowledge acquired by local people through the accumulation of experiences, informal experiments and a close understanding of the environment in a given culture” (Anandaraja & Rathakrishnan, 2008). Traditional knowledge systems are dynamic and change after human innovation and interaction with other knowledge systems (Anandaraja & Rathakrishnan, 2008; Warren, 1998). Research recommends that for sustainable development, integration of traditional knowledge with modern thoughts knowledge is essential (Warren, 1998).

Some research claims that traditional knowledge is vulnerable to modern technology (Chiwanza, Musingafi, & Mupa, 2013), but by supplementing modern weather forecasts the impact of traditional knowledge can be leveraged using modern technologies (Baliscan, 2001; United-Nations, 2004; Warren, 1998).

2.1 Informal Representations of Weather Lore

In a traditional way of life, the ability to observe and interpret traditional weather indicators is based on learning from the elders and daily interaction with the environment (Abdulrashid, 2013; Zuma-netshiukhwi, Stigter, & Walker, 2013). Traditional knowledge is passed between generations in the form of stories, songs, folklore, proverbs, cultural values, norms, beliefs, rituals, local languages, and cultural practices (Alcock, 2014; Anyira & Onoriode, 2010; Green, Billy, & Tapim, 2010; Mapara, 2009; Warren, 1998). Traditional elders coach young people about historical experiences that they should imitate, emulate or evade (Mapara, 2009). Unlike in science that relies on instrumentation, in traditional knowledge local language and terminologies

are important as they are used in conversations, stories, and oral histories (Huntington, Callaghan, Fox, & Krupnik, 2004). Despite challenges in the representation and patenting of traditional knowledge (United-Nations, 2004), research recommends that it needs to be recognized, and standardized after validation (Chinlambianga, 2011).

2.2 The Use of Visual Weather Lore in Traditional Communities

Visual weather lore entails predicting weather from astronomical and meteorological observations (Pasztor, 2010). Traditional experts, for instance farmers, make short-term observations of atmosphere and astronomical conditions before making decisions (Baliscan, 2001; Okonya & Kroschel, 2013; Shoko, 2012). Modern meteorologists also observe atmospheric and astronomically observable facts (such as the sky and clouds) to model weather forecasts (Baliscan, 2001; Mansoor, Bhargavi, & Rahima, 2012).

The challenge in using visual weather lore is the visibility which is determined by geographical location and the actual weather at the location (Pasztor, 2010). High costs associated with human observers have prompted meteorologists to use modern technology to detect and quantify visual weather indicators (Calbo & Sabburg, 2008), but human input is still valuable in clarifying the patterns of visual weather indicators (Mansoor, Bhargavi, & Rahima, 2012).

The appearance concepts such as clouds and moon are usually followed to make judgement on an approaching bad or good weather (Mansoor, Bhargavi, & Rahima, 2012) – for instance when the moon is tipped, then it can be a dry moon; if straight it can be a wet moon (Cannell, 1933). An observed new moon with horns pointing towards the earth signifies that the weather will be rainy until the moon changes (Cannell, 1933; Kidd, 1984). Thick cloud cover indicates that the rain is near (Mansoor, Bhargavi, & Rahima, 2012).

The following are examples of some of astronomical and meteorological weather lore sayings.

“A misty sun early in the morning indicates rain; a clear sun, fair weather”;

“They say a red sun has water in its eye”;

“A deep-blue sky is always an indication of beautiful weather for the rest of the day”.

A comprehensive list of some traditional meteorological and astronomical visual indicators and their characteristics can be found in Hyatt, (2002); Johansson & Achola(2013).

2.3 The Concept of Weather Forecasting

Modern weather forecasting is a scientific process that estimates weather prospects to concepts such as heat and rainfall (Risiro, Mashoko, Tshuma, & Rurinda, 2012). Some modern methods predict daily weather based on fuzzy concepts and testing of meteorological premises (Xue, 2014). Reliable predictions of daily (or the next few days') and seasonal (or the next few months') weather forecasts can be useful in economic sectors such as agriculture (Baliscan, 2001).

In both traditional and modern human lifestyle, scheduling of activities is influenced by weather conditions (Yi Zhang & Hanby, 2007). This is evident by research on subjective and numerical methods (Risiro, Mashoko, Tshuma, & Rurinda, 2012) used to seek clues to upcoming weather (Acharya, 2011b). Subjective methods that infer daily observations to future weather are simple and cheap compared to numerical methods that require modern technology such as radar to simulate long-term weather conditions (Risiro, Mashoko, Tshuma, & Rurinda, 2012).

The vast varieties of weather concepts are dynamic, making the weather forecasting process a challenge (Mansoor, Bhargavi, & Rahima, 2012). Climate variability creates challenges in the weather forecast process, leading to reliance on weather forecasts using probabilities (Xue, 2014). Modern weather forecasting relies on empirical, statistical, dynamical or a combination of these methods (Enock, 2013; Lo & Pielke, 2008; Mansoor, Bhargavi, & Rahima, 2012; Masinde, Bagula, & Muthama, 2013). In situations where there is sufficient data, the empirical methods are useful for predicting short-term weather (Rahul & Khurana, 2012). The dynamical approaches are useful for simulating long-term weather phenomena, therefore may not provide efficient short-term weather forecasts (Rahul & Khurana, 2012).

2.3.1 Measure of Climate and Change Using Seasonal Climate Forecasts

Previous researchers have advocated for seasonal climate forecasts as a measure to represent the impact of climate change (Ziervogel & Downing, 2004) by providing indicators of how climate might be compared to historical climate observations. Seasonal climate forecasts can help to

prepare for and adapt to climate variability and change. Seasonal climate forecasts can also be used to refer to seasonal weather forecasts. Modern meteorologists observe sea surface temperatures as boundary conditions to predict the probability of climate outcomes (Ziervogel & Downing, 2004).

When planning for activities such as crop management strategies, seasonal climate forecasts can aid deciding for short-term decisions as well as long-term decisions (Chagonda et al., 2015; Ziervogel & Downing, 2004). Seasonal climate forecasts for developing adaptation policies for climate change exist in both the modern scientific world and the traditional ways of life (Chagonda et al., 2015). Seasonal climate forecasts can benefit communities by allowing them to anticipate varying climates and to come up with adaptations that will reduce their sensitivity to negative climate outcomes (Stern & Easterling, 1999).

In the traditional way of life, seasonal climate forecasts are conserved in the cultures and passed from generation to generation. Traditional farmers, for instance, used their knowledge of traditional seasonal forecasting to decide on cropping variety, planting dates, and mitigation measures, so as to realize crop yields that could sustain them in the coming seasons (Wetterhall, Winsemius, Dutra, Werner, & Pappenberger, 2014; Zuma-netshiukhwi, Stigter, & Walker, 2013). The integration of scientific seasonal climate forecasts with traditional short-term climate forecasts can be handy in supplementing and improving human activity planning and decision-making strategies (Zuma-netshiukhwi, Stigter, & Walker, 2013). The integration can further be improved by embedding adaptation strategies in communities' traditional knowledge on climate variability (Chagonda et al., 2015).

Modern meteorologists and researchers can play an ideal role in enhancing existing responses of traditional seasonal climate forecasts by investigating traditional responses to seasonal climate variability (Chagonda et al., 2015). Seasonal climate forecasts can be applicable in coming up with several human decisions. For example, rainfall and temperature forecast information can be used to influence the decision on cropping strategies, drought anticipation or developing response plan to food shortages (Weisheimer & Palmer, 2014).

2.3.2 Contrast between Weather Lore and Seasonal Climate Forecasts

Applying traditional knowledge in seasonal climate forecasting could be useful in decision-making at community levels through exploiting the seasonal variation of weather in order to increase adaptation (Okonya & Kroschel, 2013; Oviedo et al., 2008). Even with lack of means to count months, weeks, years as used in the modern world, traditional communities rely on traditional knowledge to understand, conserve and adapt to their changing environment. The documentation and integration of traditional knowledge in seasonal climate forecasting is a hopeful method that is still under exploration so that it could be used in timing of human activities such as cropping decisions (Enock, 2013). With exploration the traditional communities could use traditional knowledge for determining short-term and long-term seasonal climate forecasts (Risiro, Mashoko, Tshuma, & Rurinda, 2012) which will further enhance their adaptation.

While traditional communities rely on biophysical indicators of the environment as well as spiritual methods to forecast weather, the scientific method relies on weather and climate models of measurable meteorological data. Unlike the widely researched scientific knowledge, there is a rare documentation of traditional knowledge on seasonal weather forecasts (Masinde & Bagula, 2012). Research reveals that scientific weather forecasts are readily available and accessible but not enough for use in adaptation strategies such as cropping decisions since they are difficult to be interpreted and understood locally (Zuma-netshiukhwi, Stigter, & Walker, 2013). The lack of interpretation is partly because scientific seasonal forecasts are not location-specific and cannot be downscaled. Scientific seasonal climate forecasts representing wide geographical areas cannot be useful for people in rural or remote areas.

Communities in rural or remote areas rely mostly on traditional weather forecasting systems to obtain daily and seasonal weather forecasts with indicators derived from the environment and differing from place to place (Baliscan, 2001; Shoko, 2012). Like scientific methods, the traditional communities gather information on traditional seasonal weather forecasts before the start of the season and use the information to come up with a seasonal forecast (Shoko, 2012). Since time immemorial, traditional communities have been using weather lore (Nakashima & McLean, 2012) for making seasonal climate forecasts that guided their activities (for instance, the regular movement of the sun in the year with changes in sunrise and sunset times could be handy

in determining seasonal climate forecasts). Traditional communities also realized daily weather forecasts by observing phenomena such as clouds and moon phases (Kidd, 1984). Unlike scientific seasonal climate forecasts, traditional knowledge focuses on elements of significance for local livelihoods and as a result, is essential for climate change adaptation (Nakashima & McLean, 2012).

Traditional knowledge systems are complex in nature (Chiwanza, Musingafi, & Mupa, 2013; Narasimhan & Nayar, 2002) and require some modelling to make them useful in the modern research world. The use of fuzzy cognitive mapping can be handy in formally representing traditional knowledge on weather forecasting.

2.4 Fuzzy Cognitive Maps Methods for Human Knowledge Representation

Fuzzy cognitive mapping (a combination of fuzzy logic and cognitive mapping) is a way to represent knowledge in systems that are characterized by uncertainty and complex processes (Kosko, 1986). Fuzzy logic is derived from fuzzy set theory dealing with reasoning that is approximate rather than precisely deducible from classical predicated logic (Jones, 2010). A cognitive map is a representation and reasoning model on causal knowledge (Guerram, Maamri, & Sahnoun, 2010) in the form of a directed, labelled and cyclic graph whose nodes represent causes or effects and whose arcs represent causal relations between these nodes. Cognitive maps represent beliefs (knowledge) which are laid out about a given domain of interest and are useful as a means of decision support (Din & Cretan, 2014; Maitra & Banerjee, 2014; Yousef, 2014).

Fuzzy cognitive mapping (FCM) has proven efficient for solving problems in which a number of decisions and uncontrollable variables are causally interrelated (Maitra & Banerjee, 2014). FCMs are fuzzy-signed diagraphs with feedback that describes the causal links between concepts (Dissanayake & AbouRizk, 2007). FCMs can be used to exploit the causal knowledge and experience accumulated over a certain period on a complex phenomenon (Chinlapianga, 2011; Guerram, Maamri, & Sahnoun, 2010; Mago et al., 2013; Prigent, Fontenelle, Rochet, & Trenkel, 2008; Xirogiannis & Glykas, 2004). A Fuzzy Cognitive Map is developed using human knowledge experts that know the operation of system and its behaviour in different circumstances (Chrysostomos & Peter, 1999). FCM is a powerful tool in decision-making which

aims at capturing the functioning of a complex system based on human understanding (Pramod & Abhishek, 2013).

FCMs work efficiently with missing data to model systems with nonlinearities and surrounding uncertainty (Karagiannis & Groumpos, 2013). FCMs use artificial neural networks techniques that incorporate ideas from fuzzy logic, to create decision support systems (Carvalho, 2010; Chrysafiadi & Virvou, 2013; Karagiannis & Peter P Groumpos, 2013; Chrysostomos D Stylios, Georgopoulos, & Manis, 2013). To come up with a universal FCM, knowledge from different experts can be accumulated through combining several FCMs into a big FCM by merging same concepts (Din & Cretan, 2014; Maitra & Banerjee, 2014; Yousef, 2014).

2.4.1 Models of Fuzzy Cognitive Maps

Cognitive maps aim at representing causal relationships among concepts that could be assigned values (Nasserzadeh, Jafarzadeh, Mansouri, & Sohrabi, 2008). Causal relationships between two concepts can be –categorized as positive, negative or neutral (Calais, 2008; Kanagasabhapathy & Kumaravel, 2014; Pramod & Abhishek, 2013). Increase in the value of a concept yields a corresponding positive or negative increase at the concepts connected to it (Mago et al., 2013). Bart Kosko (Kosko, 1986) introduced the notion of fuzziness to cognitive maps and created the theory of FCMs. FCMs consist of factor-concepts as inputs and decision-concepts as outputs (Chrysafiadi & Virvou, 2013). The relationship between two concepts in FCMs can take a value in an interval (-1 to 1) called weight (Din & Cretan, 2014; Kanagasabhapathy & Kumaravel, 2014; Maitra & Banerjee, 2014).

An FCM is represented as a directed graph where each node represents a concept (Din & Cretan, 2014; Gulati, 2014; Kanagasabhapathy & Kumaravel, 2014; Maitra & Banerjee, 2014). The characteristic of a system representing events, actions, goals, values and trends can be modelled by an FCM (Din & Cretan, 2014; Gulati, 2014; Maitra & Banerjee, 2014; Wei & Linzhi, 2014; Yousef, 2014). In an FCM each arc (C_i, C_j) is directed as well as weighted, and represents a causal link between concepts (Din & Cretan, 2014), showing how concept C_i causes concept C_j . In Figure 1, nodes C_i represent concepts while arcs (C_i, C_j) to represent causal links.

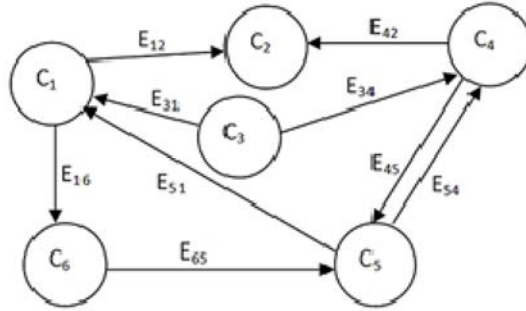


Figure 2-1 : Depiction of an FCM

An example of an FCM based on Indigenous Knowledge (IK) and Weather Lore (WL) that can be used to depict that the number of boys born and quantity of wild fruits influences rain is shown below.

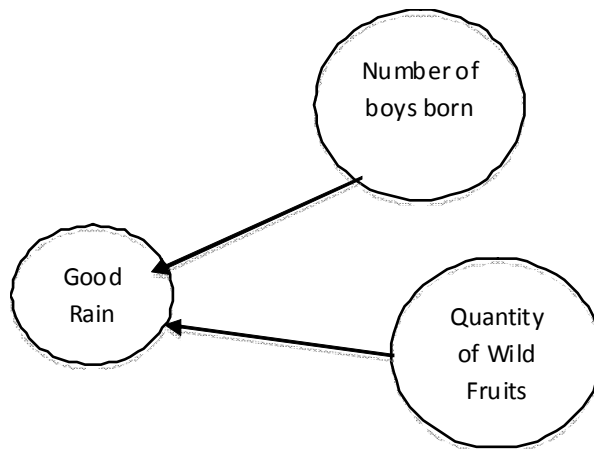


Figure 2-2: An FCM showing influence between IK concepts

FCMs are fuzzy signed directed graphs with feedback (Maitra & Banerjee, 2014). A directed edge E_{ij} from causal concept C_i to concept C_j , measures how much C_i causes C_j , with edges E_{ij} taking values in a fuzzy causal interval $[0,1]$ or $[-1, 1]$ based on system specifics (Aguilar, 2005).

$E_{ij} = 0$ indicates no causality.

$E_{ij} > 0$ indicates causal increase i.e. C_j increases as C_i increases (or C_j decreases as C_i decreases).

$E_{ij} < 0$ indicates causal decrease or negative causality i.e. C_j decreases as C_i increases (and or C_j increases as C_i decreases).

FCMs consist of concepts (also called vertices, nodes, factors or elements) and arrows representing either positive or negative. The direction of arrows represents causal relations between two concepts while the weights characterize the strength of the causal relations (Din & Cretan, 2014; Yousef, 2014). In an FCM, the state of a node C_i is determined by the sum of its inputs modified by causal link weights (Din & Cretan, 2014; Maitra & Banerjee, 2014) , and a nonlinear transfer function S (Equation 1) (Carvalho, 2010).

$$c_i(t+1) = S\left(\sum_{j=0}^{n-1} c_j(t) \bullet w_{ij}\right) \dots \dots \dots \text{Equation 2-1}$$

Updating the states of an FCM includes feeding the FCM with a stimulus state vector until it converges (Aguilar, 2005; Uygur & Stacy, 2004) with one of the three possibilities: state vector remains unchanged; a sequence of state vectors keep repeating; or the state vector keeps changing indefinitely . The evolved states of an FCM can be useful in decision support (Din & Cretan, 2014; Kanagasabhpathy & Kumaravel, 2014; Maitra & Banerjee, 2014; Yousef, 2014). FCMs can be used in problem domain analysis (Din & Cretan, 2014; Gulati, 2014; Kanagasabhpathy & Kumaravel, 2014; Maitra & Banerjee, 2014; Wei & Linzhi, 2014) by determining concepts significance; degree of influence on other concepts; impact of a change in a concept on other concepts and the evolution of a system with time given a set of values for all concepts at a point in time.

When the nodes of the FCM are fuzzy sets, then they are called fuzzy nodes (Maitra & Banerjee, 2014). FCMs with edge weights or causalities from the set $\{-1, 0, 1\}$ are called simple FCMs (Cai, 2011; Hossein, Zarandi, Khademian, & Minaei-bidgoli, 2012). An FCM with cycles is said to have a feedback, which is called a dynamical system (Carvalho, 2010; Rad, Akbari, & Taher, 2012; Rangarajan et al., 2012; Zaghdoud & Al-kahtani, 2013).

A finite number of FCMs can be combined together to produce the joint effect of all the FCMs (Praveena et al., 2012; Stylios, Georgopoulos, & Manis, 2013). If $\{E_1, E_2, E_3 \text{ up to } E_p\}$ are the adjacency matrices of the FCMs with nodes $\{C_1, C_2, \dots, C_n\}$, then the combined FCM is found by adding all the adjacency matrices $\{E_1, E_2, \dots, E_p\}$.

The combined FCM adjacency matrix is denoted by $E = \{E_1 + E_2 + \dots + E_p\}$.

2.4.2 Applications of Fuzzy Cognitive Mapping

In decision-making systems, FCMs have been useful in cases where important information is missing, unreliable, conflicting or difficult to integrate with other information (Guerram, Maamri, & Sahnoun, 2010; Karagiannis & Groumos, 2013; Luo, 2010; Sperry & Jetter, 2012; Stylios, Georgopoulos, & Manis, 2013; Uygur & Stacy, 2004). To predict forecasts (Zaghdoud & Al-kahtani, 2013), the concept of fuzzy logic can be combined with fuzzy cognitive maps (FCM) to determine the relation between various input factors.

Modelling and controlling of complex problems qualitatively can make use of FCMs as a tool for answering ‘what if’ questions during the solution-planning stage (Din & Cretan, 2014; Gulati, 2014; Maitra & Banerjee, 2014; Wei & Linzhi, 2014; Yousef, 2014). To facilitate reasoning in complex systems (Din & Cretan, 2014; Kanagasabhpathy & Kumaravel, 2014; Wei & Linzhi, 2014; Yousef, 2014), fuzzy logic and FCMs can model complex social problems (Din & Cretan, 2014; Maitra & Banerjee, 2014; Wei & Linzhi, 2014; Yousef, 2014) and the dynamic causal relationships of the context variables in a virtual world where the variables update their states with respect to different update times.

FCMs are simple graphical representation (Din & Cretan, 2014; Gulati, 2014; Maitra & Banerjee, 2014; Yousef, 2014) that can be used to make knowledge widely available through computer systems. FCMs are able to incorporate experts’ knowledge and represent knowledge in a symbolic manner to relate states, processes, policies, events, values and inputs (Din & Cretan, 2014; Maitra & Banerjee, 2014).

FCMs have also been used effectively in medical fields for decision-making, diagnosis and predictive classification (Stylios, Georgopoulos, & Manis, 2013), with the experience of many experts and knowledge from historical data combined to form the FCMs.

In addition, FCMs can be used to represent individual mental models or group knowledge and beliefs such that individual FCMs can be aggregated together, compared across individuals within the context of group interaction, or created collectively by individuals within a group context (Chrysafiadi & Virvou, 2013; Kwon & Mustapha, 2013). FCMs can also be drawn across multiple locations, where each location has its own system of practice (Pramod & Abhishek, 2013). Through characterizing the diversity in human perceptions, FCMs can help

visualize data by showing how variables relate to one another in a causal web (Aguilar, 2004) with the FCMs matrices summed up to give a combined FCMs for multiple knowledge sources.

Fuzzy cognitive mapping is a simple procedure through which input from participants of diverse backgrounds may be structured and synthesized (Chia-chien, 2007). Further, the net causal effects can be calculated from the transitive closure of the FCMs which can then be used to identify key determinants within an individual perspective, and the degree of consensus, or controversy, among FCMs representing different perspectives. FCMs can allow a structured process of identifying areas of conflicting perceptions and also areas where stakeholders with different interests might be able to gain common ground (Din & Cretan, 2014).

FCMs can also help scenario planners to integrate the qualitative and partial knowledge of multiple individuals and overcome information-processing limitations (Din & Cretan, 2014). A mental model is a mix of images and propositions that consists of both qualitative and spatial relationships (Elpiniki Papageorgiou & Groumpos, 2007; Guerram, Maamri, & Sahnoun, 2010; Najafi & Afrazeh, 2008). Through combining conceptual mapping tools with fuzzy logic and techniques for neural networks applications (Din & Cretan, 2014; Kanagasabhpathy & Kumaravel, 2014; Yousef, 2014), FCMs can be designed for the representation and formalization of soft knowledge domains (such as politics and education).

FCMs have been used to capture dependencies between assets, and then FCM-based reasoning performed to calculate risks (Pramod & Abhishek, 2013). An important feature of FCMs is the capability of addressing uncertainty (Karagiannis & Groumpos, 2013; Pang, 2013; Pramod & Abhishek, 2013; H. Singh, G. Singh, & Bhatia, 2013; Yousef, 2014) and as prediction tool with application based on forward chaining analysis to predict future behaviour (Din & Cretan, 2014; Maitra & Banerjee, 2014; Wei & Linzhi, 2014). It is, however, worth noting that, in order to perform tests and optimize the use of FCMs, an effort should be made at sufficient data collection (Pramod & Abhishek, 2013; H. Singh, G. Singh, & Bhatia, 2013; Stylios, Georgopoulos, & Manis, 2013). Some studies (Carvalho, 2010; Elpiniki, 2011; Najafi & Afrazeh, 2008; Pang, 2013; Rad, Akbari, & Taher, 2012; Stylios, Georgopoulos, & Manis, 2013) generated FCM models from input historical data, without any human intervention based on genetic algorithms and supervised learning (Mwagha & Masinde, 2014).

FCMs are more applicable when the data is unsupervised and is based on the opinion of experts (Din & Cretan, 2014; Pang, 2013; H. Singh, G. Singh, & Bhatia, 2013; Stylios, Georgopoulos, & Manis, 2013). FCMs can combine as many diverse knowledge sources as possible from different degrees of expertise into one FCM without restricting on the number of experts or the number of concepts (Elpiniki, 2011; Uygur & Stacy, 2004). FCMs for the forecasting of concept states can be validated using data from real world concepts (Elpiniki, 2011; Papageorgiou, 2008).

2.4.3 The Process of Designing Fuzzy Cognitive Maps

FCMs constructed by experts using prior knowledge do not acquire the implicit knowledge directly from the data store of systems. In a dynamical system, the behaviour is controlled by representing knowledge and reasoning based on FCMs (Din & Cretan, 2014; Kanagasabhapathy & Kumaravel, 2014; Yousef, 2014). In designing an FCM, a prediction and control model based on a fuzzy cognitive map can be developed, followed by constructing an algorithm for finding the connection matrix of the FCM (Chrysostomos & Peter, 1999; Chun-mei, 2009; Hossein, Zarandi, Khademian, & Minaei-bidgoli, 2012).

Fuzzy cognitive map models can be tested dynamically through simulations where scenarios are introduced and predictions made by viewing dynamically the consequences of the corresponding actions (Din & Cretan, 2014; Karagiannis & Groumpos, 2013; Mago et al., 2013; Pramod & Abhishek, 2013; Văidianu, 2013). To get complex personal knowledge concerning concepts, controlled interviews can be used and information transcriptions from recorded interviews to the concept maps formalized. Fuzzy cognitive maps are recorded in the form of matrices of relations between concepts (Din & Cretan, 2014; Kwon & Mustapha, 2013; Pramod & Abhishek, 2013; Văidianu, 2013).

Learning methods can be employed to improve the speed of the learning process and the quality of learning FCMs with more nodes to construct causal graph based on historical data (Pang, 2013). FCMs can be constructed using a systematic approach where concepts are gathered from survey respondents followed by taking into account the expert judgment in causal relationships between the concepts (Chia-chien, 2007; Fairweather et al., 2006; Kwon & Mustapha, 2013; Pramod & Abhishek, 2013; Sperry & Jetter, 2012).

Prediction algorithms can be constructed in fuzzy cognitive maps using fuzzy c-means clustering algorithms where a genetic algorithm is applied to learn weights of the FCM. This way, a fully learned fuzzy cognitive map can be used to represent, store fuzzy logic relationships of fuzzy time series and realize predictions. Fuzzy cognitive maps can be designed using crisp decision trees (well-known intelligent techniques that extract rules from both symbolic and numeric data) that have been fuzzified (Maitra & Banerjee, 2014; Rangarajan et al., 2012; Yousef, 2014). Fuzzy rules can be combined and used to express non-monotonic causality in fuzzy cognitive maps along with aggregation operators for combining multiple causal influences. In situations where domain experts are not able to express the causal relationships data-driven methods for learning FCMs can be used.

FCM construction can be accomplished in the following steps: (a) identification of concepts and its interconnections determining the nature (positive, negative or null) of the causal relationships between concepts; (b) initial data acquisition by the expert opinions and/or by an equation analysis when the mathematical system model is known; (c) submitting the data from the expert opinions to a fuzzy system, in which the output represents the weights of the FCM; (d) weight adaptation and optimization of the initially proposed FCM, adjusting its response to the desired output; and (e) validation of the adjusted FCM. The process of gathering and integrating knowledge from experts in the form of fuzzy cognitive maps can be enhanced with choices of graph-based learning methods in order to improve effectiveness of the final digraphs (Nasserzadeh, Jafarzadeh, Mansouri, & Sohrabi, 2008).

2.4.4 Procedures in Fuzzy Cognitive Mapping

Developing a fuzzy cognitive map involves the selection of the FCM factors or concepts which have impact on some phenomenon of interest (Calais, 2008; Din & Cretan, 2014; Mago et al., 2013). To identify the FCM concepts a group of experts can be provided with questionnaires or brain-storming sessions (Din & Cretan, 2014; Maitra & Banerjee, 2014; Yousef, 2014).

Causal relationships (positive, negative, or neutral) amongst the various concepts are established using analysis the values of concepts change with time (Calais, 2008; Din & Cretan, 2014; Kanagasabhapathy & Kumaravel, 2014; Wei & Linzhi, 2014; Yousef, 2014).

The concepts' linguistic variables are fuzzified using fuzzy membership functions (Fuzzy Logic can be used to convert the concepts relations into values between 0 and 1) before input into the fuzzy cognitive system (Mago et al., 2013; Maitra & Banerjee, 2014).

Utilization of appropriate learning algorithms can be used to overcome the potential convergence of FCMs to some undesired states by recalculating the weights when new strategies are adopted, increasing the efficiency and robustness of FCMs. This process modifies the FCM weight matrix (Papageorgiou, 2008; Rangarajan et al., 2012).

The learning algorithm assigns each concept an activation level having an initial value ranging in the interval $[0, 1]$. The learning algorithm gives FCMs the ability to learn arbitrary nonlinear mappings, and the capability to generalize situations, adaptively. (Calais, 2008; Papageorgiou, 2008)

The concepts interact, resulting in the concepts' values changing during iterations. The quantity of concepts and the quantity and complexity of relationships necessitates the system to undergo several cycles before it reaches equilibrium (Calais, 2008; Mago et al., 2013). After several iterations the values of the concept must be recorded.

To compare and visualize the FCM concepts' influence, plots can be made in groupings, against the concepts being investigated (Mago et al., 2013; Văidianu, 2013). Increasing the value of concepts with a positive effect should increase the value of investigated concepts gradually converging to a positive value while increasing the value of concepts with a negative effect, should decrease the value of investigated concepts (Karagiannis & Groumpos, 2013; Mago et al., 2013).

Network analysis is used to compare the degree of impact each of the concepts exerts on the FCM. During network analysis, the initial value of a single concept is varied (from 0 to 1) while keeping the initial values of all other concepts fixed, except maybe for the concepts under investigation (Mago et al., 2013).

To conduct the network analysis the initial values for all concepts are set at a constant level to monitor the investigated concepts after a number of iterations. Measures of centrality such as degree centrality and closeness centrality can also be used to analyze the most influential factors.

Degree centrality of each concept (node), in a given weighted and directed graph, is defined as the sum of the absolute values of the weights of the outgoing and incoming edges. Closeness centrality of a concept is the inverse of the sum of the lengths of the shortest paths between that node and all other nodes (Karagiannis & Groumpos, 2013; Mago et al., 2013).

During a simulation run, each factor's level evolves simultaneously with all other factors (Calais, 2008; Carvalho, 2010). The system improves if the new equilibrium state is better than the old equilibrium state. (for example, "In a hypothetical fuzzy cognitive map, the system improves when it produces a lower level of drug availability and drug usage related problems in America"(Calais, 2008)).

In FCM inference the multi-rule process and multi-variable fuzzy reasoning can be used (Carvalho, 2010; Gulati, 2014; Rad, Akbari, & Taher, 2012). The inference of FCM includes "forward evolved inference" and "backward evolved Inference." The backward evolved inference uses the transposing of the FCM matrix, yielding a specific concept node value that should be accompanied with a given consequence (Chun-mei, 2009). The forward inference process of FCM starts with a stimulus vector as input into the FCM. The procedure multiplies the stimulus vector to the FCM matrix nonlinearly, transforming the result vector in each iteration until it yields fixed state (the state vector remains unchanged for successive iterations) or a limit cycle with a state vector repeating patterns (Chun-mei, 2009).

2.4.5 Inference Mechanisms in Fuzzy Knowledge

Fuzzy inference is a means of decision-making that uses fuzzy logic in mapping given inputs to outputs (Mathworks, 2015). Fuzzy logic has been used for the classification of data sets (Venkat, 2015). Fuzzy inference mechanisms have been applied in weather prediction (Ramesh, Kesarkar, Bhate, Ratnam, & Jayaraman, 2015), speech recognition systems (Nereveetil, Kalamani, & Valarmathy, 2014), air traffic and vehicle control modelling (Hossain, Rahman, Hossen, Iqbal, & Hasan, 2011; Subbulakshmi, 2014), among other fields.

Designing fuzzy inference systems requires the application of human knowledge and experience (Jignesh et al., 2014). In fuzzy sets, input variables can have partial or full (crisp) membership (Jignesh et al., 2014; Perić, 2015). The fuzzy inference process consists of four sub-processes, including: the fuzzifier, rule sets, inference engine, and defuzzifier (Singhala, 2014). In fuzzy

inference process rule sets are defined which can consist of linguistic variables as inputs and outputs (Xue, 2014). Fuzzy inference processes take inputs and determine appropriate fuzzy sets where it belongs via membership functions. In fuzzy inference systems decisions are based on the testing of every rule, then aggregating outputs to arrive at decisions (Mathworks, 2015). The input for the defuzzification process is a fuzzy set (the aggregate output fuzzy set) and the output is a single value (Mathworks, 2015). An advantage of fuzzy inference systems is that they can work with inaccurate data (Mathworks, 2015).

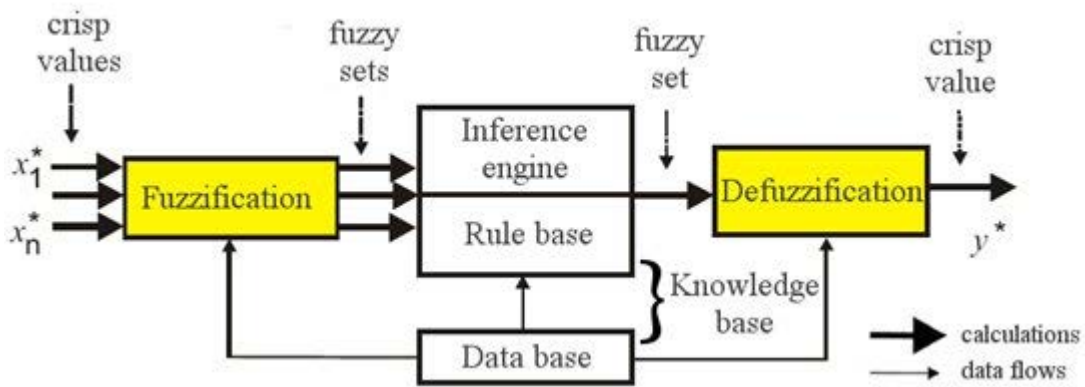


Figure 2-3: Fuzzy Inference process (source: Mathworks, 2015)

To represent traditional human forms of visualizing weather, a means is required to mimic the human visual perception for use as input to fuzzy cognitive mapping models. The reality of such a mechanism relies on the image recognition that is discussed in the next section.

2.5 Computer Vision for Mimicking Human Visual Perception

Computer vision allows computer applications to make decisions based on visual input (Clemons, Jones, Perricone, Savarese, & Austin, 2011; Setayesh, M. Zhang, & Johnston, 2008). Computer vision involves a big class of problems and techniques including: image mining, feature extraction, pattern recognition, visual action analysis and machine learning (Hema, 2013; Clemons, Jones, Perricone, Savarese, & Austin, 2011; Lang, 2009; Xiaojun Wang, Pan, & Weihong, 2015).

This field has been of interest for many computer scientists in recent years (Kobayashi, 2013; Pooja, Sonam, & Sonu, 2013) with image recognition and classification an emphasis in solutions of computer vision applications (Dilipsinh, Mahasweta, & Vikram, 2014; Eldib & Onsi, 2011;

Elissa, Mariya, Abhinav, Xinlei, & Ishan, 2015; Karel Lenc & Mishkin, 2014; Lowe, 2004; Chong Wang & Huang, 2014). Considerable attempts have been made to improve the efficiency of computer vision algorithms (Karel Lenc & Mishkin, 2014) and the design of algorithms with different characteristics and features.

Current computer vision applications are developed with the ability to perceive the real world in the same way as it is visualized by humans (Elissa, Mariya, Abhinav, Xinlei, & Ishan, 2015; Nixon & Aguado, 2002; Xiaolan & Afzal, 2010), but it is still a challenging process for the computer to recognize complicated scenes (Law, Thome, & Cord, 2014). Computer scientists partly clarify the scene recognition difficulties as attributed to image features, choice of image training sets, and also choice of classification algorithms (Vondrick, Khosla, Pirsiavash, Malisiewicz, & Torralba, 2015). An important image feature that is challenging to recognize is texture, particularly in situations where there is change of scale variation and scene cluttering (Zhang J, 2006).

Image content retrieval (Mishra & Silakari, 2012; Paresh, 2011) and segmentation (Soma & Dhandra, 2015) are some of the processing tasks done to images before detecting image features for extraction (Adel & Elmogy, 2014; Dhawan & Dogra, 2012; Khatib, Karajeh, Mohammad, & Rajab, 2015; Mandloi, 2014; Mavrantza & Argialas, 1997) over regions of interest (Boureau, 2012) and performing image classification tasks (Stanchev, 2003).

2.5.1 Challenges in Computer Vision Systems

The computer vision image analysis approach is quite different from human vision. It is challenging for the computer to perform image perception in real dimensional space and employ background knowledge as in the case with human beings (Yang, 2009). The recognition and extraction of features that fully reveal the content of images is current research in computer vision (Kamavisdar, Saluja, & Agrawal, 2013; Tian, 2013) for it is critical to find dependable correspondence between sets of images (Babu & Shankar, 2015).

Image feature recognition and retrieval has been highly studied (Lavoué, 2011; Sukhpreet, 2013). A number of algorithms have been tested (Wadhe, Mohod, & Khalsa, 2015) but still not found to be perfect when working with shadowed and low-contrasted images (Nagaraju, Srinu, & Rao, 2013). Clutter in image background horizon (Calbo & Sabburg, 2008; Khatib, Karajeh,

Mohammad, & Rajab, 2015), increases dimensionality which passes a challenge in the process of feature extraction when there are fewer training samples (Xudong, Bappaditya, & Alex, 2009). Image recognition in varying appearance and illumination is also problematic (Appati, Fosu, & Gogovi, 2014; Wong, Lam, & Siu, 2004). The mentioned challenges bring visual ambiguity (Rahat, Cécile, Damien, & Ducottet, 2015) leading to ineffective representations in image categorization (Nowak, Jurie, & Triggs, 2006) which lead to producing approximate classification results. In some image-processing tasks, low-level visual image features retrieved may not correspond to high-level image semantics (Deng, Manjunath, Kenney, Moore, & Shin, 2001).

There are many image data complexity issues (Benco, Hudec, Kamencay, Zachariasova, & Matuska, 2014), prompting computer vision researchers to propose de-noising before image processing (Soma & Dhandra, 2015). Research suggests a need to make image colours be constant to ensure that the supposed colour of images stands out with changes in lighting (Z. Jun & Youssef, 2012). Other research reveals that working with only one classifier cannot deal efficiently with the complete task of image classification (Lorca et al., 2007). There is also a need to select suitable feature spaces for use in the construction of image classification models (Yuan, Minjing, & Menglu, 2013).

2.5.2 Applications of Image Recognition

Computer vision has been applied in remote sensing to forest developing management applications (Benz, Hofmann, Willhauck, Lingenfelder, & Heynen, 2004; Hermosilla, 2005; Subba & Naga, 2011). Applying computer vision in the detection and recognition of remotely sensed images such as clouds is still an open research area (Benqin et al., 2014; Yuan, Minjing, & Menglu, 2013). In some research attempts image feature extraction and classification have been used for cloud cover analysis and air traffic applications (Calbo & Sabburg, 2008; Heinle, Macke, & Srivastav, 2010; Kuril & Saini, 2013). Image classification techniques have been applied in rapid retrieval of information after natural disasters (Martha & Kerle, 2012; Mavrantza & Argialas, 1997). Image recognition has also been applied in the testing of computer-aided design and manufacturing applications (Xiaolan & Afzal, 2010). The applications of computer vision in the fields mentioned, including that of weather forecasting (Bajwa, Naweed, Asif, &

Hyder, 2009), require fast access and a sufficient quantity of images (Nikolaou & Papamarkos, 2002).

Some studies have applied computer vision in pedestrian protection in open environments (Lorca et al., 2007), place recognition by identifying mobile devices (Lowe, 2004), communications and access control applications (Mohamed, Heshmat, Girgis, & Elaw, 2013), social applications that can evaluate environmental damage, monitoring of land use, radiation monitoring, urban planning and growth regulation (Perumal & Bhaskaran, 2010). Other fields where computer vision has been applied include military services, criminology, entertainment, education, robot navigation assistive driving applications (Thepade, Das, & Ghosh, 2015). In domains such as sports, image segmentation has been used in extracting features of interest for post-event scene investigations (Campos et al., 2011).

Another interesting domain where computer vision is useful is person identification by the recognition, matching and extraction of features such as human faces, palm prints and fingerprints (P. Bhowmik, K. Bhowmik, Azam, & Rony, 2012; Chora, 2007; Feifei, Lijian, & Zhe-ming, 2015; Mandloi, 2014; Nagaraju, Srinu, & Rao, 2013; Pachouri, 2015). This has been extended to recognizing people's positions and actions in crowd detections (Biglari, Ahsan, & Rahi, 2014; Rajan & Mole, 2015). Person identification has enabled the development of commercial applications for biometrics, criminal identification, airport security systems and film processing (Kakarwal & Deshmukh, 2012; Mohanaiah, Sathyanarayana, & Gurukumar, 2013; Rouhi, Amiri, & Irannejad, 2012; Vijayarani & Priyatharsini, 2015).

In the medical fields, computer vision has been employed to classify medical images for disease type diagnose lung tissue classification (Yang, 2013), detecting and quantifying breast cancers (Singh Laxman et al., 2012), and counting cell types based on contained features (Ponuchamy, 2012).

Image recognition has also been applied in content-based image retrieval (Wengert, Douze, & Herve, 2011), image search (Anurag, Raffay, Robinson, & Neel, 2013; Dhawan & Dogra, 2012), handwriting recognition applications (Pradeep, 2011), font recognition (Solli, 2011), logo recognition (Soma & Dhandra, 2015), and retrieving images in huge databases (Deng, Manjunath, Kenney, Moore, & Shin, 2001; Wasim, Shiv, Neetesh, & Nilofar, 2011).

2.5.3 The Process and Techniques Image Acquisition

The object recognition system requires scanned images as an input in some specified format. The current advances of multimedia and hardware technologies allow easy capture and processing of images (Zhao & Zhai, 2015). The process of image recognition requires sufficient sets of images acquired by high-resolution satellite sensors (Benz, Hofmann, Willhauck, Lingenfelder, & Heynen, 2004; Ruiz, Recio, Fernández-Sarría, & Hermosilla, 2009), through scanners, digital cameras and other digital input devices (Adel & Elmogy, 2014; Verhoeven, Karel, Doneus, Trinks, & Pfeifer, 2015). Some computer vision systems encompass graphical user interfaces for capturing images using built-in camera modules (Sukhpreet, 2013). These systems process the images acquired in real time. Other systems access images that are stored in databases for processing. With the advance in hardware technologies and fast internet links, it has become relatively easier for researchers to acquire, store and exchange images (Tirilly, Claveau, & Gros, 2009). Some researchers combine images from digital cameras and images from internet sources to create large-image classifier training sets. In the medical field sectional and 3D images are acquired using a process of X-Ray tomography (Nejad, Motekhasas, Zakeri, & Mehrabi, 2015).

In order to obtain sequential images, sky cameras can be programmed to capture scenes at specific time intervals and in appropriate formats (Heinle, Macke, & Srivastav, 2010). In effectively acquiring specific type of images such as clouds, a series of dynamic continuous images has to be acquired (Viazzi et al., 2014; Yuan, Minjing, & Menglu, 2013). Acquiring dynamic continuous images of the same scene necessitate that image capture positions should be consistent to minimize the variation of noise (Dilipsinh, Mahasweta, & Vikram, 2014). Multiple camera setups can be employed for various image position orientations (Biglari, Ahsan, & Rahi, 2014; Campos et al., 2011; Rajan & Mole, 2015) . A more promising low-cost approach of acquiring sky images is the deployment of drones to acquire scenes at regular time intervals (Dworkin, 2008; UNEP, 2013).

2.5.4 Techniques of Image Pre-Processing

Image pre-processing is the term given to handling images at the basic level. Images that are corrupted by some distortion such as noise, bad illumination or blurring require pre-processing (Nikolaou & Papamarkos, 2002), a regular procedure for reducing the dimension of

feature vectors to optimize image classification (Hema, 2013; Pandit, Kolhar, & Patil, 2015; Piera et al., 2005). The image pre-processing procedures enhance the image content quality by suppressing undesired distortions (Rajendran & Madheswaran, 2010; Soma & Dhandra, 2015).

Image pre-processing tasks include principal component analysis, noise reduction, filtering, resizing, normalization, colour transformation as well as segmentation (Chary, Lakshmi, & Sunitha, 2012; Chora, 2007; Kamavisdar, Saluja, & Agrawal, 2013; Nikolaou & Papamarkos, 2002). Noise introduced during the image acquisition process can be reduced using noise reduction filters such as median, mean, adaptive, linear and predefined filters. Image noise reduction process sets each image pixel to the mean or median of the pixel values in the neighbourhood of the corresponding input pixels (Sindhu, 2015; Pandit, Kolhar, & Patil, 2015; Rajendran & Madheswaran, 2010; Vijayarani & Priyatharsini, 2015). A more simple and efficient process of image noise reduction can be achieved by applying order statistics filters that combine both median and mean filtering to remove noise from images by determining the pixel value in the noiseless images (Sindhu, 2015).

To make an object sharp and with outstanding edges the image intensity is normalized by computing an average image intensity histogram (Rajendran & Madheswaran, 2010; Sindhu, 2015). During image pre-processing task images are resized into pre-defined image sizes (Nikolaou & Papamarkos, 2002), aligned and region of interest selected (Feifei, Lijian, & Zheming, 2015). Other image pre-processing tasks include: colour reduction by converting from Red, Green and Blue (RGB) colour model into greyscale, and removing shadows or light spots (Khatib, Karajeh, Mohammad, & Rajab, 2015).

2.5.5 Clustering and Classification of Images

Advances in imaging technologies have led to the formation of a huge number of various images requiring methods of image indexing and retrieval. Image clustering is a process used to efficiently organize and extract images for classification tasks (Bhateja, Sehrawat, & Bhardawaj, 2013). The image clustering process is also called unsupervised image classification since images in a dataset are identified as a member of one category of image collection without using any prior knowledge (Mishra & Silakari, 2012; Olaode, Naghdy, & Todd, 2014; Saritha & Parthasarathy, 2014). The image clustering process partitions the images data set into several

clusters so that the correspondence within a single cluster is larger than that of whole data set (Rajan & Mole, 2015).

Image clustering is done using dimension reduction and unsupervised classification algorithms to come up with compact image representations (Olaode, Naghdy, & Todd, 2014; Rahat, Cécile, Damien, & Ducottet, 2015). During image clustering feature descriptors are grouped corresponding to visual words whose quality depends on the choice of a clustering algorithm (Jiang, Y. Jun, & Chongwah, 2007; Tian, 2013; Tirilly, Claveau, & Gros, 2009).

Image clustering builds a visual dictionary by grouping a large set of feature descriptors which then associates each image to a histogram of occurrences of the visual words (Lavoué, 2011). Since image clustering algorithms do not determine the best possible number of clusters, the vocabulary size must be fixed to a specific number of clusters (Tirilly, Claveau, & Gros, 2009). Having a small vocabulary reduces image discrimination power as different images may be assigned into the same cluster. A large vocabulary is less general and has additional processing overhead (Jiang, Y. Jun, & Chongwah, 2007; Tirilly, Claveau, & Gros, 2009). Research reveals that larger vocabularies prove to be superior in image clustering but can discriminate irrelevant variations including image noise (Toldo, Castellani, & Fusiello, 2009).

Image clustering can be achieved using either parametric or non-parametric techniques. The parametric technique involves defining a measure of dissimilarity between image samples for assessing the degree of difference between images (Manjunath, 2014; Olaode, Naghdy, & Todd, 2014). Some image clustering techniques use partitioning methods, density-based methods, grid-based methods, model-based methods, k-means algorithm, graph-based model, hierarchical clustering, mixture resolving, mode-seeking algorithms, nearest neighbour clustering, fuzzy clustering, evolutionary clustering and spectral clustering (Manjunath, 2014; Olaode, Naghdy, & Todd, 2014; Saritha & Parthasarathy, 2014; Sridhar, 2012). Non-parametric techniques are simple but not very suitable for clustering high dimensional images (Olaode, Naghdy, & Todd, 2014). Fuzzy C-means (FCM) image clustering uses fuzzy logic where each image has a possibility of being grouped into different specific clusters (N, A, & V, 2010). Image segmentation uses the means clustering to partition an input image into foreground and background regions (Pandit, Kolhar, & Patil, 2015). Some current research used a clustering

technique based on unsupervised neural nets and self-organizing maps (Manjunath, 2014). A multi-clustering approach can be achieved by applying different clustering techniques to sets of images to obtain several visual words (Toldo, Castellani, & Fusiello, 2009). Support vector machines algorithms can also be used for image clustering (Pachouri, 2015).

2.5.6 Extraction and Representation of Image Features

Image features extraction (the process of locating specific points in an image) is an essential step before image recognition (Jain & Salankar; Ruiz, Recio, Fernández-Sarría, & Hermosilla, 2009; Tian, 2013; Vijayarani & Priyatharsini, 2015). In video applications, feature extraction is used to estimate the trajectory of an object in the image plane (Kamavisdar, Saluja, & Agrawal, 2013). Current research in image recognition and retrieval has been focused extracting different visual features of an object in order to identify the object from the image (Kuril & Saini, 2013; Olaode, Naghdy, & Todd, 2014; Thakur & Dhole, 2013) with the intention of allowing computer applications and users to search or recognize specific objects in an image (Kuril & Saini, 2013; Pachouri, 2015; Saritha & Parthasarathy, 2014; Thakur & Dhole, 2013). Image features are also known as the signatures of the image (Jain & Salankar; Nikolaou & Papamarkos, 2002).

The task of image feature extraction can only be complete when objects have been identified and recognized by the machine (Saritha & Parthasarathy, 2014). The purpose of image feature extraction is to represent an image in compact and unique form of single values or matrix vectors (Kuril & Saini, 2013; Ponuchamy, 2012; Soma & Dhandra, 2015). In this process the visual content of the images is mapped into a new feature vector (Chora, 2007; Kakarwal & Deshmukh, 2012; Nikolaou & Papamarkos, 2002). To improve performance and memory management after image extraction, only appropriate features are selected to reduce the number of features used in the image classification task (Chora, 2007; Pradeep, 2011; Rahat, Cécile, Damien, & Ducottet, 2015).

The human eye perceives images with a combination of features including: colour, texture, and shape (Benčo & Hudec, 2007). The key to a working computer vision system is the choice of features extracted to represent an image (Nikolaou & Papamarkos, 2002; Sridhar, 2012). Visual object distinguishable features that can be extracted include: colour, texture and shape (Chora, 2007; Mohanaiah, Sathyanarayana, & Gurukumar, 2013; Olaode, Naghdy, & Todd, 2014;

Saritha & Parthasarathy, 2014; Thakur & Dhole, 2013; Vijayarani & Priyatharsini, 2015; Wasim, Shiv, Neetesh, & Nilofar, 2011). Once these visual image features have been extracted, the image retrieval and recognition process reduces to measuring the similarities between the features (Thakur & Dhole, 2013). Other basic features that can be used to recognize visual objects include contour, diameter, length, width, area, perimeter, size, shape, composition and location (Chary, Lakshmi, & Sunitha, 2012; Faizal, Jabal, Hamid, Shuib, & Ahmad, 2013; Piera et al., 2005; Sindhu, 2015).

The techniques of geometry-based feature extraction (Gabor wavelet transform), appearance-based techniques, colour segmentation-based techniques, template-based feature colour histograms, colour moments and edge histogram descriptors are used to extract image features (Dhawan & Dogra, 2012; Dubey, Choubey, & Bhattacharjee, 2010). The choice of a technique relies on factors such as image scale, illumination variation, variation noise and orientation (Dhawan & Dogra, 2012; Olaode, Naghdy, & Todd, 2014). The feature extraction techniques chosen must enhance the discriminative power of feature descriptors, making the classification task less difficult (Vamvakas, Gatos, & Perantonis, 2009; Yang, 2013). An extraction technique that is able to retain the neighbourhood associations among image pixels is advantageous (Nikolaou & Papamarkos, 2002). Programming tools are available for image feature extraction with a diversity of methods to describe the properties of visual objects (Ruiz, Recio, Fernández-Sarría, & Herмосilla, 2009).

2.5.6.1 Colour Descriptors

Colour is an important and widely used feature for visual object representation (Alamdar & Keyvanpour, 2011; Mandloi, 2014; Sridhar, 2012; Zhao & Zhai, 2015). The human vision system uses colour for recognition and discrimination of objects (Bhardwaj, Di, R. Hamid, Piramuthu, & Sundaresan, 2013; Nikolaou & Papamarkos, 2002; Tian, 2013; Jun Zhang, Barhomi, & Serre, 2012). Extracting colour visual information is useful in content-based image retrieval (Chora, 2007; Jain & Salankar; Mandloi, 2014; Nikolaou & Papamarkos, 2002; Sridhar, 2012; Wasim, Shiv, Neetesh, & Nilofar, 2011). Compared to shape and texture features, colour is more constant, making it insensitive to image transformation such as scaling, translations, lighting, rotations and zooming (Mandloi, 2014; Sridhar, 2012). The detection of dark colours indicates that the object is high-density (Lang, 2009).

Colours in digital images are represented as sets of matrices which define pixel values of the images such as grey scale values in black and white images and RGB values in colour images (Agarwal & Bedi, 2015). In a true colour image, a pixel can have an RGB value from a combination of 16777216 different colours (Paresh, 2011). Colour features are extracted based on colour spaces that are mathematical representations of a sets of colours (Biglari, Ahsan, & Rahi, 2014; Paresh, 2011). The commonly used colour models are Red, Green, Blue (RGB), Hue, Value, Saturation (HSV) or Cyan, Magenta, Yellow, and Key (CMYK) (Biglari, Ahsan, & Rahi, 2014; Jain & Salankar; Sridhar, 2012; Tian, 2013; Vijayarani & Priyatharsini, 2015). The colour spaces can be derived from the common RGB format while retaining compatibility with display devices (Biglari, Ahsan, & Rahi, 2014). The RGB colour space is mostly used in computer graphics. The red, green, and blue are three primary additive colours represented by a three-dimensional, Cartesian coordinate system with varying amounts of each primary component, representing various grey levels (Biglari, Ahsan, & Rahi, 2014).

Image colour distribution can be described using colour moments, colour histograms, and colour coherence vectors (Alamdar & Keyvanpour, 2011; Pachouri, 2015; Sridhar, 2012). The choice of colour representation method used is significant for extracting colour distribution (Anurag, Raffay, Robinson, & Neel, 2013). In colour histograms bar graphs are used to depict the amount of colour in an image (Chora, 2007; Dubey, Choubey, & Bhattacharjee, 2010; Jain & Salankar; Mishra & Silakari, 2012; N. Sharma, Rawat, & J. Singh, 2011). Colour histograms are easy to compute, requiring low storage, and are robust to image viewpoints (Chora, 2007; Deng, Manjunath, Kenney, Moore, & Shin, 2001; Jain & Salankar; Wasim, Shiv, Neetesh, & Nilofar, 2011). The use of the three colour moments including first order (mean), second order (variance) and third order (skewness) have been proved to be efficient and effective in representing colour distributions of images (Chora, 2007; Mishra & Silakari, 2012; Thakur & Dhole, 2013). During image analysis the Euclidean distance is determined to measure the similarity of two colour moments (Thakur & Dhole, 2013). A colour correlogram characterizes the colour distributions of pixels and spatial correlation of pairs of colours (Chora, 2007; Mishra & Silakari, 2012).

Approaches to colour extraction for object recognition involve applying shape-based image descriptors on individual colour channels, for example, HSVSIFT, OpponentSIFT and CSIFT descriptors (Z. Jun & Youssef, 2012). The Colour SIFT method extracts colour feature points

from HSV image (Babu & P. R. Shankar, 2015). The Grid-Based-Colour-Moments (GBCM) function can be used to extract the colour moments of an image (Thakur & Dhole, 2013).

2.5.6.2 Texture Descriptors

Texture is a very important feature in the analysis and classification of images (Al-momen, George, & Naji, 2015; Benco, Hudec, Kamencay, Zachariasova, & Matuska, 2014; Ramana, Mani, & Kumar, 2009; Wasim, Shiv, Neetesh, & Nilofar, 2011). Texture relates to visual patterns with properties of homogeneity and can be said to be fine, uniform, dense, coarse, or smooth; rippled, mottled, irregular, or lineated (Haralick & Shanmugam, 1973; Sridhar, 2012). In texture visual patterns can also be described in terms of granularity, directionality, and repetitiveness (Mishra & Silakari, 2012). In the presence of clutter it is challenging to recognize objects using texture (Zhang J, 2006).

Statistical-based texture descriptors explore the grey-level spatial dependence while structural or transform-based texture descriptors rely on some transform such as DWT (Mishra & Silakari, 2012; Sridhar, 2012). Entropy (a statistical measure of randomness), local range and standard deviation measures are used to measure texture features (Mishra & Silakari, 2012). Statistical-based methods such as co-occurrence matrices, Law's texture energy measures, Fourier transform domain, Markov random field models, local linear transforms, Gabor and wavelet transform can be used to extract textures in images (Mishra & Silakari, 2012; Ramana, Mani, & Kumar, 2009).

Texture features can be extracted by exploiting the high redundancy depicted by high-intensity similarities among various pixels. Structural methods describe texture by identifying structural primaries and their rules (Mishra & Silakari, 2012). The Cubic Spline, Haar wavelet transform and Discrete Wavelet Transform (Al-momen, George, & Naji, 2015; Kuril & Saini, 2013) can be used to measure texture of an image individually or in combination.

Grey relations exist between two pixels within the specific positions of the 2-Dimensional image plane (Shuang, 2015). The GLCM (grey-level co-occurrence matrix) extracts the second order statistical texture features by describing a co-occurrence matrix relating neighbouring grey levels in pixels of an image (Benco, Hudec, Kamencay, Zachariasova, & Matuska, 2014; Benčo & Hudec, 2007; Mohanaiah, Sathyanarayana, & Gurukumar, 2013; Shuang, 2015; Uddin, Islam, &

J.-myon Kim, 2014). GLCM computes four statistical features (energy, entropy, contrast, and homogeneity) of the image (Ruiz, Recio, Fernández-Sarría, & Hermosilla, 2009; Sridhar, 2012; Yuan, Minjing, & Menglu, 2013). Gabor filters can be used to extract discernible texture features from a filtered image corresponding to a specific scale and orientation (Benčo & Hudec, 2007; Uddin, Islam, & J.-myon Kim, 2014) . The Differential Box Counting (DBC) method has successfully been used to calculate the fractal dimension distinguishing texture by image roughness (Al-momen, George, & Najj, 2015). Gabor filters and GLCM methods have been proved as efficient in image retrieval using texture features (Benco, Hudec, Kamencay, Zachariasova, & Matuska, 2014).

2.5.6.3 Shape Descriptors

Shape is an important low-level feature that can be used to recognize images for indexing and retrieval (Calbo & Sabburg, 2008; Mathew & Balas, 2015; Mohanaiah, Sathyanarayana, & Gurukumar, 2013; Toldo, Castellani, & Fusiello, 2009; Xiaolan, Afzal, & Asim, 2008). The human eye exploits shapes to identify and recognize real-world objects (Tian, 2013). In shape-based image retrieval the similarity between shapes represented by their features is measured (Chora, 2007; Hermosilla, 2005). The features that can be used to define an object shape include length, width and area (Faizal, Jabal, Hamid, Shuib, & Ahmad, 2013). Advanced features such as polygons and object skeletons can also be derived from the basic features (Benz, Hofmann, Willhauck, Lingenfelder, & Heynen, 2004).

Shape feature extraction techniques are classified based on contour and region (Kamavisdar, Saluja, & Agrawal, 2013; Mathew & Balas, 2015; Medjahed, 2015; Tian, 2013). The contour method, such as the Fourier descriptor and skeleton description, calculates shape features only from the boundary of the shape (Mathew & Balas, 2015). The region-based method extracts features from the entire image region such as invariant moments and the region area. Shape features can also be extracted from the limits of the objects (Ruiz, Recio, Fernández-Sarría, & Hermosilla, 2009). Region-based methods use Geometrical moments, Zernike moments and Legendre moments descriptors (Mathew & Balas, 2015). Region-based shape descriptors, such as statistical moments, are used when shapes have complex boundaries (Mathew & Balas, 2015). Contour-based shape descriptors, such as Fourier descriptors, are not appropriate for describing shapes consisting of several disjoint regions (Mathew & Balas, 2015). The choice of a shape

representation descriptor should be invariant to translation, rotation and scaling (Mishra & Silakari, 2012).

In the current image recognition research, shape descriptors are replaced by using descriptors such as interest points and corner points (Solli, 2011). (Solli, 2011) showed that colour descriptors outperform shape-based approaches in image classification.

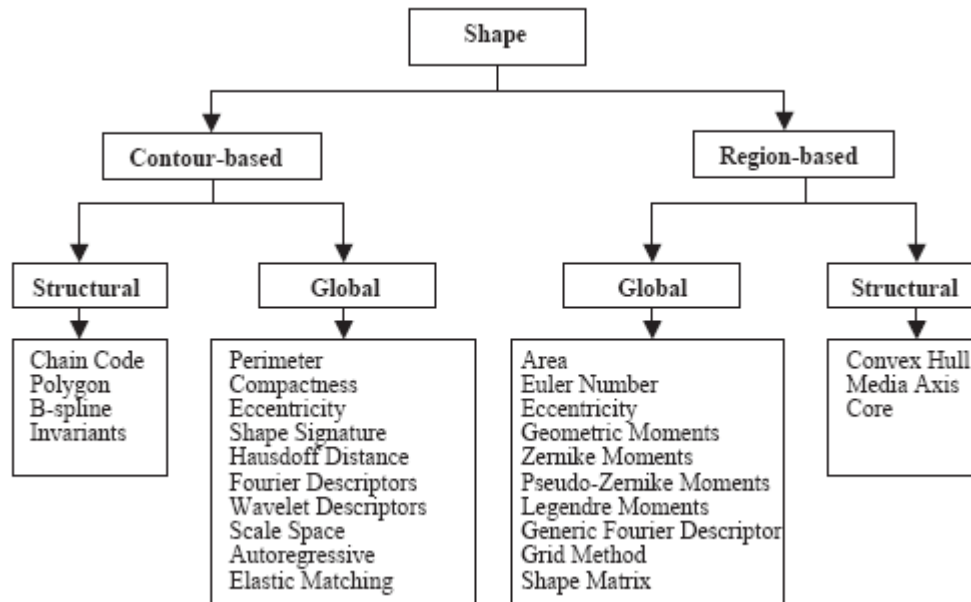


Figure 2-4: Approaches for shape representation. (Source: D. Zhang, G. Lu, 2004)

2.5.6.4 Region Descriptors

Region descriptors based on a similarity measure between neighbouring pixels and an object of interest have been considered as an effective and most frequently used technique in image processing (Singh Laxman et al., 2012; Yaxin, Zhihua, & Yubo, 2015). Extracting features based on focused regions can help improve the performance by integrating image regions which are relevant and not exhibiting uniform visual characteristics (Sindhu, 2015; Yaxin, Zhihua, & Yubo, 2015). Before image feature extraction begins, regions of interest (ROI) have to be specified (Faizal, Jabal, Hamid, Shuib, & Ahmad, 2013; Sindhu, 2015).

2.5.7 Techniques of Image Features Extraction

2.5.7.1 The GIST (Global Image Spatial Features)

Many researches on image recognition have focused on using the GIST descriptor (Douze, Amsaleg, & Schmid, 2009). The GIST descriptor uses low-dimensional feature vectors to describe the shape of an object (Sikiric & Brkic, 2013) without requiring image segmentation (Douze, Amsaleg, & Schmid, 2009). In GIST the perceptual properties of human vision – such as naturalness, openness, roughness, expansion and ruggedness – are used to represent the structure object (Douze, Amsaleg, & Schmid, 2009; Oliva, 2005; Sikiric & Brkic, 2013). The GIST focuses on the shape and the relationship between the outlines of the object (Sikiric & Brkic, 2013). Compared to the BoW, model the GIST descriptor has a drawback due to its fixed spatial layout that does not recognize images from a variation of viewpoints (Douze, Amsaleg, & Schmid, 2009).

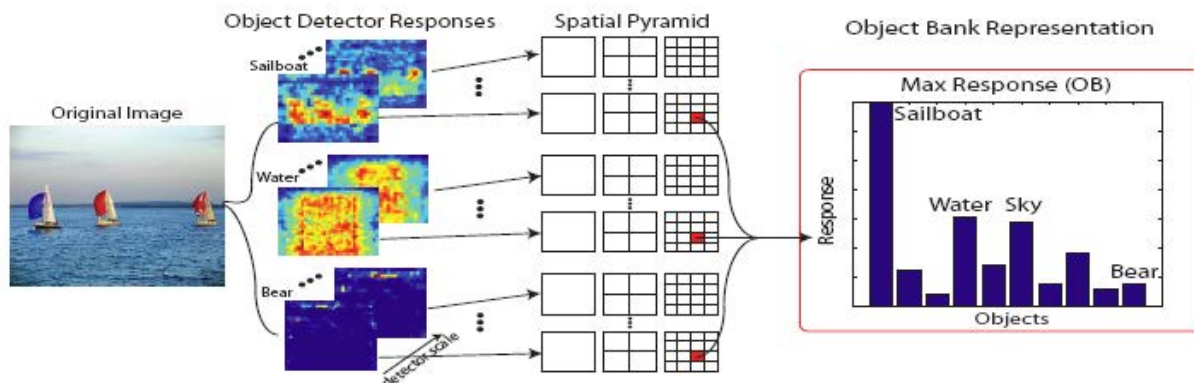


Figure 2-5: GIST feature extraction. (Source Li-Jia L, et al., 2009)

2.5.7.2 The Gabor Filters

A Gabor filter is a linear filter used for edge detection. Gabor filters' frequency and orientation representations are similar to those of the human visual system. Gabor filters can be applied to an entire image or to selected regions of interest so that regions near a pixel are described by the responses to different frequencies and orientations centred at that pixel position (Andrysiak & Choras, 2005). Gabor filters have been used for different computer vision and pattern recognition applications relying on texture segmentation and texture feature extraction (Andrysiak & Choras, 2005). Gabor filters are noise-efficient and can aid in reducing image redundancy (Andrysiak & Choras, 2005). Before processing, images can be decomposed into components corresponding to

different scales and orientations using Gabor filters (Andrysiak & Choras, 2005). The Gabor filtering process can also be used to extract grey-scale histograms from images (Sikiric & Brkic, 2013). Gabor feature vectors extracted from an image can be transformed or input directly into classification algorithms (Grigorescu, Petkov, & Kruizinga, 2002). An advantage of Gabor filters is that they can work in invariant image conditions but are computationally expensive than GLCM (Jagdish, Sunil, & Ankit, 2013).

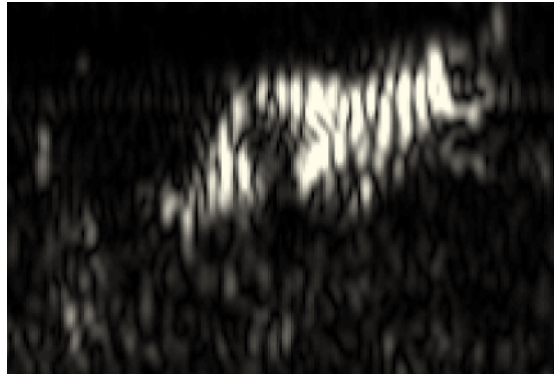


Figure 2-6; Extracted feature from Zebra Image using Gabor filter. (Source: V. Shiv Naga Prasad, 2005)

2.5.7.3 Grey Level Co-Occurrence Matrix

The Grey Level Co-occurrence Matrix (GLCM) can be used to extract spatial distribution properties of the grey levels in texture images (Deepak, 2014; Jagdish, Sunil, & Ankit, 2013). GLCM indicates how often a pixel with the intensity value i occurs in a specific spatial relationship to a pixel with the value j . GLCM texture features commonly exploited include: Energy, Contrast, Correlation, and Homogeneity (Deepak, 2014). Some research reveals that the use of the GLCM descriptor in image recognition provides better results than Gabor filters (Jagdish, Sunil, & Ankit, 2013).

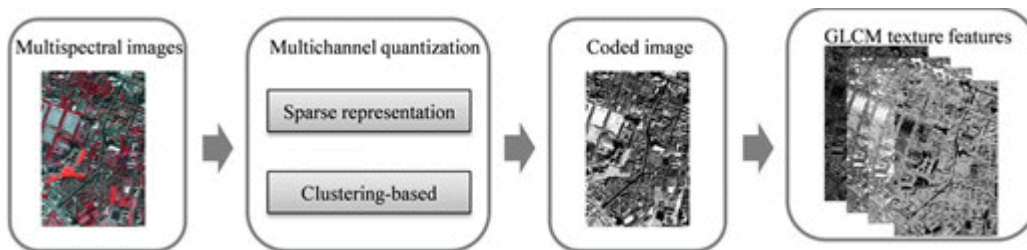


Figure 2-7; Grey Level Co-Occurrence Matrix (GLCM) feature extraction process

2.5.7.4 Principal Component Analysis

Principal Component Analysis (PCA) is a technique used to identify variations in a dataset. It has been used to identify unknown trends in image data (Vipul, 2014) decreasing image noise and reducing image dimensionality. PCA can also work with the SIFT descriptors (Lisin, 2006; Manisha & Neeraj, 2014; J. Wang et al., 2007; Xu, Jonathan Li, Shu, & Peng, 2014). PCA can be used to extract specific features in images, for instance eyes in faces (Dagher, Sallak, & Hazim, 2014) and in image and video compression (Griefahn, Wollnack, & Hintze, 2014; Olubunmi, Olusayo, Bola, & Ayodeji, 2015). To achieve compression, de-correlation and dimensionality reduction the representation of an image is obtained by projecting it to the coordinate system defined by the principal component subspace (Olubunmi, Olusayo, Bola, & Ayodeji, 2015). Principal component analysis using locally learned features has been able to represent structural features, for example image edges and texture (Xu, Jonathan Li, Shu, & Peng, 2014)

2.5.7.5 Linear Discriminant Analysis

Linear Discriminant Analysis (LDA) is a popular method used for image dimensionality reduction and pattern recognition for image feature extraction (Dagher, Sallak, & Hazim, 2014; Olubunmi, Olusayo, Bola, & Ayodeji, 2015). Features recognition using LDA works by projecting an input image to the same feature-space for classification (Dagher, Sallak, & Hazim, 2014; Manisha & Neeraj, 2014). LDA methods have a drawback in that their optimality criteria are not directly related to the classification ability of the obtained feature representation (Manisha & Neeraj, 2014). LDA is also not flexible when working with complex datasets and relies on models containing the exact number of components (Siddiqi et al., 2014).

2.5.7.6 The Scale Invariant Feature Transform

The Scale Invariant Feature Transform (SIFT) extracts descriptors from an image with invariance to translation, rotation or scaling. SIFT descriptors are also robust to image transformations such as viewpoints, noise, blur, contrast changes and scene deformation (Hyun-Woong Jang, 2014; Rey-otero & Delbracio, 2014) and in such are widely used in matching pairs of images, object recognition and video stabilization (Hyun-Woong Jang, 2014; Khan, Mccane, & Wyvill, 2011). The SIFT algorithm relies on the detection of interesting points (i.e. keypoints) and the extraction of a descriptor associated to each keypoint (Khan, Mccane, & Wyvill, 2011; Panchal, 2013). The keypoints are also called visual words that characterize an image (Hyun-

Woong Jang, 2014). The SIFT technique has an advantage of high accuracy of matching image features but is slower compared to SURF (Hyun-Woong Jang, 2014).



Figure 2-8: Image matching using Scale Invariant Feature Transform (SIFT) (David Lowe, 2004)

2.5.7.7 Speeded Up Robust Features

Speeded Up Robust Features (SURF) is sometimes called approximate SIFT (Khan, Mccane, & Wyvill, 2011). Detecting image features using SURF detectors based on the approximated Hessian Matrix is more efficient than using SIFT (Pandya, Chitaliya, & Sandip, 2013). The low dimensionality SURF descriptor determines a distribution of Haar-wavelet responses within the image regions of interest (Pandya, Chitaliya, & Sandip, 2013). SURF employs keypoint detection and keypoint description. Keypoint detection uses integral images to compute approximate Laplacian of Gaussian images using a box filter, rather than using DoGs as in SIFT. Determinants of the Hessian Matrix are then used to detect the keypoints (Khan, Mccane, & Wyvill, 2011). The SURF descriptors are computed by constructing a square window centred on the keypoints (Khan, Mccane, & Wyvill, 2011). SURF builds its scale space by keeping the image size constant while varying the filter size (Khan, Mccane, & Wyvill, 2011). SURF is fast compared to SIFT but less accurate.



Figure 2-9: Speeded Up Robust Features (SURF) features on an image (source: Mathworks, 2015)

2.5.7.8 Histogram of Oriented Gradients

Histogram of Oriented Gradients (HOG) is an image feature descriptor that characterizes objects through their shapes (Prates, Schwartz, & Menotti, 2013). The aim of the HOG method is to describe an image by a set of local histograms. These histograms count occurrences of gradient orientation in a local part of the image (Suard, Rakotomamonjy, & Benschrair, 2006). To obtain such discriminant information, the image is divided into cells and for each cell is computed a histogram of oriented gradients. Each pixel within the cell contributes with a weighted vote for an oriented histogram based on the values of the computed gradients (Prates, Schwartz, & Menotti, 2013). HOG, like SIFT descriptors, captures edge and gradient structure that is very characteristic of object local shape with invariance to local geometric and photometric transformations (Dalal & Triggs, 2005). The histograms of oriented gradients are also called Dense-SIFT extracts that describes local image features from each of the uniformly spaced cells on an image (Olaode, Naghdy, & Todd, 2014).



Figure 2-10: Histogram of Oriented Gradients (HOG) image features (source: Mathworks, 2015)

2.5.7.9 Bag of Words

The Bag of Words (BoW) – also called Bag of Features (BoF) or Bag of Keypoints (BoP) – segments an image into grids and extracts visual features from each grid to form feature vectors (Jinho Kim, B.-S. Kim, & Savarese, 2011; Solli, 2011; Yaxin, Zhihua, & Yubo, 2015). The BoW technique extracts the image features by using the threshold method (Faizal, Jabal, Hamid, Shuib, & Ahmad, 2013). After extraction of the feature vectors a vocabulary of visual words is constructed by clustering the feature vectors which represent images as histograms of visual words (Jinho Kim, B.-S. Kim, & Savarese, 2011; Yaxin, Zhihua, & Yubo, 2015). The BoW model has become an important image content representation method and is widely used in image annotation and retrieval (Yaxin, Zhihua, & Yubo, 2015).

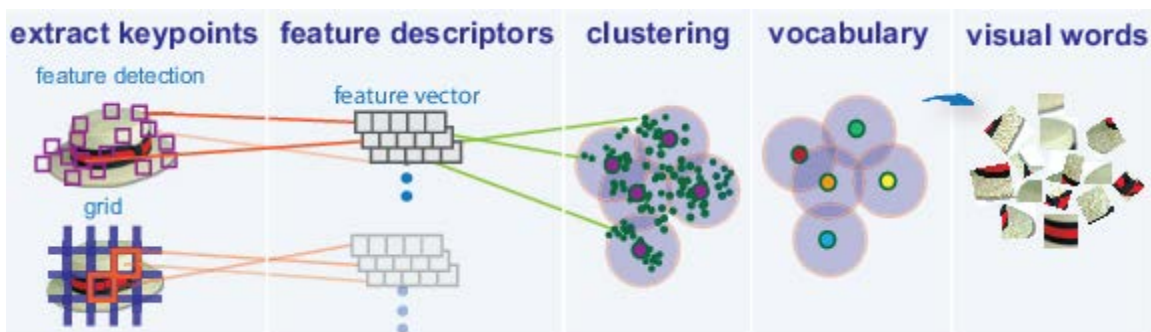


Figure 2-11: Bag of Visual Words (source: Mathworks, 2015)

The BoW has two key concepts: local features and a codebook. The essential aspect of the BoW concept is to extract global image descriptors and represent images as a collection of local properties calculated from a set of small sub-images called patches. Codebook is a way that an image can be represented by a set of local features. The idea is to cluster the feature descriptors of all patches based on a given cluster number and each cluster represents a visual word that will be used to form the codebook. After obtaining the codebook, each image can be represented by the BoW frequency histograms of the visual vocabulary of the codebook. The similarity of images can be measured by comparing between the BoF histograms (Douze, Amsaleg, & Schmid, 2009; Xiaoli, Jing, Zengchang, & Tao, 2011). Local features extractors that utilize BoW image representation technique include: SIFT; SURF; and HOG (Anurag, Raffay, Robinson, & Neel, 2013). Using BoW to extract features from locations covering the entire area of an image rather than few selected locations provides additional information which may improve the accuracy of an image classifier. The SIFT (Xiaolan, Afzal, & Asim, 2008) and SURF feature are sparse feature extraction algorithms because they only detect and describe features at chosen locations on an image (Olaode, Naghdy, & Todd, 2014). The HOG descriptor operates on localized cells, and is also invariant to geometric transformation of an image (Olaode, Naghdy, & Todd, 2014).

The output from image recognition techniques can be transformed to represent visual concepts mimicking human perceptions and used as input to fuzzy cognitive mapping and predictions process. The quality of results after running of fuzzy cognitive mapping scenarios can be evaluated against reality. The process of verification relying on results from fuzzy cognitive mapping scenarios is discussed in the next section.

2.6 The Role of Computing in Traditional Weather Forecasts Verification

Assessing the output quality of weather forecasting systems has been challenging in meteorological research (Casati et al., 2008; Mailier, Jolliffe, & S. David, 2006). The advent of modern technologies and ICT allow forecast users (such as farmers and other decision-makers) to seek weather forecasts from various sources with varying qualities of forecast information (Mailier, Jolliffe, & S. David, 2006).

Traditional knowledge is widely used in rural communities despite the fact that it has not been documented and verified, making it inaccessible to the outside world (Owiny & Marezki, 2014). Some studies revealed that the most common weather lore could have scientific bases (Baliscan, 2001). The correctness of forecasts derived from weather lore needs to be scientifically verified to enable traditional weather forecasts to be applied on the same level as conventional weather forecasts (Shoko, 2012). Verifying traditional knowledge will lead to increased adaptation (Chiwanza, Musingafi, & Mupa, 2013; Nakashima & McLean, 2012) while effectively meeting the needs of scientists and researchers (Casati et al., 2008). Recognizing and building traditional knowledge for production and representation of scientific forecasts must be employed in ways that do not devalue the cultural notions in relationship to communities (Roncoli, Ingram, & Kirshen, 2002).

Scientific verification is significant for standardizing traditional knowledge (such as for use in healthcare), as the process must include sound scientific authentication and verification (United-Nations, 2004). The United Nations recognizes traditional knowledge as a resource from the scientific point of view. With the wealth of useful information embedded in traditional knowledge many researchers have recognized the need of integrating the scientific and traditional systems of knowledge (United-Nations, 2004). However, the process requires the extraction of relevant traditional knowledge through a process of scientific verification (Chinlapianga, 2011; United-Nations, 2004).

2.6.1 The Process of Verification Using Forecast Skills

Weather forecast skill verification is a process of assessing the quality of forecast information (Fajman, 2011). Sometimes forecast verification is used to imply the measure of quality between forecasts and actual weather observations (Mailier, Jolliffe, & S. David, 2006; Mariani & Casaioli, 2008; Oberkampf & Trucano, 2002; Oreskes, Shrader-frechette, & Belitz, 2010; Tressa, Tara, & Barbara, 2012; Ziervogel & Downing, 2004). The term ‘verification’ is also regarded as a method of testing model forecasts during the validation process (Abramova & Kovriga, 2008; Lo & Pielke, 2008).

The process of verifying output from a forecast model aims at demonstrating the truth which will imply the reliability of the forecast model in for decision-making (Green, Billy, & Tapim, 2010;

Mariani & Casaioli, 2008; Oreskes, Shrader-frechette, & Belitz, 2010; Pinson, 2013). As a technique of determining the validity of a computational model's predicted values relative to actual data and not the internal working of the model, the verification process is also known as external validation (Carley, 1996). In some verification processes forecasts are compared to the observations recorded at various weather stations (Huntington, Callaghan, Fox, & Krupnik, 2004; Savvidou, Lagouvardos, Michaelides, Kotroni, & Constantinides, 2010; Xue, 2014). Sometimes a scientific verification process is conducted in the lack of sufficient data (Johansson & Achola, 2013), hence conducting a forecast verification process may not prove output accuracy for all possible scenarios but provide evidence that the forecast tool forecasts with sufficient accuracy and reliability (Oberkampf & Trucano, 2002; Oreskes, Shrader-frechette, & Belitz, 2010; Thacker et al., 2004). The verification process also can provide some tests on forecast model ability to represent unpredictable and dynamical weather systems (Randall & Wood, 2007).

2.6.2 Preparing Weather Data for Verification

Different data crowdsourcing methods (such as mobile sensors, social networks and human computation) can be used to obtain actual (or ground) truth for use in running scenarios to verify weather forecast models (Calais, 2008; Steven et al., 2015).

Crowdsourcing is a method of utilizing a variety of techniques and strategies (such as human computation, sensor networks, mobile technologies etc) for performing tasks (such as data gathering) to consequently reduce the effort of solving problems (Yuen, King, & Leung, 2011). The process of crowdsourcing information using more than one technique and from two or more independent sources with different forms of data such as text and images can clearly confirm and verify knowledge in near real-time (Habibi & Popescu-belis, 2012; Krause & Smeddinck, 2011).

2.6.2.1 Acquiring Verification Data Using Human computation

Crowdsourcing systems can employ human input and computation where there is incomplete knowledge, and where subjective comparisons of knowledge are needed (Castelein, Grus, Crompvoets, & Bregt, 2010; Franklin, Kossmann, Kraska, S. Ramesh, & Xin, 2011; Kuo & Hsu, 2010; Little, 2011). In human crowdsourcing strategy, data quality is a major concern since volunteered information is a claim and carries no assurance that can lead to trust in legitimately

created data (Chengjin LI, 2012; Goodchild & Glennon, 2010; Morris & Mcduff, 2012), hence motivating factors such as pay per result and incentives can be employed to increase data collection and performance of crowd workers (Goodchild, 2006; Kuhn, 2007; Pipek, Landgren, & Palen, 2012) where generation of solutions can be performed by paid workers rather than ad-hoc volunteers (Ahn, 2005; Goodchild & Glennon, 2010; Pipek, Landgren, & Palen, 2012). Previous studies reveal that crowd workers are willing to put their solutions forward in exchange for a chance to win compensation (Massung, Coyle, Cater, Jay, & Preist, 2013; Morris & Mcduff, 2012; Sunny, Mike, Bing, & Daying, 2012). Crowdsourcing techniques and strategies can be used to enhance classification of information (Haoqi et al., 2012; Mccall, Martinez, & Verplanke, 2013; Preist, Massung, & Coyle, 2014) as well as in evaluation of data in information systems (Goodchild, 2006; Haoqi et al., 2012; Kuhn, 2007; Quinn & Bederson, 2010).

2.6.2.2 Acquisition of Verification Data Using Wireless Sensors

Wireless sensors are now embedded in most of modern communication devices such as drones (Dworkin, 2008; Molnar, Mansour, Saulnier, Thompson, et al., 2014; Richard, 2013; UNEP, 2013), phones and digital assistants and also attached to most movable objects such as robots, vehicles and animals (Gekas, 2012; Lane et al., 2010; Xiuchao, Kenneth, & Cormac, 2014). Most of the modern communication devices can be programmed (Franklin, Kossmann, Kraska, S. Ramesh, & Xin, 2011; Lane et al., 2010) and are coming up with advanced categories of cheap and powerful embedded sensors (such as an accelerometer, digital compass, GPS, microphone, and cameras) which are now making it possible for the emergence of personal, group, and society-level sensing applications (Abbasi, 2010; Chengjin LI, 2012; Franklin, Kossmann, Kraska, S. Ramesh, & Xin, 2011; Goodchild, 2006). Sensor-equipped mobile phones have revolutionized many sectors of the economy, including business, healthcare, social networks, environmental monitoring and prediction (Kuhn, 2007; Lane et al., 2010; Mccall, Martinez, & Verplanke, 2013; Sunny, Mike, Bing, & Daying, 2012). In the application of mobile sensing technology the technical limitations are mostly encountered when performing resource-sensitive reasoning with noisy data (Abbasi, 2010; Habibi & Popescu-Belis, 2014; Hoefler, Schneider, & Lumsdaine, 2010; Kuo & Hsu, 2010; Yuen, King, & Leung, 2011). The use of information-sensing networks can facilitate effective data gathering by providing an efficient and continuous collaborated flow of information (Massung, Coyle, Cater, Jay, & Preist, 2013; Pipek, Landgren, & Palen, 2012; Preist, Massung, & Coyle, 2014; Xiuchao, Kenneth, & Cormac, 2014).

2.6.3 Strategies in Weather Forecast Verification

With sufficient pairs of actual data and weather forecasts a variety of statistical confirmation techniques can be applied to verify forecasts (Lo & Pielke, 2008). The key in verification is to test the accuracy of predictions against the ground truth (Ahmad K, 2012; Messenger & Faure, 2012; Stern & Easterling, 1999). Forecast skill verification can either be objective – statistical comparison of forecast and observed values with no human interpretation; or subjective – involve human verification of forecasts and observations (World-Meteorological-Organization, 2000).

Different choices of methods (such as using spatial verification plots, the summary of measures, forecast skill scores and diagnostic techniques) are used for forecast verification (Casati et al., 2008; Maini, 2008; Mariani & Casaioli, 2008). Uncertainty in making forecasts is a major issue in forecast verification models (Bougeault, 2003; Djam, 2013; Stern & Easterling, 1999) calling for adequate manual verification by human experts for quality checks (Uygar & Stacy, 2004). The process of forecast verification follows a sequence of steps including: gathering actual observations; choice of strategies to use in verification; the aggregation of results pairs; choice of appropriate statistics for summarizing verifications; and interpretation of the statistical significance of the skill scores (Bougeault, 2003). The choice of strategies relies on the type and quality of actual observations, which can be estimates containing information in varying time and space scales.

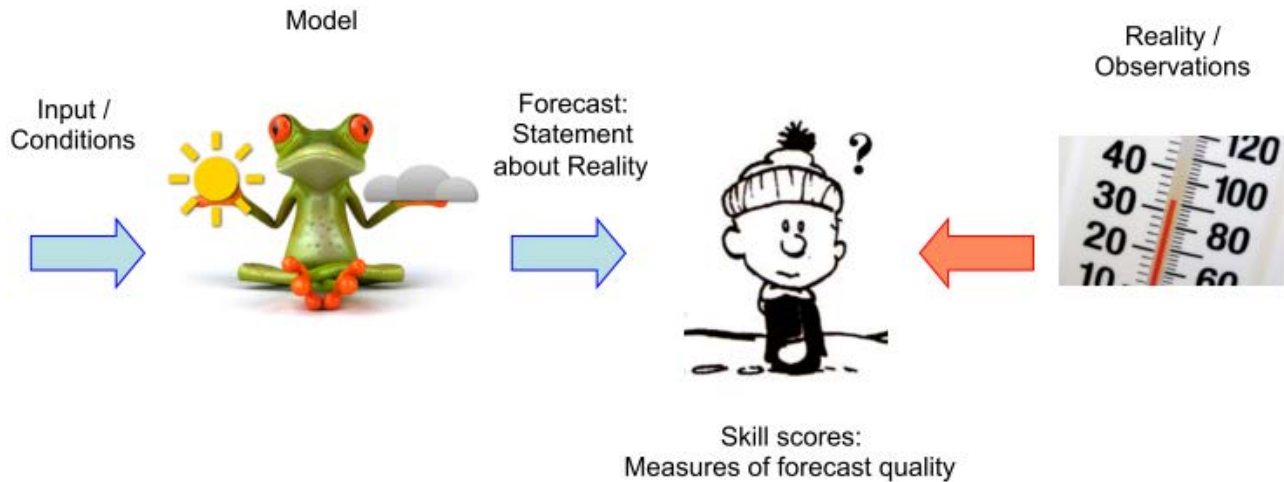


Figure 2-12: Forecast Skill Scores as Measure of Forecasts Quality (Source: Christoph Frei, 2014)

With a series of weather forecasts and actual observations in duration of times, metrics such as Mean Error (ME) and Root Mean Squared Error (RMSE) can be employed to evaluate the accuracy of weather forecasts against ground truth (Atger, 2001; Chai & Draxler, 2014). The ME highlights the biases in forecast models while the RSME evaluates the overall accuracy of forecasts (Ahmad K, 2012; Atger, 2001; Mailier, Jolliffe, & S. David, 2006).

Given forecast, F , and observations, O , in a time frame $i = 1 : n$, then the error margin, e_i , can be calculated as $e_i = F_i - O_i$. The values of ME and RSME can be calculated using the following equations.

$$ME = \frac{1}{n} \sum_{i=1}^n |e_i| \dots \dots \dots \text{Equation 2-2}$$

$$RMSE = \sqrt{\frac{1}{n} \sum_{i=1}^n |e_i|^2} \dots \dots \dots \text{Equation 2-3}$$

Qualitative forecasts (for instance, “likely to have moderate winds”) are difficult to verify since they can be interpreted differently by forecast users and researchers (Mailier, Jolliffe, & S. David, 2006). These non-quantitative forecasts can be made definite by introducing thresholds (for instance, “likely to have moderate winds” can be defined as having probability not exceeding 0.5 or a categorical value). To verify descriptive forecasts suitable strategies can be

employed depending on the definitions. In fuzzy cognitive mapping models domain experts as well as cross-validation strategies have been combined and used as a verification method (Djam, 2013; 2010; Pang, 2013).

Chapter Three: Research Methodology

3.1 Introduction

This chapter presents the procedures undertaken and techniques used for verification of visual weather lore. The main aim of this chapter is to explain the methodologies and how they have been applied. First are the methods for preliminary studies and understanding of the weather lore domain. The research design and specific methodologies used to examine the application of visual weather lore by traditional communities for predicting weather outcomes are then discussed. The use of case study methods to determine if some causal effects exist between metrological and visual weather lore is also highlighted. This is followed by the methods for analyzing case study results to come up with combined knowledge representations in the form of fuzzy cognitive maps. Finally, the methods used for implementing the software model for experimenting visual weather lore verification using a mixture of techniques and metrics are discussed.

The procedures used in this research are organized into seven sections: section 3.1 introduces this chapter and highlights the sections and methodologies used in this research; section 3.2 provides a description of the research design; section 3.3 describes the case study method as applied in understanding the visual weather lore domain; section 3.4 describes the procedures and methods in developing a visual weather lore verification tool; section 3.5 describes the experiments and tests of methods for predicting weather outcomes using visual weather lore; section 3.6 describes the procedures for verification of predicted weather outcomes; finally section 3.7 describes the procedures used in evaluating the objectives of this research.

The case study research process was qualitative, with its major interest being to inquire into the experience of individual humans and how they comprehend the subjective phenomenon of complex weather prediction in a traditional context. The case study method focused on understanding the deliberate behaviours and actions of humans as they shared their experience of visual weather phenomenon.

The following are definition of some of the terms used in this research:

Case study:– in this research a case study is an in-depth study of an event in a selected area using selected individuals

Data analysis – the interrogation of acquired data to come up with summaries and trends in the study variables

Ethics – the standards held to guard the research participants from risks and exploitation

Structured interview – a set of predefined questions to guide the researcher and respondents in the answering of questions

Judgmental sampling (also called purposive sampling) – the use of prior knowledge to select respondents to research questions

Open-ended questions: questions to which respondents are free to give their own responses

Pilot/Pre-test study – a trial study to gauge the adequacy of research tools and redefine questionnaires

Population – the set of all people in the communities' studies

Qualitative research – research focusing on descriptive data and responses

Quantitative research – research focusing on number of responses

Questionnaire – a set of questions to aid respondents in providing answer to questions

Reliability – the ability to replicate consistent results when used in different case studies

Research design – a plan for conducting research

Sample – a subset of a population

Validity – the degree of a result to reflect the meaning of a tested variable

3.2 Research Design

This research is based on mixed research design (Duan & Hoagwood, 2013) where both qualitative and quantitative techniques were combined to suit specific objectives of this research. The qualitative approach (Nakashima & McLean, 2012) was noteworthy in investigating human understanding and use of visual weather lore for weather prediction. The quantitative methods (Ahmad K, 2012) were substantial in investigating means of representing visual weather lore knowledge and applying the knowledge to predict weather outcomes.

3.2.1 Data Sources

There is limited documented information on weather lore validation. In addition, the weather lore concept is complicated (Mwagha & Masinde, 2015) to explain analytically. Thus, most of the literature reviewed in this research (refer to Chapter Two) are focussed mainly on the available weather lore, fuzzy cognitive mapping, weather sensing, visual recognition processes and forecast verification. This literature review was useful in directing the design of verification methods and platform as well as choice of software tools used. Literature reviewed was also used to enhance and align research objectives to research the methodology.

The sources of data considered for investigating the weather lore domain were both primary (acquired using questionnaire-based interviews and case studies) as well as secondary data through literature review. The scope of this investigation was to identify astronomical (Kunkle & Ristvet, 2013) and meteorological (Ziervogel et al., 2014) aspects as used in the context of traditional weather forecasts (Baliscan, 2001). The intention of acquiring data from both the primary and secondary sources was to extract facts for comparison, scientific validation and preservation of the essential information to integrate into modern weather prediction systems.

3.2.2 Data Collection Techniques

A series of three structured interviews were adopted from (Duan & Hoagwood, 2013; Preist, Massung, & Coyle, 2014) for use in these two phases. The first phase was carried out in a South African community in KwaZulu- Natal while the second phase was carried out both in Kenya (Taita-Taveta) and repeated in South Africa (KwaZulu-Natal).

During the first phase of the interview, sample astronomical and meteorological images were presented to informants for identification and description of associated weather. Phase II interviews involved the capturing of astronomical and meteorological images, identification of the images and description of associated weather. In each of the case study locations, social places were used as venues for interview sessions.

The people interviewed were members of the studied communities. The purposive sampling method (Risiro, Mashoko, Tshuma, & Rurinda, 2012) was used to select 50 respondents (perceived knowledgeable persons) comprising both traditional farmers and herdsmen and local residents. Data was collected with the help of research assistants (university students on vacation and volunteers) from the communities selected with the help of the University (Central University of Technology, Free State – CUT) research supervisor. The research assistants were trained with regard to interpretation of the questionnaire, interviewing guidelines and research ethics. An introductory letter from CUT was used to introduce the researchers.

The collected data was digitized for storing in a computer and for transferring to the main researcher. A spreadsheet was used for easy storage and retrieval of data. For safety and recovery of information, back-up copies of the data were made and stored separately.

Structured interviews (Stern & Easterling, 1999) using questionnaires proved satisfactory to gather qualitative information. The data collection method permitted the respondents enough time and capacity to question their opinions on the visual weather lore domain. The focus points of the interviews were decided by the researcher since there were aspects in the weather lore domain the researcher was interested in exploring (visual astronomical and meteorological). The main objective of using structured interviews was to understand the respondent/s' point of view so that individual opinions about the visual weather lore could be analyzed.

Qualitative research (Duan & Hoagwood, 2013) was used to describe the causal links between visual weather lore and weather outcomes. Quantitative methods were used to establish statistically significant conclusions about the populations in the case study locations by analyzing the collected data from the representative sample of the population.

3.2.4 Sampling Techniques

This research used purposive sampling (Meier, 2011) to target a particular category of respondents. The study targeted respondents in the rural communities of KwaZulu-Natal (South Africa) and Taita-Taveta (Kenya) where farmers and people that rely on weather for their activities were located. The research incorporated other categories of people, such as teachers, since most farmers and herdsmen are difficult to contact during daytime working hours. All categories of adult respondents who were residents in the case study locations were considered no matter of professions.

3.2.5 Data Analysis and Interpretation

The data analysis involved identifying key indicators of causal effects between visual weather lore and weather outcomes (also referred to as ‘concepts’ in this research). These indicators were recorded by scales of magnitude of effects (see Data Collection Instrument in the Appendices section) between the concepts (strong negative, negative, none, positive and strong positive).

The collected data was set up in a Statistical Package for Social Sciences (SPSS) codebook with some scales of semi-informal transformations. In order to derive common knowledge, the data was analyzed using both quantitative (such as percentage or number of respondents) and descriptive statistics (such as mode and mean of categorical responses). The analyzed data was represented as group knowledge (on visual astronomical and meteorological weather concepts and the causal effects on short term weather) using statistical summaries.

The responses for all the respondents in the case study locations were collected, analyzed, and summarized to answer the research questions. The analysis was categorized in terms of the following sections that provided answers to specific research objectives:

- (a) Study area and demographic information of the respondents – the interest at this point was to understand the way of life and economic activities of the people. This was also reflected in the experience and length of stay in the communities;
- (b) Impact of weather on daily activities of the respondents – the interest of this was to determine if weather affects the daily activities of the people in the communities. The

answers to this section provided a clue as to whether or not the communities relied on weather and therefore they used some means of predicting weather;

- (c) Means of forecasting weather as used by respondents – the interest at this point was to determine the frequently used methods of predicting weather outcomes. Since some communities in rural areas do not rely on modern technology, answers to this provided a clue as to whether the people relied on traditional visual weather indicators;
- (d) Respondent/s’ knowledge of visual (meteorological and astronomical) weather indicators – the interest in this was to determine if the people had knowledge of visual (astronomical or meteorological) weather indicators. The knowledge of this indicator provided an indication of whether or not they used visual weather lore to predict weather outcomes;
- (e) Causal links and effects between the visual weather indicators and weather outcomes – the interest of this was to determine if people could recognise links between visual weather indicators and weather outcomes. The analysis results of this section gave a judgement on whether links exist between visual weather indicators and weather outcomes; and
- (f) Identification of weather seasons’ characteristics – the interest at this point was to determine the pattern in weather seasons between the case studies and to come up with a general trend in the weather seasons.

3.2.6 Ethical Considerations

The respondents/participants were informed that the rights of ownership of the information remained with them as the knowledge holders and would be protected. During the interviews, consent were obtained from the respondents through completion of a ‘Consent form’ (see Data Collection Instruments in Appendices section) that identified the specifics of this research including the purpose and how the collected data would be used. The information collected from the respondents is the intellectual property of the knowledge holders and is held in trust by the researcher. The gathered knowledge was reviewed before reporting. The confidentiality and safety of participants was protected; therefore, the informants were allowed to make a voluntary decision about whether to take part in the research.

3.2.7 Pilot Study

Informants from the KwaZulu-Natal province of South Africa were recruited for a pilot study. A test questionnaire was designed (with various visual astronomical and meteorological concepts

identified from literature including weather outcomes and open-ended questions) and administered to respondents from the Zulu community (working at the Central University of Technology, Free State) to provide feedback. The respondents described causal relationships between visual astronomical and meteorological traditional weather concepts (indicators) to expected weather outcomes. The opinions of the Zulu people were considered valuable because they mostly rely on weather outcomes for success of their activities such as early farming and planting. The feedback allowed for the revision of the questions as well as for improving the understandability of the questions. The preliminary questionnaire-based data collection tools are found in the Appendix: Phase 1 Data Collection Instruments.

3.3 Use of Case Studies

The case study methodology (Hammersley, Foster, & Gomm, 2000) was used to recruit informants from KwaZulu-Natal province of South Africa for a pilot study. Since weather affects every person's daily activities, the preliminary study considered the general categories of local people (not only farmers) that include people in formal employment and students. The opinions of local people such as farmers and teachers were considered relevant and valuable. A test questionnaire was designed (various visual astronomical and meteorological concepts identified from literature including weather outcomes with open-ended questions) and administered at the pilot location between the months of March and April 2015. The informants described causal relationships between visual astronomical and meteorological traditional weather concepts (indicators) and expected weather conditions. The preliminary questionnaire-based data collection tools are found in the Appendix: Phase I Data Collection Instruments.

3.3.1 Data Collection Procedures

The second phase of visual weather lore domain understanding consisted of conducting two case studies using restructured questionnaires with a reduced number of concepts. The questionnaires were administered in two locations (KwaZulu-Natal province in South Africa and Taita-Taveta County in Kenya) between the months of May and July 2015. As in the preliminary study, consent forms and guidelines of conducting the interviews were provided in each set of questionnaires (see Appendix: Phase II Data Collection Instruments). The two case studies were conducted by interviewing respondents about how visual astronomical and meteorological weather concepts cause weather outcomes.

3.3.2 Data Analysis Procedures

In each case study the data collected was set up in a codebook with some scales of semi-informal transformations. In order to derive common knowledge, the data was analyzed using both quantitative (percentage of respondents) and descriptive statistics (mean and mode of categorical responses). The analyzed data was represented as group knowledge (on visual astronomical and meteorological weather concepts and the causal effects on short-term weather outcomes) using statistical summaries. The final analysis involved cross-unit comparisons between the case studies followed by overall aggregation and group knowledge representation.

The research of visual weather lore was a complex phenomenon that occurs within some complex weather lore and complex weather phenomena. Case study research (Randall & Wood, 2007) proved significant in empirical inquiries that could investigate contemporary phenomena within some real-life context when the boundaries between phenomena and context are not clearly obvious.

The advantage of the generalization benefit of the case study methodology was considered to employ its purposive sampling technique to recruit representatives from the selected communities. Selected members from the representative communities were asked to gain insights into the communities' perceptions of weather lore. The representatives were also instrumental in describing weather lore (in the form of Fuzzy Cognitive Mapping) based on weather images and conditions respective to their geographic locations. After the case studies, weather lore representations from individual respondents' beliefs were aggregated to FCMs representing group knowledge.

Since weather affects every person's daily activities (Enock, 2013), the case study considered the general categories of local people (not just farmers), people in formal employment, students among others (this was aimed at countering the challenges of contacting the informal categories of people such as herders). Conducting two case studies was preferred so that the results attained from one case could be confirmed with the other case study. The two case studies also permitted replication of data collection and analysis procedures so that results could be confirmed. The replication allowed the research to draw a more general picture of the visual weather lore domain before coming up with aggregate visual weather lore-based knowledge representations.

The case study method was suitable since there was little knowledge in the weather lore domain and specifically in the context of how it is applied for weather prediction in developing countries. In this research, it was envisaged that similar trends in the use of visual weather lore would be given by the majority of respondents. Some previous researchers (Meier, 2011; Ziervogel et al., 2014) have used multiple case studies approaches to confirm or contradict commonalities between research outcomes.

The use of the case studies approach also provided an opportunity for detailed information exploration on the visual weather lore domain. The looser format of case studies allowed the interview process to begin with general questions and then narrowed the focus to more specific aspects of the weather lore domain. To reduce bias during the case studies, this research used pilot interview (test) to come up with preliminary results.

3.4 Solution Design Process

An integrated design for validation of visual weather lore was developed using Unified Modelling Language (UML) tools (Kennedy, 2010). The design integrated together weather sensors for real-time weather data gathering, fuzzy cognitive maps for weather lore mapping, computer vision for detecting visual weather concepts from sky scenes, and verification procedures for checking concurrences between visual weather lore-based predicted weather outcomes to actual weather observations.

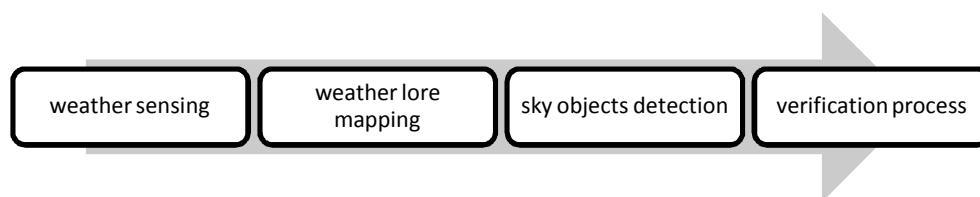


Figure 3-1: Soutlion Design Process

3.4.1 Seasonal Knowledge Representation

A fuzzy cognitive mapping (FCM)-based prediction scenario process consisting of six steps (described in section 2.4), was used. This process has been used by previous researchers to come up with fuzzy cognitive maps-based scenario prediction systems (Jetter, 2011).

The first FCM step was the clarification of information requirements (Jones, 2010). This step was achieved by using the literature review together with preliminary studies that were aimed at understanding the visual weather lore domain. In this step, the scope of the visual weather lore domain to be investigated was defined. The second step was to define a plan for gathering relevant weather lore-related information. This step allowed the identification of the sources of visual weather lore knowledge as well as selection of appropriate methods for gathering visual weather lore knowledge. The third step involved gathering of knowledge that was achieved through two case studies. In this step, the final output was data that was organized with causal relations between visual weather lore and weather outcomes. In the fourth step conceptual seasonal fuzzy cognitive maps were designed. The fifth step was the design of detailed fuzzy cognitive maps that had represented weather lore causal effects between the combined case studies. In this step the selection of input variables and functions for fuzzy cognitive maps were designated. The final step involved testing the fuzzy cognitive maps, interpretation of resulting predicted weather outcomes (outputs) as well as validation of the resultant outcomes.

First a plan for information gathering was realized by identifying relevant information target sources such farmers, herdsman, teachers, students, and published research, as well as the means by which the knowledge should be captured. The researcher used preliminary studies and personal discussions with the supervisor at CUT, Free State, as well as the analysis of sources of indigenous knowledge publications. The sources of weather lore information and gathering techniques were chosen with considerations of balancing the domain and human bias as well as circumventing cognitive limitations of respondents from the different case study locations.

In the second step, two case two studies were conducted. The questionnaires (see Appendix: Data Collection Tools) were split into three separate sections to acquire substantial information from the individual respondents. In the first section the knowledge of weather lore of the participant was sought using well-known visual weather lore concepts. This was to enable the respondents to understand the requirements of the study and to prepare for the next section. The second section gauged the participants' use of visual weather lore during their daily activities. This was to stimulate the participants' minds to recognize any possible visual weather scenarios that can lead to weather outcomes. The final section anticipated capturing relationships between visual weather objects and weather outcomes. Various scales of magnitude such as strong, very

strong and none were used to capture categorical responses. The magnitudes of relationships provided by the participants were aimed at representing the interaction between the visual weather concepts (visual weather cognitive maps). This process was repeated for each of the four weather seasons.

The knowledge from individual respondents was coded in a common spreadsheet for analysis. The analysis aimed at coming up with common representations of the interactions between visual weather objects and for each of the weather seasons.

The causal links between visual weather concepts were investigated using the combined case studies in which results were aggregated to build up common knowledge (Strickert, Samarasinghe, & Davies, 2009). The joint averages of the majority of responses from the case studies were determined for each set of interacting concepts. The results of statistical knowledge were used to formally represent seasonal weather knowledge using fuzzy cognitive maps in the form of connection matrices (Din & Cretan, 2014).

In step three the represented knowledge was investigated for consistency. Some of the relationships which proved to be biased were eliminated and other causal links streamlined using knowledge trends from the four weather seasons. The dynamics of the represented knowledge were investigated (Rangarajan et al., 2012), so as to understand the significance of visual weather concepts with high dynamics.

In step four simulation input was used to investigate scenarios in the different weather seasons with different combination of input states (Papageorgiou, 2008). The aim was to investigate the combination of inputs which can produce the desired state (Steven et al., 2015) of predicted weather outcomes.

In step five the simulation scenarios' results (Sperry & Jetter, 2012) were used to refine the causal strengths in the seasonal fuzzy cognitive maps so as to represent the knowledge better to realize optimal outputs.

Additional knowledge from literature and discussions with the research supervisor was used for modification of the represented seasonal fuzzy cognitive maps. This was to take care of possible weather scenarios that were not factored during the prior investigations.

3.4.2 Recognition of Sky Objects

Image scenes were acquired from the field using an all-weather sky camera on a daily basis. The cameras accumulated this data for use in the image pre-processing (Pandit, Kolhar, & Patil, 2015) and sky object recognition tasks (Dagher, Sallak, & Hazim, 2014).

The different techniques used for objects detection in images have been discussed in the literature review section. The sky objects detection process was exploited on the colour, texture and the shape characteristics of visual sky objects. In this research experiments were made to uncover the best feature that can represent sky objects. The feature type selection was achieved through representing the target sky objects using shape and texture followed by cross technique comparisons. The features of the visual objects are illustrated, as well as the pre-processing tasks crucial for detection process.

After the sky objects were identified using the right techniques, the identified features were exploited by detectors that filtered them for false detections and extracted detected visual objects. Detection of objects was carried out using vision cascade classifiers (Xinggang Wang, Feng, Bai, W. Liu, & Jan, 2014) and a benchmark function that determined the similarity between the extracted sky objects and corresponding ground truths.

Detection of sky objects using Histogram of Oriented Gradients/Linear Binary Patterns classifiers and performance results are presented. The performances of the detectors were tested under three different sets of conditions using massive data sets and results are presented. Lastly the presentation of tests and results in the benchmark process which computes scores of detected visual objects in reference to some ground truth (otherwise referred to as ideal visual sky objects in some sections of this research). The results from the benchmark process were transformed to visual sky concepts.

Image sets representing visual weather concept were extracted from a collection of known images to label positive training samples (Olaode, Naghdy, & Todd, 2014; Xudong, Bappaditya, & Alex, 2009). Using positive samples the finest actual images of objects were then extracted and specified as base (ideal object). Samples of negative images were also extracted and specified as negative image training sets.

Regions of interest (Feifei, Lijian, & Zhe-ming, 2015; Sindhu, 2015) that define visual objects (Feifei, Lijian, & Zhe-ming, 2015; Sindhu, 2015) were delineated from the sets of positive samples. For each set of positive samples a corresponding set was specified with negative samples consisting of scenes with different objects to the object concept.

An input sky scene was subjected to a processing component where consecutive detectors recognize objects representing the various concepts. The output from this process was a set of extracted objects corresponding to the various sky concepts.

The process of checking similarity between extracted and ideal objects involved computing the distance between the compared objects (Mohamed, Heshmat, Girgis, & Elaw, 2013; Sridhar, 2012). Similar objects had a minimal distance, while the distance increases as the objects increasingly becomes wider. This process was vital to supplement the object detection procedure in the eventuality of false positives (Neiting & Aftery, 2007). The set of similarity scores was used to compute the vector that represented the detected sky objects.

The visual sky objects were transformed to a form suitable for verification. Appropriate tools for data transformation were implemented to handle errors and incompatibilities. All transformed weather concepts were logged in the form of input vector representing the sky weather concepts.

3.4.3 Weather Outcomes Prediction

A fuzzy cognitive mapping middleware was integrated into the weather lore verification tool for mapping detected visual weather concepts to weather outcomes. The learning algorithms (Papageorgiou & Salmeron, 2014) and procedures in the FCM middleware were tested before integration. An incremental prototyping approach was used as continually check the suitability and appropriateness of techniques implemented.

The numbers of nodes (Najafi, 2011) in the FCM process (or concepts) were determined dynamically by computing the size of the input concept vector. The weights (causal relationships between concepts) were represented in adjacency matrices distinguished by the four weather seasons (summer, autumn, winter and spring). The numeric values represented in seasonal matrices varied corresponding to the strengths of relationship between the concepts in the

different seasons. During simulation runs the weights were resolved from the specific seasons by determining numeric data in the matrices.

The seasons were represented such that each of the seasons S_i had previous and next seasons represented as S_{i-1} , and S_{i+1} respectively. The onset and cessation of seasons had timing characteristics of early or late, while the season progress was specified as either continuous or interrupted. To mimic the circular and overlapping nature of the weather seasons (such as the onset/cessation timing and progress) and weather season selection procedure was employed.

Simulations were run for the state of input concepts (c_i^k) by computing new concepts (c_i^{k+1}) using the seasonal knowledge represented in adjacency matrices (Din & Cretan, 2014). The input to a simulation run was a vector of n concepts determined using information from the object detector component. An activation function (Cai, 2011; Uygur & Stacy, 2004) was used in predicting the new state of concepts.

To restrict the concepts' values to be in the interval $[0, 1]$ a transformation function (Chrysafiadi & Virvou, 2013) was applied per iteration. This transformation function generated concepts values in the range $0 \leq c(i) \leq 1$ with a prospect that the maximum likelihood was positive but infinitely small (for instance 0.4×10^{-70}). Alleviation of this prospect was achieved using a min-max normalization (Luo, 2010; Najafi, 2011; Xirogiannis & Glykas, 2004) function that scaled the predictions in the range $[0, 1]$.

Appropriate statistical learning (Rahat, Cécile, Damien, & Ducottet, 2015) tools were employed to discover patterns between fuzzy cognitive map predictions during iterations. An iterative learning (Karagiannis & Groumpos, 2013; Rangarajan et al., 2012) process was implemented via a transformation function. The purpose was to update the strengths of causal links in the season connection matrix before it was used in the next concept activation (Stylios, Georgopoulos, & Manis, 2013) iteration. This function also ensured that the strengths of causal links were confined within the range $[-1, 1]$ prior to activation of new concepts states. The learning function also removed self loops (Obiedat, 1994) to ascertain that a concept could not have a causal effect on itself.

On the final run of a simulation process the output was generated in the form of a vector (Mago et al., 2013) consisting of selected values of predicted weather outcomes. These values were in the range $[0, 1]$ representing the expectation (probability) of the weather outcomes. The predicted weather outcomes formed the main input to the (prediction against observation) verification process.

The predicted weather outcomes were visualized using bar charts to depict the variation of the expected weather outcomes. The new causal effects between the concepts were also visualized using a network graph (H. Singh, G. Singh, & Bhatia, 2013) depicting the new relations and strengths of causal effects between the concepts. Since the predicted weather outcomes were in probability values $[0, 1]$, a transformation function was used to convert these probability values into human understandable form (linguistic terms (Papageorgiou & Salmeron, 2014) describing the likeliness of the predicted weather outcomes). The strongest outcome was also described as the major outcome (in order of the magnitudes of the strongest outcomes).

3.4.4 Weather-sensing Platform

A wireless weather-sensing platform with real-time sensor nodes was integrated to gather weather parameters and conditions in Bloemfontein, Free State. The data was transmitted through wireless transmission protocols (Lane et al., 2010) to the base station. To build up sufficient data for evaluation of the predictions the automated (using wireless sensor nodes) weather station in the field logged periodic actual weather observations.

3.4.5 Image Data Gathering

Weather images (daily sky scenes) were gathered in real time through sky cameras at the test locations. The images were logged by date and geographic position (GPS) (Laliberte & Rango, 2011) for concurrence with the weather sensor data. Data gathering was done incrementally and on daily basis to guarantee a sufficient data set for the experimentation procedures.

3.5 Experimentation Process

Daily system simulations were run using the implemented tool to predict and record probabilities of weather outcomes (rain, heat index/hotness, dry, cold index). Weather observations were captured periodically by use of a wireless weather station. The weather logging process was

repeated daily (for periods extending more than a month) until there was sufficient data to use for in the verification process. The actual weather observations data sets (weather measurements) were transformed to categorical values [0, 1] to match with the range of the predicted weather outcomes (Nurmi, 2003; Stanski, L. Wilson, & Burrows, 1871).

3.6 Verification Procedure

In the verification process comparisons were made between the actual observations and weather outcome predictions, values by computing residuals (error values) from the observations. The error values and the squared error were used to compute the (MSE) Mean Squared Error and the (RMSE) Root Mean Squared Error forecast skill scores for each predicted weather outcome (Casati et al., 2008; Shrestha, Robertson, J.Wang, Pagano, & Hapuarachchi, 2013). Contingency tables (Hamill, 2006) were computed to determine prediction rates and Threat Scores.

3.7 Evaluation Procedures

The integrated tool for visual weather lore verification was tested with independent data acquired from a selected location (in CUT, Free State, South Africa).

The validity of the visual weather lore verification model was assessed using actual experiments and data from the second case study location (Taita-Taveta County of Kenya). This data was organized in the form of daily sky scenes and weather parameters acquired from Voi meteorological weather station, during the month of December 2015.

To evaluate the methods used in this research, relationships between visual weather lore (expected weather) to logged weather images and actual weather data were analyzed using appropriate forecast skills (Hamill, 2006). Validation tests were performed in Kenya to estimate performance of the visual weather lore verification tool. In order to benchmark the weather lore verification tool using fuzzy cognitive maps based on symbolic image classifiers, comparative analyses (Randall & Wood, 2007) of accuracies were made with some modern weather validation techniques.

Chapter Four: Weather Lore Investigation and Verification Tool Design

4.1 Introduction

This chapter presents the results for investigation of knowledge in the visual weather lore domain followed by a description of a visual weather lore verification tool. The preliminary task was to recognize the visual weather lore domain through statistical analysis of interview responses concerning traditional knowledge of visual weather aspects. Upon understanding of the domain, the next step was to formulate the definition of requirements, outputs and definition of mathematical logic that entail the visual weather lore verification tool. The investigation and planning procedures followed a sequence of sub-tasks (a) to (e), as depicted in Figure 4-1 and described in subsequent sections.

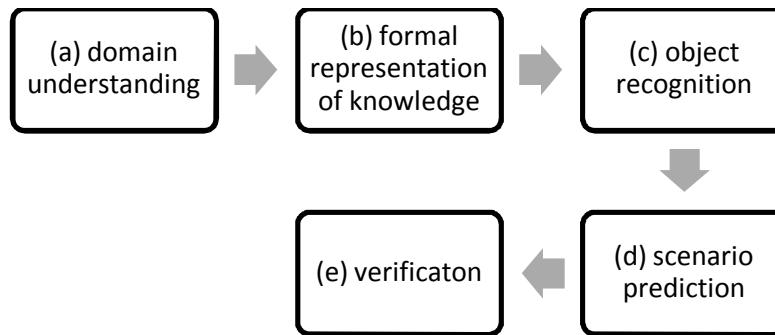


Figure 4-1 Analysis and Design Procedure

4.2 Identification of Concepts and their Relations in the Visual Weather Lore Domain

An endorsement from literature shows that, since time immemorial, people have been interacting with the natural environment, and with experience they have developed some sense on predicting weather changes in their surroundings (Fishman & Amico, 1994; Mwangi, Wetterhall, Dutra, Giuseppe, & Pappenberger, 2014; Nakashima & McLean, 2012). The traditional predictions have been applied in lifestyles such as deciding on farming schedules in the course of the seasons (Hornidge & Antweiler, 2012; Kidd, 1984). With interference from climate change and other factors such as population growth and urbanization, the interactions between humans and environment have been reducing (Abdulrashid, 2013; Enock, 2013; Owiny & Marezki, 2014). This has contributed to the erosion of important knowledge being witnessed today, hence the uncertainty of events dependent on weather outcomes. Weather patterns are complex and arise

from multiple weather concepts that dynamically interact with each other within an uncertain environment (Calbo & Sabburg, 2008; Narasimhan & Nayar, 2002). In order to understand the characteristics of the weather concepts, it is necessary to apply computational techniques that mimic human senses and decision-making (Chiwanza, Musingafi, & Mupa, 2013; Enock, 2013; Zuma-netshiukhwi, Stigter, & Walker, 2013). This calls for the identification of relevant human knowledge and understanding of how the complex weather concepts interact. Once understood, these processes can be validated (Acharya, 2011a; Shoko, 2012) and integrated with models that simulate weather phenomenon.

4.2.1 The Aim and Scope of Visual Weather Lore Investigations

This research is aimed at understanding the relations between visual weather concepts and examining their computational applicability in mimicking human sense and decision making. To achieve this objective, this research investigated the most significant weather concepts that humans exploit for decision-making in the process of planning for their daily activities. Given that effects of weather outcomes vary from one group of people (such as farmers and rural inhabitants) to another, information sought was locality-specific (KwaZulu-Natal in South Africa and Taita in Kenya). The scope of this study was limited to the identification of visual astronomical and meteorological weather aspects as applied in traditional ways of weather forecasting. A comparative case study method was used, followed by aggregation of seasonal knowledge from the two case study areas.

To hasten the domain understanding process, local research assistants were employed to relay information about the research and identify questionnaire respondents. The informants were informed that the right of ownership of the information collected from them is held in trust by the researcher. The informants completed consent forms (see Consent Form in Appendix: Phase I Data Collection Instruments) that identified the specifics of this ,including the purpose and the use of the resulting knowledge. The informants participated in the interview voluntarily and had power to decide to withdraw or not to answer parts of research questions.

4.2.2 Range of Visual Weather Lore Knowledge

This study considered visual weather lore aspects from the world perspective; for this, literature was reviewed to gain insights into the global perceptions of weather lore. A wide variety of

visual astronomical and meteorological weather indicators were identified from literature (Mwagha & Masinde, 2015) and considered for further investigation (Table 4—1).

Table 4—1: Collection of Visual Weather Indicators

Object	Indicators
Cloud colour	White; grey
Cloud types	altocumulus; altostratus; cirrocumulus; cirrostratus; cirrus; cumulonimbus; stratocumulus; stratus
Cloud shape	cauliflower; towers
Cloud patterns	feathery; layered; rippled; uniform; filaments
Cloud levels	low; medium; high
Sun	halo around
Stars	dull; twinkle; filled; few
Moon phase	new; full; dark; transition; halo around
Night sky	clear; dark; red
Lightning	high; low
Rainbow	morning; evening

4.2.3 Identification of Visual Astronomical and Meteorological Weather Lore Concepts

The respondent(s) were asked to state their perceptions on the degree of causal effect (strong positive, positive, none, negative and strong negative) of astronomical and meteorological indicators to weather outcomes (rain, dry, hot, cold, calm, windy and cloudy). The results were organized in a summary (Table A—1) derived by grouping of the responses.

4.2.4 Reduction of the Identified Visual Weather Concepts

Based on clouds patterns, colour and shape characteristics, the following cloud characteristics were linked to specific cloud types: cirrus, cirrostratus, cirrocumulus, high clouds, low clouds, medium clouds, blue clouds, brown clouds, cauliflower clouds, feathery clouds, filaments clouds, grey clouds, layered clouds, nimbus, red clouds, rippled clouds, tower clouds, uniform clouds and white clouds.

Using knowledge of associations and characteristics of clouds, the clouds concepts were re-grouped according to levels. For instance, high clouds consisted of cirrus, cirrostratus and cirrocumulus clouds which were characterized by being white and taking the shapes of feathers, filaments or hair. The high clouds appeared yellow or red at sunset. The regroupings of major cloud levels with associations to type and characteristics is shown in Table 4—2 below.

Table 4—2: Grouping of Clouds by levels

Cloud Group	Cloud Type	Characteristics
High clouds	Cirrus	feathery, white, filaments, hair-like, yellow/red at sunset/-rise
	Cirrostratus	creates halo around sun/moon, white, can cover all sky, hair-like, smooth
	Cirrocumulus	clusters of small round white patches, ripples/grains,
Middle clouds	Altostratus	grey/bluish cloud sheets, thin so can reveal sun
	Alto cumulus	white/grey patches, rounded masses or rolls
Low and Vertical clouds	Stratus	a fog not far from ground, grey cloud layer, a uniform base
	Stratocumulus	layered, grey or whitish patch, honeycomb appearance, rounded masses or rolls
	Nimbostratus	dark rainclouds, covers sky, blocks sun, grey, continuous raincloud, results from thickening altostratus
	Cumulus	fair weather, cauliflower, detached, rising mounds, domes or towers
	Cumulonimbus	brings and goes with rain, thunderstorm cloud, mountain or huge tower

Using knowledge of concept associations, the initial concepts were condensed by clustering similar and restating opposing concepts leading to a fewer number of concepts. The notion of condensing the concepts was necessitated by uncertainty in the occurrence of concepts, meaning that some concepts could override (such as occurrence of the different cloud types) and inherit characteristics of other concepts. The clouds concepts were reduced to high, medium and low level clouds respectively. The dark sky and clear sky were considered to be opposing each other; by identifying one concept, the other could be determined as the converse. Twinkling and many stars were combined to represent one concept, while dull and few stars were combined to come up with a new concept. Similarly, the twinkling/many and dull/few stars were determined as stars; hence, by identifying one the other is determined as the converse. The rainbows occurring

at any time of the day were reduced to represent a single concept. The concepts relating to lightning (much and less) were taken to represent a single concept. Due to the fact that changes in weather outcomes occur mostly between the full/visible to dark moon transitions, the concepts dark moon, full moon, decreasing moon, increasing moon and new moon were condensed to two concepts: full/visible moon and partial/dark moon. The weather outcomes were reduced to only four concepts (rain, hot, cold and dry) which proved significant to the daily activities of humans. The concepts cloudy and clear skies were considered redundant since they represented opposing characteristics, while the concepts of windy and calm were considered having non-visual characteristics. The final list of interacting concepts were determined as: high clouds; low clouds; medium clouds; clear sky; many stars; rainbow; lightning; partial/dark moon; full/visible moon; rain; dry; hot; and cold

4.3 Causal Effects of Visual Astronomical & Meteorological Concepts

4.3.1 Case One: KwaZulu-Natal Province of South Africa

4.3.3.1 Description of the Study Area

KwaZulu-Natal (see map in Figure 4-2 and Figure 4-3) is South Africa's third-smallest province with a total area of 94361 square kilometres and taking up 7.7% of South Africa's land area (South Africa Statistics, 2015). The province has the second-largest population in South Africa (with 10.3 million people in 2015). Climate in the coastal areas of KwaZulu-Natal is subtropical, with summer temperatures rising to over 30 °C. KwaZulu-Natal gets the most rain (over 1 000mm a year) in South Africa, which occurs between the months of October and April and mostly during the summer months of December to February in which thunderstorms can occur almost every afternoon. During winter seasons, the temperatures are usually mild to warm (average over 20 °C) and the probability of raining is low. KwaZulu-Natal has fertile soils, making agriculture the major economic activity.



Figure 4-2: Location of KwaZulu-Natal in South Africa



Figure 4-3: Data Collection Points at KwaZulu-Natal

Note: The data collection points selected are represented by the triangles. The selection of the locations was based on the research assistants' familiarity with the places.

4.3.2 Demographics of Respondents

A sample of 51 respondents consisting of 60% females and 40% males was drawn using purposive sampling (Duan & Hoagwood, 2013) from the villages of KwaZulu-Natal province of South Africa. The majority of the respondents were middle-aged, with 56% over 35 years of age while 40% were aged between 18 and 35 years. Most of the respondents were educated: 75% had a minimum of secondary education with a third of these having post-secondary qualifications. Two-thirds of the respondent(s) were working class, of which 28% were self-employed and, interestingly, 37% seeking academic qualifications in either secondary schools or universities. The main economic activity in the province is farming, represented by 76% of the respondents,

while some people do business and mining, as indicated by the remaining respondents. Most of the respondents have lived in KwaZulu-Natal a long time, with 75% indicating that they had stayed for over five years, of which over 50% have lived there for over 20 years.

4.3.3 Significance of Weather on Daily Activities

The respondents were asked to provide their opinion on how weather affects their daily activities: 58% of them stated that weather sometimes affected their activities; against 33% who indicated that weather often affected their activities. Of the total number of the respondents, only 5% stated that weather rarely affected their activities, while the rest (1%) said weather did not affect their daily activities. The majority (51%) of the respondents indicated that they often checked for weather forecasts while 41% stated they sometimes checked for the forecasts. The rest (8%) stated that they rarely checked for weather forecasts. The respondents indicated that they were interested in daily (52%), seasonal (29%) and fortnight (15%), weather forecasts respectively; 55% of the respondents stated that they got their weather forecasts from the radio, while 39% indicated that they relied on traditional weather forecasts. About 4% of the respondents got their weather forecasts from the newspapers and the internet. The respondents showed some confidence in their methods of weather forecasts as 49% indicated that they had some confidence in the forecasts, 21% having great confidence and 29% having little confidence in the accuracy of the forecasts.

The results reveal that traditional people (over 50%) still rely on weather information to plan for their daily activities (such as farming). The communities show some confidence (over 50%) in the methods and forecasts that they make using the various methods.

4.3.4 Knowledge of Meteorological and Astronomical Weather Indicators

The respondents were asked to state their knowledge and significance of the visual weather indicators. Of these, 51.7% stated that they knew some astronomical or meteorological weather indicators, 40% indicated that they knew only a few indicators, while 8.3% of the respondents stated that they knew a substantial number of the indicators. When asked to indicate the indicators they knew best, 63.3% of the respondents selected both sun and clouds as indicators, 73.3% knew stars, 70% rainbows, 93.3% clouds, and 90% lightning. When asked if the indicators assisted them in predicting weather, 51.7% of them indicated that very often the

indicators help them predict weather, 45% stated that sometimes the indicators are useful, while the rest stated that the indicators were not useful in predicting weather.

4.3.5 Characteristics of Weather Seasons in KwaZulu-Natal Province of South Africa

The respondent(s) were asked to state the local names (in isiZulu, the language mostly spoken by the communities living in KZN) of weather seasons, times and the corresponding signals of onset and cessation as well as if the seasons were interruptible. The summer season (October to February) is locally known as *ihlobo*. Autumn, locally known as *intwasabusika*, is the long rainy season that occurs from March to May. The cold season (winter) is locally known as *ubusika* and occurs from May to July. The spring (short rainy season), locally known as *intwasahlo*, occurs from August to October. Table 4—3 summarizes the weather seasons and their characteristics in KwaZulu-Natal.

Table 4—3: Characteristics of Weather Seasons in KwaZulu-Natal

Season	Local name	Onset signs	Cessation signs	Start	End	Season interrupts
Summer	<i>ihlobo</i>	lightning very hot daytime rain	cold winds temperature lowers rain stops	Oct	Feb	Yes
Autumn	<i>intwasabusika</i>	trees shed leaves grass turns colour	very cold	Mar	May	Yes
Winter	<i>ubusika</i>	mists	clear sky in the morning birds build new nests trees look dry	May	July	Yes
Spring	<i>intwasahlo</i>	lot of wind	very hot	Aug	Oct	Yes

4.3.6 Causal Effects of Astronomical and Meteorological Indicators to Weather Outcomes

The respondents were asked to link any causal effects between visual weather concepts and short term weather outcomes. They stated their perceptions on causal effects of astronomical and meteorological indicators to weather outcomes. The percentage of respondents associated with each causal effect, mode and mean were determined for each set of interacting concepts. The results were categorized into the four weather seasons (winter, summer, autumn and spring).

The complete results of statistical analysis of the responses were summarized in Table A—2 to Table A—6.

4.4 Case Two: Taita Taveta County of Kenya

4.4.1 Description of the Study Area

Taita-Taveta County (see Figure 4-4 and Figure 4-5) is an arid and semi-arid (ASAL) county in Kenya covering an area of 17083.9 km². The county lies between 2° 46' north to 4° 10' north and longitudes 37° 36' east to 30°14' east. The altitude of Taita-Taveta varies between 481m above sea level in the lowlands to 2200m above sea level for highlands, giving two distinct climatic characteristics, with the hills experiencing lower temperatures (as low as 18.2°C) compared to the lower zones with an average temperature of 24.6°C (Taita Taveta County Government Profile, 2015). The average temperature in the county is 23°C. The county is divided into highlands zone, dry lowlands zone and some volcanic foothills. The highlands receive high rainfall and are suitable for horticultural farming. The county experiences two rain seasons: the long rains between the months of March and May and the short rains between November and December. The rainfall distribution is uneven in the county, with the highlands receiving higher rainfall than the lowland areas. The major economic activities include ranching and farming (such as maize and sisal growing) (Taita Taveta County Government Profile, 2015).



Figure 4-4: Location of Taita-Taveta County in Kenya

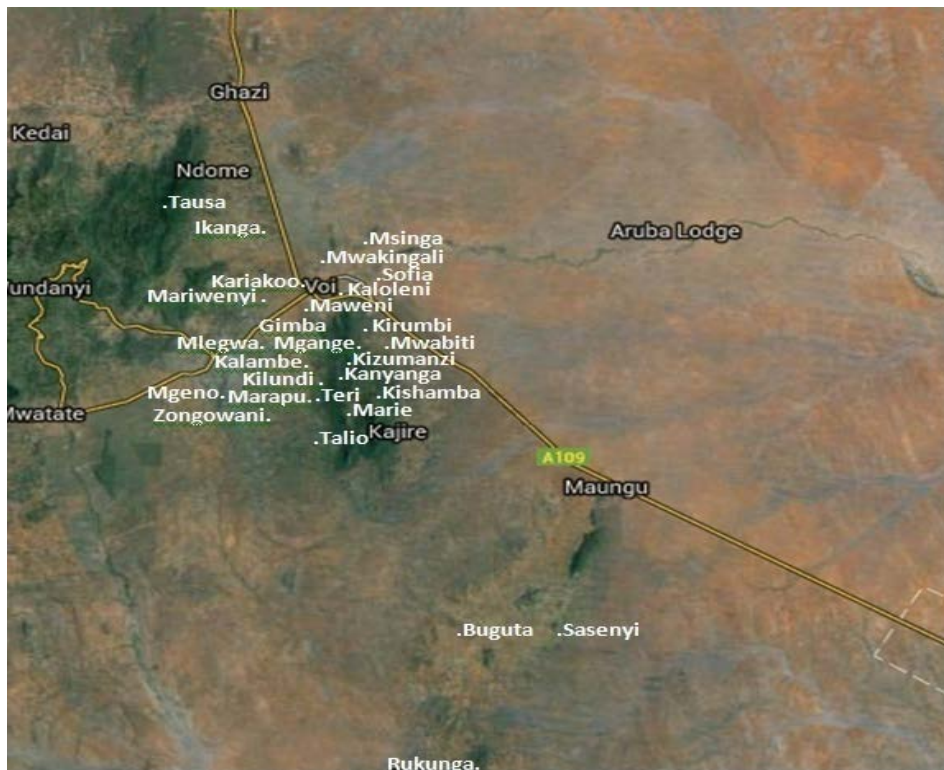


Figure 4-5: Data Collection Points in Taita-Taveta County of Kenya

Note: The data collection points were identified by the named places on the map. The selected locations were identified with major shopping centres in the constituency.

4.4.2 Demographics of Respondents

A sample of respondents comprising 51.7% females and 48.3% males was drawn using purposive sampling (Duan & Hoagwood, 2013). The majority (i.e. 68%) of the respondents were between 46 to 55 years of age while 15% were aged between 36 to 45 years; 6.7% of the respondents were between 56 to 65 years while 8.3% were over 66 years of age. Young people aged 18 to 35 years represented only 1.7% of the sample. More than half (55%) of the respondents had a minimum of secondary education while 22% had primary education; 44% were self-employed and 15% in formal employment. The main economic activity in the constituency is farming (61.7%), followed by cattle keeping (16.7%). Other economic activities are mining (8.3%), sand-harvesting (5%), ranching (3.3%), brick-making (3.3%) and business (1.7%) respectively. Most of the respondents are permanent residents in the county, as indicated by 51.7% staying over 20 years while 41.7% stayed for over 10 years.

4.4.3 Significance of Weather on Daily Activities

The respondents were asked to state the impact of weather on their activities and their preferred forecasts methods: 71.7% of them stated that sometimes weather affects their daily activities, while 28.3% indicated that weather often affects their activities; 53.3% of the respondent(s) indicated that they sometimes check for weather forecasts while 43.3% stated they often check for the forecasts. Only 3.3% of the respondents stated that they rarely check for weather forecasts. The respondents indicated that they were interested in seasonal (56.7%), next two days (41.7%) and next week's (1.7%) weather forecasts respectively. Almost all of the respondents (91.7%) stated that they checked weather by observing the environment.

4.4.4 Knowledge of Meteorological and Astronomical Weather Indicators

The respondents were asked to state their knowledge of visual weather concepts and how it helps in predicting weather: 51.7% of them stated that they knew some astronomical or meteorological weather indicators, 40% indicated that they knew only a few indicators, while 8.3% of the respondents stated that they knew a substantial number of the indicators. When asked to state the

indicators they knew, 63.3% confirmed that they knew both sun and clouds as indicators, 73.3% knew stars, 70% rainbows, 93.3% clouds, and 90% lightning. When asked if the indicators assisted them in predicting weather, 51.7% of the respondents indicated that very often the indicators helped them predict weather, 45% stated that sometimes the indicators were useful, while the rest stated that the indicators were not useful in predicting weather.

4.4.5 The Characteristics Weather Seasons in Taita-Taveta County of Kenya

The respondents were asked to state the local names (in Taita dialects, the language mostly spoken in the county) of weather seasons, occurrence times and the corresponding signals of onset and cessation. The summer season (December to February) is locally known as *kaskazi* or *kiangaza*. The autumn, locally known as *ishika* (name close to isiZulu *one-ubusika*), is the long rain season from March to May. The cold season (winter) is locally known as *mtsuo*, occurring from July to September. There is a hot spell known as *kwalazi* or *kwari* that occurs towards the end of winter (August and September) signifying a transition to the short rain season. The spring (short rains season), locally known as *vuli*, occurs from October to December. Table 4—4 summarizes the weather seasons and their characteristics.

Table 4—4: Characteristics of Weather Seasons in Taita-Taveta, Kenya

Season	Local name	Onset signs	Cessation signs	Start	End	season interrupts
Summer	<i>kaskazi/ kiangaza</i>	Clear day/night Warm evening/night Hot day Wild fires Warm breezes Sky blue Long day hours	grass dry Hot humid Cool nights mosquitoes appear less sun sweating tired of activities	Dec	Feb	Yes
Autumn	<i>ishika</i>	Clouds accumulate Dark evenings Evening rains Temperature drop Trees flower Short days Long nights	Clear day skies Crops stagnant Rains disappear Thick vegetation Temperatures lower Trees lose leaves flowers blossom	Mar	May	Yes
Winter	<i>mtsuo</i> <i>kwalazi / kwari</i>	Bird/bees nesting high Birds migrating Cold evenings Cold mornings Cold nights Cloudy day times Winds Pests move in houses	Warm evenings Warm mornings Warm nights Clouds accumulate Evening winds Clear sky Hot sun	Jun	Sep	Yes
Spring	<i>vuli</i>	Dark nights Evening rain Hot mornings Leaves bud/flowers Hot nights Lightning Migrating butterflies	Baobab fruits ripen Clear sky Grass mature Hot sun Trees yellow leaves	Oct	Dec	Yes

4.4.6 Causal Effects of Astronomical and Meteorological Indicators to Weather Outcomes

The respondents were asked to state their perceptions of causal effects of astronomical and meteorological indicators to weather outcomes. Weather varies significantly during the seasons and depending on the phases of the moon, unexpected weather change might occur during any of the seasons.

Table A—11 depicts the statistical analysis of the responses. The tables present a summary of the percentage of responses for each class of causal effect (strong positive; positive; none, negative and strong negative). The tables show the mean and mode of responses for each set of interacting concepts.

4.4.7 Comparison of Case Studies

4.4.8 Significance of Weather on Daily Activities and Knowledge of Visual Weather Indicators

The analysis of the two case studies indicates that weather has significant effect on human activities. This is depicted by the statistics that the majority of people (58% in South Africa and 71% in Kenya) stating that weather affects their daily activities. The majority of the respondents in both case studies stated that they often checked for weather forecasts. On the knowledge of visual weather indicators most of the respondents in both case studies stated that they knew some visual indicators and that the visual indicators help them to predict weather. The trend of the significance and knowledge of visual weather indicators in the two case studies is depicted in Figure 4-6.

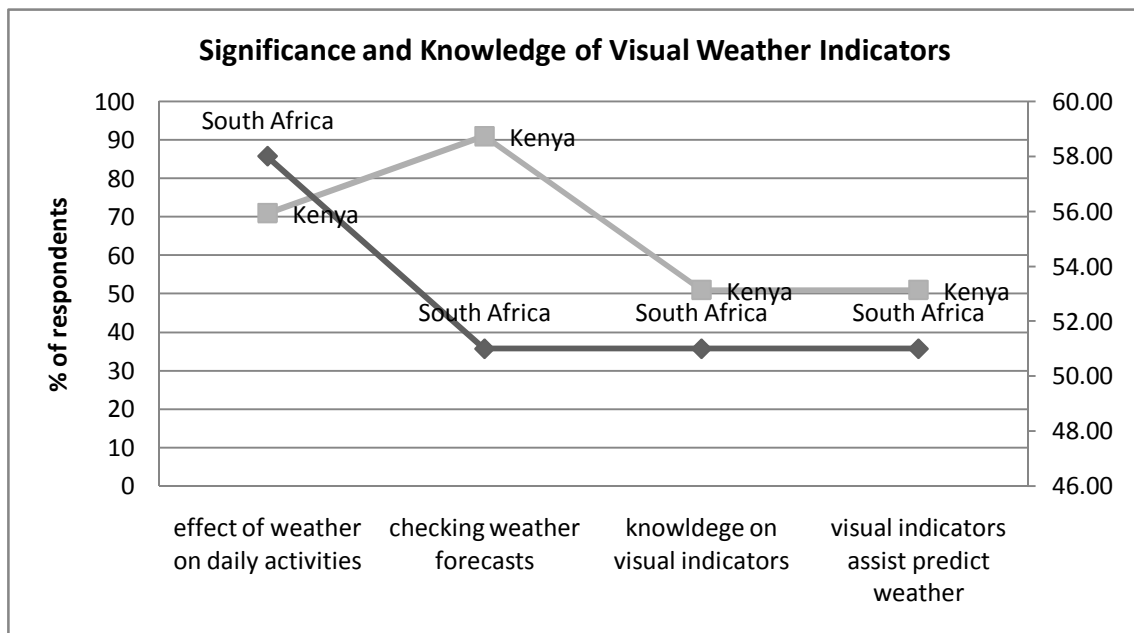


Figure 4-6: Trends of Knowledge of Weather in Kenya and South Africa

4.4.9 Causal Effects between Astronomical and Meteorological Concepts: Kenya vs. South Africa

The mode and mean knowledge (separately for Kenya and South Africa) were determined for each set of interacting concepts. The analysis showed that the weather season's patterns in Kenya and South Africa correspond but the extremes (high and low values) vary significantly. The comparison of the mode and mean knowledge of the causal effects to the various weather outcomes in the various seasons (for both Kenya and South Africa) are depicted in Table 4—5 to Table A—20. The values in the table represent the strength (range -1 to 1) based on computed average of responses.

Table 4—5: Comparison of Mode and Mean Knowledge for the Relations in Weather Concepts

Concept to Concept	Causal Effect (mode Values)		Causal Effect (mean Values)	
	Kenya	South Africa	Kenya	South Africa
high clouds to low clouds	.0	.0	-.1	-.2
high clouds to medium clouds	.0	.0	-.1	-.3
high clouds to clear sky	.5	.5	.5	.5
high clouds to many stars	.0	.0	-.1	-.1
high clouds to rainbow	.0	.0	-.1	.0
high clouds to lightning	-1.0	-1.0	-.8	-.9
high clouds to partial/dark moon	.0	.0	.0	.0
high clouds to full/visible moon	.0	.0	.1	.1
medium clouds to low clouds	.0	.0	.0	.0
medium clouds to clear sky	-.5	-.5	-.5	-.5
medium clouds to many stars	.0	.0	-.2	-.2
medium clouds to rainbow	.0	-1.0	-.3	-.5
medium clouds to lightning	.0	.0	.1	.1
medium clouds to partial/dark moon	.0	.0	.1	.1
medium clouds to full/visible moon	.0	-1.0	-.2	-.5
low clouds to clear sky	-1.0	-1.0	-.8	-.9
low clouds to many stars	.0	.0	-.1	-.1
low clouds to rainbow	.0	.0	-.1	.0
low clouds to lightning	.0	.0	.1	.0
low clouds to partial/dark moon	.0	.0	.1	.0
low clouds to full/visible moon	.0	.0	-.2	-.1
clear sky to many stars	.0	.0	.2	.1
clear sky to rainbow	.0	.0	.1	.1
clear sky to lightning	-1.0	-1.0	-.8	-.8
clear sky to partial/dark moon	.0	.0	-.2	-.5
clear sky to full/visible moon	.0	.0	.2	.2
many stars to rainbow	.0	.0	.2	.1
many stars to lightning	.0	.0	-.2	-.1
many stars to partial/dark moon	.0	-.5	-.2	-.3
many stars to full/visible moon	.0	.0	.3	.3
rainbow to lightning	.0	.0	-.3	-.2
rainbow to partial/dark moon	.0	.0	.0	.0
rainbow to full/visible moon	.0	.0	.1	.1
lightning to partial/dark moon	.0	.0	.2	.1
lightning to full/visible moon	.0	.0	-.2	-.1
partial/dark moon to full/visible moon	.0	.0	-.2	-.1

4.4.10 Variation of Knowledge between Case Studies

Performing separate analysis using mode and mean and comparing between the case studies (Figure 4-7 -Figure C-4) depicted some trends in knowledge of causal effects. The mode of responses was steadier (the mode knowledge between the two case studies override) than the mean (the mean knowledge values do not override between the two case studies).

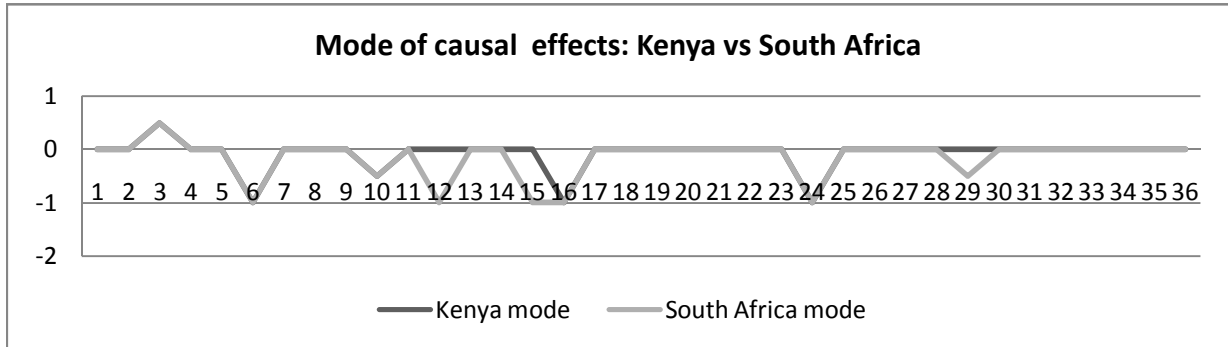


Figure 4-7: Comparison of Modal Causal Effects between Kenya and South Africa

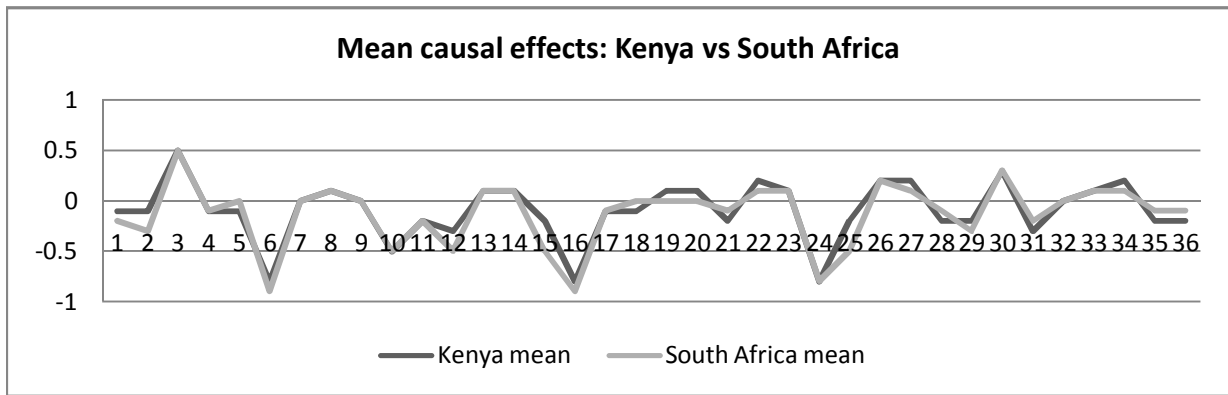


Figure 4-8: Comparison of Mean Causal Effects between Kenya and South Africa

Table 4—6: Summary of Modal Seasonal Causal effects in Kenya and South Africa

Concept to Outcome	Seasonal Causal Effects (modal Values)							
	Winter		Summer		Autumn		Spring	
	Kenya	South Africa	Kenya	South Africa	Kenya	South Africa	Kenya	South Africa
high clouds to rain	-1.0	.0	-1.0	-1.0	-1.0	-.5	-1.0	-.5
low clouds to rain	.5	.5	.0	1.0	1.0	1.0	.5	.5
medium clouds to rain	.0	.5	.5	.5	.5	.5	-.5	.5
clear sky to rain	-1.0	.0	-1.0	-.5	-1.0	-1.0	-1.0	-.5
many stars to rain	-1.0	.0	-.5	-1.0	-1.0	-1.0	-1.0	-1.0
rainbow to rain	-.5	-.5	-.5	-.5	-.5	-1.0	-.5	-.5
lightning to rain	.5	.5	.0	1.0	1.0	.5	1.0	1.0
partial/dark moon to rain	.5	.0	.5	.5	.5	.5	.5	.5
full/visible moon to rain	.0	.0	-.5	-1.0	-.5	-.5	-.5	-1.0
high clouds to dry	1.0	1.0	1.0	1.0	1.0	.5	1.0	.5
low clouds to dry	.5	1.0	-1.0	-1.0	-1.0	-1.0	-.5	.5
medium clouds to dry	-.5	1.0	-.5	-.5	-.5	-1.0	.5	-.5
clear sky to dry	1.0	1.0	1.0	1.0	1.0	.5	1.0	.5
many stars to dry	.5	1.0	1.0	1.0	1.0	-1.0	1.0	.5
rainbow to dry	.0	1.0	.5	.5	.5	.5	.5	-.5
lightning to dry	-.5	-1.0	-1.0	-1.0	-1.0	-.5	-1.0	-1.0
partial/dark moon to dry	-.5	-.5	-.5	-1.0	-.5	-.5	-.5	-1.0
full/visible moon to dry	.5	.5	1.0	1.0	.5	.5	.5	-1.0
high clouds to hot	.5	-.5	1.0	1.0	.5	.5	1.0	.5
low clouds to hot	-1.0	-.5	-1.0	-1.0	-.5	-.5	-.5	-.5
medium clouds to hot	-.5	-.5	-.5	1.0	.5	-1.0	.5	-.5
clear sky to hot	.5	.5	1.0	1.0	1.0	.5	1.0	1.0
many stars to hot	.5	.5	1.0	1.0	1.0	-1.0	1.0	.5
rainbow to hot	.5	.5	1.0	.5	.5	.5	.5	.5
lightning to hot	-.5	-1.0	-1.0	-.5	-.5	-.5	-1.0	-.5
partial/dark moon to hot	-.5	.0	-.5	-1.0	-.5	-.5	-.5	-.5
full/visible moon to hot	.5	.5	1.0	1.0	1.0	.5	.5	1.0
high clouds to cold	-.5	1.0	-1.0	-1.0	-1.0	.5	-1.0	-1.0
low clouds to cold	1.0	1.0	.5	.5	.5	.5	.5	.5
medium clouds to cold	.5	1.0	.5	-1.0	.5	.5	.5	.5
clear sky to cold	-.5	.5	-1.0	-1.0	-1.0	.5	-1.0	-1.0
many stars to cold	-.5	.5	-.5	-1.0	-.5	.5	-1.0	-1.0
rainbow to cold	-.5	.5	-.5	-1.0	-.5	.5	.5	-.5
lightning to cold	.5	1.0	.5	.5	1.0	.5	1.0	.5
partial/dark moon to cold	.5	1.0	-.5	.5	.5	.5	.5	.5
full/visible moon to cold	-.5	1.0	-1.0	-1.0	-.5	.5	-.5	-1.0

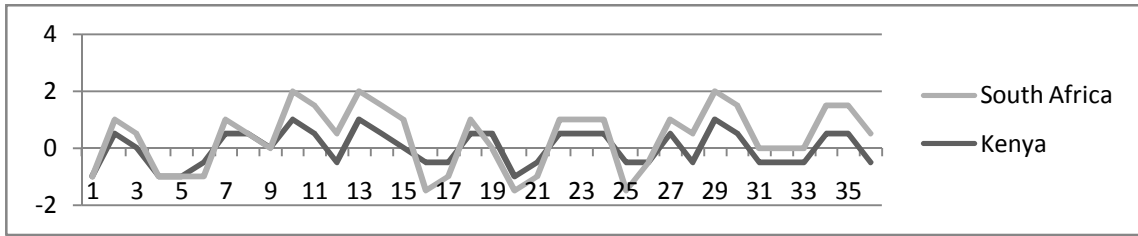


Figure 4-9: Modal Causal Effect in Kenya and South Africa Winter

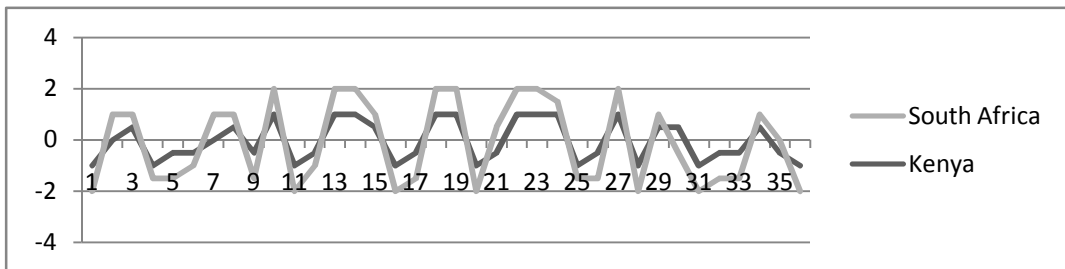


Figure 4-10: Modal Causal Effect in Kenya and South Africa Summer

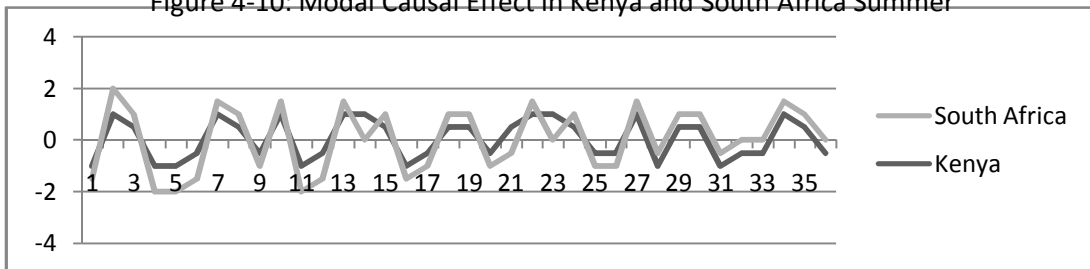


Figure 4-11: Modal Causal Effect in Kenya and South Africa Autumn

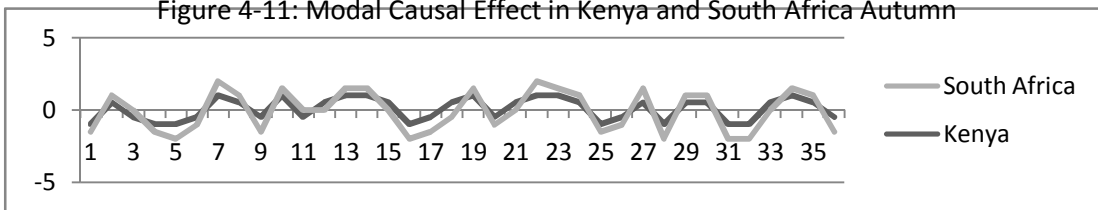


Figure 4-12: Modal Causal Effect in Kenya and South Africa Spring

Mean analysis was done in similar fashion (see Table A—20) and the results summarized from Figure C-1 to Figure C-4.

4.4.11 Aggregation of Seasonal Knowledge from Case Studies

To represent common knowledge for the two case studies, joint statistics (mode and mean values) were determined for:

- (1) between the visual astronomical and meteorological concepts and
- (2) between the astronomical and meteorological concepts to weather outcomes in the various seasons.

Aggregated mode and mean values for the four weather seasons were summarized in Table 4—7 and Table 4—8. Depiction in the trends of the mode and mean causal effects between the astronomical and meteorological concepts are shown in Figure 4-13, while Figure 4-14 – Figure 4-17 depict the trends in the aggregated (mode and mean) causal effects for the winter, summer, autumn and spring seasons.

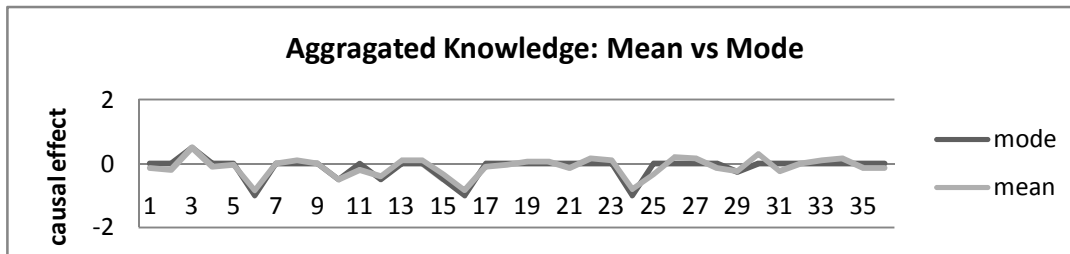


Figure 4-13: Comparison of Mean and Modal Aggregated Knowledge

Table 4—7: Aggregated Mode and Mean Knowledge on Concepts

Aggregated Causal Effect (Kenya and South Africa)		
Concept to Concept	mode	mean
high clouds to low clouds	0	-0.15
high clouds to medium clouds	0	-0.2
high clouds to clear sky	0.5	0.5
high clouds to many stars	0	-0.1
high clouds to rainbow	0	-0.05
high clouds to lightning	-1	-0.85
high clouds to partial/dark moon	0	0
high clouds to full/visible moon	0	0.1
medium clouds to low clouds	0	0
medium clouds to clear sky	-0.5	-0.5
medium clouds to many stars	0	-0.2
medium clouds to rainbow	-0.5	-0.4
medium clouds to lightning	0	0.1
medium clouds to partial/dark moon	0	0.1
medium clouds to full/visible moon	-0.5	-0.35
low clouds to clear sky	-1	-0.85
low clouds to many stars	0	-0.1
low clouds to rainbow	0	-0.05
low clouds to lightning	0	0.05
low clouds to partial/dark moon	0	0.05
low clouds to full/visible moon	0	-0.15
clear sky to many stars	0	0.15
clear sky to rainbow	0	0.1
clear sky to lightning	-1	-0.8
clear sky to partial/dark moon	0	-0.35
clear sky to full/visible moon	0	0.2
many stars to rainbow	0	0.15
many stars to lightning	0	-0.15
many stars to partial/dark moon	-0.25	-0.25
many stars to full/visible moon	0	0.3
rainbow to lightning	0	-0.25
rainbow to partial/dark moon	0	0
rainbow to full/visible moon	0	0.1
lightning to partial/dark moon	0	0.15
lightning to full/visible moon	0	-0.15
partial/dark moon to full/visible moon	0	-0.15

Table 4—8: Aggregated Mode and Mean Knowledge for the Various Weather Seasons

Kenya and South Africa Aggregated Seasonal Causal Effects								
Concept to Outcome	Winter		Summer		Autumn		Spring	
	mode	mean	mode	mean	mode	mean	mode	mean
high clouds to rain	-0.5	-0.4	-1	-0.75	-0.75	-0.65	-0.75	-0.65
low clouds to rain	0.5	0.45	0.5	0.5	1	0.8	0.5	0.55
medium clouds to rain	0.25	0.25	0.5	0.3	0.5	0.6	0	-0.05
clear sky to rain	-0.5	-0.45	-0.75	-0.65	-1	-0.8	-0.75	-0.75
many stars to rain	-0.5	-0.4	-0.75	-0.7	-1	-0.85	-1	-0.85
rainbow to rain	-0.5	-0.55	-0.5	-0.55	-0.75	-0.7	-0.5	-0.55
lightning to rain	0.5	0.5	0.5	0.55	0.75	0.7	1	0.8
partial/dark moon to rain	0.25	0.2	0.5	0.35	0.5	0.6	0.5	0.55
full/visible moon to rain	0	0.05	-0.75	-0.65	-0.5	-0.55	-0.75	-0.7
high clouds to dry	1	0.8	1	0.85	0.75	0.7	0.75	0.7
low clouds to dry	0.75	0.7	-1	-0.8	-1	-0.85	0	0.05
medium clouds to dry	0.25	0.15	-0.5	-0.5	-0.75	-0.75	0	0.05
clear sky to dry	1	0.8	1	0.85	0.75	0.75	0.75	0.65
many stars to dry	0.75	0.65	1	0.8	0	0	0.75	0.6
rainbow to dry	0.5	0.45	0.5	0.5	0.5	0.55	0	0.05
lightning to dry	-0.75	-0.7	-1	-0.75	-0.75	-0.65	-1	-0.8
partial/dark moon to dry	-0.5	-0.5	-0.75	-0.6	-0.5	-0.55	-0.75	-0.7
full/visible moon to dry	0.5	0.5	1	0.75	0.5	0.55	-0.25	-0.05
high clouds to hot	0	0.1	1	0.85	0.5	0.45	0.75	0.6
low clouds to hot	-0.75	-0.65	-1	-0.85	-0.5	-0.5	-0.5	-0.5
medium clouds to hot	-0.5	-0.5	0.25	0.15	-0.25	-0.05	0	-0.2
clear sky to hot	0.5	0.55	1	0.85	0.75	0.65	1	0.85
many stars to hot	0.5	0.5	1	0.85	0	-0.05	0.75	0.65
rainbow to hot	0.5	0.5	0.75	0.65	0.5	0.65	0.5	0.55
lightning to hot	-0.75	-0.65	-0.75	-0.65	-0.5	-0.55	-0.75	-0.65
partial/dark moon to hot	-0.25	-0.2	-0.75	-0.7	-0.5	-0.5	-0.5	-0.5
full/visible moon to hot	0.5	0.5	1	0.85	0.75	0.65	0.75	0.75
high clouds to cold	0.25	0.2	-1	-0.85	-0.25	-0.15	-1	-0.85
low clouds to cold	1	0.8	0.5	0.45	0.5	0.55	0.5	0.55
medium clouds to cold	0.75	0.65	-0.25	-0.15	0.5	0.55	0.5	0.55
clear sky to cold	0	0	-1	-0.8	-0.25	-0.1	-1	-0.8
many stars to cold	0	0.05	-0.75	-0.65	0	0	-1	-0.8
rainbow to cold	0	0	-0.75	-0.7	0	0	0	0
lightning to cold	0.75	0.65	0.5	0.55	0.75	0.65	0.75	0.7
partial/dark moon to cold	0.75	0.65	0	0.05	0.5	0.6	0.5	0.5
full/visible moon to cold	0.25	0.15	-1	-0.85	0	0	-0.75	-0.6

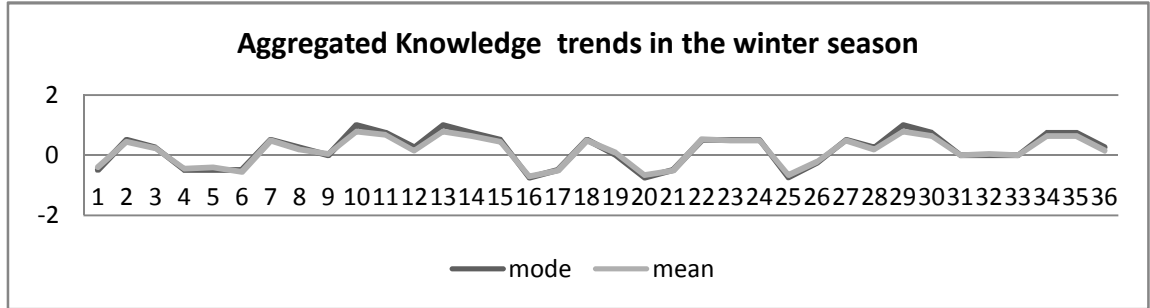


Figure 4-14: Trend of Aggregated Mean and Mode for the Winter Season

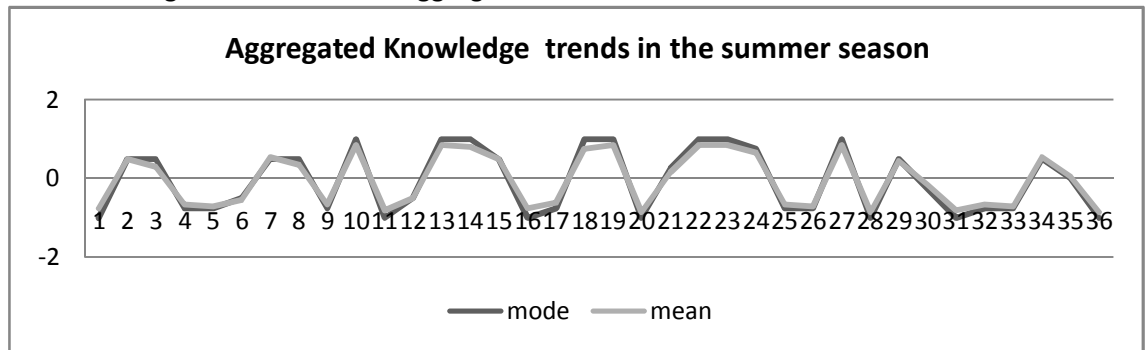


Figure 4-15: Trend of Aggregated Mean and Mode for the Summer Season

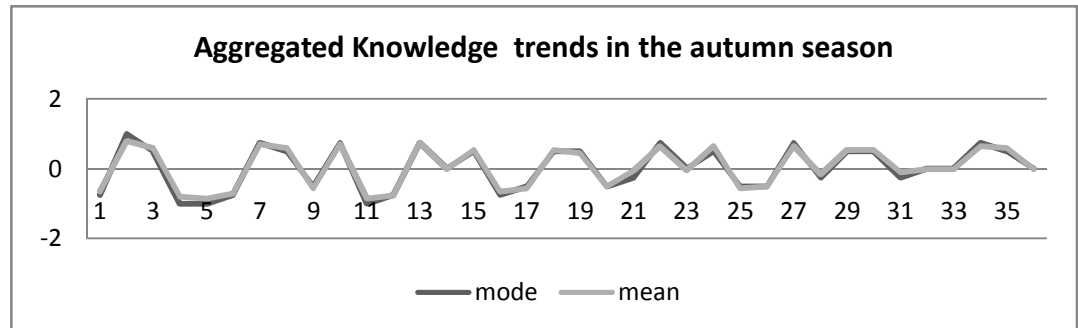


Figure 4-16: Trend of Aggregated Mean and Mode for the Autumn Season

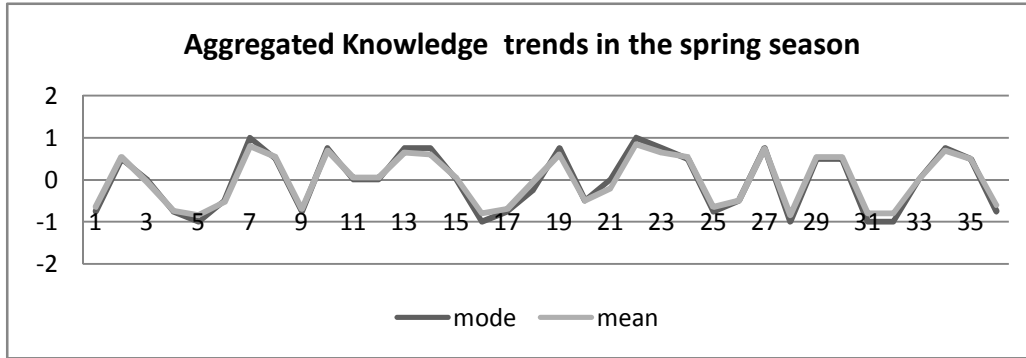


Figure 4-17: Trend of Aggregated Mean and Mode for the Spring Season

4.4.12 Representations of Aggregated Knowledge

In the joint analysis, the mean statistic considered all the possible responses (*strong-negative, negative, none, positive, strong-positive*) from the two case studies. Results of statistical analysis for seasons such as winter (South Africa was colder than Kenya), and summer (South Africa was hotter than Kenya) portrayed that the causal effects vary significantly (see Figure 4-14 to Figure 4-17 on the knowledge trends for the various seasons). The analysis of all responses using mean depicted a poor aggregate of causal effects; hence the mean aggregate was not preferred as the best statistic to represent the mutual causal effects for the case studies.

The joint averages of majority responses from the case studies were determined for each set of interacting concepts. The knowledge variation between the modal values in the two case studies was not extreme as that of the mean (see Figure 4-14 to Figure 4-17 on the knowledge trends for the various seasons). This observation led to the preference of the averages of probability (modal values) in favour of the mean for representing the interactions between the concepts. Table 4—9 and Table 4—10 show the preferred values representing causal effects between the interacting visual astronomical and meteorological concepts.

Table 4—9: Aggregated Causal Effect (Kenya and South Africa)

Concept to Concept	value
high clouds to low clouds	0
high clouds to medium clouds	0
high clouds to clear sky	0.5
high clouds to many stars	0
high clouds to rainbow	0
high clouds to lightning	-1
high clouds to partial/dark moon	0
high clouds to full/visible moon	0
medium clouds to low clouds	0
medium clouds to clear sky	-0.5
medium clouds to many stars	0
medium clouds to rainbow	-0.5
medium clouds to lightning	0
medium clouds to partial/dark moon	0
medium clouds to full/visible moon	-0.5
low clouds to clear sky	-1
low clouds to many stars	0
low clouds to rainbow	0
low clouds to lightning	0
low clouds to partial/dark moon	0
low clouds to full/visible moon	0
clear sky to many stars	0
clear sky to rainbow	0
clear sky to lightning	-1
clear sky to partial/dark moon	0
clear sky to full/visible moon	0
many stars to rainbow	0
many stars to lightning	0
many stars to partial/dark moon	-0.25
many stars to full/visible moon	0
rainbow to lightning	0
rainbow to partial/dark moon	0
rainbow to full/visible moon	0
lightning to partial/dark moon	0
lightning to full/visible moon	0
partial/dark moon to full/visible moon	0

Table 4–10: Kenya and South Africa Aggregated Seasonal Causal Effects

Concept to Outcome	Winter	Summer	Autumn	Spring
high clouds to rain	-0.5	-1	-0.75	-0.75
low clouds to rain	0.5	0.5	1	0.5
medium clouds to rain	0.25	0.5	0.5	0
clear sky to rain	-0.5	-0.75	-1	-0.75
many stars to rain	-0.5	-0.75	-1	-1
rainbow to rain	-0.5	-0.5	-0.75	-0.5
lightning to rain	0.5	0.5	0.75	1
partial/dark moon to rain	0.25	0.5	0.5	0.5
full/visible moon to rain	0	-0.75	-0.5	-0.75
high clouds to dry	1	1	0.75	0.75
low clouds to dry	0.75	-1	-1	0
medium clouds to dry	0.25	-0.5	-0.75	0
clear sky to dry	1	1	0.75	0.75
many stars to dry	0.75	1	0	0.75
rainbow to dry	0.5	0.5	0.5	0
lightning to dry	-0.75	-1	-0.75	-1
partial/dark moon to dry	-0.5	-0.75	-0.5	-0.75
full/visible moon to dry	0.5	1	0.5	-0.25
high clouds to hot	0	1	0.5	0.75
low clouds to hot	-0.75	-1	-0.5	-0.5
medium clouds to hot	-0.5	0.25	-0.25	0
clear sky to hot	0.5	1	0.75	1
many stars to hot	0.5	1	0	0.75
rainbow to hot	0.5	0.75	0.5	0.5
lightning to hot	-0.75	-0.75	-0.5	-0.75
partial/dark moon to hot	-0.25	-0.75	-0.5	-0.5
full/visible moon to hot	0.5	1	0.75	0.75
high clouds to cold	0.25	-1	-0.25	-1
low clouds to cold	1	0.5	0.5	0.5
medium clouds to cold	0.75	-0.25	0.5	0.5
clear sky to cold	0	-1	-0.25	-1
many stars to cold	0	-0.75	0	-1
rainbow to cold	0	-0.75	0	0
lightning to cold	0.75	0.5	0.75	0.75
partial/dark moon to cold	0.75	0	0.5	0.5
full/visible moon to cold	0.25	-1	0	-0.75

4.5 Formal Representations of Visual Weather Lore Knowledge

4.5.1 Representation of Concepts in Fuzzy Cognitive Maps

The concepts identified during weather lore domain understanding and analysis (*high clouds; low clouds; medium clouds; clear sky; many stars; rainbow; lightning; partial/darkmoon; full/visible*

moon; rain; dry; hot; cold) were uniquely structured by their respective positions in an n state vector as follows:

$$C = \{c_1, \dots, c_n\} \dots \dots \dots \text{Equation 4-1}$$

The state of a concept c , was represented by the probability of occurrence with term sets taking real values, p , in the closed set of range $0 \leq p \leq 1$. The corresponding membership functions, which describe each linguistic variable (probability of occurrence), were represented as follows:

$$c(p) = \begin{cases} 1, full_presence \\ \vdots \\ \downarrow decreasing_presence \dots \dots \dots \text{Equation 4-2} \\ \vdots \\ 0, full_absence \end{cases}$$

The set of states of the concepts (both indicators and outcomes) were mathematically represented by an n state vector, C , consisting of the presence probabilities of the concepts.

$$C_{states} = \{c_1(p), \dots, c_n(p)\} \dots \dots \dots \text{Equation 4-3}$$

such that n is the number of interacting concepts

4.5.2 Representation of Causal Effects

The causal effects between the concepts (weather indicators) were declared using the variable “causal effect” which takes values, w in a closed set of range $-1 \leq w \leq 1$ with term sets T , proposed to comprise five variables. Using five linguistic variables, the different degrees of causal effects between concept(s) were determined. The five derivable variables according to degrees of the causal effects were represented by T (causal effect) such that;

$$T (\text{causal effect}) = \{strong\ positive, positive, none, negative, strong\ negative\}.$$

During a scenario simulation the causal effects between concepts change states. The final causal effects correspond to weights within a range in which membership functions describe the terms of causal effects using a linguistic variable. Unlike the probability values $[0, 1]$, the membership

functions for the terms of the causal effect were classified to take values of in the range [-1, 1], taking the range of strong positive to strong negative effects as follows:

$$\begin{aligned}
 0.5 &< \textit{strong_positive} \leq 1 \\
 0 &< \textit{positive} \leq 0.5 \\
 0 &= \textit{none} \\
 -0.5 &< \textit{negative} < 0 \\
 -1 &\leq \textit{strong_negative} < -0.5
 \end{aligned}$$

4.5.3 Representation of Concepts Relations Using Fuzzy Cognitive Maps

The relations between the concepts were represented by a statistically weighted $n \times n$ adjacency matrix W , which mapped the causal weights at the intersection of concepts pair's i.e.

$$W = \begin{bmatrix} w_{11} & \dots & w_{1j} \\ \vdots & & \vdots \\ w_{i1} & & w_{ij} \end{bmatrix} \dots\dots\dots \text{Equation 4-4}$$

The value n represents the number of interacting concepts that falls in the range $1 \leq (i, j) \leq n$

The general rule of fuzzy cognitive maps (Din & Cretan, 2014; Najafi & Afrazeh, 2008) was applied i.e. for any concept c_i , the causal effect of concept c_i on another concept c_j is w_{ij}

The final (Kenya and South Africa) fuzzy cognitive maps (Table A—12 to Table A—19) were formulated as $n \times n$ matrices W , using the results of statistical analysis (see Table A—12 to Table A—19). The adjacency matrices were filled with values w_{ij} indicating the strength of the relationship between interacting concepts at position c_{ij} . A positive sign (+ or no sign) was used before the value to indicate an enhancing effect while a negative sign (-) was used to indicate a depressing effect. The value of zero (0) was used to mean that concept c_i has no causal effect to an adjacent concept c_j

4.5.4 Formation of Group Knowledge by Aggregation of Fuzzy Cognitive Maps

A simple form of learning was represented by aggregating knowledge from corresponding seasonal fuzzy cognitive map matrices (Kenya and South Africa) into single units. This was done by adding the adjacency matrices of the seasonal FCM W_i to form an overall FCM connection matrix W . The resultant matrix had values outside the range $[-1, 1]$; hence to scale the combined matrix was divided by N .

$$W = \frac{1}{N} \sum_{i=1}^N W_i \dots \dots \dots \text{Equation 4-5}$$

The object W represented the overall seasonal FCM, N corresponds to the number FCMs, and W_i corresponds to the FCM connection matrix of i^{th} season. The final fuzzy cognitive map connection matrices consisted of collective knowledge from both Kenya and South Africa (Table 4–11 and Table 4–12).

Table 4–11: Final Fuzzy Cognitive Map for Winter Season

Concepts	high clouds	low clouds	medium clouds	clear sky	many stars	rainbow	lightning	partial/dark moon	full/visible moon	rain	dry	hot	cold
high clouds	0.00	0.00	0.00	0.50	0.00	0.00	-1.00	0.00	0.00	-0.50	1.00	0.00	0.25
low clouds	0.00	0.00	0.00	-1.00	0.00	0.00	0.00	0.00	0.00	0.50	0.75	-0.75	1.00
medium clouds	0.00	0.00	0.00	-0.50	0.00	0.00	0.00	0.00	-0.50	0.25	0.25	-0.50	0.75
clear sky	0.00	0.00	0.00	0.00	0.00	0.00	-1.00	0.00	0.00	-0.50	1.00	0.50	0.00
many stars	0.00	0.00	0.00	0.00	0.00	0.00	0.00	0.00	0.00	-0.50	0.75	0.50	0.00
rainbow	0.00	0.00	0.00	0.00	0.00	0.00	0.00	0.00	0.00	-0.50	0.50	0.50	0.00
lightning	0.00	0.00	0.00	0.00	0.00	0.00	0.00	0.00	0.00	0.50	-0.75	-0.75	0.75
partial/dark moon	0.00	0.00	0.00	0.00	0.00	0.00	0.00	0.00	0.00	0.25	-0.50	-0.25	0.75
full/visible moon	0.00	0.00	0.00	0.00	0.00	0.00	0.00	0.00	0.00	0.00	0.50	0.50	0.25
rain	0.00	0.00	0.00	0.00	0.00	0.00	0.00	0.00	0.00	0.00	0.00	0.00	0.00
dry	0.00	0.00	0.00	0.00	0.00	0.00	0.00	0.00	0.00	0.00	0.00	0.00	0.00
hot	0.00	0.00	0.00	0.00	0.00	0.00	0.00	0.00	0.00	0.00	0.00	0.00	0.00
cold	0.00	0.00	0.00	0.00	0.00	0.00	0.00	0.00	0.00	0.00	0.00	0.00	0.00

Table 4–12: Final Fuzzy Cognitive Map for Summer Season

Concepts	high clouds	low clouds	medium clouds	clear sky	many stars	rainbow	lightning	partial/dark moon	full/visible moon	rain	dry	hot	cold
high clouds	0.00	0.00	0.00	0.50	0.00	0.00	-1.00	0.00	0.00	-1.00	1.00	1.00	-1.00
low clouds	0.00	0.00	0.00	-1.00	0.00	0.00	0.00	0.00	0.00	0.50	-1.00	-1.00	0.50
medium clouds	0.00	0.00	0.00	-0.50	0.00	0.00	0.00	0.00	-0.50	0.50	-0.50	0.25	-0.25
clear sky	0.00	0.00	0.00	0.00	0.00	0.00	-1.00	0.00	0.00	-0.75	1.00	1.00	-1.00
many stars	0.00	0.00	0.00	0.00	0.00	0.00	0.00	0.00	0.00	-0.75	1.00	1.00	-0.75
rainbow	0.00	0.00	0.00	0.00	0.00	0.00	0.00	0.00	0.00	-0.50	0.50	0.75	-0.75
lightning	0.00	0.00	0.00	0.00	0.00	0.00	0.00	0.00	0.00	0.50	-1.00	-0.75	0.50
partial/dark moon	0.00	0.00	0.00	0.00	0.00	0.00	0.00	0.00	0.00	0.50	-0.75	-0.75	0.00
full/visible moon	0.00	0.00	0.00	0.00	0.00	0.00	0.00	0.00	0.00	-0.75	1.00	1.00	-1.00
rain	0.00	0.00	0.00	0.00	0.00	0.00	0.00	0.00	0.00	0.00	0.00	0.00	0.00
dry	0.00	0.00	0.00	0.00	0.00	0.00	0.00	0.00	0.00	0.00	0.00	0.00	0.00
hot	0.00	0.00	0.00	0.00	0.00	0.00	0.00	0.00	0.00	0.00	0.00	0.00	0.00
cold	0.00	0.00	0.00	0.00	0.00	0.00	0.00	0.00	0.00	0.00	0.00	0.00	0.00

An FCM network for the spring season and as part of the complex network of weather seasons is depicted in Figure 4-18. The network depicts the interaction between the concepts with values of edges representing the strength of causal effect between the interacting concepts.

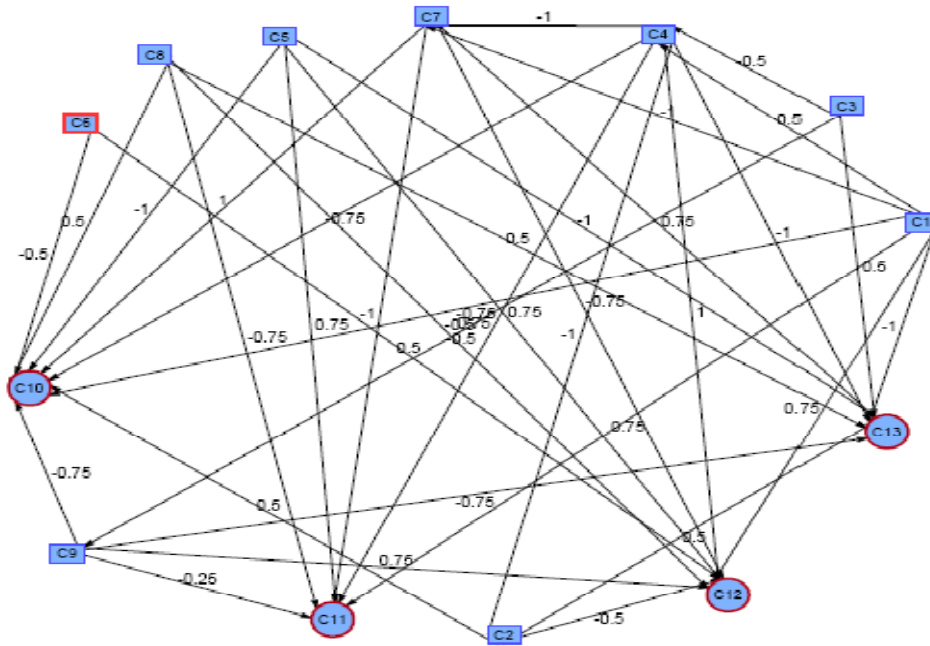


Figure 4-18: FCM for the Spring Season

Key: (C1=high clouds; C2=low clouds; C3=medium clouds; C4=clear sky; C5=many stars; C6=rainbow; C7=lightning; C8=partial/dark moon; C9=full/visible moon; C10=rain; C11=dry; C12=hot; C13=cold)

The significance outdegree (outgoing nodes), indegree (incoming nodes) and centrality (total incoming and outgoing nodes) of the visual weather concepts were analyzed and presented in Table 4—13.

Table 4—13: Analysis of the Importance of Nodes (Concepts) for Spring Season

Concepts	Outdegree	Indegree	Centrality
high clouds	4.75	0.00	4.75
low clouds	2.50	0.00	2.50
medium clouds	1.50	0.00	1.50
clear sky	4.50	2.00	6.50
many stars	3.50	0.00	3.50
Rainbow	1.00	0.00	1.00
Lightning	3.50	2.00	5.50
partial/dark moon	2.25	0.00	2.25
full/visible moon	2.50	0.50	3.00
rain	0.00	5.75	5.75
Dry	0.00	4.25	4.25
Hot	0.00	5.50	5.50
Cold	0.00	6.00	6.00

4.6 The Blueprint of Weather Lore Verification Tool

This section describes the weather lore verification tool consisting of input, processing components and output. The input to the system is in the form of sky image scenes and actual weather observations from wireless weather sensors. The image recognition component performs three sub tasks including: objects (concepts) detection from image scenes, extraction of detected objects, and to approximate presence of the concepts by comparing extracted objects to ideal objects. The prediction process involves the use of approximated concepts to simulate scenarios using the knowledge represented in the fuzzy cognitive maps generated in the previous section. The verification component evaluates the variation between the predictions and actual weather observations to determine prediction errors and accuracy. Figure 4-19 and Figure 4-20 depicts the architecture and the use case diagrams of the weather lore verification tool. This is followed by discussion of the working for each sequential component.

In the architecture the tool works by accepting sky images that are passed through an image recognition component. The detected objects are benchmarked then passed to an FCM based prediction component. The predictions are then verified against actual sensor weather records.

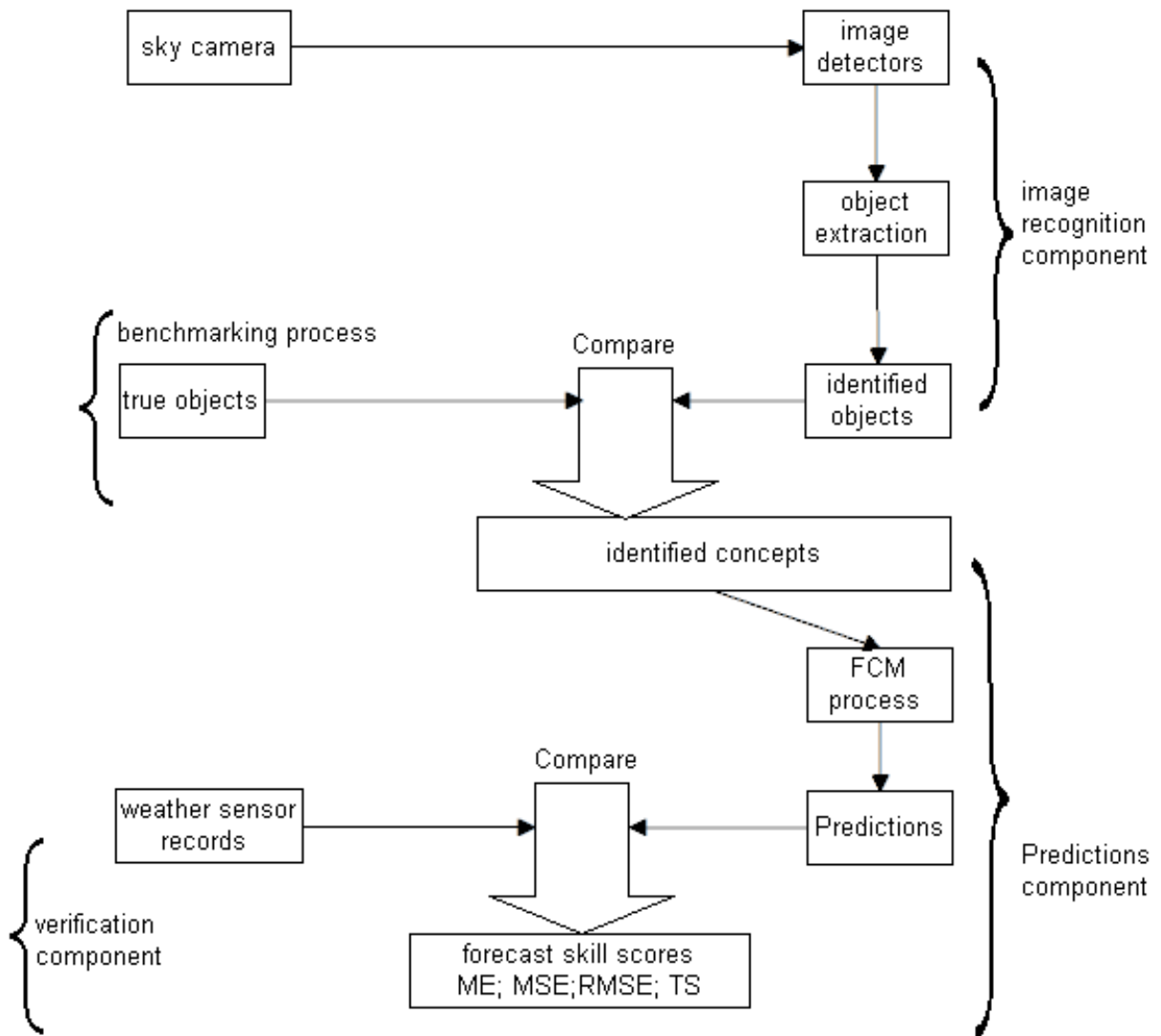


Figure 4-19: Architecture of the Visual Weather Lore Verification Method

The use case diagram for the visual weather lore verification tool is depicted below (Figure 4-20). In the use diagram the knowledge expert identifies visual weather lore that is used to develop seasonal weather fuzzy cognitive maps. The designer uses the techniques of computer vision and FCMs to develop programs for training detectors and verify predictions. The user (who is a meteorologist) can then use the tool to add new images and actual weather data for purposes of verification.

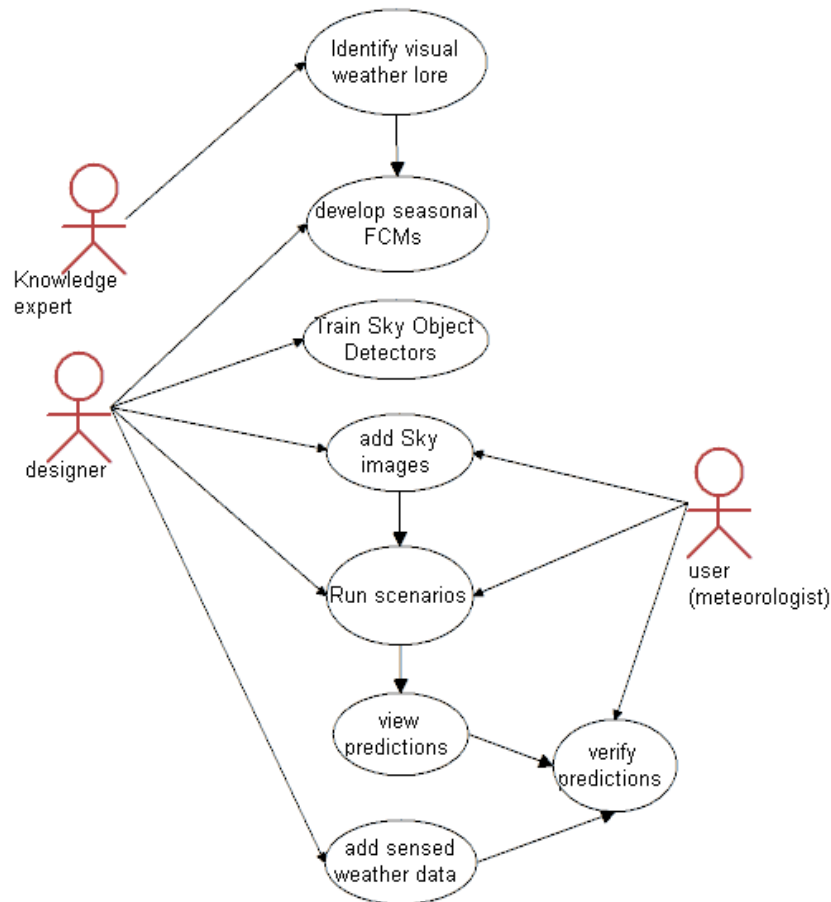


Figure 4-20: Use Case Diagram for the Weather Lore Verification Tool

4.6.1 Object Recognition in Visual Sky Scenes Using Machine Learning

The object recognition process identifies specific objects in a digital sky image using machine learning and pattern recognition algorithms. This process involves a series of subtasks as depicted in the process flow diagram (Figure 4-21) and explained in subsequent sections.

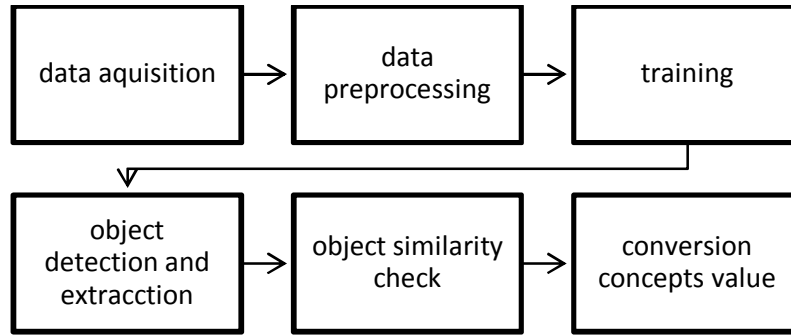


Figure 4-21: The Object Recognition Process

4.6.2 Data Format and Acquisition Methods

Image scenes are acquired from the field using all-weather sky cameras at specific time intervals. The automated cameras accumulate this data for use in the image pre-processing and object recognition tasks. To build up sufficient data for evaluation of the predictions an automated (using wireless sensor nodes) weather station in the field logs periodic actual weather observations.

4.6.3 Pre-processing Objects Sets from Image Data

Image sets representing the visual weather concept are extracted from a collection of known images to label positive training samples. Using positive samples the finest actual images of objects are then extracted and specified as base (ideal object). Samples of negative images are also extracted and specified as negative image training sets. The process of identifying positive samples iterates (see Figure 4-22) until there are sufficient quantities of images to represent each visual concept.

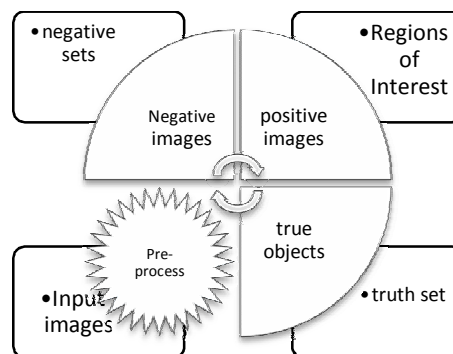


Figure 4-22: Process of Preparing Image Sets for Detector Training

4.6.4 Training of Sequential Object Detectors

Regions of interest that define visual objects are delineated from the sets of positive samples. For each set of positive samples, a corresponding set is specified with negative samples consisting of scenes with different objects to the object concept. The procedure of training object detectors for each concept is depicted in Figure 4-23.

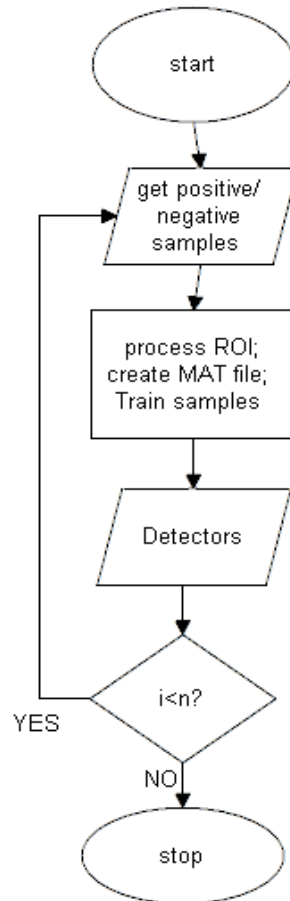


Figure 4-23: Flow Chart for Training Detectors

4.6.5 Object Detection and Extraction from an Input Sky Scene

An input sky scene is subjected to a processing component (Figure 4-24) where predefined consecutive detectors recognize objects representing the various concepts. The output from this process is a set of extracted objects corresponding to the various concepts. Visual objects that are

undetected are represented with value zero (meaning the probability of the concept presence is zero) and consequently by pass the test of extraction and similarity check procedures.

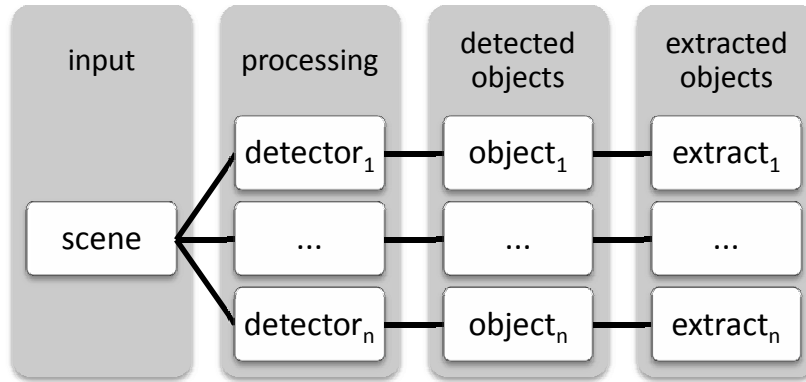


Figure 4-24: Object Detection and Extraction Process

4.6.6 Similarities Check between Detected and Ideal Objects

The process of checking similarity (Figure 4-25) between extracted and ideal objects involves computing the distance or the difference between the objects (Figure 4-25). Similar objects will have a distance of zero, while the distance between objects increases as the objects increasingly becomes more different. This process is vital to supplement the object detection procedure in the eventuality of false positives. The image colour, shape and texture intensity variations (specified as benchmarks or similarity scores) are the output in this process.

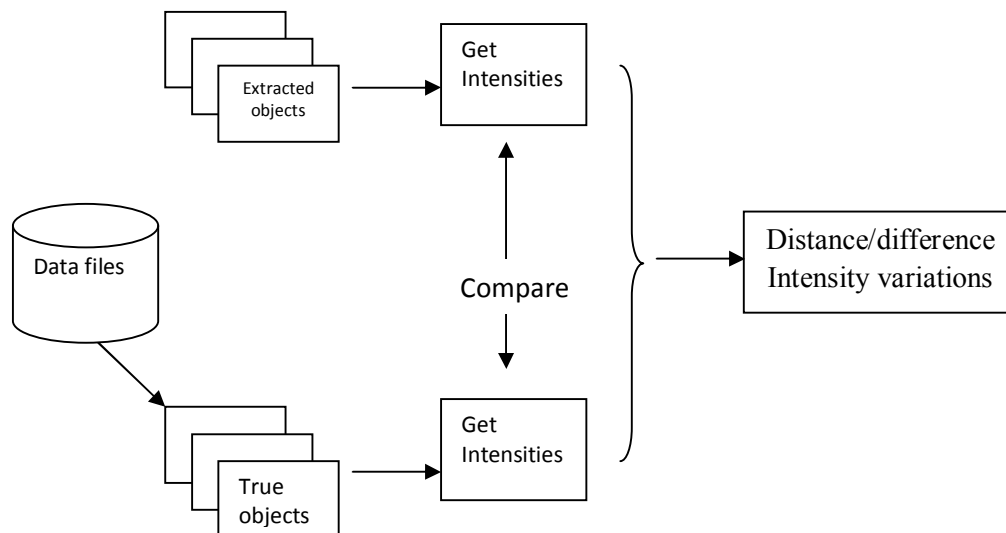


Figure 4-25: Similarity Check between Detected and True Objects

4.6.7 Computing the Presence Probabilities of Detected Objects

The set of objects differences or similarity (S) scores are used to compute the likelihood (P) of presence for the detected objects. The transformation from the similarity scores to the concept values (probability of object presence) is depicted in a flow chart (Figure 4-26).

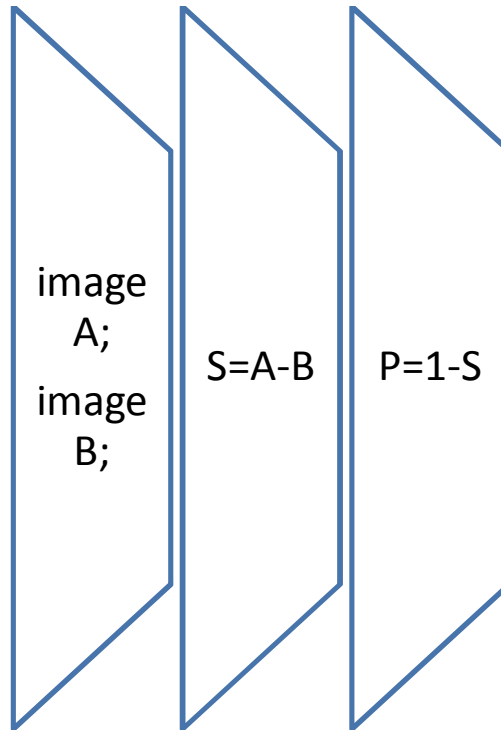


Figure 4-26: Estimating the Presence Concepts from Detected Objects

4.7 Fuzzy Cognitive Mapping Technique for Weather Outcome Scenarios Processing

4.7.1 Determination of the Number of Nodes and Concepts Values

Given an input consisting of benchmarked sky concepts, the numbers of nodes (or concepts) are determined dynamically by computing the size of the input concept vector. This can also be determined from the weights matrices by determining the row or column size of the matrices. The values of concepts are then determined in a straight forward approach by using the indices of the values in the input concepts vector. The sequence of determination of the number and values of concepts is depicted in Figure 4-27.

Number of Nodes (Concepts) = size (Concepts-Vector, Row) **OR**

Number of Nodes = size (Weights-Matrix, Row or Column)

Value of Concept =input (index)

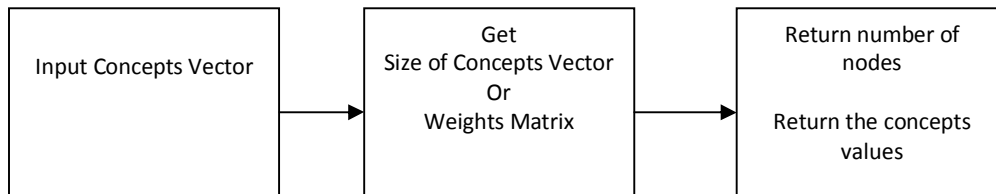


Figure 4-27: Process Flow of Generating Number and Probability of Nodes in FCM

4.7.2 Representation of Causal Relationships between Concepts

The weights (causal relationships between concepts) are represented in adjacency matrices distinguished by the four weather seasons (summer, autumn, winter and spring). The numeric values represented in seasonal matrices vary corresponding to the strengths of relationship between the concepts in the different seasons. During simulation runs the weights are resolved from the specific seasons by determining numeric data in the matrices.

4.7.3 Choice and Status of a Seasonal Fuzzy Cognitive Map

The seasons are represented as a circular linked list where season S_i has a previous and next season(s) represented as S_{i-1} , and S_{i+1} respectively. The onset and cessation of seasons take timing characteristics of early or late, while the season progress is specified as either continuous

or interrupted. To mimic the circular and overlapping nature of the weather seasons (such as the timing and progress) a selection routing procedure is employed (

Figure 4-28). The overlapping nature of the weather seasons during the months is illustrated in Figure 4-29.

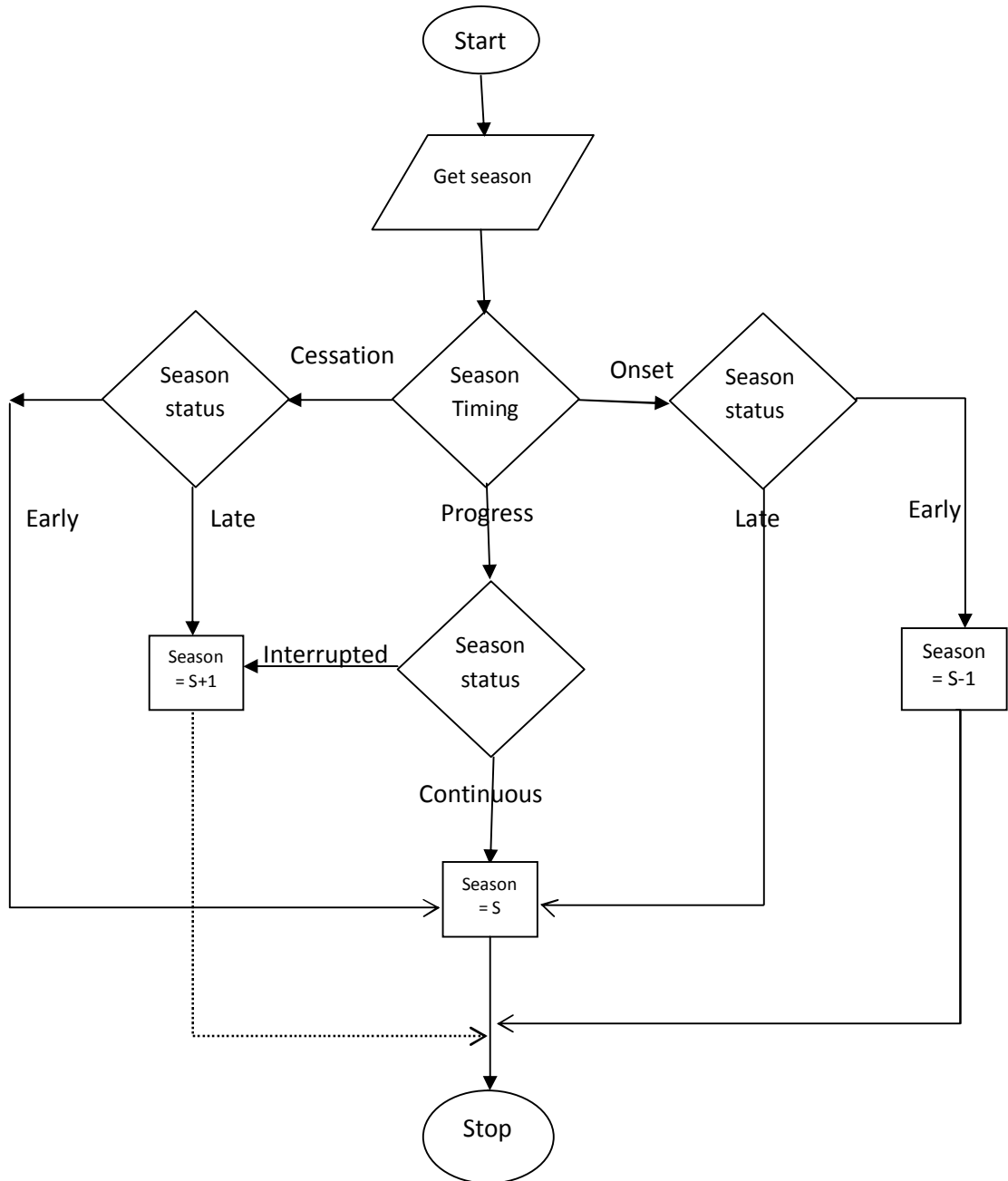


Figure 4-28: Flowchart for Selection of Weather Seasons

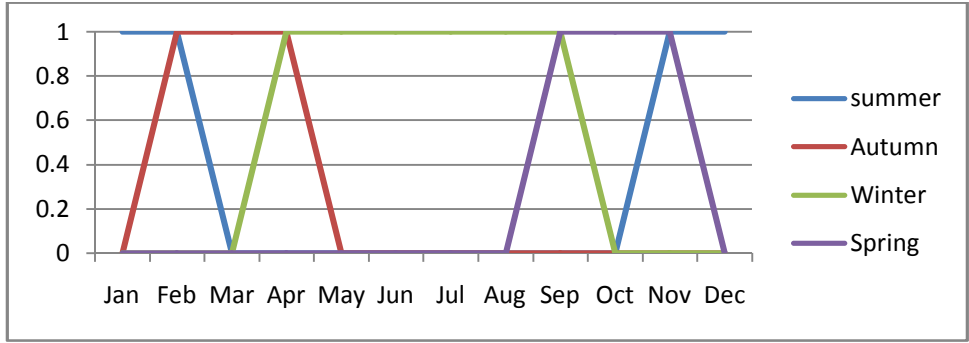


Figure 4-29: The Overlapping Nature of the Weather Seasons

4.7.4 Activation of New Concepts States and States of Equilibrium

Simulations are run for the state of input concepts (c_i^k) by computing new concepts (c_i^{k+1}) using the seasonal knowledge represented in adjacency matrices. The input to a simulation run is a vector of n concepts determined using information from the object detector component. An activation function (Cai, 2011; Uygur & Stacy, 2004) is used in predicting the new state of concepts. The number of iterations of the simulations per concept is set to be equal to the number of concepts (nodes). The procedure of activating new states of concepts is shown in Figure 4-30. Since the state vectors of the fuzzy cognitive map at iteration n is completely determined by the state vector at iteration $(n-1)$, the state of equilibrium is detectable during simulation runs by comparing two successive state vectors.

$$c_i^{(k+1)} = f \left(\sum_{\substack{j \neq i \\ j=1}}^n c_j^{(k)} \cdot w_{ji} \right) \dots \dots \dots \text{Equation 4-6}$$

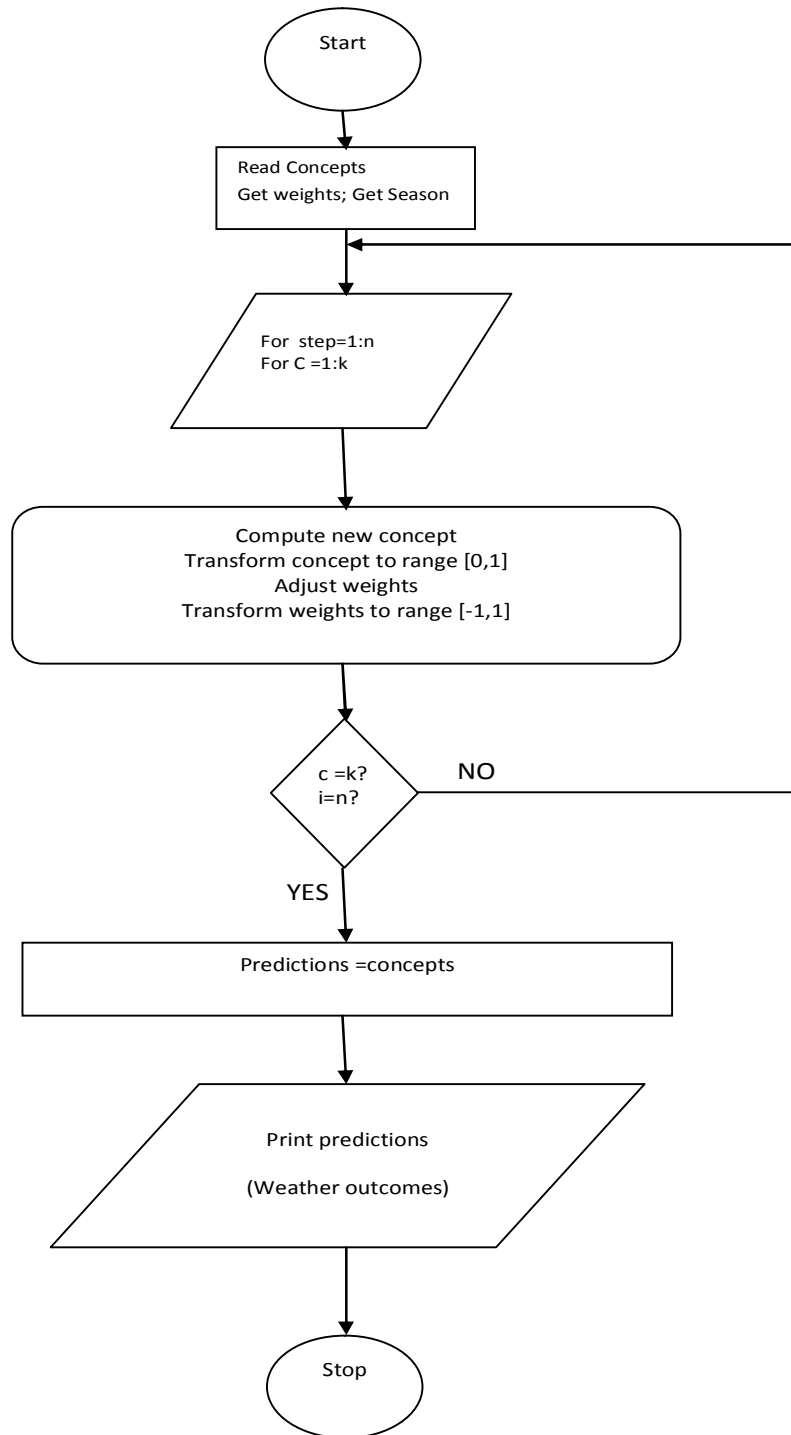


Figure 4-30: Flowchart for Activation of New Concepts states

4.7.5 Limiting the New Concepts States Using a Transformation Function

To restrict the concepts values to be in the interval $[0, 1]$ a transformation function is applied per iteration. This transformation function generates concepts values in the range $0 \leq c(i) \leq 1$ with a prospect that the maximum likelihood is positive but infinitely small (for instance 0.4×10^{-70}). Alleviation of this prospect is achieved using a min-max normalization (Luo, 2010; Najafi, 2011; Xirogiannis & Glykas, 2004) function that scales the predictions in the range $[0, 1]$. The concept state limiting process runs through the stages depicted in

Figure 4-31 and Figure 4-32.

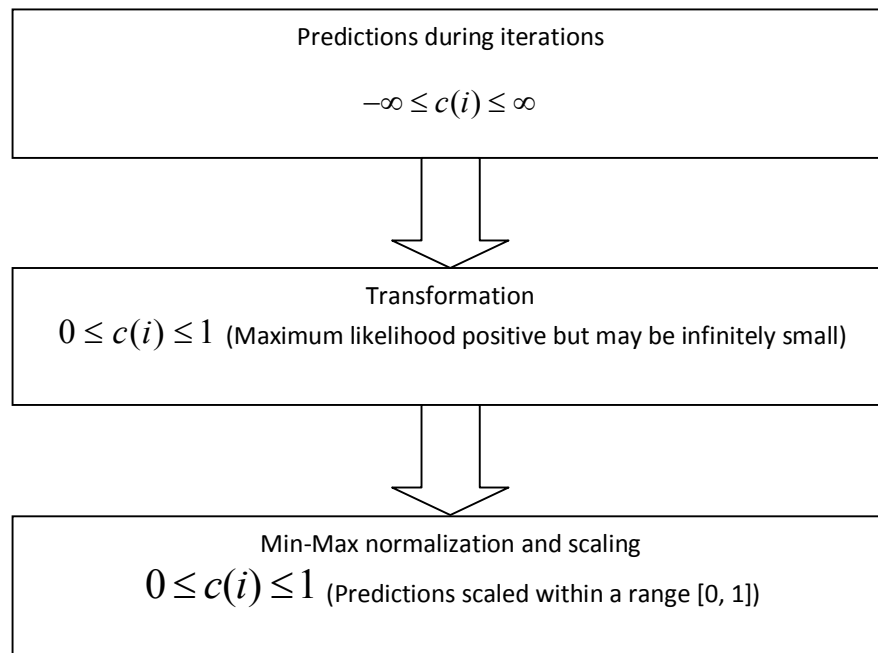


Figure 4-31: Process Flow in Predictions Transformation and Normalization

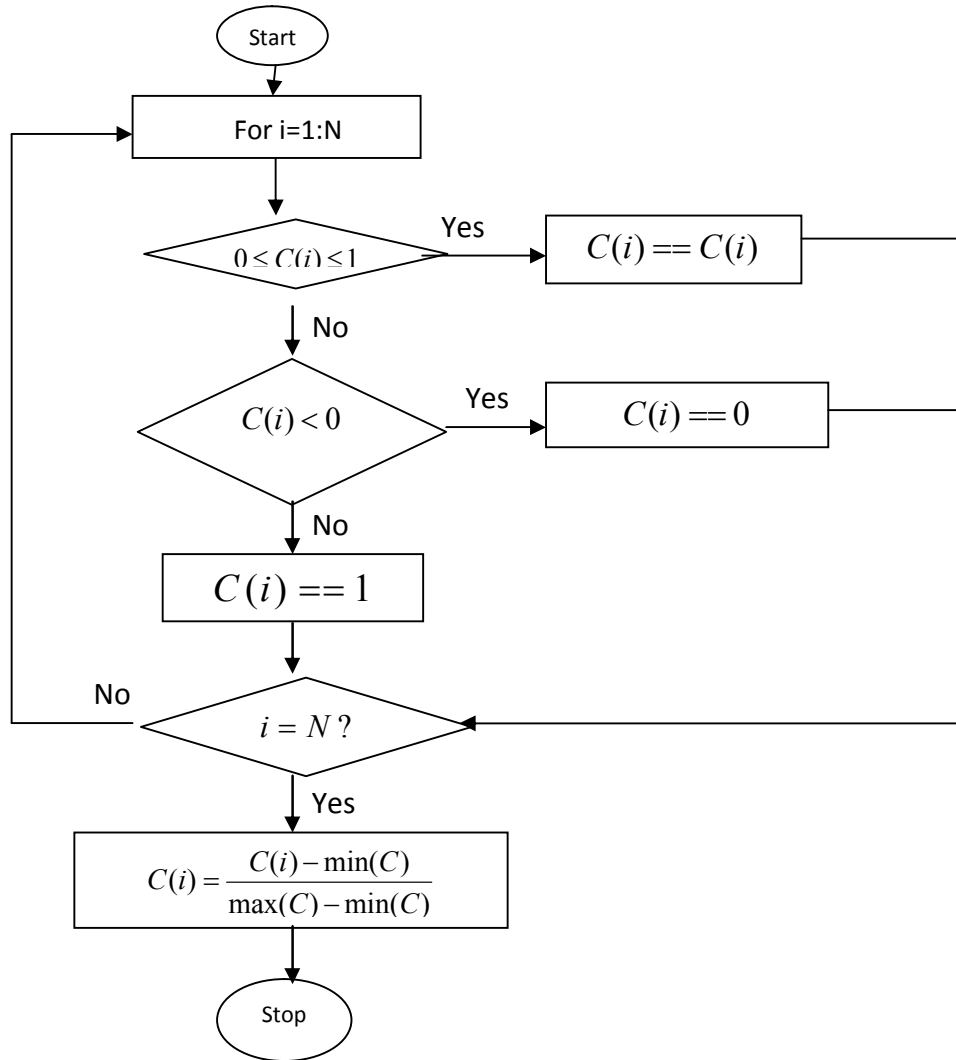


Figure 4-32: Flowchart for Transforming Concepts

4.7.6 Iterative Learning of New Causal Weights in Fuzzy Cognitive Maps

An iterative learning (Karagiannis & Groumos, 2013; Rangarajan et al., 2012) process takes place via a transformation function. The purpose is to update the strengths of causal links in the season connection matrix before it is used in the next concept activation iteration. This function also ensures that the strengths of causal links are within the range $[-1, 1]$ prior to activation of new concepts states. The learning function also removes self-loops to ascertain that a given concept cannot have a causal effect on itself (Figure 4-33).

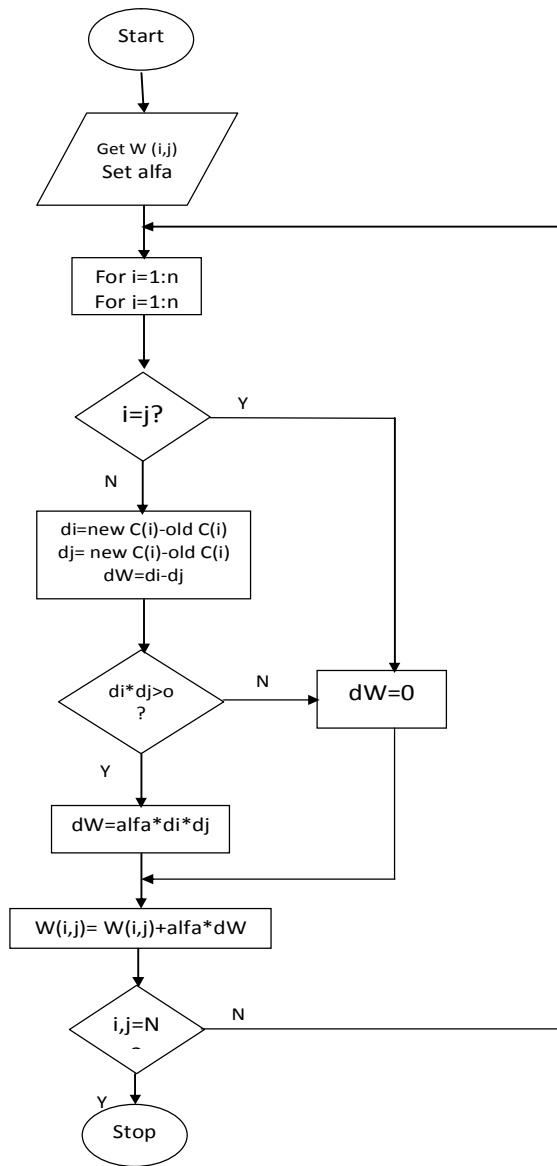


Figure 4-33: Learning Process in FCM

4.7.7 The Likelihoods of Weather Outcomes

On the final run of a simulation process, the output is generated in form of a vector consisting of predicted values of selected weather outcomes. These values are in the range [0, 1] representing the expectation (probability) of the weather outcomes in the next 12-24 hours. The predicted weather outcomes form main input to the (prediction against observation) verification process.

4.7.8 Visualization of Predicted Weather Outcomes

The predicted weather outcomes are visualized using bar charts to depict the variation of the expected weather outcomes. The new causal effects between the concepts are also visualized using a network graph (Figure 4-34) depicting the new relations and strengths of causal effects between the concepts. Since the predicted weather outcomes are in probability values with range [0, 1], a transformation function is used to convert these probability values into human understandable form (linguistic terms describing the likeliness of the predicted weather outcomes). The strongest outcome is also described as the major outcome.

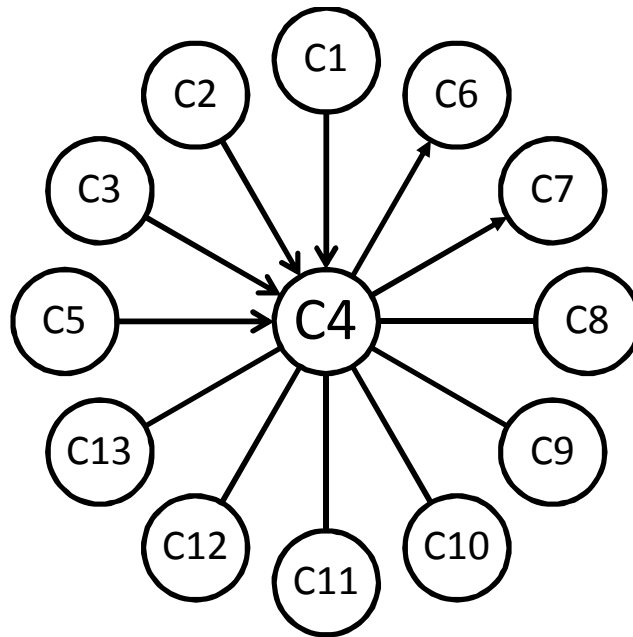


Figure 4-34: Sample Network Graph Depicting Connection in Concepts

4.8 Determination of Forecast Skills for Verification of Visual Weather Lore

4.8.1 Simulation Scenario Outcomes Vs Observations

Daily system simulations are run to predict and record probabilities of weather outcomes (*rain, heat, dry, cold*). Weather observations are captured periodically by use of a wireless sensor weather station. This process is repeated several times until there is sufficient data to use for in verification process. The actual weather observations (measurement) are transformed and normalized to categorical values [0, 1] to match the range of the predicted weather outcomes. The observations are transformed to categorical values (see Table 4–14).

Table 4–14: Transformation Values for Human Weather Descriptions

Observation level (linguistic)	Rain	Dry	Heat	Cold	Values (numeric)
None					0
very low					1
very low					1
very low – low					1
Low					1
low – medium					1
Medium					1
medium – high					1
High					1
high- very high					1
very high					1

To make the verification process simple a procedure is employed to organize the data sets with updated history using time stamps of observed and predicted values (Table 4–15).

Table 4–15: Representation of Observations and Predictions Summary

Concept	Predicted (P)	Observed (O)		Predicted (P)	Observed (O)
	day=1	day=1	...	day=n	day=n
C ₁	P ₁ (1)	O ₁ (1)		O ₁ (n)	P ₁ (n)
.					
C _n	P _n (1)	O _n (1)		O _n (n)	P _n (n)

4.8.2 Verification using Forecast Skills

In the verification process (Figure 4-35 and

Figure 4-36) comparisons are made between the actual observations (O_i) and weather outcome predictions (P_i), values by computing residuals (error values) from the observations. The error values, E_i and the squared error (E_i)² are used to compute the (MSE) Mean Squared Error and the (RMSE) Root Mean Squared Error (Casati et al., 2008; Shrestha, Robertson, J.Wang, Pagano, & Hapuarachchi, 2013) forecast skill scores for each predicted weather outcome.

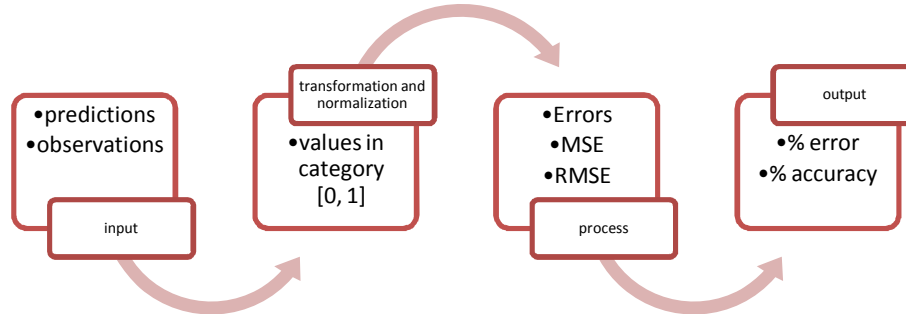


Figure 4-35: Process for Verification of Forecast Skill

The formulae $MSE = \frac{1}{n} \sum_{t=1}^n |E_t^2|$ and $RMSE = \sqrt{\frac{1}{n} \sum_{t=1}^n |E_t^2|}$ are used to compute the verification forecast skills. The MSE and RMSE values are analyzed where smaller MSE indicate that the predictions are closer to the observations. Large values for RMSE are indicative of large errors in prediction. RMSE is a measure of the spread (Mariani & Casaioli, 2008; Thornes & David B Stephenson, 2001) of the observed values about the predicted values. The verification statistics are represented in both summary form and visualized in graphic charts. The process of computing the metrics is as follows.

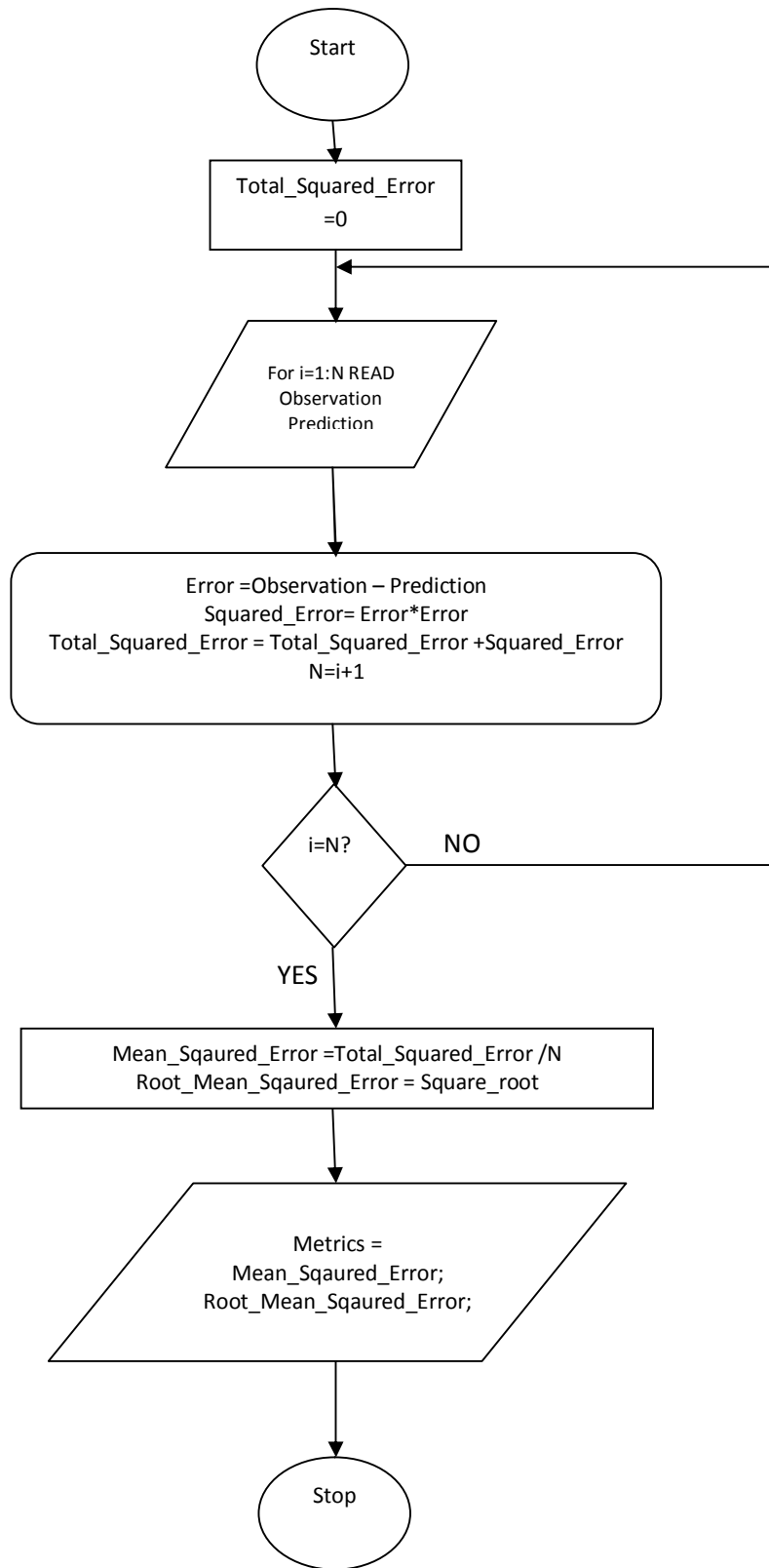


Figure 4-36: Flowchart for Computing Verification Statistics

4.8.3 Summary of the Verification Tool Design

This chapter presented an understanding of the visual weather lore domain. This was followed by the formulation and the definition of requirements, outputs and definition of mathematical logic that entail the visual weather lore verification tool. In Chapter Five, the implementation and working of the visual weather lore verification tool are presented through a series of subsections.

Chapter Five: Implementation of Visual Weather Lore Verification Tool

5.1 Overview of the Tool

This chapter presents the functioning and test results of a visual weather lore verification tool, which is ascertained through experiments in a series of sub components and presenting of results. To start with, a description concerning the vital computational hardware and software configuration of the model is presented. Tests are presented on machine learning methods for sky objects detection. The outcomes of a verification process based on comparison of weather predictions to actual weather observations (using various forecast skills metrics) are presented. For experimental purposes, a configuration of wireless weather sensors are employed as a method of acquiring actual weather observations in real-time. To make evident the validity of the visual weather lore verification model, experiments and results using actual data acquired from Bloemfontein municipality during the month of October/December 2015 are presented. The structure of the sub-components is based on the architecture of the verification tool presented in Chapter Four. The discussions concerning the specifics of the techniques used to realize a working model for visual weather lore verification were presented in the literature review section.

The computational platform for visual weather lore verification consists of data transformations results processing cycles. The combination of data acquisition devices (hardware) and human interaction was important to enhance the results of the visual weather lore verification model. Sky imagers and wireless weather sensor were the main devices for acquiring experimentation data for this type of a verification model. The hardware and software components of visual weather lore verification model form essential parts of discussions in this chapter. The procedural components of the visual weather lore verification model were programmed in parallel. This rendered the model an incremental software artefact that was continuously enhanced during and after development. The realization of individual components consisted of mock-up tests, run in command line to gauge whether the components generate acceptable outputs. After the development, real tests were run by entering data through the model user interface. The model was enhanced with file data logging environment for output post processing and analysis. The visual weather lore verification model presented provides users of the system with an interactive platform for input and output visualizations.

5.2 Detection of Sky Objects

5.2.1 Training of Cascade Detectors for Sky Objects

5.2.1.1 Data Sources and Acquisition

The training of sky objects detectors followed the analysis and designs (Chapter Four). The training was carried out using only selected target sky objects (refer to the discussion on concepts identified in the analysis section). The scope of training data involved valid and quality sky scenes (sky images) obtained using a sky camera.

The detection of sky objects and representation into visual sky concepts relied on the independent (restricted by features of the sky objects) pre-processing of each sky object to match appropriate feature classifiers and object detection techniques. The relationship between the discernible features in sky objects and the classifiers used was vital to successful sky concepts representation. The features of the sky objects dictated the choice of classifiers, while the type of classifiers determined the final detected sky objects. For reliable representation of sky concepts some transformations were necessary to strike some balance between the classifiers' results and each of the final detected sky objects.

In the literature review the various shortcomings allied with visual objects detection (including geometric and photometric changes) were discussed. Apart from the shape and texture contained within sky objects, colour was also a significant feature in the process of recognizing sky objects. Bearing in mind the object detection shortcomings, an initial emphasis was placed on the identification of features associated with sky objects in variations of day and night conditions. In the literature review section it was clearly stated clearly that variations in visual features of an object is the main cause of false positives. This makes the selection of sky objects and their features vital for successful detection of sky objects and representation to visual sky concepts.

The training process was conducted using images in any scale and graphic formats. Scale transformation functions were put in place to handle memory overflow resulting from high resolution sky images. The training sky scenes were provided in both day and night conditions. In experimentation cycles, image metadata were processed to enhance the representation and outputs (see the next section).

5.2.1.2 Meta-Data of the Sky Objects

```
objdate =
16-Oct-2015 06:45:28
```

Figure 5-1: Object Time and Date Meta-Data

```
Command Window
LOC =
    GPSVersionID: [2 2 0 0]
    GPSLatitudeRef: 'S'
    GPSLatitude: [29 6 55.9286]
    GPSLongitudeRef: 'E'
    GPSLongitude: [26 11 25.1829]
    GPSAltitudeRef: 0
    GPSAltitude: 0
    GPSTimeStamp: [16 44 24]
    GPSProcessingMethod: [1x64 double]
    GPSDateStamp: '2015:10:22'

X =
    29.0000    6.0000    55.9286

Y =
    26.0000   11.0000   25.1829

University Rd, Bloemfontein, 9301, South Africa
Park West, Bloemfontein, 9301, South Africa
Bloemfontein, South Africa
Bloemfontein, 9301, South Africa
Bloemfontein, South Africa
Motheo, South Africa
Free State, South Africa
South Africa
```

Figure 5-2: GPS Meta-Data

Sky objects meta-data (Figure 5-1 and Figure 5-2) were processed with date-time zone in 24-hour clock format and GPS coordinates (latitudes, longitudes, compass direction) in degrees, minutes and seconds. The GPS coordinates were transformed to decimal degrees (positive or negative) for mapping in web map and prediction location identification.

5.2.1.3 Selecting Features Descriptors for Identification of Sky Objects

In order to effectively detect a visual object from an input sky scene, the properties of each sky object were described with uniqueness. To achieve this, it was necessary to determine unique feature descriptors that were repetitive and invariant to transformations such as scale, rotation, viewpoint and illumination.

Sky objects were classified to a particular category only if they had similar feature descriptors. The pre-processing of features of sky objects formed the backbone of subsequent detection tasks, since it was necessary to represent high level information about the sky objects (using features as colour, texture and shape). The features identified in pre-processing were the basis in the training of the cascade of sky objects detectors.

The aim of investigating features in sky objects was to exploit the raw pixel information so that the variations between sky objects that had the same features (inter-features variations) were not preserved while variations between features of different sky objects (between-object variations) were preserved.

The detection of sky objects demanded for the best selection of visual features to be extracted. The Local Binary Patterns (LBP), commonly used for extracting image texture features; and the Histogram of Oriented Gradients (HOG), commonly used for getting object shape information, were the considered descriptors of sky objects.













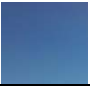





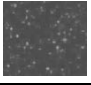




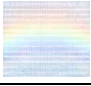


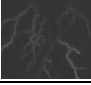






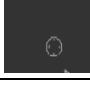


The visual objects on which the cascade classifiers were trained had to be pre-processed satisfactorily for optimal results of the detections. The concern was to generate efficient feature descriptors for the visual sky objects which present excellent robustness under conditions of illumination, scale and clutter that could distort the objects in sky scenes. Some deliberate pre-processing was necessary to uncover the finest feature space which allowed the features from individual sky objects to be distinguished from the rest of the features in an input sky scene. To minimize the constraint of illumination and background in visual sky objects, independent conditions of day and night were pre-processed for use in ultimate decision regarding visual sky concepts representation.

The pre-processing for the visual objects features was realized using a collection of sky images obtained from the open skies of Bloemfontein, Free State, South Africa. The main interest was to

obtain as much as possible a variation of the sky objects required for the detectors training process. The sky scenes were chosen to represent the selected sky objects in various day-time and night-time illumination conditions.

To determine the best feature to use in the detection procedure, the texture, edge and shape feature models were evaluated using test images for the different sky objects. Some sky objects emerge both in day and night; hence where appropriate objects in both illumination conditions were tested (Table 5—1). Several experiments were done to investigate the features of each sky object. The table below shows the visual objects and the features tested as well as an indication of best feature.

Table 5—1: Comparison of Features Descriptors in Sky Objects

Sky Objects	visual features of target object				Best Feature
	Original	Edge	Texture	Shape	
high clouds					Shape
low clouds					Shape
medium clouds					Shape
clear sky					Shape
stars					Shape
rainbow					Shape
lightning					Shape
dark moon					Shape
visible moon					Shape

Similar to other objects recognition tasks, sky objects detection conditions were dictated by the actual conditions intended for the recognition process. The detection of sky objects was a complex task since sky scenes contained rotated, scaled as well as blurred sky objects. The analysis of best feature descriptor showed that shape descriptor could represent the near actual sky object information less invariant to colour and other conditions.

5.2.1.4 Dimensionality Reduction in Sky Objects

Quality sky images contained data that had very high dimensional (in both resolution and quantity), computationally demanding and time-consuming to process. High dimensionality in sky scenes was tackled by eliminating the dimensions that seemed irrelevant for each sky object. This ensured that the sky objects were transformed from the high dimensional spaces to a lower

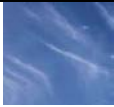



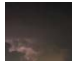


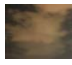



















dimensional space while preserving the important features of the sky objects for subsequent detection tasks. This procedure offered computational payback resulting from processing a smaller amount of data in the sky scenes. Reducing the feature space also facilitated elimination of redundancies in the features of sky objects. The dimensionality reduction process was significant as the final features in sky objects were represented in a more compact and effective way, which enhanced the performance of the detectors.

The input sky scenes were resized by specifying the dynamic size of the output image. To avoid distorting the output images and to maintain the same aspect ratio as the input image, the height was specified to NaN, for dynamic calculation of dimension that can preserve the aspect ratio of the scaled image. The Nearest-neighbour interpolation method (Kennedy, 2010) was applied to assign the output pixels, values that their exact points fell within. The median filtering method was also applied to remove noise (outliers) without distorting the sharpness of the scaled output image.

5.2.1.5 Specification of Data for Training Sky Objects Detectors

Further from determining the features of sky objects and performing dimensionality reduction, choosing training samples to represent the visual objects was of extreme importance. The quality of the training samples was indispensable in the performance of the sky object detectors. The training of cascade detectors for sky objects required specification of positive instances and corresponding sets of negative instances. For each visual object, a variation of 250 images were acquired, and where possible to represent as much as possible similar objects in varying scale and illumination during day and night conditions (Table 5—2).

Table 5—2: Sample Variation of Sky Objects

Sky Object	Orientation	Scale	Illumination
high clouds			
low clouds			
medium clouds			
clear sky			
stars			
rainbow			
lightning			
dark moon			
visible moon			

5.2.1.6 Specifications of Negative Instances for Visual Sky Objects

A collection of 1750 images per sky object were used as ‘negative samples’. These were the objects that associated to the non-target sky objects. To supplement the ‘negative samples’ datasets, several images that did not contain target objects were collected from NASA photos in the flickr website (<https://www.flickr.com/photos/gsfrc/>). For better detection accuracy, objects that resembled targeted sky object (false positives) were also incorporated into their respective sets of negative samples. These datasets were duplicated by rotating the images to obtain 3500 samples. More negative samples were generated from the existing samples by varying the object brightness. Thus, a total of 7000 samples per sky object were used as negative samples. During the training of ‘object detectors’, the negative training samples were not specified explicitly as the detector function automatically generated negative samples from the supplied negative

instances that did not contain the target sky objects. Given that the detector function worked in stages, detected false positives were automatically generated as negative samples in subsequent training stages.

In the sky panorama, there were a quite a number of unrelated (Figure 5-3) objects (such as clear-sky and white clouds; moon and round clouds) which during experimentation, the sky object detectors erroneously identified as similar objects. The confusion mainly resulted from colour and the shape information of sky objects.



Figure 5-3: Samples of Similar Sky Objects

5.2.1.7 Specifications of Test Samples and Positive Instances for Visual Sky Objects

A variation of 250 new images for each sky object were acquired, and where applicable, with varying illumination (during day and night conditions). To comprehensively represent test instances for each of the sky objects, the test samples were specified into three categories. The first test set consisted of sky scenes containing target sky objects. The second test set consisted of scenes that did not contain the target sky objects. The third test set contained objects that looked like the target sky objects. The test samples were duplicated at run time by rotating the images to obtain 500 samples. More positive test samples were generated at run time from the existing samples by varying object brightness. In total, 1000 samples containing target objects were tested for each object detector. For each detector the other two (sets of non-target objects; and sets containing only similar to target objects) test samples consisted of 1000 samples respectively. These test sets were derived from the difference between the target sets and that of other sky objects followed by duplications using geometric and photometric transformations.

The positive training sets consisted of 250 images per sky object. The sets were duplicated (Figure 5-4), by rotating and flipping the images to generate 500 samples. This number was doubled by varying object brightness, generating a total of 1000 samples per sky object. To reduce the memory requirement and enable easy comparisons of sky objects the images in the

training sets were transformed to a common resolution of 252 by 127 pixels. The positive samples were specified via rectangular Regions of Interest (ROI) in the whole images where appropriate. The ROI contained the location in coordinates of the objects of interest. Another approach that was used is that of cropping out the object of interest from the whole image and then supplying the coordinates of the whole images as ROI. In this research the majority of rectangular ROI in the whole images were specified by using the ‘Training Image Labeller’ application to delineate ROIs with bounding boxes, followed by generating outputs represented by array of structures for use as positive training instances.

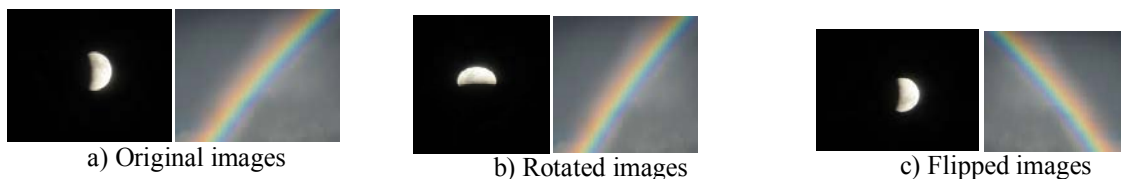



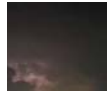












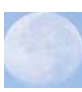


Figure 5-4: Example of some manipulated sky objects

5.2.1.8 Benchmarks of Visual Objects

A specification of benchmark sky objects were provided for each sky object. The benchmark formed the ground truth for evaluating the quality (similarity) of detected target sky objects. In appropriate circumstance two benchmark sky objects were specified for the day and night images respectively. The dimensions of the benchmarks were transformed to common size of 252 by 127pixels. The day and night images (Table 5—3) were designated dynamically based on the time meta-data of detected sky scene.

Table 5—3: The Ground Truths for Visual Sky Objects

<i>visual sky</i>	<i>day image</i>	<i>night image</i>
high clouds		
low clouds		
medium clouds		
clear sky		
stars		
rainbow		
lightning		
dark moon		
visible moon		

5.2.1.9 Feature Based Sky Objects Detectors

In literature review, the exploitation of colour as a feature in objects detection tasks has been found to be problematic. This is because it is subject to changes in illumination and lighting; the same object can generate different colour information. The inherent problem made the colour features unreliable for exploitation by sky objects detectors. However, the Histogram of Oriented Gradients (HOG) was acknowledged as feature descriptors widely used for shape-based image classification tasks. In addition, the Local Binary Pattern (LBP) and Haar image features

descriptor are binary descriptor used to extract texture feature in images. In literature review complete discussions on the working of the techniques of representing image features using descriptor were presented. Confirmation tests in this study showed that it was computationally expensive to train sky object detectors using the Haar descriptor. Thus, in this study, sky objects detection was based on a cascade of classifiers trained using HOG image feature descriptors. The training and testing data were generated using the procedures discussed under the data for training the sky objects detectors.

To detect sky objects in input sky scenes, target sky object specific cascade detectors were used to scan the input scene at multiple window positions with varying scales. At each scanned positions, the detectors assessed sub-windows for classification as containing target sky object. The concept of using sliding windows was an intentional task that enabled the detection of multiple sky objects in one input sky scene.

Each sky object detector worked in multiple stages that were ensembles of weak learners or simple classifiers. The weak learners in detectors stages were trained using an adaptive boosting technique which enabled the training of perfect sky object detectors. The adaptive boosting technique computed a weighted average of the resolutions from the weak learners at each of the detectors training stages.

During training and detection stages the classifiers marked the sub-window defined by the present position of the sliding window as either contained or did not contain a target sky object. A positive value was used to indicate that a target sky object was found while a negative value was used to indicate the target sky object was not found. If a position was marked with a negative value, the classification of the position was completed with a decision that the target sky object was not found, and the detector adjusted the window to the next position. Positions marked using positive values were moved for processing in the next detection stage. If the final detection stage assigned a positive value to the moved position, then the detectors could account for sky object as found at the window position. The use of multiple stages permitted the detectors to reject non target sky objects soonest possible. The assumption was that the majority of the scanned window positions did not contain the target sky objects. The use of a multistage detector increased the accuracy of detecting sky objects at the same time reducing the processing time.

The multistage detectors used both simple (with few number of features) and complex (with more number of features) classifiers. The simple classifiers were employed in early stages of detection to discard most of the false positives, while complex classifiers were used in the later detection stages to discard more complex sub-windows.

5.2.1.10 Important Factors Considered for Sky Objects Detectors

The training of the final sky objects detectors was cascaded by using the results of detections in the previous stages to train subsequent stages. Prior to the training of new stages, a cascade function tested the detector consisting of the stages already trained on parts of the supplied negative instances. The assumption was that some positions in the negative instances might be assigned positive values leading to false positives. The classifier moved the detected false positives to the next training stage as negative instances. The cascading of classifiers allowed subsequent training stages of the detectors to correct mistakes made in the previous training stages.

During detectors training and detection process, three different situations were expected to occur. The first (an ideal situation) was that the detectors correctly identified target sky objects leading to true positives. Second, false positives were expected when the detectors erroneously assigned negative instances as positive values (meaning that target sky objects were present). The third situation was that false negatives were expected when the detectors erroneously assigned positive sky objects negative values (i.e. target sky objects were not found). In the third situation, when a detector training and detection stages had a low false negative rate, the detector erroneously marked a positive sky object as negative. In this situation, the detection process completed, and the detector could not correct the mistake. In the second situation, the detectors made use of high false positive rates, enabling the correction of mistakes by subsequent stages if negatives instances were assigned positive values.

The overall false positive rates (Table 5—4) of the detectors were determined by multiplying the false positive rate (F) and the number of training stages (S). The value F was the false positive rate per visual sky object detector stage (lying in the open interval (0 1)). Likewise, the overall true positive rate per sky object detector were determined by multiplying the true positive rate per (T) the number of training stages (S). The value T, was the true positive rate per detector stage (lying in the open interval (0 1)). Experiments revealed that increasing the number of

training stages reduced the overall false-positive rate while reducing the overall true positive rate. To make sky objects comparison easier, a common false and true positive rates ($F=0.2$ and $T=0.98$) was used for all detectors.

Table 5—4 : Evaluation of the Training Factors for Sky Objects Detectors

Detectors	number of samples		Number of Training Stages (S)	False Positive Rate (F)	True Positive Rate (T)	F*S	T*S
	positive	negative					
high clouds	1000	7000	18	0.2	0.98	3.6	17.64
low clouds	1000	7000	15	0.2	0.98	3	14.7
medium	1000	7000	15	0.2	0.98	3	14.7
clear sky	1000	7000	10	0.2	0.98	2	9.8
stars	1000	7000	10	0.2	0.98	2	9.8
rainbow	1000	7000	15	0.2	0.98	3	14.7
lightning	1000	7000	15	0.2	0.98	1	14.7
dark moon	1000	7000	10	0.2	0.98	2	9.8
visible moon	1000	7000	10	0.2	0.98	2	9.8

Reducing the detector false positive rates led to some difficulty in the generating of negative instances between the training stages. This difficulty was alleviated by pre-processing as many negative instances (7000 samples) for each of the sky objects detectors as achievable.

The selection between using fewer detector training stages with a lower false positive rate per stage or more training stages with a higher false positive rate per stage was very critical. Training sky object detectors stages' using lower false positive rates led to difficulty as the majority of the final trained stages contained weak learners. The sky object detectors were trained using stages with a higher false positive rate and as a result they contained the minority of weak learners.

The training results of the sky objects detector provided important information on the rate of false positives and true positives that occurred after using specific number of training stages. Tuning of the number of training stages, the false alarm and true positive rates, was done considering the information arising from training results so that the requirements of individual sky object detectors were satisfied.

Ideally, it was attractive to train the sky object detectors with a greater number of stages since the overall false positive rates reduced at each stage. On the other hand, increasing the number of detector training stages raised the false negative rate which increased the probability of

erroneously discarding positive sky object instances. To obtain a balance between the training factors the sky objects detectors were trained using a maximum of twenty stages and a lower false negative rate (since using less number of training stages with a lower false negative rate gave satisfactory overall false positive rates).

5.2.1.11 Features Preference in of Sky Objects Detectors

The sky objects detectors were trained using two types of features descriptors: Local Binary Patterns (LBP) and Histograms of Oriented Gradients (HOG). Using the HOG provided advantages over LBP feature descriptors. This is because the HOG descriptor proved reliable when operating on localized image cells (Table 5—5), hence sustaining invariance to geometric and photometric transformations of the sky objects.

The sky object detectors (based on LBP and HOG features) were independently tested using bulk sets consisting of 1000 target sky objects at various scales and orientations; the aim of this test was to find the best feature model (Table 5—5) for the final sky objects detectors. The conditions of the test instances were as explained in the section regarding specifications of test instances.

Table 5—5: Evaluation of Feature Models for Sky Objects Detectors
% of positive (negative) detections using 1000 samples containing target (non-target) sky objects

Detectors	% of positive (negative) detections using 1000 samples containing target (non-target) sky objects		best feature model
	LBP features	HOG features	
high clouds	88.004, (14.94)	90.812, (17.446)	HOG
low clouds	89.642, (17.442)	88.472, (12.442)	LBP
medium clouds	90.344, (16.608)	91.28, (12.442)	HOG
clear sky	89.876, (22.446)	88.238, (13.276)	LBP
stars	88.472, (14.944)	91.28, (10.77)	HOG
rainbow	90.578, (22.446)	89.174, (10.774)	LBP
lightning	89.642, (19.944)	90.11, (18.28)	HOG
dark moon	90.11, (18.28)	91.046, (14.94)	HOG
visible moon	88.706, (18.28)	90.578, (11.604)	HOG

5.2.1.12 Normalized Image Intensity Histograms/ Histogram Equalization

HOG feature descriptors were used for symbolic representation of visual sky objects. The features of sky objects had considerable intra-class variations in each sky object that were difficult to represent and preserve. Histogram contrast normalization was used to minimize the intra class variations. The processing of HOG descriptor involved dividing an image into small connected regions (cells) and for each cell calculating a histogram of gradient directions (edge orientations) for the pixels within the cell. The combination of these histograms of edge orientations was used to represent the HOG descriptor. The performance in using the HOG descriptors was enhanced by normalizing the contrast of the local histograms for the sky objects. The normalization process rendered the sky objects to a common resolution. The normalization was done before partitioning the sky objects into equal-sized grid blocks as well as computing the HOG features of the blocks. To normalize, the intensity value across larger sky object blocks were computed and the resulting value used to normalize the values of all the cells within the sky object block. The significance of the normalization process was that it enhanced the sky images, building an add-on to HOG invariance to changes in sky object illumination and shadowing. The normalization procedure was necessary before the training and testing of the sky objects detectors. This was due to the fact that, the representation of each sky objects consisted of distinctive features associated with its blocks. Adjusting the cell size of HOG descriptors influenced the descriptor parameters on the sky objects detection. The detectors were trained using the default cell size of 8x8, which proved to be the finest by its smallest rate of false positives.

5.2.1.13 Representations of Sky Objects Detectors as XML Files

A mechanism of representing the trained sky object detectors in symbolic form was essential before subjecting the detectors to experimental tests with input sky scenes. The trained sky object detectors were self-sufficient and liberated of any samples of training objects since all the information on sky objects features were represented in the form of decision trees. Self-defining Extensible Mark-up Language (XML) detectors (Figure 5-5) were generated. The structure of the detectors was embedded in the XML files, thus new sky objects were detected without rebuilding the detectors, making it possible for the features of the sky objects to be dynamically re-generated within the XML representations.

```

<?xml version="1.0"?>
<opencv_storage>
<!-- Created using Computer Vision System Toolbox(tm) for MATLAB(R) -->
<!-- Version 8.3.0.532 (R2014a) -->
<!-- Compatible with OpenCV 2.4 -->
<cascade>
  <stageType>BOOST</stageType>
  <featureType>HOG</featureType>
  <height>32</height>|
  <width>36</width>
  <stageParams>
    <boostType>GAB</boostType>
    <minHitRate>9.8000001907348633e-01</minHitRate>
    <maxFalseAlarm>2.0000000298023224e-01</maxFalseAlarm>
    <weightTrimRate>9.4999999999999996e-01</weightTrimRate>
    <maxDepth>1</maxDepth>
    <maxWeakCount>100</maxWeakCount></stageParams>
  <featureParams>
    <maxCatCount>0</maxCatCount>
    <featSize>36</featSize></featureParams>
  <stageNum>6</stageNum>
  <stages>
    <!-- stage 0 -->
    <_>
      <maxWeakCount>1</maxWeakCount>
      <stageThreshold>1.</stageThreshold>
      <weakClassifiers>
        <_>
          <internalNodes>
            0 -1 1 8.6157033219933510e-03</internalNodes>
          <leafValues>
            1. -1.</leafValues></_></weakClassifiers></_>
    <!-- stage 1 -->
    <_>
      <maxWeakCount>1</maxWeakCount>
      <stageThreshold>1.</stageThreshold>
      <weakClassifiers>
        <_>
          <internalNodes>
            0 -1 6 2.8644487261772156e-02</internalNodes>
          <leafValues>
            -1. 1.</leafValues></_></weakClassifiers></_>
    <!-- stage 2 -->
    <_>
      <maxWeakCount>1</maxWeakCount>
      <stageThreshold>1.</stageThreshold>
      <weakClassifiers>

```

Figure 5-5: Segment of XML Representation of Detectors

5.2.1.14 The Performance of Sky Objects Detectors

The performance of each sky object detector was independently assessed by computing the rate of positive detection, which was the percentage of positive detections in pre-processed collections of test sky scenes. A performance evaluation function (see code below) was implemented in parallel with detector tests to account for the percentage rates of detection in each of the three test situations.

```
read (bulk set)  
n=number of objects;  
for object=1:n  
    begin  
        count=0;  
        detection procedure;  
            if(detected)  
                extract procedure;  
                count=count+1;  
            else  
                count=count;  
            endif  
        performance=count/n*100;  
    end for
```

During sky objects detections the descriptors corresponding to the regions of the sky objects within the detection window were generated. These descriptors were then classified according to the decision trees models in the XML files illustrated in section 5.2.1.13. The detection process allowed positive values to be assigned at multiple sub-window locations, and at varying scales determined by the minimum and maximum bounding box specifications. The assignments of positive values in this way led to multiple sky objects detections occurring at different image locations and scales. The multiple detections occurred to both the patterns of recurring objects (such as high clouds) and distinct sky objects (such as the moon) in the input sky scene. The multiple detections resulted from training the sky object detectors to be insensitive to small localization errors in sky objects. The multiple detections (Figure 5-6) also appeared as overlaps around the background of the detected sky objects. During training of the sky object detector the consistency of true positives was greater than that of false alarms (overlaps). The information arising from overlaps around detected sky objects was useful in reducing the false alarms and combination of true sky object detections.

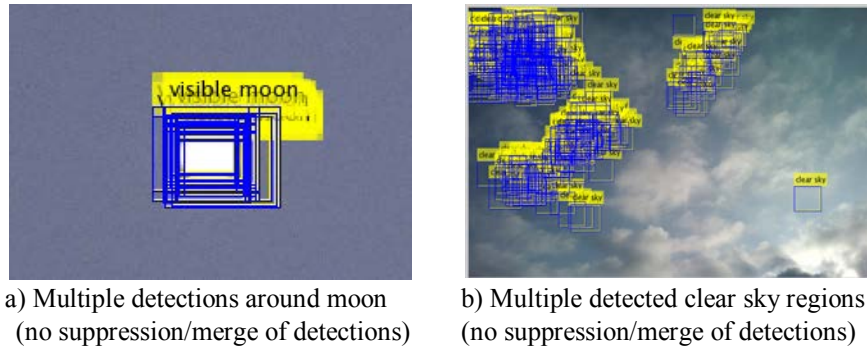


Figure 5-6: Multiple Bounding Boxes (selection) Around detected Objects

The multiple sky objects detections were processed in various approaches. The simplest approach was to select the strongest detection (scoring the detections and selecting the one with maximum confidence score). A second approach was to compute the average of the bounding boxes at each detected sky object location (in the normal flow of sky objects detections). The averages of the detected bounding boxes were also weighted using their confidence scores.

The detectors were tested using sets of one thousand images to gauge their performance, and obtain some useful statistics (Table 5—6). The merge thresholds were amplified to limit false detections and reduced to return strong positives in unlimited detections. The testing of sky objects detectors provided information on the rate of true positives that occurred when varying merge thresholds were applied to the specific test (with target object; with objects similar to target object; and with non-target objects) sets.

Table 5—6: Determination of Optimal Merge Thresholds for Sky Object Detectors

detector	merge threshold	% of positive detections in 1000 test samples		
		set with target object	set with objects like target object	set without target object
high clouds	1	91.6667	80.6452	75.6098
	2	58.5366	50	22.5806
	3	29.6667	21.2683	3.2258
	4	19.3333	18.5122	3.2258
low clouds	1	100	100	47.6190
	2	96.7742	64.5161	38.0952
	3	96.7742	58.0645	33.3333
	4	96.7742	41.9355	33.3333
medium clouds	1	100	100	52.3810
	2	100	50	33.3333
	3	100	42.8571	20
	4	93.5484	23.8095	15
clear sky	1	90.2439	85.4271	84.4444
	2	80.4878	62.3116	48.8889
	3	65.8537	52.7638	42.2222
	4	53.6585	43.7186	33.3333
rainbow	1	88.8889	75	19.0476
	2	68.7500	60	0
	3	68.7500	37.7778	0
	4	62.5000	26.6667	0
lightning	1	100	91.6667	47.6190
	2	100	88.3333	42.8571
	3	100	86.6667	42.8571
	4	100	83.3333	42.8571
dark moon	1	100	74.1935	57.1429
	2	88	41.9355	30.9524
	3	56	22.5806	9.5238
	4	36	9.6774	2.3810
visible moon	1	85.4271	25.8065	28.6585
	2	83.4171	16.1290	12.1951
	3	81.4070	12.9032	6.0976
	4	79.8995	9.6774	4.8780

By analyzing the test results, the default settings of the merge threshold parameters were adjusted accordingly to optimize the outcomes of each sky object detectors. To enhance the sky objects detectors accuracy merge threshold (Figure 5-7) functions were applied before extracting the final detected sky objects.

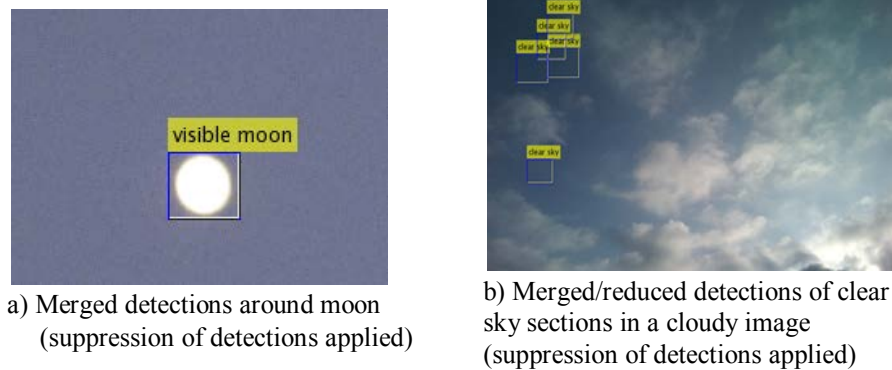


Figure 5-7: Effect of Merge Threshold (Mathworks 2014 Software was used)

5.2.1.15 Benchmarks between Detected and Ideal Sky Objects

The rationale of sky objects detection process was to identify the presence of specific sky objects in input sky scenes. The identified visual objects were expected to appear contradictory in different sky panorama, hence the results on the detected sky objects needed to be reviewed based on input occasion and the determination of appropriate ground truths. The benchmark process did the task of extracting the detected sky objects and pre-processing them, selecting an appropriate ground truth and representing the extracted sky object in the form of a sky concept. The representation of a sky object as a sky concept (a value in the range $(0, 1)$; which was also the probability of the extracted object matching to specified ground truth), enabled some exploitation in the weather scenario prediction component based on fuzzy cognitive mapping.

5.2.1.16 Extractions of Detected Visual Sky Objects from Sky Scenes

The extraction (Figure 5-8) of detected sky objects was a pre-processing task in the process of approximating the presence of visual sky objects in sky scenes. Before extraction the results from the sky objects detectors were reviewed to determine for each sky object the best detections. The position (coordinates) values of detected sky objects that were recomputed by the merge threshold function were a critical ingredient to the extraction process. The positions of detected sky objects in the input sky scene were marked for extraction. Once the extraction was completed, the extracted sky objects were represented as independent object files that were isolated from the input sky scenes. The process of extracting sky objects relied on the detection results as follows:

```
if (Detected object)
    extraction object;
    save as independent object;
    other procedures;
endif
```

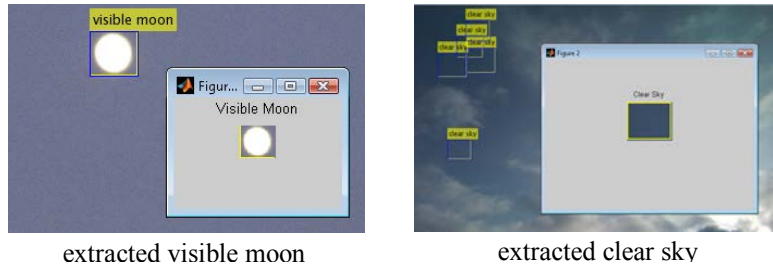


Figure 5-8: Independent Extracted Object

5.2.1.17 Symbolic Representation of the Presence of Sky Concepts

The performance sky object detectors (in terms of percentage of correct detections and false positive rates) were not enough to symbolize the presence of sky objects in sky scenes. The results provided by detectors had to be processed, to provide some dependable truths about the sky objects. The detected sky objects were accounted for by estimating their presence in input sky scenes. The extracted sky objects were benchmarked based on their association to some precise objects (in some sections referred to as the ground truth). The detected sky objects needed to be represented as sky concepts for further computation in the predictions component.

The tasks of representing sky objects to sky concepts were detector dependent; the extracted sky objects were scored at the detector levels based on how accurate the detectors generate bounding boxes that were comparable to the ground truth. The extracted sky objects were pre-processed and benchmarked using techniques of object similarity measures. In some similarity measures the match values were inversely proportional to the metric between the extracted sky object and the ground truths.

5.2.1.18 Elective Day and Night Ground Truths

The ground truth on some of the sky objects (such as visible moon and clear-sky) varied depending on lighting conditions. As a pre-processing process, sets of sky objects for both day and night lighting conditions were specified. Histogram equalization was necessary to reduce variations in brightness and contrast of the sky objects within the specific lighting conditions (day or night).

```
visiblemoonExtract = imresize(visiblemoonExtract, [252 127], 'nearest');  
if (day_startTsec<scene_time2)||(day_startTsec==scene_time2)&&(scene_t...  
ime2<day_endTsec)||(day_endTsec==scene_time2)  
    visiblemoon_base=imread(*);  
else  
    visiblemoon_base=imread(*);  
end
```

5.2.1.19 Similarity Scoring of Extracted Sky Objects

Similarity scoring of extracted sky objects was of great significance in the attempts to account for the correspondence between detected sky objects and some positional ground truths. The scoring of extracted sky objects was based on testing a combination of well-known features humans use for visual perception, with a consideration that the human visual cognition system is well tailored for discriminating structural information from visual objects. The benchmark tests were not meant to penalize the quality of the extracted sky objects, but to compute some proximity of detected objects to specified ground truths. Apart from producing outputs for use in the prediction component, the similarity scoring acted as a supplementary quality assessment process for the results of sky objects detectors. The assumption here was that similar sky objects did not qualify as perfect matches to their principal objects but did contain some acceptable deviation in distances. In the benchmarking section, algorithms for extracting shape, colour and texture information in visual objects was investigated as candidates for sky objects benchmarking, and their performances compared using a collection of 1000 positive/negative instances per sky object. The rationale for testing both positive/negative instances was due to the fact that while the sky objects detectors were expected to generate positive detections, the number of false positives detected should be negligible.

5.2.1.20 Shape-based Benchmark Tests

Histogram of Oriented Gradients

The HOG features of extracted sky object were generated by first computing the magnitudes of gradients and their orientations (directions) over the entire object.

The magnitude of the gradients was computed by:

$$|G| = \sqrt{I_x^2 + I_y^2} \dots\dots\dots \text{Equation 5-1}$$

And the orientation of the gradients was computed by:

$$\theta = \arctan \frac{I_y}{I_x} \dots\dots\dots \text{Equation 5-2}$$

The gradients that had small magnitudes were transformed to zeros. The image grid cells were aligned to the object position. Orientation histograms were generated for each object cell, by quantizing the gradient directions. The gradient thresholds were added in orientation bins. The orientation histograms were stacked into one vector of length N*C. (The value of N represented the number of orientation bins while the values C representing the number of object cells.) After stacking the resultant vector was normalized to a unit length with the normalization factor using either of the forms:

$$f = \sqrt{\frac{v}{\|v\|_1 + e}} \dots\dots\dots \text{Equation 5-3}$$

$$f = \frac{v}{\|v\|_1 + e} \dots\dots\dots \text{Equation 5-4}$$

$$f = \frac{v}{\|v\|_2^2 + e^2} \dots\dots\dots \text{Equation 5-5}$$

The unit vector consisted of the HOG features that uniquely represented the extracted sky object.

5.2.1.21 Edge Based Benchmark Tests

Edge detection methods were used to discover points in extracted sky objects where brightness changed abruptly (mathematically referred to as discontinuity). The discontinued points in

extracted objects were organized into sets of segments with curved lines (edges). Edge features were extracted objects using the canny and LoG edge detection algorithms.

Canny edge algorithm of detecting discontinuities in image intensities was devised by John Canny (an Australian computer scientist). The Canny edge algorithm aims at the derivation of an optimal smoothing filter for minimizing multiple responses to single edge detections. In Canny, the edge points are determined using points in an image where the magnitude of gradients presume local maximum in the gradient direction.

The procedure of deriving a Canny edge in extracted sky objects follows these steps:

- I. The first step was to apply a Gaussian smoothing filter to an extracted sky object using the formula:

$$S[i, j] = G[i, j, \sigma] * I[i, j] \dots \dots \dots \text{Equation 5-6}$$

The value I [i,j] represented the extracted object; G[i,j,σ] was the Gaussian smoothing filter, and σ was the spread of the Gaussian that was used to control the smoothing degree. The outcome of the convolution of an extracted object with the Gaussian filters led to an array matrix representing a smoothed object S[i, j]

- II. The second step was to calculate the magnitudes of gradients and orientations in the smoothed objects. This was achieved by using gradient of the smoothed array matrix S[i, j] to generate x and y partial derivatives, followed by applying the finite-difference method to approximate the partial derivatives.

$$\frac{\partial S}{\partial x} = S[i, j] * G_x$$

$$\frac{\partial S}{\partial y} = S[i, j] * G_y$$

$$M[i, j] = \sqrt{\frac{\partial S^2}{\partial x} + \frac{\partial S^2}{\partial y}} \dots\dots\dots \text{Equations 5-7}$$

$$\theta[i, j] = \arctan\left(\frac{\partial S / \partial y}{\partial S / \partial x}\right)$$

III. The third step was to establish object edge directions by applying non-maxima suppression to the magnitudes of the gradients. Successful establishment of the edge directions was followed by the alignment of the edges to the directions that can be traced in an object. For each and every pixel (i,j) in an object some the direction was computed that can best approximate the direction of the object pixel.

IV. The final step was applying the double threshold algorithm that links edges in an object.

Laplacian of Gaussian

The Laplacian of Gaussian edge feature extraction process was done in two steps. The first step was to apply a Laplacian derivative filter to determine areas of abrupt variation (or edges) in an extracted object. The second step was to smooth the object by applying the Gaussian filter.

$$L(x, y) = \nabla^2 f(x, y) = \frac{\partial^2 f(x, y)}{\partial x^2} + \frac{\partial^2 f(x, y)}{\partial y^2} \dots\dots\dots \text{Equation 5-8}$$

The Laplacian and Gaussian functions can be combined to obtain a single equation that includes the smoothing Gaussian filter as follows:

$$LoG(x, y) = -\frac{1}{\pi \sigma^4} \left[1 - \frac{x^2 - y^2}{2\sigma^2} \right] e^{-\frac{x^2 + y^2}{2\sigma^2}} \dots\dots\dots \text{Equation 5-9}$$

The LoG (Laplacian of Gaussian) operator obtained the second derivative of the object. Object parts that are uniform gave LoG values of zero, while abrupt changes occurring in an object gave LoG values that were positive.

5.2.1.22 Texture -based Benchmark Tests

An image texture is a metric that can be used to depict in sequence the spatial arrangement of colour or intensities in an image. Texture is an important feature in distinguishing image contents. Various methods (such as Entropy and GLCM) were used to extract texture in sky objects.

Entropy

Entropy measured the randomness to represent the texture of an extracted sky object using the formula:

$$\text{sum}(p \cdot \log_2(p)) \dots \dots \dots \text{Equation 5-10}$$

The value p was a count of object histograms that were determined from an RGB object.

Mathematically the entropy can be represented by:

$$Entropy_i = \frac{1}{MN} \sum_{x=1}^M \sum_{y=1}^N I_i(x,y) (-\ln I_i(x,y)) \dots \dots \dots \text{Equation 5-11}$$

where $I_i(x,y)$ is an object with dimension $M \times N$

Grey Level Concurrence Matrix

The procedures of calculating extracted objects texture features utilized the values of the GLCM to measure the variation in intensity or texture between extracted object pixels. A GLCM comprises information regarding the locations of object pixels that have similar grey levels. To come up with a GLCM a displacement vector $d = (dx, dy)$ was determined. From the vector d, pairs of image pixels that have grey levels (i,j) and separation d were counted. A $n \times n$ dimensional GLCM was formed, where n is the number of grey levels determined from an extracted sky object.

5.2.1.23 Colour Based Benchmark Tests

Colour was not reliable in detection tasks, since visual objects changed colour subject to geometric transformations and varying illumination. However, in the task of matching predefined sky objects, colour information proved important. To compare extracted sky objects the three independent colour channels (red, green and blue) were extracted from the pairs of detected objects and ground truths for matching purpose.

Euclidean Distance

The Euclidean Distance (Delta-E) is a single number representing the distance between colour channels images. Delta-E was determined by calculating the Euclidean distance difference between the red, green and blue channels in extracted objects and ground truths. The change in the distance ΔE_{ab} between the objects was computed by using the formula

$$\Delta E_{xy}^* = \sqrt{(r_x^* - r_y^*)^2 + (g_x^* - g_y^*)^2 + (b_x^* - b_y^*)^2} \dots\dots\dots \text{Equation 5-12}$$

Where r^* is the red colour channel, g^* is the green colour channel and b^* the blue colour channel of the objects (x= ground truth; y=extracted object).

Structural SIMilarity Index

The technique of Structural SIMilarity (SSIM) index was used in determining the correspondence between extracted object and ground truths. The SSIM measure was considered as a quality comparison of an image to another image that is of perfect quality. In SSIM the ground truth was assumed to be a perfect and distortion-free image. The SSIM index was measured on a range of common-size windows of extracted object and ground truth. Given two windows (x=ground truth and y=extracted object), of size N×N the SSIM was determined by:

$$SSIM(x, y) = \frac{(2\mu_x\mu_y + c_1)(2\sigma_{xy} + c_2)}{(\mu_x^2 + \mu_y^2 + c_1)(\sigma_x^2 + \sigma_y^2 + c_2)} \dots\dots\dots \text{Equation 5-13}$$

5.2.1.24 Comparison between the Benchmarks

The above bench mark tests were subjected to bulk data sets containing 1000 images per sky concept and in three varying sets of situations. Detected sky objects were subjected for similarity benchmark; the preferred scores were greater than or equal to 0.5 for detected sky objects. A

transformation function was used in parallel with benchmarks tests to account for the percentage of objects benchmarked with scores greater than 0.5 in each of the three situations. The rationale for setting scores greater than 0.5 was that the extracted sky objects were expected to resemble an average similarity to their corresponding ground truths.

```
read (bulk set)
n=number of objects;
for object=1:n
  begin
    count=0;
    detection procedure;
    if(detected)
      extract procedure;
      benchmark procedure;
      if(benchmark>threshold)
        count=count+1;
      else
        count=count;
      endif
    else
      count=count;
    endif
    performance=count/n*100;
  end for
```

The benchmark results (Table 5—7 and Table 5—8) were useful in comparing the similarity check methods. The percentage scores for each feature were represented in the table, with the best measure identified in the last column.

Table 5—7: Performance of Measures for Benchmarking Negative Instances to Ground Truths

Sky Objects	Percent of Scores > 0.5 per 1000 Samples of Positive Instances							Selected Benchmark
	Delta E (Colour Based)	SSIM (Colour Based)	Canny (edge Based)	log (edge Based)	Entropy (Texture)	SIFT (Texture Based)	HOG (Shape Based)	
High clouds	88.3333	26.6667	41.6667	41.6667	88.3333	88.3333	88.3333	HOG
Low clouds	96.7742	16.1290	58.0645	54.8387	100	100	100	HOG
Medium clouds	100	19.3548	67.7419	67.7419	100	100	100	HOG
Clear sky	80.4878	78.0488	4.8780	4.8780	80.4878	80.4878	80.4878	HOG
Stars	40.4762	2.3810	23.8095	35.7143	100	88.0952	100	HOG
Rainbow	68.7500	0	0	0	75	75	75	HOG
Lightning	84.4444	0	93.3333	95.5556	93.3333	88.8889	100	HOG
Dark moon		32	100	96	100	100	100	HOG
Visible moon	80.4020	48.7437	0	0	83.4171	83.4171	83.4171	HOG

Table 5—8: Performance of Measures for Benchmarking Negative Instances to Ground Truths

Sky Objects	Percent of Scores>0.5 per 1000 Samples of Negative Instances							Selected Benchmark
	Delta E (Colour Based)	SSIM (Colour Based)	Canny (edge Based)	log (edge Based)	(Texture Based)	(Texture Based)	HOG (Shape Based)	
High clouds	22.5806	12.9032	19.3548	19.3548	22.5806	22.5806	22.5806	LoG
Low clouds	40	8.3333	16.6667	16.6667	40	38.3333	40	LoG
Medium clouds	50	25	18.3333	23.3333	50	48.3333	50	LoG
Clear sky	48.8889	35.5556	2.2222	2.2222	48.8889	48.8889	48.8889	LoG
Stars	26.6667	6.6667	6.6667	6.6667	26.6667	26.6667	26.6667	LoG
Rainbow	19.0476	0	0	0	19.0476	19.0476	19.0476	LoG
Lightning	0	0	0	0	4.7619	4.7619	4.7619	LoG
Dark moon	4.7619	9.5238	9.5238	9.5238	9.5238	9.5238	9.5238	HOG
Visible moon	9.1463	9.1463	0	0	11.5854	12.1951	12.1951	LoG

5.2.1.25 Joint Features Benchmarks Tests

Joint benchmark features were realized by combining set of features (such as colour; texture; shape; and edge) that were unique to sky objects. The major importance of employing joint features to benchmark sky objects was that there were rare possibilities for joint features to be ambiguous. The assumption was that two or more sky objects with the same colour features could not have the same edge, shape and texture features. Computation of joint feature histograms was computationally more intensive (as several features tests and comparisons needed to be processed) than single feature tests, but led to better performance in sky object benchmark results. Tests were conducted using 1000 positive instances to evaluate benchmarks.

With single benchmarks, averages of 10 images were processed per second, while the joint benchmark tests processes an average of 2 images per second.

5.2.1.26 Restraining of Complementary Sky Concepts

The relationships between the detected sky concepts were evaluated for proper representation of overriding and overlapping complementary and supplementary sky concepts. The distinction between related sky concepts led to variation in terms of their values. The accumulative and combined effect of related sky concepts was considered when handling complementary and supplementary sky concepts. For instance, if the sky concept (moon) was detected, then the value of the contradictory sky concept (dark moon) was not anticipated. For the concepts clear sky, if the detection was 100%, then it was necessary to restrict values of co-occurring concepts (such as low clouds and medium clouds). A simple rule was that if two sky concepts A and B have an opposing effect on each other, then if both the concepts were detected, their values were to be regulated using some joint probability transformation to reflect the co-occurrence. The restraining of the complementary and supplementary relationships reduced the probability that co-occurring sky concepts hinder each other and subsequently nullify resulting effects during the prediction process. The detection of visible moon for instance automatically rendered the value of dark moon to zero as shown below.

```
if (visiblemoon_value==0)
    darkmoon_value=darkmoon_value;;
else
    darkmoon_value=0;
end
...
```

Co-occurring sky concepts were dealt with by computing the joint existence relationships (the union of the sky concepts probabilities) as shown below.

```
if(clearSky_value>threshold)&&((meddiumClouds_value>threshold)||...
(lowClouds_value>threshold))&&(highClouds_value> threshold)
clearSky_value=clearSky_value*meddiumClouds_value*lowClouds_value*highClouds_value;
else
clearSky_value=clearSky_value;
end
if(highClouds_value>threshold)&&((meddiumClouds_value>threshold)||...
(lowClouds_value> threshold))&&(clearSky_value> threshold)
```

```

highClouds_value=highClouds_value*meddiumClouds_value*lowClouds_value*clearSky_value
;
else
highClouds_value=highClouds_value;
end

```

5.2.1.27 Confidence on Detected Sky Concepts

The percentage difference of the union of co-occurring sky concepts was determined to approximate the level of co-existence between two sky concepts. The average of the differences was taken for all co-occurring concepts to determine the overall level of confidence for all the detected sky concepts. A simple procedure was as follows:

If the probability of a sky concept x (p_x) existing alone was 1, then the probability of x (p_x) and y (p_y) existing jointly was $x*y$. The percentage negation of this joint existence was $100*(1-x*y)$ taken as the confidence level for the sky concepts A and B. This procedure followed for all co-occurring sky concepts with the average taken as the overall confidence level. A sample computation was as follows

```

clearsky2lowclouds=100*(1-clearSky_value*lowClouds_value);
clearsky2mediumclouds=100*(1-clearSky_value*meddiumClouds_value);
clearsky2lightining=100*(1-clearSky_value*lightining_value);
darkmoon2fullmoon=100*(1-darkmoon_value*visiblemoon_value);
highclouds2lowclouds=100*(1-highClouds_value*lowClouds_value);
highclouds2mediumclouds=100*(1-highClouds_value*meddiumClouds_value);
confidencelevel=(clearsky2lowclouds+clearsky2mediumclouds+clearsky2lightining+...
darkmoon2fullmoon+highclouds2lowclouds+highclouds2mediumclouds)/6;

```

The significance of the confidence level was that of dynamically determining the value of alpha that was applied in the prediction component. The statistical significance of alpha ($alpha = 100\% - confidence\ level$) signified the level of rejecting the sky objects detections so that the predictions were computed based on the level of confidence.

Some normalization was done to fix the values in an acceptable range, while the scaling was done to represent the concepts in a range (0,1). The final sky concepts were normalized and scaled using the formula shown below.

```

concepts = cell2mat(detected_values);
concepts = (concepts - min(concepts))/(max(concepts) - min(concepts));
range2 = 1 - 0.0;

```

$concepts = (concepts * range2) + 0.0;$

Finally the scaled sky concepts were organized in a symbolic mathematical vector that had a distinct position for each of the sky concepts as shown below.

$detected_values = \{highClouds_value, lowClouds_value, meddiumClouds_value, clearSky_value, \dots, stars_value, rainbow_value, lightning_value, darkmoon_value, visiblemoon_value, rain, dry, hot, cold\};$

This vector, together with the confidence levels, determined from the detections process, formed the input to the prediction component. The aim of the rigorous benchmarking process should be understood not to penalize the sky objects detectors but to provide some clue to the predictions component pertaining to the quality of the detection process. The determination of detections confidence levels was meant to influence the outcome of the predictions component. Using confidence levels for self-learning in later sky objects detection tasks was achievable to influence the sky object detectors to fine-tune the merge thresholds in suppressing false positives.

5.2.1.28 Review of Sky Objects Detection and Sky Concepts Representation

The sky objects detection component used input from sky scenes and detected sky objects successively extracting and representing them as sky concepts. The sky objects were detected based on pre-trained cascade classifiers that perform multiple detections merging and improving results using input meta-data (time stamps). The procedure of benchmarking-extracted sky objects used appropriate day or night truths to represent the detected sky objects as sky concepts. Confidence levels on the final sky concepts were determined based on complementary and supplementary relationships between the benchmarked sky objects. The three measures (detections, benchmarks, and confidence) in determining sky concepts were meant to increase model self-reliance in representing sky concepts. The final sky concepts were structured and represented in the form of a mathematical vector, for use in the predictions component. The experiments and results of the fuzzy cognitive maps-based predictions component form the major focus in the next section.

5.3 Simulation of Weather Outcomes through Fuzzy Cognitive Maps Simulations

5.3.1 Overview of Scenario Simulations

The previous section presented in detail the results of the sky objects detection component with the final output being sky concepts structured and represented in the form of mathematical vectors. This section discusses the experimental results of simulating weather outcomes scenarios using fuzzy cognitive mapping techniques. The predictions rely on fuzzy cognitive map connection matrices, which represent seasonal knowledge on sky weather concepts to weather outcomes. The outcomes of predictions are logged using input time stamps for further analysis. Finally, a range of fuzzy cognitive maps experimental results, including human-friendly predictions with graph visualizations are presented.

Fuzzy cognitive mapping techniques were used to symbolically represent and depict the model of a complex visual sky weather lore domain. Descriptions were given (in terms of sky concepts) of the different characteristics of the visual sky weather lore domain. Each sky concept represents a characteristic of the visual sky weather lore system, where the sky concepts interact with each other resulting in changes in weather outcomes.

5.3.2 Model Visual Sky Concepts

In organizing fuzzy cognitive maps model to predict weather outcomes the visual sky concepts identified during the analysis phase were used. A total of nine visual sky concepts and four categories of weather conditions (see Table 5-9) were used to act as the nodes the seasonal fuzzy cognitive maps with statistically determined edge weights as described in subsequent sections.

For each seasonal fuzzy cognitive map, a set of thirteen concepts {C1, C2, C3, C4, C5, C6, C7, C8, C9, C10, C11, C12 and C13} were specified as the key nodes in the experiments. The names of the concepts were specified together with their description and their probable range of their values (Table 5—9).

Table 5—9: Description of Concepts

Concept Symbol	Concept Name	Description of Concepts	Possible
C ₁	High Clouds	sky object	(0,1)
C ₂	Low Clouds	sky object	(0,1)
C ₃	Medium Clouds	sky object	(0,1)
C ₄	Clear Sky	sky object	(0,1)
C ₅	Stars	sky object	(0,1)
C ₆	Rainbow	sky object	(0,1)
C ₇	lightning	sky object	(0,1)
C ₈	Dark Moon	sky object	(0,1)
C ₉	Visible Moon	sky object	(0,1)
C ₁₀	Rain/Wet	weather outcome	(0,1)
C ₁₁	Dry	weather outcome	(0,1)
C ₁₂	Hot/Heat	weather outcome	(0,1)
C ₁₃	Cold	weather outcome	(0,1)

5.3.3 The Seasonal Connection Matrices

Connection matrices were used to represent the weights of the relationships between the thirteen concepts in each seasonal the fuzzy cognitive map. Each connection matrix had thirteen rows and thirteen columns. In the connection matrices the weights, which range between [-1, 1], were determined during the analysis phase.

5.3.4 Inputs of Prediction Model

The weather outcomes prediction model used sky concepts (a vector) and weights (a matrix) as inputs.. In graphical terms, the sky concepts inputs were represented by nodes, while the weights inputs were represented by arrows with some values between the sky concepts (nodes). Each sky concept was a node with its inputs and/or outputs. In the graph below (Figure 5-9) the inputs were indicated by dashed arrows that equate to the sky concepts. The outputs were other sky concepts that interact with the sky concept. Inputs to the prediction model used only detected sky concepts with provision that additional inputs need to be incorporated into connection matrices and associated object detectors trained as well.

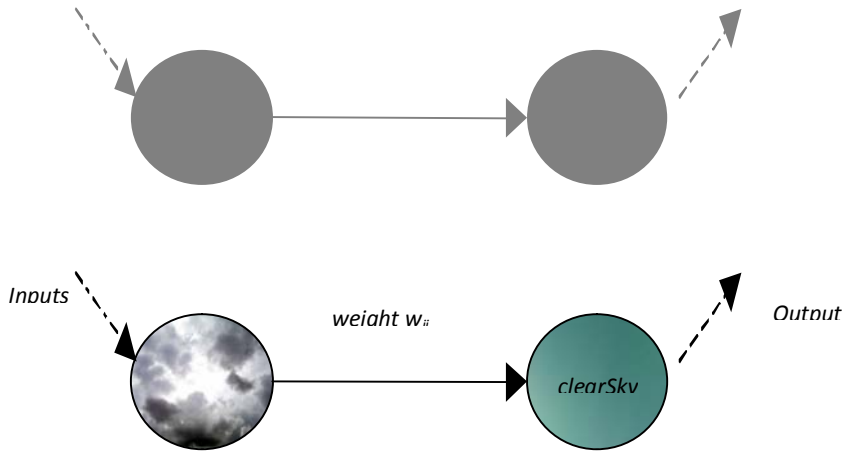


Figure 5-9: Graphical Depiction of Prediction Inputs and Outputs

The input sky concepts acted as either causal or effect concepts dependent on the direction of the arrow in the weight inputs. For instance in the graph above,

$$lowClouds \xrightarrow{\text{causes}} clearSky, \text{ by some weight } w_{ji} \dots \dots \dots \text{Equation 5-14}$$

The sky concept lowClouds was the causal concept of the weight w_{ji} , while the sky concept clearSky was the effect concept of weight w_{ji} . In the implementation of causal effect relationships, a sky concept could be both a causal concept of one causal relationship and an effect concept of different causal relationship.

The two inputs (sky concepts vector and weights matrix) to the weather prediction model had influential quantity values, the sky concept status values and the weight values. The status values of the sky concepts showed the situation of the sky concepts. The weight values specified the strengths of causal effects from one sky concept to another sky concept.

The two inputs (sky concepts vector and weights matrix) were specified by some input set, Input, which was represented by a two tuple

$$Input = \{C, W\} \dots \dots \dots \text{Equation 5-15}$$

where C was a real valued vector that represents the set of input sky concepts in the range [0,1], and W was a real valued matrix that represents the set of causal effect weights between sky concepts in the range [-1,1].

In mathematical terms

$$C = \{x_i \mid x_i \in [0, 1]; i = \overline{1,13} \text{ and } x \in \mathbb{R}\} \dots\dots\dots \text{Equation 5-16}$$

$$W = \{w_{ij} \mid w_{ij} \in [-1, 1]; i = \overline{1,13}; j = \overline{1,13} \text{ and } w_{ij} \in \mathbb{R}\} \dots\dots\dots \text{Equation 5-17}$$

In the predictions model the status of a sky concept was a positive numeric value in between [0, 1]. A sky concept with a state of zero (0) value indicated that the sky concept was inactive. A higher numeric value in the state of a sky concept indicated that the sky concept was active. The maximum activity rate in a sky concept was (1), meaning that the sky concept was in maximum cause or effect.

The causal or effect weight values, w_{ji} of the sky concepts were in the range [-1, 1]. A positive w_{ji} indicated that the state value of the effect sky concept C_i changed proportionately with the state value of the cause sky concept C_j . Negative w_{ji} indicated that the changes of the effect concept C_i were inversely proportional to the state value of the cause concept C_j .

To realize the representation of fuzzy sky concepts and fuzzy causal effects between sky concepts the weather predictions model used a bipolar in range [-1, 1] for the cause effects and the probability interval [0, 1] for the sky concepts states. The fuzzy (overlap) nature of the inputs was implemented to map the human approximate way of thinking.

The characteristics and qualities of the sky concepts and weights inputs described above powers critical interactions in predictions component as was desired. The sky concepts interacted with the predictions model through activation weights values to map sky concept state values. The causal effect weights values interacted with the sky concepts to transform a real causal activation values to the some new weights value. The final causal effect weights values were adjusted using relationship function that relies on the state values of the sky concepts. This quality of the inputs introduced fuzziness in the determination of the final values of sky concepts.

5.3.5 Model Simulation Experiments

The simulation of predictions consisted of a series of sub-steps. First the systems obtained the input of the sky concepts state values and confidence levels from the detections component. At

this point the user is optionally allowed to alter/adjust the sky concepts to reflect the human opinion. The user can opt to select a seasonal connection matrix or rely on automated system procedure. The system also allowed the user to provide levels of desired accuracy which prompted the iteration to terminate once target accuracy was realized. This step was followed by a series of iterations until final output was displayed. A simple flow chart that guided the predictions is depicted (Figure 5-10).

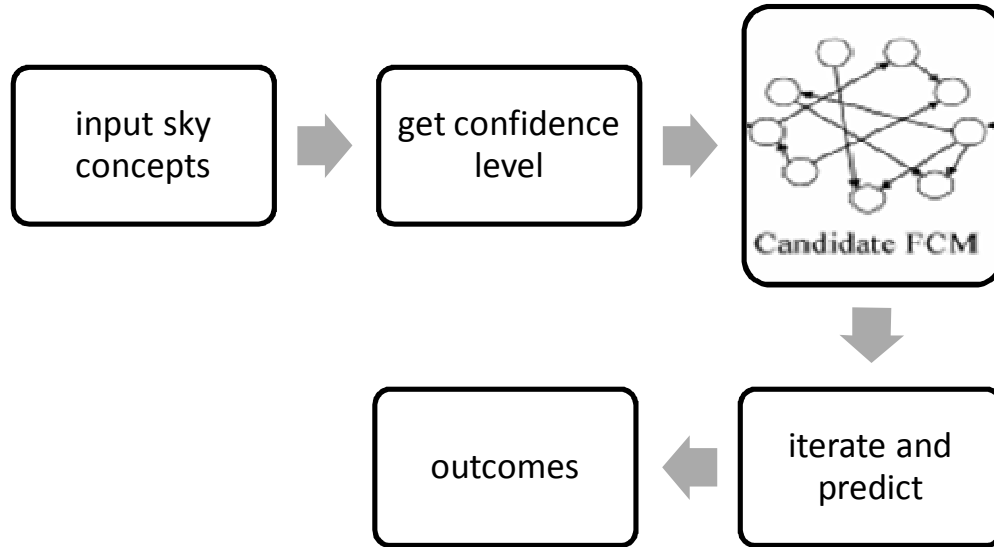


Figure 5-10: Prediction Steps

5.3.6 Activations to New Sky Concepts States

The sky concepts states were the values represented as a real valued vector C_i taking probability values between $[0, 1]$. The activation of new sky concepts states was realized by transforming previous sky concepts vector. The transformation considered all the causal sky concept nodes that influenced the given sky concept node. The transformation of sky concepts values to new state values used the two inputs described earlier:

Given that there were 13 sky concepts (nodes) in the sky concepts vector, a 13x13 weights connection matrix W was used:

$$W = \begin{bmatrix} w_{1,1} & w_{1,2} & w_{1,3} & \dots & w_{1,13} \\ w_{2,1} & w_{2,2} & w_{2,3} & \dots & w_{2,13} \\ w_{3,1} & w_{3,2} & w_{3,3} & \dots & w_{3,13} \\ \dots & \dots & \dots & \dots & \dots \\ w_{13,1} & w_{13,2} & w_{13,3} & \dots & w_{13,13} \end{bmatrix} \dots \text{Equation 5-18}$$

A 1x13 sky concepts vector C was also generated

$$C = [C_1, C_2, C_3, \dots, C_{13}] \dots \text{Equation 5-19}$$

The sky concepts vector C was multiplied by the connection matrix W to get a new 1x13 vector C' as follows:

$$C' = CxW$$

$$C' = [C_1, C_2, C_3, \dots, C_{13}] x \begin{bmatrix} w_{1,1} & w_{1,2} & w_{1,3} & \dots & w_{1,13} \\ w_{2,1} & w_{2,2} & w_{2,3} & \dots & w_{2,13} \\ w_{3,1} & w_{3,2} & w_{3,3} & \dots & w_{3,13} \\ \dots & \dots & \dots & \dots & \dots \\ w_{13,1} & w_{13,2} & w_{13,3} & \dots & w_{13,13} \end{bmatrix}$$

$$= C' = [C'_1, C'_2, C'_3, \dots, C'_{13}] \dots \text{Equation 5-20}$$

Statistically the new sky concepts state vector C' was given by:

$$C'_i = \sum_j w_{ij} C_j \dots \text{Equation 5-21}$$

In the new sky concept activation process, a general assumption worth to note was that a sky concept cannot have a causal effect on itself.

The value C'_i was given by the sum of the products between the state values of all the causal sky concepts of concept C_i and the weight values between pairs of relating sky concept nodes. The value C'_i represented the new status of sky concept C_i considering the influence of all of its causal sky concepts.

5.3.7 Threshold, Max Min Normalization and Scaling Function

In each stage of activating the new states of sky concepts a threshold function was used to regulate the resultant vector. In the last iteration the final stable sky concepts were standardized by using a max-min normalization function, and then scaled using the confidence level range.

```

new_vector=oldvector*con_matrix
for i = 1: oldvector.length
if ((new_vector (i)> 0) && (new_vector (i)< 1))
    new_vector (i)= new_vector (i);
else
if new_vector (i)< 0
    new_vector (i) = 0;
else
    new_vector (i)=1;
if new_vector (i) == 0
    new_vector (i) = 0;
end
end
end
end

```

```

transformed = (new_vector - min(new_vector))/(max(new_vector) - min(new_vector));
new_vector =transformed;

```

```

rng=confidencel;
range2=(rng/100)-0;
predictions = (new_vector *range2) + 0;

```

5.3.8 Iterative Learning and Update of Cause Effects Relationships

The prediction of the states of sky concepts used fuzzy cognitive map learning. Iterative learning permitted the weights matrix to be updated as new concepts states were computed at each stage. This enabled the input sky concepts to interact with their desired weights values and adjust their cause effects relationships until stability.

Iterative learning was a feedback mechanism used by the predictions component to enhance the quality of final predicted sky concepts. The procedure used is as follows:

1. Initialize current sky concepts vector and the current weight matrix;

2. Determine the state values by the relationship functions between weight and its causal concept by multiplying the sky concept state vector by the weight matrix calculate
3. Normalize the resultant sky concepts vector;
4. Check error margin between resultant sky concepts nth outputs relative to nth-1 output
5. If the error margin is unsatisfactory, increase the state value of the counter concept;
6. Use the resultant state values of sky concepts as a new input vector;
7. Repeat these steps until the values of the output sky concepts become stable; and
8. If the state value of the counter concept reaches/exceeds a target value, adjust the state value of the parameter concept.

The analysis of seasonal fuzzy cognitive maps scenarios allowed the determination of stable states for use in predicting sky concepts outcomes. The state of new sky concepts was determined by multiplying an input vector of sky concepts with the seasonal connection matrix. Depending on the strengths of the sky concepts connection matrix the cause and effect of input sky concept were transmitted from one sky concept to connected sky concepts. The process was iteratively repeated until the final sky concepts vector converged to a steady state. The convergence method enforced a number of iterations until stability. The simulation halted when the limit of the resultant sky concepts vector was reached, i.e. when

$$C'_k - C'_{k-1} < \varepsilon = 0.001 \dots \dots \dots \text{Equation 5-22}$$

so that ε was an error margin, whose value could be dynamically specified.

The running of scenario involved the adjustment of sky concepts (nodes) by varying to high and low value respectively. The final values of sky concepts in a scenario run were then compared to the iteration states results (Table 5—10) to see if the value of the concept increased or decreased.

Table 5—10: Concepts Values at Various Iterations

Iteration	C1	C2	C3	C4	C5	C6	C7	C8	C9	C10	C11	C12	C13
1 (initial values)	0	0	0	0	0	0	0	0	0	0	0	0	0
2	1	1	1	0	1	1	0	1	0	0.3623	0	0.1074	0
3	0.1965	0.0055	1	0	0.1965	0.1965	0	0.1965	0	0	0.25	1	0
4	0.0672	0.0402	1	0	0.0672	0.0672	0	0.0672	0	0.1933	0	0.6462	0
5	0.0369	0.0183	1	0	0.0369	0.0369	0	0.0369	0	0.4159	0	0.3472	0
6	0.0327	0.0174	1	0	0.0327	0.0327	0	0.0327	0	0.4519	0	0.3079	0
7	0.0325	0.0174	1	0	0.0325	0.0325	0	0.0325	0	0.4579	0	0.3005	0
8	0.0326	0.0175	1	0	0.0326	0.0326	0	0.0326	0	0.4581	0	0.3002	0
9	0.0326	0.0175	1	0	0.0326	0.0326	0	0.0326	0	0.4581	0	0.3002	0
10	0.0326	0.0175	1	0	0.0326	0.0326	0	0.0326	0	0.4581	0	0.3002	0
11	0.0326	0.0175	1	0	0.0326	0.0326	0	0.0326	0	0.4581	0	0.3002	0
12	0.0326	0.0175	1	0	0.0326	0.0326	0	0.0326	0	0.4581	0	0.3002	0
13	0.0326	0.0175	1	0	0.0326	0.0326	0	0.0326	0	0.4581	0	0.3002	0
14	0.0326	0.0175	1	0	0.0326	0.0326	0	0.0326	0	0.4581	0	0.3002	0
15	0.0326	0.0175	1	0	0.0326	0.0326	0	0.0326	0	0.4581	0	0.3002	0
16	0.0326	0.0175	1	0	0.0326	0.0326	0	0.0326	0	0.4581	0	0.3002	0
17	0.0326	0.0175	1	0	0.0326	0.0326	0	0.0326	0	0.4581	0	0.3002	0
18	0.0326	0.0175	1	0	0.0326	0.0326	0	0.0326	0	0.4581	0	0.3002	0
19	0.0326	0.0175	1	0	0.0326	0.0326	0	0.0326	0	0.4581	0	0.3002	0
20	0.0326	0.0175	1	0	0.0326	0.0326	0	0.0326	0	0.4581	0	0.3002	0
21	0.0326	0.0175	1	0	0.0326	0.0326	0	0.0326	0	0.4581	0	0.3002	0

The graphical representation of the convergence is as shown below (Figure 5-11). The constant lines after the 8th iteration indicate that the values of predictions do not change even with computations of more iterations.

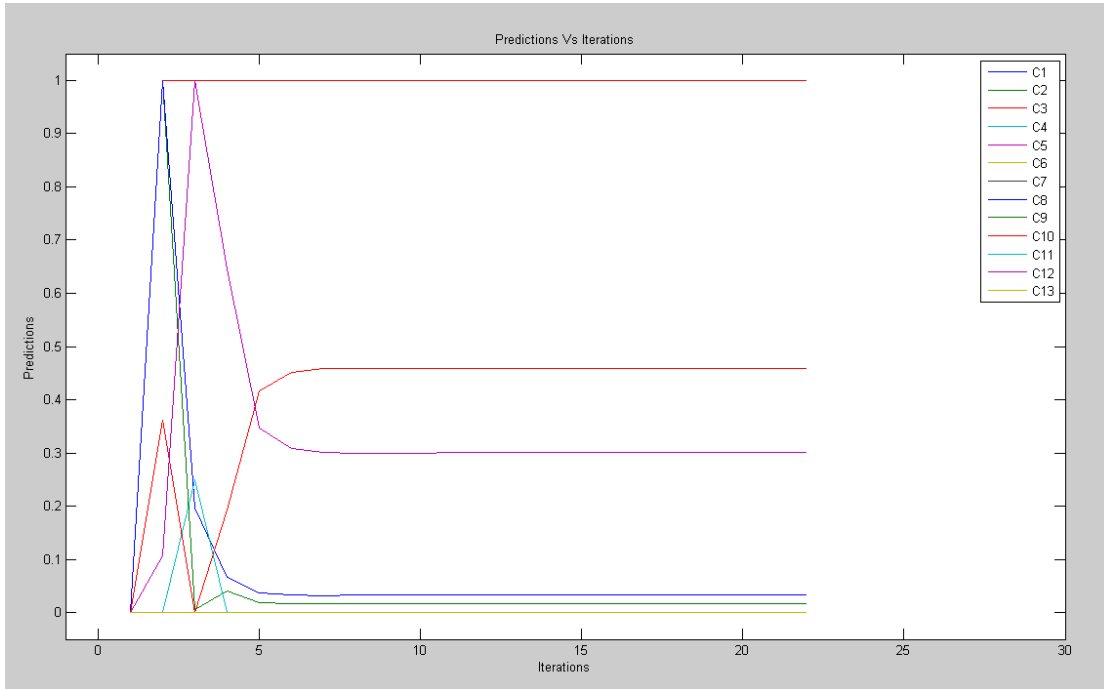


Figure 5-11: Iterative Predictions Convergence Graph

5.3.9 Mapping of Predicted Weather Outcomes

In the sky concepts all the concepts represent some change to some new state. The sky concepts were defined in the same way using a common set of membership function representing a certain amount of change ranging from [0, 1].

The predicted values were mapped to an incremental log file for use in the verification component that approximated the validity of the predicted concepts against actual weather outcomes. Considering the nature of humans, who often use their inaccurate expressions such as ‘very much’, ‘much’, ‘little’, and ‘very little’ to make prediction statements, the outputs from final predicted sky concepts (in the range [0, 1]) were transformed to human-understandable form. Defuzzification allowed the analysis and understanding of the predicted sky concepts. The simulated sky concepts were used to generate human comprehensible decisions that are instantly

handy for further decisions. The outcomes were interpreted in scales ranging from 0% to 100% chances of weather prospects.

%Log Process

```
oldData = get('*');
newData = get('*');
nRows = (size(oldData,1));
nRows = nRows + 2;
a = make_str(nRows);
b = join('A', a);
c = join('C', a);
save('*', time_date,'predictions',b);
save('*', newData,'predictions',c);
```

%Location Determination

```
lat1=join(directionlat,X11);lon1=strcat(directionlon,Y11);
lat=str2num(lat1);lon=str2num(lon1);
url=sprintf('http://maps.googleapis.com/maps/api/geocode/xml?latlng=%.4f,%.4f&sensor=true'
, lat, lon);
try
buffer = urlread(url);
results = regexp(buffer, '<formatted_address>(.*?)<', 'tokens' );
for k = 1 : length(results), fprintf('%s\n', results{k}{1}) ; end
%xb=results;location=xb{3}{1};
xb=results;location1=xb{1}{1};location2=xb{2}{1};location3=xb{3}{1};
```

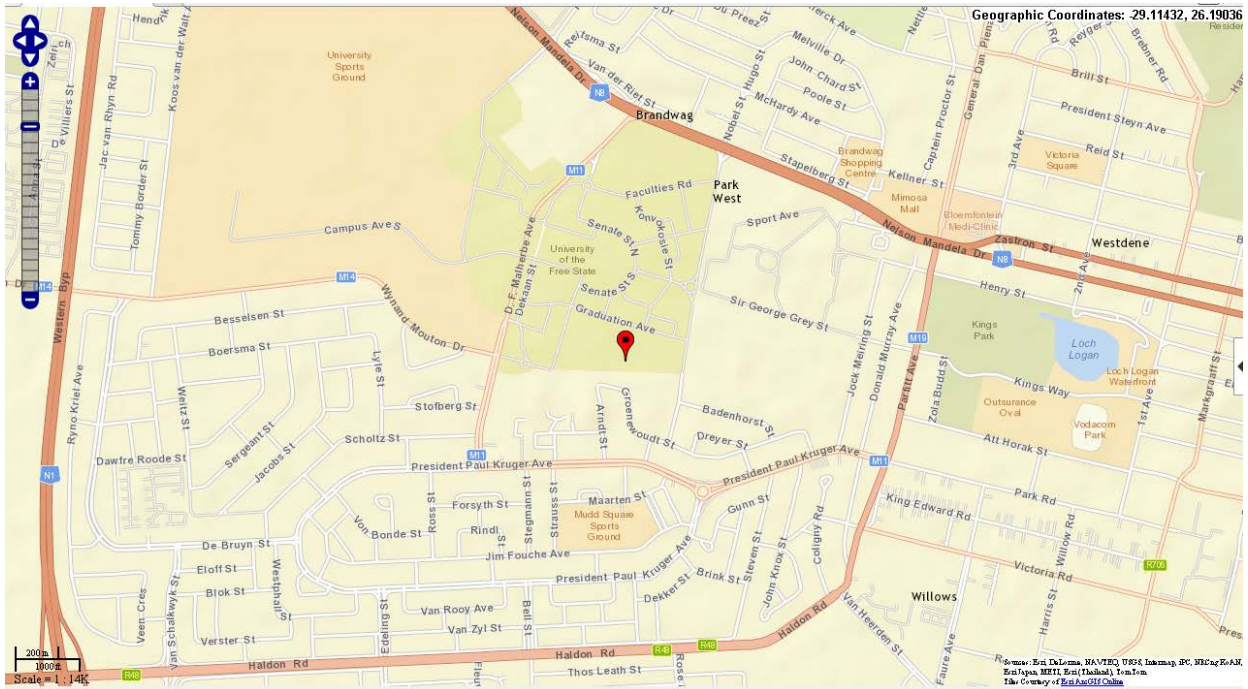


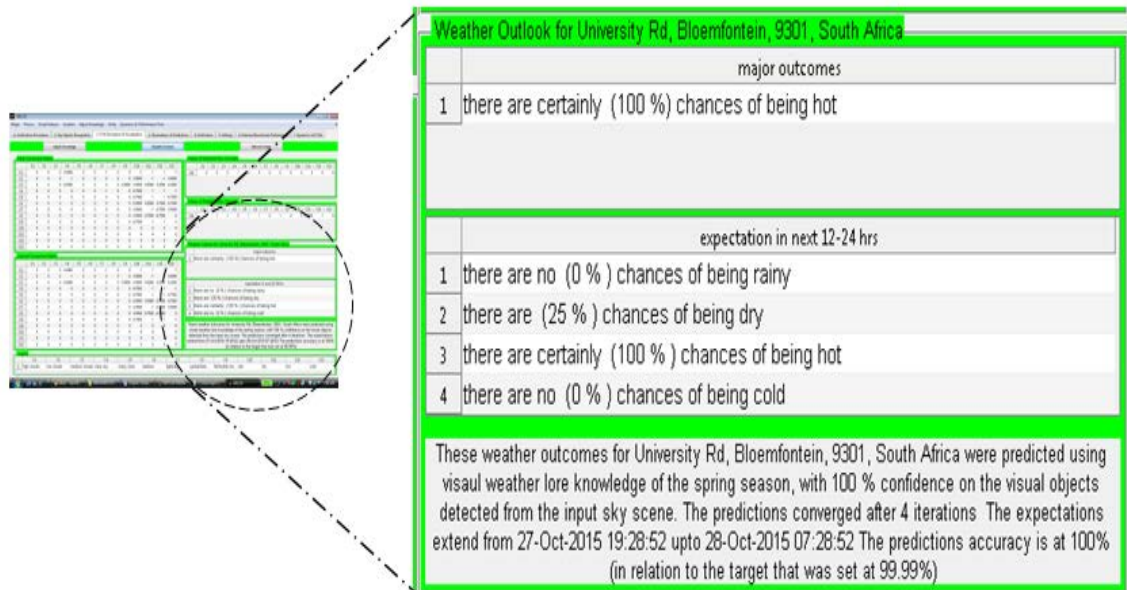
Figure 5-12: Depiction of Prediction Location in Map

Outcomes Transformation

```

predictions= get('*');
nRows = (size(predictions,1));
nRows = nRows +1;
d = num2str(nRows);
e = strcat('C', d);
f = strcat('F', d);
range=[e,':',f];
read_row=get('*','predictions',range);
v=read_row;
n=size(v,2);
p=(v*100);
for i=1:n
if (0<v(i)<0.2)      z(i)={'statements'};
elseif (0.19<v(i)<0.3)  z(i)={'statements'};
elseif (0.29<v(i)<0.4)  z(i)={'statements'};
elseif (0.39<v(i)<0.5)  z(i)={'statements'};
elseif (0.49<v(i)<0.6)  z(i)={'statements'};
elseif (0.59<v(i)<0.7)  z(i)={'statements'};
elseif (0.69<v(i)<0.8)  z(i)={'statements'};
elseif (0.79<v(i)<0.9)  z(i)={'statements'};
elseif (0.89<v(i)<1.0)  z(i)={'statements'};
else
z(i)={'statements'};
end
end
z;
concepts={'rainy';'dry';'hot';'cold'};
for i=1:n
    outcomes(i)=strcat(z(i),{' (}',num2str(p(i)),{' % ) chances of being ' },concepts(i));
end
outcomes;
save('*','outcomes');
ind=find(v==(max(max(v))));
size_ind=size(ind,2);
for j=1:size_ind
major_outcomes(j)=strcat(z(ind(j)),{' (}',num2str(p(ind(j))),{' % ) chances of being '
},concepts(ind(j)));
end

```



5.3.10 Ne

The intera

Figure 5-13: Snapshot of Major Predicted Outcomes

visualization. For this network files were implemented to visualize the seasonal knowledge in radial graphical layout with straight edge types. In the connection matrices rows were used to generate source nodes (the influence sky concepts) and the matrix columns were used to represent the sinks (nodes representing affected sky concepts). A generated network graph for the summer season as depicted (Figure 5-14).

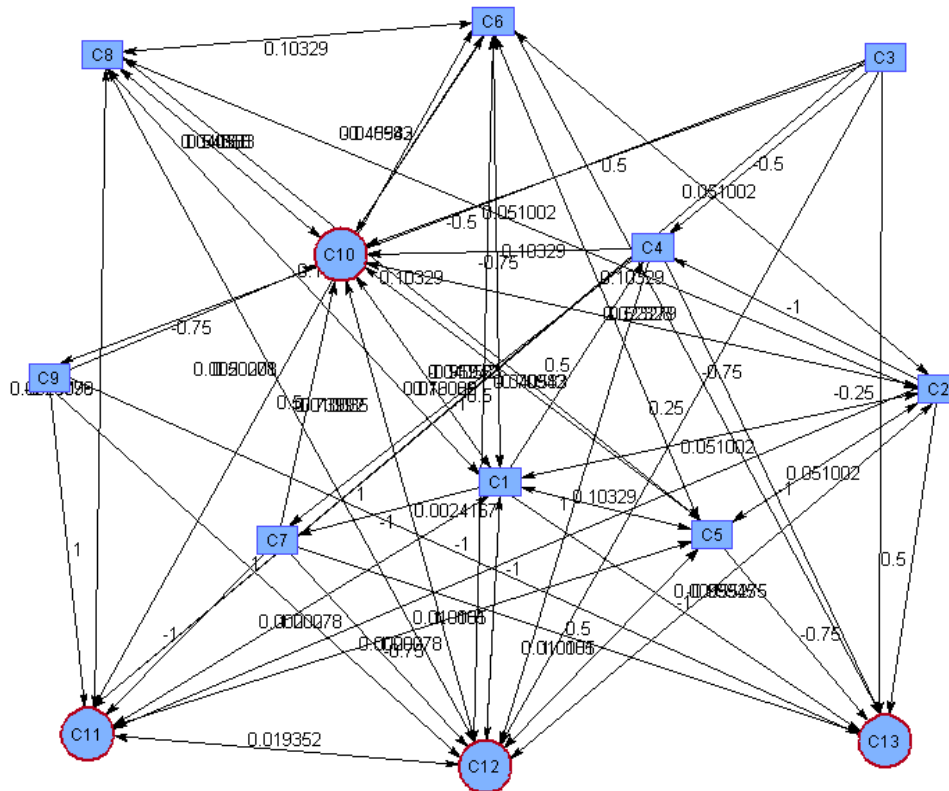


Figure 5-14: Graphical depiction of the Summer Weather Season

5.3.11 Dynamics of Seasonal Fuzzy Cognitive Maps

The seasonal fuzzy cognitive maps were analyzed to determine and interpret the relations between the sky concepts. This analysis presented more understanding concerning the structural properties and dynamics of the seasonal fuzzy cognitive maps. To analyze the type and the role of each sky concept within the fuzzy cognitive maps the density, indegree, outdegree and centrality measures were determined.

5.3.12 Density of the Seasonal Connection Matrices

The densities, D , of the seasonal fuzzy cognitive maps were determined to depict how highly connected the sky concepts were to each other. For each seasonal fuzzy cognitive map, the densities were computed by dividing the number of countable connections, Z , by the number of possible connections between N sky concepts.

Given that the relationships in the seasonal connection matrices depict no self-loops, then the main diagonal of the connection matrices consisted only of zeros. The maximum number of sky concepts connections was given by $N(N-1)$. The densities in the seasonal fuzzy cognitive maps were determined by:

$$D = \frac{Z}{N(N-1)} \dots \dots \dots \text{Equation 5-23}$$

The implementation significance of density was that seasonal fuzzy cognitive maps with many connections per sky concept had higher density provided increased alternative of manipulating the sky concepts.

5.3.13 Indegree, Outdegree and Centrality of Sky Concepts

The indegree was computed by summing the counts of all the absolute values of incident arrows. In the connection matrices this was the sum of the columnar sky concepts. The outdegree was determined by summing the counts of all the absolute values of outgoing arrows. In the connection matrices this was the sum of the row sky concepts. The absolute values were used to give equal importance to recognize both negative and positive causal effects weights between sky concepts.

$$\text{in degree} = \sum_{k=1}^N a_{ki} \dots \dots \dots \text{Equation 5-24}$$

$$\text{out degree} = \sum_{k=1}^N a_{ik} \dots \dots \dots \text{Equation 5-25}$$

The centralities of all the sky concepts for each seasonal fuzzy cognitive map were determined (see Table 5—11to Table 5—14). The centrality was also called the total degree of the sky concepts (i.e. the sum of the indegree and outdegree per sky concept). The centrality was used to measure the importance of the sky concepts. Sky concepts with high centrality were given special attention.

Table 5—11: Summer Season Dynamics

Summer	C1	C2	C3	C4	C5	C6	C7	C8	C9	C10	C11	C12	C13
Indegree	0	0	0	3	0	0	2	0	1	9	9	9	8
Outdegree	6	5	6	5	4	4	4	3	4	0	0	0	0
Centrality	6	5	6	8	4	4	6	3	5	9	9	9	8

Table 5—12: Autumn Season Dynamics

Autumn	C1	C2	C3	C4	C5	C6	C7	C8	C9	C10	C11	C12	C13
Indegree	0	0	0	3	0	0	2	0	1	9	8	8	6
Outdegree	6	5	6	5	1	3	4	4	3	0	0	0	0
Centrality	6	5	6	8	1	3	6	4	4	9	8	8	6

Table 5—13: Winter Season Dynamics

Winter	C1	C2	C3	C4	C5	C6	C7	C8	C9	C10	C11	C12	C13
Indegree	0	0	0	3	0	0	2	0	1	8	6	8	8
Outdegree	6	4	3	5	4	2	4	4	4	0	0	0	0
Centrality	6	4	3	8	4	2	6	4	5	8	6	8	8

Table 5—14: Spring Season Dynamics

Spring	C1	C2	C3	C4	C5	C6	C7	C8	C9	C10	C11	C12	C13
Indegree	0	0	0	3	0	0	2	0	1	9	9	9	8
Outdegree	6	5	6	5	4	4	4	3	4	0	0	0	0
Centrality	6	5	6	8	4	4	6	3	5	9	9	9	8

5.3.14 Transmitter, Receiver and Ordinary Sky Concepts

The transmitter, receiver and ordinary factors of the sky concepts were determined. In implementation the transmitters had positive outdegree and zero indegree. The receivers had positive indegree and zero outdegree (also known as sink or ends in some other computational terms). Analysis of the transmitter sky concepts was important as they influence other sky concepts while they remain unaffected. Sky concepts with both positive indegree and outdegree were known as ordinary sky concepts.

Complexity (Table 5—15) of the sky concepts was determined by the ratio of the total transmitters to total receivers. If the ration was high, then the sky concepts relationships were regarded as highly complex. For low complexity the sky concepts relationships were externally driven.

$$Complexity = \frac{Transmitters}{Receivers} \dots\dots\dots Equation 5-26$$

Table 5—15: Seasonal FCM Dynamics

Season	Total Sky Concepts	Total Connections	Total Transmitters	Total Receivers	Total Ordinary	Complexity	Density
Summer	13	82	6	4	3	1.5000	0.5256
Autumn	13	74	6	4	3	1.5000	0.4744
Winter	13	72	6	4	3	1.5000	0.4615
Spring	13	82	6	4	3	1.5000	0.5256

5.3.15 Review of Scenario Simulations

This section presented the experiments and results of the prediction component that makes use of detected concept values to predict weather outcomes based on knowledge represented in fuzzy cognitive maps. A mechanism of influencing the results of weather predictions was achieved by acknowledging model confidence on the detected concepts. The confidence levels were based on qualitative judgments of supplementary and complementary relationships between detected concepts. Experiment results revealed that integrating detections confidence suppresses near-false prediction of weather outcomes. The predicted weather outcomes were further enhanced by integrating iterative reorganization (a simple form of learning) of the season connection matrix weights before successive steps of a simulation. The prediction component portrayed uncertainty of the weather seasons by allowing specification of the season status; or else the model utilizes object time stamps for season resolution.

5.4 Compilation of Actual Weather Observations Using Wireless Sensors

5.4.1 Overview of Wireless Sensors based Weather Station

These section present configuration and tests results of the wireless weather station used to gather actual weather observations. First, a description of the sensors and the components of the wireless station is presented. The results of data logs are presented, followed by discussions on the choice of weather parameters, transformations and representations to verifiable weather observations. The weather parameters gathered using the wireless weather sensors were benchmarked to Bloemfontein weather records (<http://www.accuweather.com/> and <http://www.timeanddate.com/> real-time weather measurement mechanisms.)

5.4.2 Components of the Wireless Weather Station

A simple star topology wireless weather data acquisition system was employed. The weather station consisted of a central base station and numerous wireless sensing nodes. Distance from the base station to the weather sensors varied to tens of metres, therefore a reliable communication was realized using a wireless network. The base station automatically synchronized the internal working clocks of the sensing nodes and received data from the wireless sensor nodes for logging in an internal central repository. The internal power consumption for the wireless sensor nodes was minimal (at 3 volts). The base station was powered both internally and externally to increase its lifetime.

The wireless weather station was used for continuous monitoring of weather conditions in order to generate a log of daily weather data. The purpose of this monitoring was to generate sufficient weather records which were useful in verification of the predicted weather outcomes. The sensor nodes had an internal buffer that temporarily stored weather readings. At distinct time intervals the wireless sensing nodes transmitted recently measured data to the base station. The base station logged and displayed data for up to seven days. This data was accumulated by transferring to an external storage through a software program.

To facilitate the collection of real-time weather data a configuration of Oregon scientific wireless sensor hardware and software was used. The Oregon scientific equipment used has been comprehensively validated in the country of origin (NIST Certification, USA) and experimented with in other countries (such as UK, France and Germany). An advantage of the Oregon Scientific variety of wireless weather stations is the capacity to introduce additional weather parameter sensors.

The wireless weather station gathered (in real time and every one hour) the indoor and outdoor temperature, precipitation, heat index, wind chill, wind direction and wind speed among other parameters. The weather sensors remotely transmitted data to the base station. A wireless weather station used is depicted below (Figure 5-15)



Figure 5-15: Oregon Scientific Weather Station

5.4.3 Sensors used in the Wireless Weather Station

The wireless weather station was positioned on the roof of the Central University of Technology (CUT) BHB building. The base station was positioned in an office on the 2nd floor of BHB building. The Oregon scientific wireless weather sensor proved reliable weather measurement equipment that meets WMO accuracy benchmarks. Essential weather parameters that were measurable by conventional weather monitoring systems were realized by this equipment.

The wireless weather station measured a wide range of meteorological parameters by allowing wireless connection of different types of sensors. The wireless weather station equipment included a range of outdoor sensors consisting of a thermo-hygrometer, an anemometer-cum-wind vane, a rain gauge and a barometer that were used to acquire actual weather parameters that the format described, as shown in Table 5—16.

Table 5—16: Weather Parameters Recorded

Parameter	Description	Range, Accuracy
Outdoor Temperatures	The indoor/outdoor temperature values were recorded as real values in Celsius.	-40°F;-40°C- 150°F;65°C 1°F;0.5°C
Outdoor humidity	The humidity that is usually the ratio of the vapour pressure of moist air to its saturation vapour pressure at its temperature was expressed in %.	0%-99%, ±3%
Wind speed and direction,	The Wind speed was recorded in kilometres per hour and wind direction was in compass points (NESW).	0 m/s -80 m/s, ±5% 0°-360°, ±3°
Precipitation	Precipitation was recorded in hourly and daily (24 hour) cumulative.	0" -393.6", 5%
Atmospheric pressure	The atmospheric pressure was recorded in millibars.	21.25inHg/540hPa 43.31inHg / 1,100hPa
Wind chill	The wind chill was recorded as the cooling effect produced by the combination of cool temperature and wind.	0%-99%, ±3%
Heat index	The measure of how hot it feels (heat index) was recorded in percentage. The values of humidity and air temperature were used to determine the humidity.	0%-99%, ±3%

To benchmark the wireless weather station, the daily meteorological parameters were obtained from the real-time weather observatories (<http://www.accuweather.com/en/za/south-africa-weather/bloemfontein>). The Bloemfontein weather observatories also make available barometric pressure, dew point, and relative humidity observations.

The wireless weather station was evaluated against the conventional weather station in Bloemfontein to guarantee dependable accuracy. The accuracy of the pre-calibrated automatic

wireless weather station was done by comparing the readings of the weather sensor with the Bloemfontein, Free State weather observations.

5.4.4 Review of Wireless Sensors-based Weather Station

These section presented configuration and tests results of the wireless weather station that was used to gather actual weather observation. The sensors setup and the components of the wireless station were discussed. The results of data logs were presented, with specifications on the chosen weather parameters and the transformations used to represent the verifiable weather observations.

5.5 Visual Weather Lore Verification Using Forecast Skills

5.5.1 Overview of Visual Weather Lore Verification Component

The previous two sections demonstrated the mechanisms of detecting weather concepts from sky scenes, predictions using fuzzy cognitive mapping techniques and gathering actual weather observations using wireless sensors. The results from the predictions component and actual weather sensor form the main ingredients of the verification component that is the focus of this section. The transformations applied to the two input verification data sets are illustrated. Verification experiments using various forecast skill metrics and results are presented.

5.5.2 Range of Verification Data

Two inputs were used in the verification component: first the predicted weather outcomes from the visual weather lore based predictions component, and secondly, the actual weather observations generated using the wireless weather-sensing component. Both data sets had time metadata to ensure correspondence in terms of prediction and observation periods. These two data sets were crucial in the validation of the visual weather lore verification model. The predictions data set consisted of daily records (wet/rain, dry, hot/heat, cold) which represented the next 12/24 hr weather prospect. The observation data set consisted of the actual records which represented the actual weather outcomes (wet/rain, dry, hot/heat, cold) for the day. A section of the data sets is shown (Figure 5-16) and graphs (Figure 5-17).

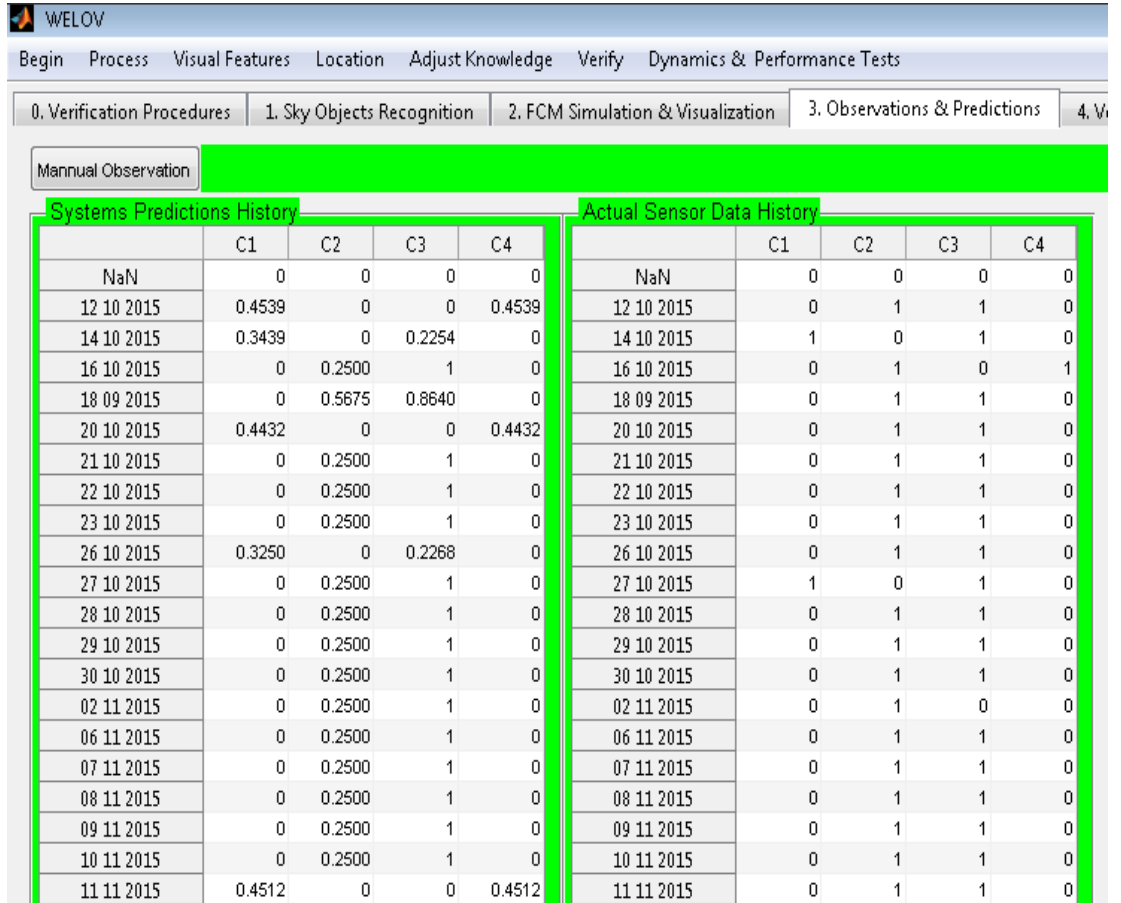


Figure 5-16: Section of Predictions/Observation Data Sets

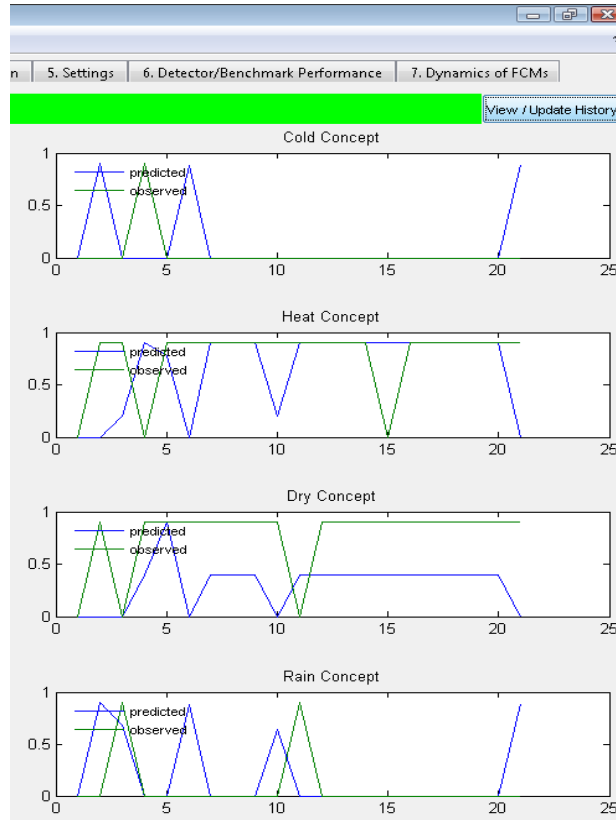


Figure 5-17: Graphs of Predictions Vs Observations

5.5.3 Transformation of Weather Observations to Categorical Variables

The observations data acquired using a wireless weather station was logged as variable strings of data containing weather parameters. The observed weather parameters were transformed to categorical weather variables (0 = non-occurrence, 1 = occurrence) that indicated the presence or absence of the weather outcomes. A value of 0 indicated a non-observed weather outcome while a value of 1 indicated an observed weather outcome. The weather records were transformed to categorical values for simplicity of verification against predicted weather outcomes. The predictions data set consisted of scaled data in the range [0, 1]. To compare the two data sets the following transformations were implemented:

Wet/Rain

$$\text{Categorical} = IF(\text{Precipitation} > 0, 1, 0)$$

Dry

Categorical =IF(Precipitation >0,0,1)

Hot/Heat

HI=IF((E3*9/5+32)<=80,E3,IF(AND(F3<13,((E3*9/5+32)>80),((E3*9/5+32)<112)),(((-42.379+2.04901523*(E3*9/5+32)+10.14333127*F3-0.22475541*(E3*9/5+32)*F3-0.00683783*(E3*9/5+32)*(E3*9/5+32)-0.05481717*F3*F3+0.00122874*(E3*9/5+32)*(E3*9/5+32)*F3+0.00085282*(E3*9/5+32)*F3*F3-0.00000199*(E3*9/5+32)*(E3*9/5+32)*F3*F3)-32)*5/9)-(((13-F3)/4)*SQRT((17-ABS((E3*9/5+32)-95))/17)),IF(AND(F3>85,((E3*9/5+32)>80),((E3*9/5+32)<87)),(((-42.379+2.04901523*(E3*9/5+32)+10.14333127*F3-0.22475541*(E3*9/5+32)*F3-0.00683783*(E3*9/5+32)*(E3*9/5+32)-0.05481717*F3*F3+0.00122874*(E3*9/5+32)*(E3*9/5+32)*F3+0.00085282*(E3*9/5+32)*F3*F3-0.00000199*(E3*9/5+32)*(E3*9/5+32)*F3*F3)-32)*5/9)+((F3-85)/10)*((87-(E3*9/5+32))/5),(((-42.379+2.04901523*(E3*9/5+32)+10.14333127*F3-0.22475541*(E3*9/5+32)*F3-0.00683783*(E3*9/5+32)*(E3*9/5+32)-0.05481717*F3*F3+0.00122874*(E3*9/5+32)*(E3*9/5+32)*F3+0.00085282*(E3*9/5+32)*F3*F3-0.00000199*(E3*9/5+32)*(E3*9/5+32)*F3*F3)-32)*5/9))))
Categorical=IF(HI>25,1,0)

Cold

Categorical =IF(HI <18,1,0)

5.5.4 Forecast Accuracy and Metrics

A set of weather predictions are considered accurate if their variations from the actual weather are sufficiently small. A statistical evaluation of the visual weather lore-based weather predictions was achieved by comparing the predicted weather outcomes to wireless weather sensor observations. Statistical evaluation was undertaken using daily inputs of weather outcomes predicted against the observed meteorological parameters. Metrics of forecast skill were computed in error terms to compare the set of weather outcomes predictions and actual weather observations. The Mean Error (ME) was computed as the arithmetic average of the set of forecast errors. The Mean Absolute Error (MAE) was computed by averaging the absolute values of the prediction errors.

$$ME = \frac{1}{n} \sum_{i=1}^n e_i \dots \dots \dots \text{Equation 5-27}$$

$$MAE = \frac{1}{n} \sum_{i=1}^n |e_i| \dots \dots \dots \text{Equation 5-28}$$

The Mean Squared Error (MSE) was computed by averaging the squares of the prediction errors. MSE was the statistically appropriate measure of weather lore-based weather outcomes prediction errors. For each weather outcome the objective was to minimize as much as possible the MSE of the predictions.

$$MSE = \frac{1}{n} \sum_{i=1}^n e_i^2 \dots \dots \dots \text{Equation 5-29}$$

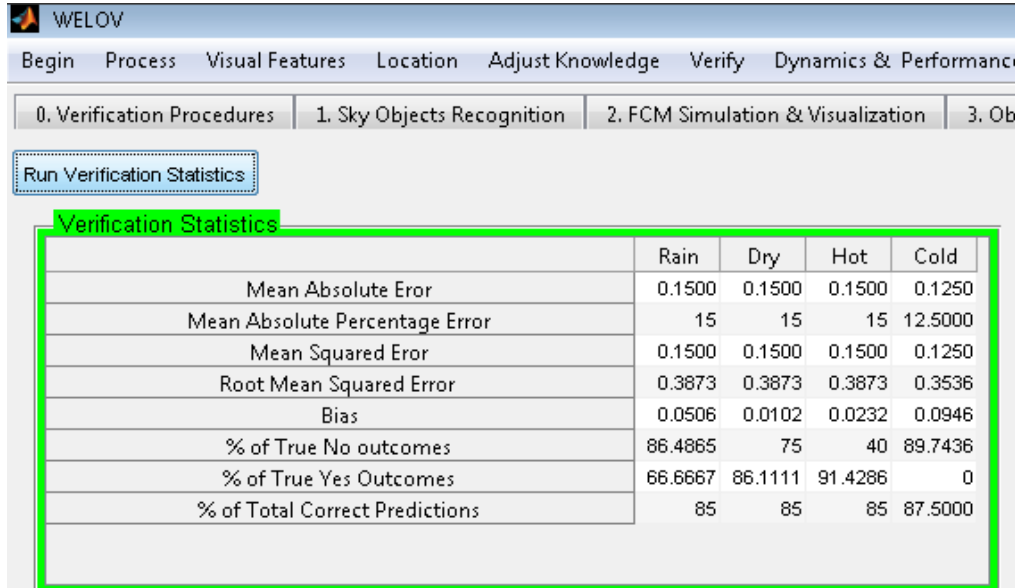
The Root Mean Squared Error (RMSE) was determined by computing the square root of the MSE.

$$RMSE = \sqrt{MSE} \dots \dots \dots \text{Equation 5-30}$$

The MAPE is the most popular aggregate measure for prediction accuracy. The MAPEs were determined by expressing the absolute magnitude of each prediction error as a percentage of the actual observation followed by computing the average of the percentages.

$$MAPE = \frac{1}{n} \sum_{i=1}^n \frac{|e_i|}{Z_i} \dots \dots \dots \text{Equation 5-31}$$

The tendencies to under- or over-predict weather outcomes (Bias) were computed.



The screenshot shows the WELOV software interface. The 'Run Verification Statistics' button is highlighted. Below it, a table titled 'Verification Statistics' displays error metrics for four categories: Rain, Dry, Hot, and Cold. The table is outlined in green in the original image.

	Rain	Dry	Hot	Cold
Mean Absolute Error	0.1500	0.1500	0.1500	0.1250
Mean Absolute Percentage Error	15	15	15	12.5000
Mean Squared Error	0.1500	0.1500	0.1500	0.1250
Root Mean Squared Error	0.3873	0.3873	0.3873	0.3536
Bias	0.0506	0.0102	0.0232	0.0946
% of True No outcomes	86.4865	75	40	89.7436
% of True Yes Outcomes	66.6667	86.1111	91.4286	0
% of Total Correct Predictions	85	85	85	87.5000

Figure 5-18: Snapshot of Error Metrics

ME – Mean Error

MAE – Mean Absolute Error

MAPE – Mean Absolute Percentage Error

MSE – Mean Squared Error

RMSE – Root Mean Squared Error

B – Bias

N_{oc} – % of correct no weather outcomes predictions (against total no observations)

Y_{occ} – % of correct positive weather outcomes predictions (against total yes observations)

PC – % of total correct predictions (against total yes and no observations).

The verification statistics were computed for the 40 records (observations and predictions). The Mean Absolute Error (MAE) between the observations and predictions were rain (0.15), dry (0.15), heat (0.15), and cold (0.125) respectively. The Mean Absolute Percentage Error (MAPE) between the observations and predictions were rain (15), dry (15), heat (15), and cold (12.5)

respectively. The Mean Squared Errors (MSE) between the observations and predictions were rain (0.15), dry (0.15), heat (0.15), and cold (0.125) respectively. The Root Mean Squared Errors (RMSE) between the observations and predictions were rain (0.3873), dry (0.3873), heat (0.3873), and cold (0.3536) respectively. The Bias between the observations and predictions was rain (0.0506), dry (0.0102), heat (0.0232), and cold (0.0946) respectively. The percentage of true non-occurrences between the observations and predictions were rain (84.48), dry (75), heat (40), and cold (89.74) respectively. The percentage of true occurrences between the observations and predictions were rain (66.66), dry (86.11), heat (91.42), and cold (0) respectively. The overall accuracy between the observations and predictions was rain (85), dry (85), heat (85), and cold (87.5) respectively. With increased scope (span and quantity of records) of verification the perceived accuracy increased considerably.

5.5.5 Contingency Tables for Weather Outcomes

In the verification process using contingency tables (Table 5—17 to Table 5—21) a collection of matching records of predictions and observations were used. The notions HIT(s), MISS(es), FALSE ALARM(s) and CORRECT-NEGATIVE(s) were used to depict a 2 by 2 contingency table for each predicted weather outcome. A ‘HIT’ was used to represent the occurrence of an observed (represented by 1) weather outcome that was also categorically predicted to occur (indicated as 1). A ‘FALSE ALARM’ was used to represent a weather outcome that was predicted to occur (represented by 1) but was not observed (indicated as 0). A ‘MISS’ was used to represent a weather outcome that was predicted not to occur (value 0) but was actually observed as positive (value 1). A ‘CORRECT NEGATIVE’ was used to represent a weather outcome that was predicted not to occur (value 0) and was actually not observed (value 0).

Table 5—17: General Contingency Table

		Visual Weather Lore Predictions		
		Yes	No	Totals
Sensor Observations	Yes	HITS	MISSES	Total Events
	No	FALSE ALARMS	CORRECT NEGATIVES	Total non-events
	Totals	Total Events Predicted	Total Non-Events	Sample size

Table 5—18: Contingency Table (Rain)

		Visual Weather Lore Predictions		
		Yes	No	Totals
Sensor Observatio	Yes	2	1	3
	No	5	32	37
	Totals	7	33	40

Table 5—19: Contingency Table (Dry)

		Visual Weather Lore Predictions		
		Yes	No	Totals
Sensor Observations	Yes	31	5	36
	No	1	3	4
	Totals	32	8	40

Table 5—20: Contingency Table (Heat)

		Visual Weather Lore Predictions		
		Yes	No	Totals
Sensor Observations	Yes	32	3	35
	No	3	2	5
	Totals	35	5	40

Table 5—21: Contingency Table (Cold)

		Visual Weather Lore Predictions		
		Yes	No	Totals
Sensor Observations	Yes	0	1	1
	No	4	35	39
	Totals	4	36	40

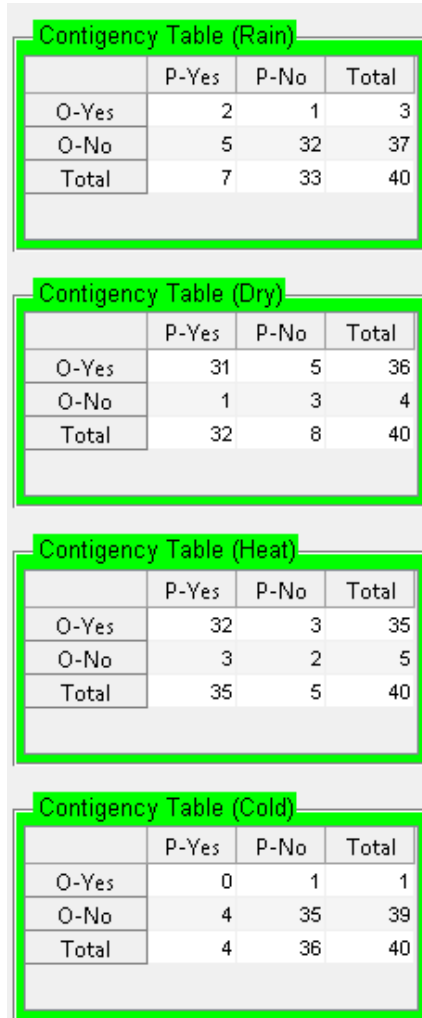


Figure 5-19: snapshot of Contingency Tables

5.5.6 Threat Score (TS) or Critical Success Index (CSI)

The TS (CSI) is a standard weather forecast verification measure which has a range of 0 to 1. The value of 1 indicates a perfect score and the score approaches zero as the weather outcome becomes rare. The TS or CSI was computed for all the weather outcomes as follows:

$$TS, CSI = \frac{a}{a+b+c} \dots\dots\dots \text{Equation 5-32}$$

Using 40 records, the weather outcome rain was rare with a score of 0.25; the score of dry weather outcome was 0.837; hot/heat was 0.842; and the cold weather outcome was scored as 0. The scores were observed to be realistic with increased number of test records.

5.5.7 Review of Verification Process

The verification component and experimental results based on a system predicted against actual weather outcomes logged from a wireless sensor station were presented in Chapter Five. The results of transformation functions on the verification data sets were presented. The results of verification experiment reveal that the visual weather lore-based predicted outcomes were close to the actual weather outcomes observed using the automatic (Oregon) wireless weather station. In Chapter Six discussions, evaluation and research conclusion are presented.

Chapter Six: Performance Evaluation, Discussion and Conclusions

6.1 Introduction

Chapter Five discussed the components and functionalities of the visual weather lore verification tool. The sub-components for detection, prediction and verification were experimented with, and in each case, the outputs were presented. The detection component was accomplished, using image recognition methods for objects recognition and approximation of the presence of visual objects in sky scenes. The performance of each detector was evaluated using bulk image data sets. The implementation and test results of fuzzy cognitive mapping techniques to represent tacit knowledge on visual weather and to predict weather outcomes based on selected visual sky concepts were discussed. A verification component that compares system predictions to actual weather observations was implemented and test results presented. The test results of the verification component that performs the key task of verification of visual weather lore, through computing various forecast skills metrics was presented.

In this chapter (Chapter Six), various assessments that were performed to quantify the achievement of the objectives set in this research are reported. This chapter also presents some innovative aspects of this research and concludes by highlighting some opportunities for extending this research.

6.2 Evaluation of Research Objectives

6.2.1 Identification of Astronomical and Meteorological Visual Aspects Weather Lore

An investigation was accomplished on the most influential visual weather concepts that humans exploit in deciding on weather outcomes in the process of planning for their daily activities. The investigation established that traditional knowledge on weather was locality specific, due to the fact that the effects of weather outcomes vary from different categories of people (such as farmers and general rural inhabitants). The identification of visual astronomical and meteorological weather aspects proved usable (over 50% of the respondents in both case studies stated that they knew some visual indicators and that the visual indicators help them to predict weather) as a traditional way of weather forecasting. The two case studies' results were found to be comparable and aggregation was used to generate seasonal knowledge from the two study areas. An analysis of a broad selection of visual astronomical and meteorological weather

indicators identified using literature review and some previous research (Mwagha & Masinde, 2015) were found to correlate to the results of the case studies in this research.

An unambiguous number of concepts were realized using the knowledge of associations between weather concepts and the initially identified visual weather concepts reduced by clustering sky objects with similar characteristics (and restating contrasting concepts). The ambiguity and overlapping characteristics in the occurrence of sky concepts (such as similar cloud types) necessitated the reduction of the number of concepts. The selected weather outcomes (rain/wet condition, hot/heat cold and dry condition) were identified as major weather conditions (as identified in onset and cessation signs of weather seasons) in influencing the daily activities of people. The ultimate list of interacting and influential astronomical and meteorological aspects (also referred to as concepts) was realized as shown in Table 6—1.

Table 6—1: List of astronomical and meteorological aspects

high clouds	low clouds	medium clouds	clear sky	stars	rainbow	lightning	partial/dark moon	full/visible moon	rain	dry	hot	cold
-------------	------------	---------------	-----------	-------	---------	-----------	-------------------	-------------------	------	-----	-----	------

6.2.2 Causal Effects between Visual Weather Lore and Weather Outcomes

In each of the two case studies conducted, group knowledge was realized by analyzing the data using both quantitative (percentage of respondents) and descriptive statistics (mean and mode of categorical responses). Cross-unit comparisons between the case studies’ results were accomplished before aggregation and group knowledge representation. The results of analysis were represented as group knowledge (on visual astronomical and meteorological weather concepts and the causal effects on short-term weather conditions) based on statistical summaries.

The results of analyzing knowledge from the two case studies (see Figure 4-6) revealed that weather is significant on human activities. This was portrayed by the result that the majority of human daily activities (58% in South Africa and 71% in Kenya) were sometimes affected by weather. The possible reason for the higher percentage in Kenya was that more elderly people (46 to 55 years representing over 68% of the respondents) were sampled in Kenya. The analysis results also depicted that majority of the respondents in both case studies often check for weather

forecasts. The results also showed that most of the respondents in both case studies knew some visual indicators and that the visual indicators help them to predict weather.

By analyzing of perceptions of individual respondents, the causal effects between visual weather concepts and short-term weather outcomes were realized. The percentage of respondents associated with each causal effect, mode and mean were represented for each pair of interacting weather concepts. The final results were categorized and represented in terms of the four weather seasons (winter, summer, autumn and spring).

Joint statistics (mode and mean values) between the visual astronomical and meteorological concepts; and the astronomical and meteorological concepts to weather outcomes in the four weather seasons enabled the realization of common knowledge between the two case studies.

Analysis and summaries of aggregated mode and mean values of causal effects for the four weather seasons (see Table 4—10) depicted and confirmed the trends for the winter, summer, autumn and spring seasons. The results of joint statistical analysis considering all the possible responses (strong-negative, negative, none, positive, strong-positive) for seasons such as winter (South Africa was colder than Kenya), and summer portrayed that the causal effects vary significantly (South Africa's summer was hotter than Kenya's summer; the depiction was similar for the winter season). The analysis using mean depicted a poor aggregate of causal effects; hence the mean aggregate was not preferred as the best statistic to represent the common causal effects between the two case studies.

The combined averages of majority responses from the two case studies were resolved for each pair of selected interacting weather concepts. The deviation between the computed mean values in the two case studies was found to be greater than that of the mode on the knowledge trends for the various seasons). This observation led to the preference of the averages of probability (modal values; see Figure 4-9) in favour of the mean values for representing the causal effects between the interacting visual astronomical and meteorological weather indicators.

6.2.3 The Role of Fuzzy Cognitive Mappings in representing Weather Role

Influential sky weather concepts (also referred to as astronomical and meteorological weather concepts in some parts of this research) were identified through weather lore domain

understanding and analysis and represented as;(high clouds; low clouds; medium clouds; clear sky; many stars; rainbow; lightning; partial/dark moon; full/visible moon; rain; dry; hot; cold).

The four seasonal fuzzy cognitive maps were accomplished by analyzing and interpreting the relations between the sky concepts. The analysis results permitted a more understanding concerning the structural properties and dynamics of the seasonal fuzzy cognitive maps. The type and the role of each sky concept within seasonal fuzzy cognitive maps were established by analyzing the density, indegree, outdegree and centrality measures (see Table). The centrality indicates clear sky has the highest strength in contribution to weather conditions. Rainbow has the least contribution to the weather conditions.

Table 6—2: Results of analysis of the importance of concepts

Concepts	Outdegree	Indegree	Centrality
high clouds	4.75	0.00	4.75
low clouds	2.50	0.00	2.50
medium clouds	1.50	0.00	1.50
clear sky	4.50	2.00	6.50
many stars	3.50	0.00	3.50
Rainbow	1.00	0.00	1.00
Lightning	3.50	2.00	5.50
partial/dark moon	2.25	0.00	2.25
full/visible moon	2.50	0.50	3.00
Rain	0.00	5.75	5.75
Dry	0.00	4.25	4.25
Hot	0.00	5.50	5.50
Cold	0.00	6.00	6.00

6.2.4 Computer Vision as a Technique for Visual Weather Lore Recognition

To achieve this objective, a sky objects detection component was implemented and tested using input from sky scenes. The detected sky objects were represented as sky concepts. The task of benchmarking extracted sky objects was realized using appropriate day or night images to represent the detected sky objects as sky concepts. Confidence levels on the final sky concepts were realized using existence relationships between the benchmarked sky objects. Three measures (detections, benchmarks, and confidence) for determining sky concepts were found significant in increasing model self-reliance in representing sky concepts. Experiments with the

sky object detectors revealed that, as the numbers of training stages for the detectors increased, the detector's overall false positive rate reduced. On analysis (see Table 5—5) the HOG feature model was identified as the best for the sky objects detectors.

6.2.5 Predicting Weather Outcomes Based On Symbolized Visual Weather Lore

To attain this objective, a prediction component that makes use of detected sky concepts values to predict weather outcomes based on knowledge represented in fuzzy cognitive maps was implemented in MATLAB. Experiment results revealed that integrating detections confidence was suppressive of false predictions of weather outcomes. The choice on the status of weather seasons (including: the current season, onset, cessation, progress, or interrupted) enabled the determination of the working weather seasons for enhancing the model predictions.

The determination of scenarios was achieved by the adjustment of values of the sky concepts (varying nodes/concepts values from high to low). The comparisons of the iterative changes in the values of the concepts (Table 5—10) were used to depict the final values of sky concepts in scenarios.

The graphical representations of the concepts convergence (see Figure 5-11) envisaged the behaviour of the predictions component. The constant lines indicated that the values of predictions did not change beyond some values even with additional iterations of scenarios.

6.2.6 Verification of the Weather Lore-Based Predictions

To achieve this objective, the validity of the visual weather lore verification tool was re-assessed using data from a second case study location. Actual data in form of daily sky scenes and weather parameters were acquired from Voi, Kenya during December 2015 and January 2016. The experimentation results using the actual images and weather data and the performance of the verification tool formulate the discussion in sections 6.2.6.1 to 6.2.6.3.

6.2.6.1 Data Acquisition and Experiments with the Verification Tool

Sky scenes (in the form of images) and corresponding actual weather records were captured in the period December 2015 to January 2016 (on a daily basis) from Voi Kenya. The images were subjected to the recognition and sky objects extraction component. The extracted objects were benchmarked and transformed to sky concepts. The generated sky concepts were subjected to

the predictions component to generate results in the form of projected 12/24-hour weather outcomes.

The predicted weather outcomes were transformed to categorical variables where values (1,0) represented expected and weather an unexpected outcomes respectively. Daily actual weather records (precipitation, humidity, wind speed/direction, temperatures) were logged and transformed to categorical weather outcomes.

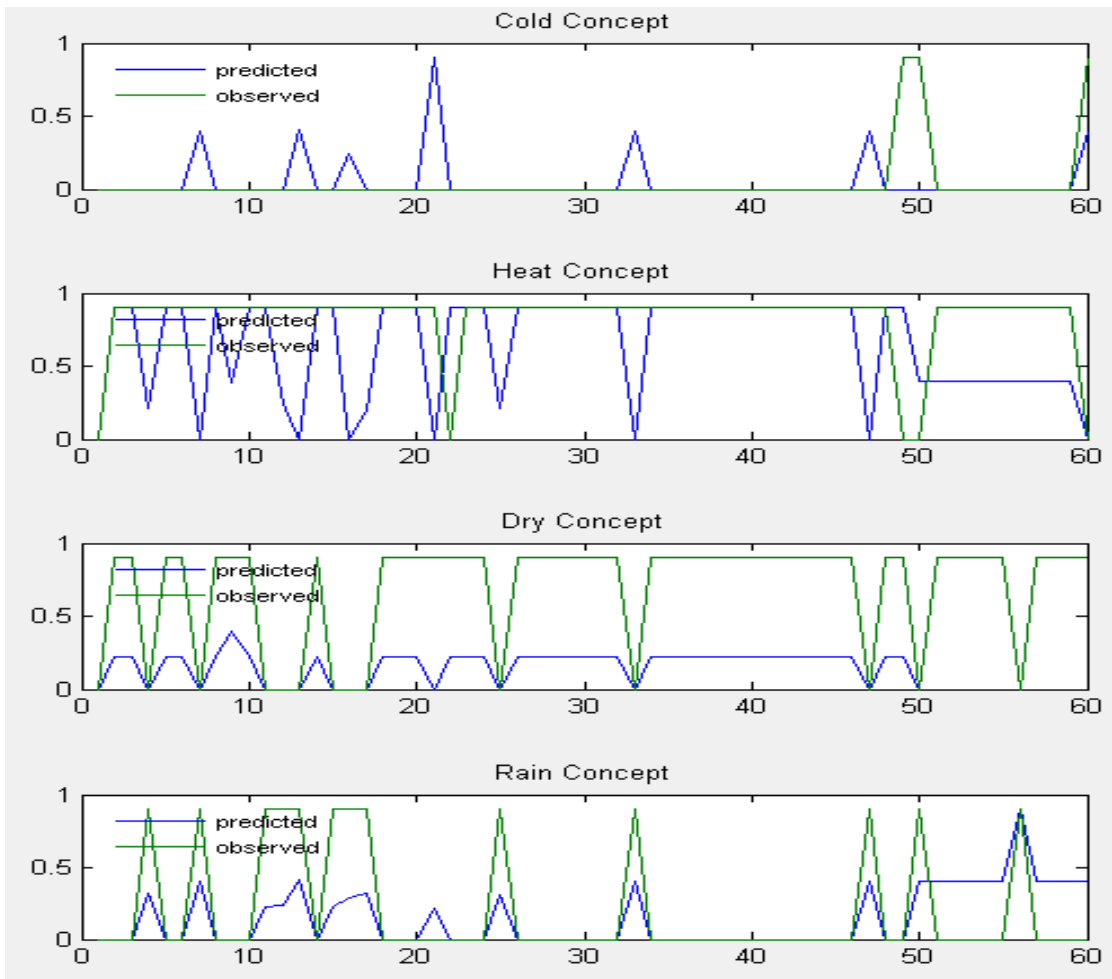


Figure 6-1: Graphs of Prediction/Observation Categorical Values

Mean Absolute Percentage Error (MAPE) between the observations and predictions was determined as rain (16.67); dry (1.67); heat (1.5); and cold (13.33) respectively. The Mean Squared Error (MSE) between the observations and predictions was determined as rain (0.1667); dry (0.167); heat (0.15); and cold (0.1333) respectively. The Root Mean Squared Error (RMSE) between the observations and predictions was determined as rain (0.4082); dry (0.1291); heat

(0.3873); and cold (0.3551) respectively. The Bias between the observations and predictions was determined as rain (0.0123); dry (0.0066); heat (0.0130); and cold (0.0193) respectively. The percentage of true non-occurrences between the observations and predictions were determined as rain (78.72); dry (99.9); heat (40); and cold (89.47) respectively. The percentage of true occurrences between the observations and predictions were determined as rain (99.9); dry (97.8); heat (89.09); and cold (33.3) respectively. The overall accuracy between the observations and predictions was determined as rain (83.3); dry (98.3); heat (85); and cold (86.6) respectively. It is worth noting that these accuracies were based on comparison to gathered actual weather observations.

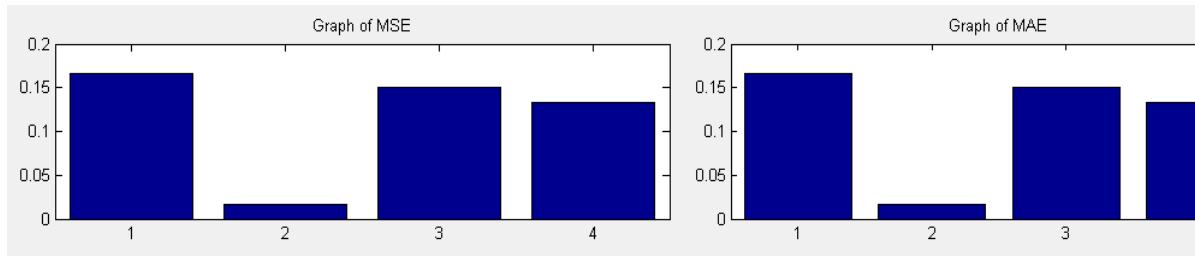


Figure 6-2: Graphs of MSE/MAE

6.2.6.2 Contingency Tables for Predicted/Observed Weather Outcomes

The HIT(s), MISS(es), FALSE ALARM(s) and CORRECT-NEGATIVE(s) were computed and represented in 2 by 2 contingency tables as show in Figure 6-3below.

Contingency Table (Rain)			
	P-Yes	P-No	Total
O-Yes	13	0	13
O-No	10	37	47
Total	23	37	60

Contingency Table (Dry)			
	P-Yes	P-No	Total
O-Yes	45	1	46
O-No	0	14	14
Total	45	15	60

Contingency Table (Heat)			
	P-Yes	P-No	Total
O-Yes	49	6	55
O-No	3	2	5
Total	52	8	60

Contingency Table (Cold)			
	P-Yes	P-No	Total
O-Yes	1	2	3
O-No	6	51	57
Total	7	53	60

Figure 6-3: Snapshot of Contingency Tables

6.2.6.3 Threat Score (TS) or Critical Success Index (CSI)

The contingency tables were used to determine the threat score of the weather outcomes. Rain was determined with a score of 0.56. The score of dry weather outcome was 0.97, hot/heat was 0.844 and the cold weather outcome was determined as 0.11.

The results of evaluating the visual weather lore verification model depict that the model works for the second case study location (Voi, Kenya). The evaluation results confirm a near-perfect match (with above 80% accuracy) between the visual weather lore-based system predictions and actual weather observations. Contingency

6.3 Innovative Aspects of the Research

A technique for verifying visual weather lore through the use of computer vision, fuzzy cognitive mapping and sensor networks techniques has been developed. The aim of the verification was intended to prove the significance of selected traditional knowledge in enhancing the accuracy of predicting weather conditions. It is important to note that shape-based features (HOG) descriptors performed best in both detection and benchmarking of sky concepts. This was evident from the higher overall detection and benchmark rates compared to other features.

FCMs were found to be a useful mechanism for representation of interactions in the complex visual weather lore phenomenon. Collections of important WL concepts were gathered and visual ones used to guide in design of the FCM. As a first step only astronomical and meteorological concepts related to cloud physics were used to come up with a model of the FCM. The results demonstrate that the stabilized FCM was efficient to predict weather condition scenarios. Fuzzy cognitive mapping for establishing links between weather knowledge and weather lore can contribute to environmental sustainability research by validation of otherwise complex phenomena such as weather lore.

The research results on the use of visual weather lore aspects for predicting weather and subsequent verification against actual weather sensor observations was successful, with over 80% accuracy. The increase in verification accuracy with increased records showed a promising trend promoting continuous research experimentation.

The results from this research were specific to traditional people and the comparisons of the two case study locations were therefore generalized. Limitations in terms of weather variability existed but had minimal influence on the overall case studies results.

The designed visual weather lore verification tool automatically analyzed visual weather data that could complement modern satellite data and weather models. The links between the visual weather lore and modern scientific weather models were used to determine the accuracy of traditional weather knowledge.

The validation results showed that the verification process can combine data from various geographical locations, since accuracy of verifications increased with increased data sets. The

verification by using data sets from different geographical locations also produced similar results.

The results of the visual weather lore validation stimulate the opportunity for integrating consistent weather lore with modern systems of weather prediction and enhancing applications offering decision support relying on weather effects.

The FCM could be enhanced by incorporating sub-FCMs from other WL aspects such as animal or plant behaviours. With the complexity of incorporation of many concepts from sub-FCM models, the FCM outputs can as well be verified by machine learning.

The use of optimized input sets of sky concepts in fuzzy cognitive maps could further be used to enhance the reliability of the predicted weather conditions.

The application of the method used for real-time weather prediction needs to be investigated in the long run for massive data and for long-range weather prediction.

6.4 Recommendations for Future Developments

- (a) This research combined hybrid techniques for verification of weather lore; this provides an entrance point for research on integrating indigenous knowledge on weather with modern numerical weather prediction systems for accurate and downscaled weather forecasts.
- (b) The verification process described in this research concentrated on only the most likely categorical weather outcomes such as presence or absence of heat/cold and dry/wet/rain. The scores presented using contingency tables do not cater for specific weather categories (such as intense rain). To better evaluate the performance of the method in these research-specific weather outcomes, further research aimed at determining particular levels of accuracies is necessary.
- (c) This research aimed at providing a scientific insight in to using selected visual weather lore for weather prediction; for this reason, considerable aspects of weather lore were not explored. Such unverified weather lore (for example sound) can be investigated where methods to verify these specific weather lore categories need to be developed. Future work could also deal with using FCMs for representing holistic characteristics of the weather lore domain.

- (d) This research was conducted within a limited time-frame, making it challenging to consider weather lore from all communities. More case studies may therefore be conducted to compare and verify the results of this research in the future. The predictions of weather outcomes using the visual weather lore verification tool could also be benchmarked by comparative analysis with most of the modern weather validation techniques.
- (e) Wireless sensors are now embedded in most of modern communication devices (such as phones and personal digital assistants) and also attached to most movable objects such as robots, vehicles and animals. Mobile devices could be programmed to enable rural communities to characterize weather lore (using predefined Fuzzy Cognitive Mapping rules) based on their weather observations and conditions respective to their geographic locations. Mobile phone users could also be used to collect and transmit in real time to a central data store the weather images and conditions that they observe. This process would generate massive data sets that could easily be verified.
- (f) The process of gathering information using more than one technique and from two or more independent sources with different forms of data such as text and images could be investigated to confirm and verify visual weather lore in near real-time. Modern web 3.0 techniques such as human computation and GIS tools could also be employed for collective weather sensing and gathering of weather images and conditions for weather lore verification.
- (g) The application of data mining techniques on visual weather lore can lead to useful information in which data mining algorithms can be used to learn patterns and evaluate the quality of visual weather lore data. Data mining validation tests could also be performed several times and results could be averaged to estimate performance of the visual weather lore verification tool.

References

- Abbasi, R. A. (2010). Discovering and Exploiting Semantics in Folksonomies. *PhD Thesis Universitat Koblenz-Landau*, (October).
- Abdulrashid, L. (2013). Sustainability of Indigenous Knowledge in Seasonal rain Forecast and farming Decision in Semi-Arid areas of Katsina State, Nigeria. *International Journal of Arts and Commerce Vol.*, 2(4), 35-46.
- Abramova, N. A., & Kovriga, S. V. (2008). Criterial Approach to Verification at Cognitive Mapping of Ill-Structured Situation Dynamics. *Institute of Control Sciences of Russian Academy of Sciences*, (1963), 1-23.
- Acharya, S. (2011a). Prediction of rainfall variation through flowering phenology of night-flowering jasmine (*Nyctanthes arbor-tristis* L .; *Verbenaceae*) in Tripura. *Indian Journal of Traditional Knowledge*, 10(1), 96-101.
- Acharya, S. (2011b). Presage Biology : Lessons from nature in weather forecasting. *Indian Journal of Traditional Knowledge*, 10(1), 114-124.
- Adel, E., & Elmogy, M. (2014). Image Stitching based on Feature Extraction Techniques : A Survey. *International Journal of Computer Applications*, 99(6), 1-8.
- Agarwal, J., & Bedi, S. S. (2015). Implementation of hybrid image fusion technique for feature enhancement in medical diagnosis. *Human-centric Computing and Information Sciences - SpringerOpen Journal*, 1-17. doi: 10.1186/s13673-014-0020-z.
- Aguilar, J. (2004). Dynamic Random Fuzzy Cognitive Maps. *Computación y Sistemas*, 7(4), 260-270.
- Aguilar, J. (2005). A Survey about Fuzzy Cognitive Maps Papers. *INTERNATIONAL JOURNAL OF COMPUTATIONAL COGNITION*, 3(2), 27-33.
- Ahmad K. (2012). STATISTICAL VERIFICATION OF TWO NUMERICAL WEATHER PREDICTION MODELS FOR QUANTITATIVE PRECIPITATION FORECAST. *International Sustainability and Civil Engineering Journal*, 1(1), 16-24.
- Ahn, L. V. (2005). Human Computation. *Communications of the Association for Computing Machinery*.
- Al-momen, S., George, L. E., & Naji, R. K. (2015). Texture classification using spline , wavelet decomposition and fractal dimension. *Applied and Computational Mathematics*, 4(1), 5-10. doi: 10.11648/j.acm.20150401.12.

- Alamdar, F., & Keyvanpour, M. (2011). A New Color Feature Extraction Method Based on Dynamic Color Distribution Entropy of Neighborhoods. *International Journal of Computer Science Issues*, 8(5), 42-48.
- Alcock, P. G. (2014). Venus Rising: South African Astronomical Beliefs, Customs and Observations. *South African Weather Service*. P.G. Alcock.
- Alonso, O. (2008). Exploiting Semantic Annotations for Information Retrieval. *ECIR Workshop, Glasgow, Sunday 30th of March 2008*.
- Anandaraja, N., & Rathakrishnan, T. (2008). Indigenous weather and forecast practices of Coimbatore district farmers of Tamil Nadu. *Indian Journal of Traditional Knowledge*, 7(4), 630-633.
- Andrysiak, T., & Choras, M. (2005). Image retrieval based on hierarchical gabor filters '. *Int.J.Appl.Math.Comput.Sci*, 15(4), 471-480.
- Anurag, B., Raffay, H., Robinson, P., & Neel, S. (2013). Palette Power : Enabling Visual Search through Colors. *KDD-Association of Computing Machinery*. Chicago, Illinois: Association of Computing Machinery.
- Anyira, I., & Onoriode, O. K. N. A. (2010). The Role of Libraries in the Preservation and Accessibility of Indigenous Knowledge in the Niger Delta Region of Nigeria. *Library Philosophy and Practice (e-journal)*.
- Appati, J. K., Fosu, G. O., & Gogovi, G. K. (2014). Face Feature Extraction for Recognition Using Radon Transform. *American Journal of Engineering Research*, 3(03), 219-224.
- Atger, F. (2001). Verification of intense precipitation forecasts from single models and ensemble prediction systems. *Nonlinear Processes in Geophysics*, 401-417.
- Babu, M. P., & Shankar, P. R. (2015). A Novel Algorithm for Color Image matching using Wavelet-SIFT. *International Journal of Scientific and Research Publications*, 5(1), 1-6.
- Bajwa, I. S., Naweed, M. S., Asif, M. N., & Hyder, S. I. (2009). Feature Based Image Classification by using Principal Component Analysis. *Journal of Graphics, Vision and image Processing*.
- Baliscan, E. S. G. C. M. (2001). TRADITIONAL WEATHER FORECASTING METHODS IN ILOCOS NORTE. *Philipp J Crop Sci*, 26(1), 5-14.
- Benco, M., Hudec, R., Kamencay, P., Zachariasova, M., & Matuska, S. (2014). An Advanced Approach to Extraction of Colour Texture Features Based on GLCM. *International Journal of Advanced Robotic Systems ARTICLE*, 11(104), 1-8. doi: 10.5772/58692.

- Benqin, S., Li, Jun, Mura, M. D., Li, P., Plaza, A., Bioucas-dias, J. M., et al. (2014). Remotely Sensed Image Classification Using Sparse Representations of Morphological Attribute Profile. *IEEE TRANSACTIONS ON GEOSCIENCE AND REMOTE SENSING*, 52(8), 5122-5136.
- Benz, U. C., Hofmann, P., Willhauck, G., Lingenfelder, I., & Heynen, M. (2004). Multi-resolution , object-oriented fuzzy analysis of remote sensing data for GIS-ready information. *ISPRS Journal of Photogrammetry & Remote Sensing*, 58, 239 - 258. doi: 10.1016/j.isprsjprs.2003.10.002.
- Benčo, M., & Hudec, R. (2007). Novel Method for Color Textures Features Extraction Based on GLCM. *RADIO ENGINEERING*, 16(4), 64-67.
- Bhaskar, R., Laxman, Srivatsan, & Smith, A. (2010). Discovering frequent patterns in sensitive data. *KDD*.
- Bhateja, P., Sehrawat, P., & Bhardawaj, A. (2013). An Analysis of Data Mining , Web Image Mining and their Applications. *International Journal of Information and Computation Technology*, 3(6), 603-608.
- Bhowmik, P., Bhowmik, K., Azam, M. N., & Rony, M. W. (2012). Fingerprint Image Enhancement And It ' s Feature Extraction For Recognition. *INTERNATIONAL JOURNAL OF SCIENTIFIC & TECHNOLOGY RESEARCH*, 1(5), 117-121.
- Biglari, O., Ahsan, R., & Rahi, M. (2014). Human Detection Using SURF and SIFT Feature Extraction Methods in Different Color Spaces. *Journal of mathematics and computer Science*, 11, 111 - 122.
- Bougeault, P. (2003). The WGNE survey of verification methods for numerical prediction of weather elements and severe weather events. *Europe*, (May).
- Boureau, Y.-lan. (2012). *Learning Hierarchical Feature Extractors For Image Recognition*.
- Boven, K., & Morohashi, J. (2002). Best Practices using Indigenous Knowledge. *NA joint publication by: uffic/UNESCO/MOST November 2002*.
- Bryan, C., & Yuhong, Z. (2014). Modeling land suitability / capability using fuzzy evaluation. *GeoJournal*, 79, 167-182. doi: 10.1007/s10708-013-9503-0.
- Cai, Y. (2011). Cognitive Teachable Agent in Virtual Learning Environment with Fuzzy Cognitive Map. *International Journal of Information Technology*, 17(2), 1-11.
- Calais, G. J. (2008). Fuzzy Cognitive Maps Theory : Implications for Interdisciplinary Reading : National Implications. *FOCUS On Colleges, Universities, and Schools*, 2(1), 1-16.

- Calbo, J., & Sabburg, J. (2008). Feature Extraction from Whole-Sky Ground-Based Images for Cloud-Type Recognition. *American Meteorological Society*, 3-14. doi: 10.1175/2007JTECHA959.1.
- Campos, D., Barnard, M., Mikolajczyk, K., Kittler, J., Yan, F., Christmas, W., et al. (2011). An evaluation of bags-of-words and spatio-temporal shapes for action recognition. *IEEE Workshop on Applications of Computer Vision* (Vol. 1). Kona, Hawaii.
- Cannell, M. (1933). Signs , Omens , and Portents in Nebraska Folklore. *University of Nebraska Studies in Language, Literature, and Criticism*, (2).
- Carley, K. M. (1996). Validating Computational Models. *Department of Social and Decision Sciences Carnegie Mellon University*, 0793(September).
- Carvalho, J. P. (2010). On the Semantics and the Use of Fuzzy Cognitive Maps in Social Sciences. *WCCI 2010 IEEE World Congress on Computational Intelligence* (pp. 18-23). Barcelona.
- Casati, B., Wilson, L. J., Stephenson, D B, Nurmi, P., Ghelli, A., Pocernich, M., et al. (2008). Review of Forecast verification: current status and future directions. *Meteorological Applications*, 18, 3-18. doi: 10.1002/met.
- Castelein, W., Grus, Ł., Cromptvoets, J., & Bregt, A. (2010). A characterization of Volunteered Geographic Information. *13th AGILE International Conference on Geographic Information Science*, 1-10.
- Chagonda, I., Mugabe, F. T., Munodawafa, A., Mubaya, C. P., Masere, P., & Murewi, C. (2015). Engaging smallholder farmers with seasonal climate forecasts for sustainable crop production in semi-arid areas of Zimbabwe. *African Journal of Agricultural Research*, 10(7), 668-676. doi: 10.5897/AJAR2014.
- Chai, T., & Draxler, R. R. (2014). Root mean square error (RMSE) or mean absolute error (MAE)? – Arguments against avoiding RMSE in the literature. *Geoscientific Model Development*, (2005), 1247-1250. doi: 10.5194/gmd-7-1247-2014.
- Chary, R. V. R., Lakshmi, D. R., & Sunitha, K. V. N. (2012). F EATURE E XTRACTION M ETHODS FOR COLOR IMAGE SIMILARITY. *Advanced Computing: An International Journal*, 3(2), 147-157.
- Chengjin LI, F. P. (2012). Crowdsourcing Database & Application. *SIGSPATIAL*.
- Chia-chien, H. (2007). The Delphi Technique: Making Sense Of Consensus. *Practical Assessment, Research & Evaluation*, 12(10).

- Chinlapianga, M. (2011). Traditional knowledge , weather prediction and bioindicators : A case study in Mizoram , Northeastern India. *Indian Journal of Traditional Knowledge*, 10(1), 207-211.
- Chiwanza, K., Musingafi, M. C. C., & Mupa, P. (2013). Challenges in Preserving Indigenous Knowledge Systems : Learning From Past Experiences. *Information and Knowledge Management*, 3(2), 19-26.
- Chora, R. S. (2007). Image Feature Extraction Techniques and Their Applications for CBIR and Biometrics Systems. *INTERNATIONAL JOURNAL OF BIOLOGY AND BIOMEDICAL ENGINEERING*, 1(1), 6-16.
- Chrysafiadi, K., & Virvou, M. (2013). A knowledge representation approach using fuzzy cognitive maps for better navigation support in an adaptive learning system. *SpringerPlus - a SpringerOpen Journal*, 2(1), 1-13. doi: 10.1186/2193-1801-2-81.
- Chrysostomos, S., & Peter, G. (1999). Mathematical Formulation of Fuzzy Cognitive Maps. *Proceedings of the 7th Mediterranean Conference on Control and Automation* (pp. 2251-2261). Haifa.
- Chun-mei, L. I. N. (2009). Adaptive Control Framework Study Based on Fuzzy Cognitive Map. *Proceedings of the 3rd WSEAS International Conference on COMPUTER ENGINEERING and APPLICATIONS* (pp. 93-96).
- Clemons, J., Jones, A., Perricone, R., Savarese, S., & Austin, T. (2011). EFFEX : An Embedded Processor for Computer Vision Based Feature Extraction, 1-6.
- Dagher, I., Sallak, N. E., & Hazim, H. (2014). Face Recognition using the most Representative Sift Images. *International Journal of Signal Processing, Image Processing and Pattern Recognition*, 7(1), 225-234.
- Dalal, N., & Triggs, B. (2005). Histograms of Oriented Gradients for Human Detection. *Proceedings of the 2005 IEEE Computer Society Conference on Computer Vision and Pattern Recognition*.
- Deepak. (2014). Content Based Image Retrieval using HSV-Color Histogram and GLCM. *International Journal of Advance Research in Computer Science and Management Studies*, 2(1), 246-253.
- Deng, Y., Manjunath, B. S., Kenney, C., Moore, M. S., & Shin, H. (2001). An Efficient Color Representation for Image Retrieval. *IEEE TRANSACTIONS ON IMAGE PROCESSING*, 10(1), 140-147.
- Dhawan, S., & Dogra, H. (2012). Feature Extraction Techniques for Face Recognition. *International Journal of Engineering, Business and Enterprise Applications*, 12(202), 1-4.

- Dilipsinh, B., Mahasweta, J., & Vikram, A. (2014). A Study on Features Extraction Techniques for Image Mosaicing. *International Journal of Innovative Research in Computer and Communication Engineering*, 2(3), 3432-3437.
- Din, M. A., & Cretan, G. C. (2014). Causal modeling of the higher education determinants regarding the labour market absorption of graduates : a Fuzzy Cognitive Maps approach. *INTERNATIONAL JOURNAL of FUZZY SYSTEMS and ADVANCED APPLICATIONS*, 1, 1-6.
- Dissanayake, M., & AbouRizk, S. M. (2007). QUALITATIVE SIMULATION OF CONSTRUCTION PERFORMANCE USING FUZZY COGNITIVE MAPS. *Proceedings of the 2007 Winter Simulation Conference* (pp. 2134-2140).
- Djam. (2013). Fuzzy Cognitive Map Based Approach for Teachers ' Performance Evaluation. *The Pacific Journal of Science and Technology*, 14(2), 176-181.
- Douze, M., Amsaleg, L., & Schmid, C. (2009). Evaluation of GIST descriptors for web-scale image search. *CIVR*, 0-7.
- Duan, N., & Hoagwood, K. (2013). Purposeful Sampling for Qualitative Data Collection and Analysis in Mixed Method Implementation Research. *Adm Policy Ment Health*. doi: 10.1007/s10488-013-0528-y.
- Dubey, R. S., Choubey, R., & Bhattacharjee, J. (2010). Multi Feature Content Based Image Retrieval. *International Journal on Computer Science and Engineering*, 02(06), 2145-2149.
- Dworkin, A. (2008). POLICY BRIEF SUMMARY DRONES AND TARGETED KILLING : DEFINING A EUROPEAN POSITION. *European Council of Foreign Relations*.
- Eldib, M. Y., & Onsi, H. M. (2011). Web Image Mining Age Estimation Framework. *ICGST-GVIP Journal*, 11(1), 1-8.
- Elissa, A., Mariya, T., Abhinav, S., Xinlei, C., & Ishan, M. (2015). Applying artificial vision models to human scene understanding. *Frontiers in Computational Neuroscience* - www.frontiersin.org, 9(February), 1-14. doi: 10.3389/fncom.2015.00008.
- Elpiniki Papageorgiou, C. S., & Groumpos, P. (2007). Novel Architecture for supporting medical decision making of different data types based on Fuzzy Cognitive Map Framework. *Proceedings of the 29th Annual International Conference of the IEEE EMBS* (pp. 1192-1195). Lyon.
- Elpiniki, P. (2011). Review study on Fuzzy Cognitive Maps and their applications during the last decade. *2011 IEEE International Conference on Fuzzy Systems* (pp. 828-835).
- Enock, C. M. (2013). Indigenous Knowledge Systems and Modern Weather Forecasting: Exploring the Linkages. *Journal of Agriculture and Sustainability*, 2(1), 98-141.

- Etemad, K., & Chellappa, R. (1997). Discriminant analysis for recognition of human face images. *Journal of Optical Society of America*, 14(8), 1724-1733.
- Fairweather, J., Hunt, L., Rosin, C., Campbell, H., Benge, J., & Watts, M. (2006). *Understanding kiwifruit management using causal mapping. ARGOS Research Report.*
- Faizal, M., Jabal, A., Hamid, S., Shuib, S., & Ahmad, I. (2013). LEAF FEATURES EXTRACTION AND RECOGNITION APPROACHES TO CLASSIFY PLANT. *Journal of Computer Science*, 9(10), 1295-1304. doi: 10.3844/jcssp.2013.1295.1304.
- Fajman, P. (2011). Improved Verification and Analysis of National Weather Service Point Forecast Matrices. *Earth Sciences Commons, and the Meteorology Commons.*
- Feifei, L., Lijian, Z., & Zhe-ming, L. (2015). Palmprint Feature Extraction Based on Curvelet Transform. *Journal of Information Hiding and Multimedia Signal Processing*, 6(1), 131-139.
- Fishman, B. J., & Amico, L. M. D. (1994). Which Way Will The Wind Blow ? Networked Computer Tools For Studying The Weather. *Conference on Educational Multimedia and Telecommunications* (pp. 209-216). Vancouver.
- Franklin, M. J., Kossmann, D., Kraska, T., Ramesh, S., & Xin, R. (2011). CrowdDB : Answering Queries with Crowdsourcing. *SIGMOD'11 - ACM.*
- Friederichs, P., & Thorarinsdottir, T. L. (2012). Forecast verification for extreme value distributions with an application to probabilistic peak wind prediction. *Meteorological Institute, University of Bonn*, 1-26.
- Gekas, J. (2012). Social Data Mining through Distributed Mobile Sensing. *International Journal of Engineering.*
- Goodchild, M. F. (2006). CITIZENS AS SENSORS: THE WORLD OF VOLUNTEERED GEOGRAPHY. *National Center for Geographic Information and Analysis, and Department of Geography, University of California*, 1-15.
- Goodchild, M. F., & Glennon, J. A. (2010). ACrowdsourcing geographic information for disaster response: a research frontier. *International Journal of Digital Earth*, 3(926057191), 231-241. doi: 10.1080/17538941003759255.
- Goswami, B. N. (1997). The Challenge of Weather Prediction. *RESONANCE, SERIES ARTICLE*, (Jan), 8-15.
- Gray, Steven, Zanre, E., & Gray, Stefan. (n.d.). Fuzzy Cognitive Maps as Representations of Mental Models and Group Beliefs. *University of Hawai'i at Mānoa; University College Cork, Coastal and Marine Research Center, Environmental Research Institute, Ireland.*

- Green, D., Billy, J., & Tapim, A. (2010). Indigenous Australians ' knowledge of weather and climate. *Climatic Change*, *100*, 337-354. doi: 10.1007/s10584-010-9803-z.
- Griefahn, D., Wollnack, J., & Hintze, W. (2014). Principal component analysis for fast and automated thermographic inspection of internal structures in sandwich parts. *J. Sens. Sens. Syst.*, *3*, 105-111. doi: 10.5194/jsss-3-105-2014.
- Grigorescu, S. E., Petkov, N., & Kruizinga, P. (2002). Comparison of Texture Features Based on Gabor Filters. *IEEE TRANSACTIONS ON IMAGE PROCESSING*, *11*(10), 1160-1167.
- Guerram, T., Maamri, R., & Sahnoun, Z. (2010). A Tool for Qualitative Causal Reasoning On Complex Systems. *International Journal of Computer Science Issues*, *7*(6), 120-125.
- Gulati, N. (2014). Knowledge Navigator for Intelligent Collaborative E-Tutoring : A Proposed Framework using Fuzzy Cognitive Agent. *International Journal of Science and Research*, *3*(6), 772-775.
- Habibi, M., & Popescu-belis, A. (2012). Using Crowdsourcing to Compare Document Recommendation Strategies for Conversations. *ACM RecSys 2012*, 15-20.
- Habibi, M., & Popescu-belis, A. (2014). Enforcing Topic Diversity in a Document Recommender for Conversations. *Proceedings of COLING 2014, the 25th International Conference on Computational Linguistics*, 588-599.
- Hamill, T., Josip Juras. (2006). Measuring forecast skill : is it real skill or is it the varying climatology ?. *Quarterly Journal of the Royal Meteorological Society*, *132*, 2905-2923. doi: 10.1256/qj.06.25.
- Haoqi, Z., Edith, L., Miller, R., Gajos, K., Parkes, D., & Horvitz, E. (2012). Human Computation Tasks with Global Constraints. *CHI'12 - ACM*.
- Haralick, R. M., & Shanmugam, K. (1973). Textural Features for Image Classification. *IEEE TRANSACTIONS ON SYSTEMS, MAN, AND CYBERNETICS*, *SMC-3*(6).
- Heinle, A., Macke, A., & Srivastav, A. (2010). Automatic cloud classification of whole sky images. *Atmospheric Measurement Techniques*, *3*, 557-567. doi: 10.5194/amt-3-557-2010.
- Hema. (2013). A SURVEY IN NEED OF IMAGE MINING TECHNIQUES. *International Journal of Advanced Research in Computer and Communication Engineering*, *2*(2), 1238-1240.
- Hermosilla. (2005). COMBINING FEATURES EXTRACTED FROM IMAGERY AND LIDAR DATA FOR OBJECT-ORIENTED CLASSIFICATION OF FOREST AREAS. *The International Archives of the Photogrammetry, Remote Sensing and Spatial Information Sciences*, *XXXVIII-4/*, 3-8.

- Hoefler, T., Schneider, T., & Lumsdaine, A. (2010). Characterizing the Influence of System Noise on Large-Scale Applications by Simulation. *IEEE*, (November).
- Hornidge, A.-katharina, & Antweiler, C. (2012). Environmental Uncertainty and Local Knowledge Southeast Asia as a Laboratory of Global Ecological Change. *transcript Verlag*, (September), 32-80.
- Hossain, A., Rahman, A., Hossen, J., Iqbal, A. K. M. P., & Hasan, S. K. (2011). Application of Fuzzy Logic Approach for an Aircraft Model with and without Winglet. *International Journal of Aerospace and Mechanical Engineering*, 5(4), 224-232.
- Hosseini, M., Zarandi, F., Khademian, M., & Minaei-bidgoli, B. (2012). A Fuzzy Expert System Architecture for Intelligent Tutoring Systems : A Cognitive Mapping Approach. *Journal of Intelligent Learning Systems and Applications*, 4, 29-40.
- Hullman, J., Krupka, E., & Adar, E. (2015). Evaluating Approaches to Crowdsourced Visual Analytics. *Collective Intelligence*, 1-4.
- Huntington, H., Callaghan, T., Fox, S., & Krupnik, I. (2004). Matching Traditional and Scientific Observations to Detect Environmental Change : A Discussion on Arctic Terrestrial Ecosystems. *Ambio*, 33(7), 20-25.
- Hyatt, H. M. (2002). *Folklore from Adams County Illinois*, (3rd Edition).
- Hyun-Woong Jang, S. C. (2014). Flickr Image Classification using SIFT Algorithm. *Life Science Journal*, 11(7), 607-611.
- Jagdish, L., Sunil, K., & Ankit, C. (2013). Fabric defect detection based on GLCM and Gabor filter: A comparison. *Optik - International Journal for Light and Electron Optics*, 1-6. Elsevier GmbH. doi: 10.1016/j.ijleo.2013.05.004.
- Jain, N., & Salankar, S. S. Color & Texture Feature Extraction for Content Based Image Retrieval. *IOSR Journal of Electrical and Electronics Engineering*, 2014, 53-58.
- Jiang, Y. G., Jun, Y., & Chongwah, N. (2007). Towards Optimal Bag-of-Features for Object Categorization and Semantic Video Retrieval. *Association of Computing Machinery*.
- Jignesh, J., with Deepak, K., Ramakrishna. (2014). A review on applying Fuzzy Logic inference system in Improving Agility Assessment of Supply Chain. *INTERNATONAL JOURNAL OF INNOVATIVE RESEARCH IN TECHNOLOGY*, 1(5), 111-117.
- Johansson, T., & Achola, S. M. (2013). Challenges for bridging the divide between scientific and traditional knowledge systems of climate prediction in the taita hills, kenya. *Africa Climate Conference 2013*. Arusha: African Insect Science for Food and Health.

- John, W., Allen, Y., Arvind, G., & Shankar, S. (2009). Robust Face Recognition via Sparse Representation. *IEEE TRANSACTIONS ON PATTERN ANALYSIS AND MACHINE INTELLIGENCE*, 31(2), 1-18.
- Jones. (2010). Modeling Situation Awareness for Army Infantry Platoon Leaders Using Fuzzy Cognitive Mapping Techniques. *Proceedings of the 19th Conference on Behavior Representation in Modeling and Simulation* (pp. 216 - 223). Charleston.
- Jun, Z., & Youssef, B. (2012). Color Image Descriptor. *Springer-Verlag Berlin Heidelberg*, 312-324.
- K, R., Raja, K. B., R, V. K., & Patnaik, L. M. (2010). Feature Extraction based Face Recognition , Gender and Age Classification. *International Journal on Computer Science and Engineering*, 02(01), 14-23.
- Kakarwal, S. N., & Deshmukh, R. R. (2012). Hybrid Feature Extraction Technique for Face Recognition. *International Journal of Advanced Computer Science and Applications*, 3(2), 60-64.
- Kamavisdar, P., Saluja, S., & Agrawal, S. (2013). A Survey on Image Classification Approaches and Techniques. *International Journal of Advanced Research in Computer and Communication Engineering*, 2(1), 1005-1009.
- Kanagasabhapathy, G., & Kumaravel, A. (2014). Construction of Primary Fuzzy Cognition Mapping For mathematical Intuition. *World Applied Sciences Journal*, 31(8), 1508-1511. doi: 10.5829/idosi.wasj.2014.31.08.2054.
- Karagiannis, I., & Groumpos, P. (2013). Input-Sensitive Fuzzy Cognitive Maps. *International Journal of Computer Science Issues*, 10(3), 143-151.
- Karel Lenc, J. R. M., & Mishkin, D. (2014). A Few Things One Should Know About Feature Extraction , Description and Matching. *19th Computer Vision Winter Workshop*. Krtiny, Czech Republic.
- Kennedy, R. P. (2010). Unstructured Content Analysis & Classification System for the IRS. *International Journal Computer Applications*, 1(4), 32-37.
- Khan, N., Mccane, B., & Wyvill, G. (2011). SIFT and SURF Performance Evaluation Against Various Image Deformations on Benchmark Dataset. *2011 International Conference on Digital Image Computing: Techniques and Applications* (pp. 501-506). doi: 10.1109/DICTA.2011.90.
- Khatib, T., Karajeh, H., Mohammad, H., & Rajab, L. (2015). Full Length Research Paper A hybrid multilevel text extraction algorithm in scene images. *academicJournals*, 10(14908), 105-113. doi: 10.5897/SRE2014.6146.

- Kidd, D. A. (1984). WEATHER LORE IN ARATUS ' PHAENOMENA. *Weather and Climate*, 4, 32-37.
- Kim, Jinho, Kim, B.-S., & Savarese, S. (2011). Comparing Image Classification Methods : K-Nearest-Neighbor and Support-Vector-Machines. *Applied Mathematics in Electrical and Computer Engineering*, 133-138.
- Kobayashi, T. (2013). BoF meets HOG : Feature Extraction based on Histograms of Oriented p . d . f Gradients for Image Classification. *IEEE Conference on Computer Vision and Pattern Recognition* (pp. 747-754). doi: 10.1109/CVPR.2013.102.
- Kosko, B. (1986). Fuzzy Cognitive Maps. *Int. J. Man-Machine Studies*, 24, 65-75.
- Krause, M., & Smeddinck, J. (2011). HUMAN COMPUTATION GAMES : A SURVEY. *19th European Signal Processing Conference, (Eusipco)*, 754-758.
- Kuhn, W. (2007). Volunteered Geographic Information and GIScience. *Position Paper for the NCGIA and Vespucci Workshop on Volunteered Geographic Information*.
- Kunkle, T., & Ristvet, B. (2013). CASTLE BRAVO: FIFTY YEARS OF LEGEND AND LORE A Guide to Off-Site Radiation Exposures. *Defense Threat Reduction Agency- Defense Threat Reduction Information Analysis Center*.
- Kuo, Y.-ling, & Hsu, J. Y.-jen. (2010). Resource-Bounded Crowd-Sourcing of Commonsense Knowledge. *Proceedings of the Twenty-Second International Joint Conference on Artificial Intelligence*, 2470-2475.
- Kuril, S., & Saini, I. (2013). Cloud Classification for Weather Information by Artificial Neural Network. *International Journal of Applied Physics and Mathematics*, 3(1), 28-30. doi: 10.7763/IJAPM.2013.V3.167.
- Kwon, S. J., & Mustapha, E. E. (2013). Exploring the Effect of Cognitive Map on Decision Makers ' Perceived Equivocality and Usefulness in the Context of Task Analyzability and Representation. *The Fifth International Conference on Information, Process, and Knowledge Management* (pp. 117-122).
- Laliberte, A. S., & Rango, A. (2011). Image Processing and Classification Procedures for Analysis of Sub-decimeter Imagery Acquired with an Unmanned Aircraft over Arid Rangelands. *GIScience & Remote Sensing*, 48(1), 4-23. doi: 10.2747/1548-1603.48.1.4.
- Lane, N. D., Miluzzo, E., Lu, H., Peebles, D., Choudhury, T., & Campbell, A. T. (2010). A Survey of Mobile Phone Sensing. *IEEE Communications Magazine - AD HOC AND SENSOR NETWORKS*, (September), 140-150.
- Lang, D. (2009). Automatic recognition and calibration of astronomical images. *PhD Thesis. Astrometry.net repository*, (11).

- Lavoué, G. (2011). Bag of Words and Local Spectral Descriptor for 3D Partial Shape Retrieval. *Eurographics Workshop on 3D Object Retrieval*.
- Law, M. T., Thome, N., & Cord, M. (2014). Bag-of-Words Image Representation : Key Ideas and Further Insight, 29-52. doi: 10.1007/978-3-319-05696-8.
- Laxman, Singh, with Zaheeruddin & Jaffery. (2012). Detection and Shape Feature Extraction of Breast Tumor in Mammograms. *Proceedings of the World Congress on Engineering* (Vol. II). London, U.K.
- Levner, I., Bulitko, V., Li, L., Lee, G., & Greiner, R. (2003). Automated Feature Extraction for Object Recognition.
- Lisin, D. A. (2006). IMAGE CLASSIFICATION WITH BAGS OF LOCAL FEATURES. *PhD Dissertation University of Massachusetts Amherst*, (May).
- Little, G. (2011). *Programming with Human Computation. Sites The Journal Of 20Th Century Contemporary French Studies*.
- Lo, J. C.-fung, & Pielke, R. (2008). Assessment of three dynamical climate downscaling methods using the Weather Research and Forecasting (WRF) model. *Journal of Geophysical Research*, 113. doi: 10.1029/2007JD009216.
- Lorca, D. F., Sotelo, M. Á., Bergasa, L. M., Toro, P. R. D., Nuevo, J., Ocaña, M., et al. (2007). Combination of Feature Extraction Methods for SVM Pedestrian Detection. *IEEE TRANSACTIONS ON INTELLIGENT TRANSPORTATION SYSTEMS*, 8(2), 292-307.
- Lowe, D. G. (2004). Distinctive Image Features from Scale-Invariant Keypoints. *International Journal of Computer Vision*, 1-28.
- Luo, X. (2010). Merging Textual Knowledge Represented by Element Fuzzy Cognitive Maps. *JOURNAL OF SOFTWARE*, 5(2), 225-234. doi: 10.4304/jsw.5.2.225-234.
- Mago, V. K., Morden, H. K., Fritz, C., Wu, T., Namazi, S., & Geranmayeh, P. (2013). Analyzing the impact of social factors on homelessness : a Fuzzy Cognitive Map approach. *BMC Medical Informatics and Decision Making*, 13(94), 1-19.
- Mailier, P., Jolliffe, I., & David, S. (2006). Quality of Weather Forecasts: Review and recommendations. *Royal Meteorological Society*, (January).
- Maini, P., with L.S.Rathore. (2008). Economic Impact Assessment of Agro- Meteorological Advisory Service of NCMRWF. *Report no. NMRF/PR/01/2008, 104pp, Published by NCMRWF, Ministry of Earth Sciences, Government of India, A-50 Institutional Area, Sector- 62, NOIDA, UP, INDIA 201 307*.

- Maitra, S., & Banerjee, D. (2014). Application of Fuzzy Cognitive Mapping for Cognitive Task Analysis in Mechanised Mines. *IOSR Journal of Mechanical and Civil Engineering*, 11(2), 20-28.
- Mandloi, G. (2014). A Survey on Feature Extraction Techniques for Color Images. *Journal of Computer Science*, 5(3), 4615-4620.
- Manisha, D., & Neeraj, K. (2014). Face Recognition based on Singular Value Decomposition Linear Discriminant Analysis Method. *International Journal of Engineering and Innovative Technology*, 3(12), 192-195.
- Manjunath. (2014). Review and Analysis of Multimedia Data. *International Journal of Innovative Research in Computer and Communication Engineering*, 2(2), 124-130.
- Mansoor, M. R., Bhargavi, R., & Rahima, T. M. H. B. (2012). AUTOMATIC IDENTIFICATION OF CLOUD COVER REGIONS USING SURF. *International Journal of Computer Science, Engineering and Information Technology*, 2(2), 159-175.
- Mapara, J. (2009). Indigenous Knowledge Systems in Zimbabwe : Juxtaposing Postcolonial Theory. *The Journal of Pan African Studies*, 3(1), 139-155.
- Mariani, S., & Casaioli, M. (2008). Forecast verification: A summary of common approaches and examples of application. *FORALPS Technical Report*, 5, 60.
- Martha, T. R., & Kerle, N. (2012). CREATION OF EVENT-BASED LANDSLIDE INVENTORY FROM PANCHROMATIC IMAGES BY OBJECT ORIENTED ANALYSIS. *Proceedings of the 4th GEOBIA* (pp. 53-57). Rio de Janeiro - Brazil.
- Masinde, M., & Bagula, A. (2012). ITIKI: bridge between African indigenous knowledge and modern science of drought prediction. *Knowledge Management for Development Journal*, 7(3), 37-41.
- Masinde, M., Bagula, A., & Muthama, N. (2013). IMPLEMENTATION ROADMAP FOR DOWNSCALING DROUGHT FORECASTS IN MBEERE USING ITIKI. *Kaleidoscope Academic Conference*.
- Massung, E., Coyle, D., Cater, K., Jay, M., & Preist, C. (2013). Using Crowdsourcing to Support Pro-Environmental Community Activism. *Association for Computing Machinery: CHI 2013, April 27–May 2, 2013, Paris, France*.
- Mathew, S., & Balas, V., Zachariah. (2015). A Content-based Image Retrieval System Based On Convex Hull Geometry. *Acta Polytechnica Hungarica*, 12(1), 103-116.
- Mathworks. (2015). Fuzzy Logic Toolbox User ' s Guide. *Matlab R2015a*.

- Mavrantza, O. D., & Argialas, D. P. (1997). IDENTIFICATION OF URBAN FEATURES USING OBJECT-ORIENTED IMAGE. *International Archives of Photogrammetry, Remote Sensing and Spatial Information Sciences*, 36, 101-106.
- Mccall, M. K., Martinez, J., & Verplanke, J. (2013). Shifting Boundaries of Volunteered Geographic Information Systems and Modalities : Learning from PGIS. *ACME: An International E-Journal for Critical Geographies*, 1-36.
- Medjahed, S. A. (2015). A Comparative Study of Feature Extraction Methods in Images Classification. *I.J. Image, Graphics and Signal Processing*, 3(February), 16-23. doi: 10.5815/ijigsp.2015.03.03.
- Meier, P. (2011). Verifying Crowdsourced Social Media Reports for Live Crisis Mapping : An Introduction to Information Forensics. *iRevolutio*; www.iRevolution.net/bio.
- Messenger, C., & Faure, V. (2012). Validation of remote sensing and weather model forecasts in the Agulhas ocean area to 57 ° S by ship observations. *South African Journal of Science*, 108, 1-10.
- Mishra, N., & Silakari, S. (2012). Image Mining in the Context of Content Based Image Retrieval :. *International Journal of Computer Science Issues*, 9(4), 69-76.
- Mohamed, W., Heshmat, M., Girgis, M., & Elaw, S. (2013). A new Method for Face Recognition Using Variance Estimation and Feature Extraction. *International Journal of Emerging Trends & Technology in Computer Science*, 2(2), 134-141.
- Mohanaiah, P., Sathyanarayana, P., & Gurukumar, L. (2013). Image Texture Feature Extraction Using GLCM Approach. *International Journal of Scientific and Research Publications*, 3(5), 1-5.
- Molnar, A., Mansour, M. J., Saulnier, A., & Thompson, S., with Bracken-Roche, C., David Lyon. (2014). Surveillance Drones : Privacy Implications of the Spread of Unmanned Aerial Vehicles (UAVs) in Canada. *A Report to the Office of the Privacy Commissioner of Canada, under the 2013-2014 Contributions Program*, (613).
- Morris, R. R., & Mcduff, D. (2012). Crowdsourcing Techniques for Affective Computing. *MIT Media Lab*.
- Muguti, T., & Maposa, R. S. (2012). Indigenous Weather Forecasting : A Phenomenological Study Engaging the Shona of Zimbabwe. *The Journal of Pan African Studies*, 4(9), 102-113.
- Mwagha, S. M., & Masinde, M. (2014). Comparison of Nearest Neighbor (ibk), Regression by Discretization and Isotonic Regression Classification Algorithms for Precipitation Classes Prediction. *International Journal of Computer Applications*, 96(21), 44-48.

- Mwagha, S. M., & Masinde, M. (2015). Scientific Verification of Weather Lore for Drought Forecasting – The Role of Fuzzy Cognitive Mapping. In P. C. A. M. C. (Eds) (Ed.), *IST-Africa 2015 Conference Proceedings* (pp. 1-13). Lilongwe, Malawi: IIMC International Information Management Corporation.
- Mwagha, S. M., Waiganjo, P. W., Moturi, C. A., & Masinde, M. (2014). Intelligent System For Predicting Agricultural Drought For Maize Crop. *INTERNATIONAL JOURNAL OF TECHNOLOGY ENHANCEMENTS AND EMERGING ENGINEERING RESEARCH*, 2(4), 51-54.
- Mwangi, E., Wetterhall, F., Dutra, E., Giuseppe, F. D., & Pappenberger, F. (2014). Forecasting droughts in East Africa. *Hydrology and Earth System Sciences*, 18, 611-620. doi: 10.5194/hess-18-611-2014.
- N, A., A, K., & V, M. (2010). Image Clustering and Retrieval using Image Mining Techniques. *IEEE International Conference on Computational Intelligence and Computing Research*.
- Nagaraju, C., Srinu, B., & Rao, E. S. (2013). An efficient Facial Features extraction Technique for Face Recognition system Using Local Binary Patterns. *International Journal of Innovative Technology and Exploring Engineering*, 2(6), 76-78.
- Najafi, A. (2011). Prediction Of The Price Transmission Performance Using Fuzzy Cognitive Maps. *Australian Journal of Basic and Applied Sciences*, 5(9), 1281-1287.
- Najafi, A., & Afrazeh, A. (2008). Using Fuzzy Cognitive Maps for Prediction of KnowledgeWorker Productivity Based on Real Coded Genetic Algorithm. *International Journal of Industrial Engineering & Production Research*, 22(1), 21-30.
- Nakashima, D. J., & McLean, K. G., Thulstru. (2012). Weathering Uncertainty Traditional knowledge for climate change assessment and adaptation. *United Nations Educational, Scientific and Cultural Organization*, 120. Paris: UNESCO, and Darwin, UNU.
- Narasimhan, S. G., & Nayar, S. K. (2002). Vision and the Atmosphere. *International Journal of Computer Vision*, 48(3), 233-254.
- Nasserzadeh, S. M. R., Jafarzadeh, M. H., Mansouri, T., & Sohrabi, B. (2008). Customer Satisfaction Fuzzy Cognitive Map in Banking Industry. *Communications of the IBIMA*, 2, 151-162.
- Neiting, T. G., & Aftery, A. E. R. (2007). Strictly Proper Scoring Rules , Prediction , and Estimation. *Journal of the American Statistical Association*, 102(477). doi: 10.1198/016214506000001437.
- Nejad, F. M., Motekhas, F. Z., Zakeri, H., & Mehrabi, A. (2015). An Image Processing Approach to Asphalt Concrete Feature Extraction. *Journal of Industrial and Intelligent Information*, 3(1), 54-60. doi: 10.12720/jiii.3.1.54-60.

- Nereveettil, C. J., Kalamani, M., & Valarmathy, S. (2014). Feature Selection Algorithm for Automatic Speech Recognition Based On Fuzzy Logic. *International Journal of Advanced Research in Electrical, Electronics and Instrumentation Engineering*, 3(3), 6974-6980.
- Ngara, R., & Mangizvo, R. V. (2013). INDIGENOUS KNOWLEDGE SYSTEMS AND THE CONSERVATION OF NATURAL RESOURCES IN THE SHANGWE COMMUNITY IN GOKWE DISTRICT , ZIMBABWE. *International Journal of Asian Social Science*, 3(1), 20-28.
- Ni, B., Song, Z., & Yan, S. (2009). Web Image Mining Towards Universal Age Estimator. *Association of Computing Machinery*, 85-94.
- Nikolaou, N., & Papamarkos, N. (2002). Color image retrieval using a fractal signature extraction technique. *Engineering Applications of Artificial Intelligence*, 15, 81-96.
- Nixon, M., & Aguado, A. (2002). *Feature extraction and Image Processing* (2nd ed.). Elsevier Ltd.
- Noh, S.-in, Bae, K., Park, Y., & Kim, Jaihie. (2003). A Novel Method to Extract Features for Iris Recognition System. *Springer-Verlag Berlin Heidelberg*, 862-868.
- Nowak, E., Jurie, F., & Triggs, B. (2006). Sampling Strategies for Bag-of-Features. *Springer-Verlag Berlin Heidelberg*, 490-503.
- Nurmi, P. (2003). Recommendations on the verification of local weather forecasts. *European Centre for Medium Range Weather Forecasts*, (December).
- Oberkampf, W. L., & Trucano, T. G. (2002). Verification and Validation in Computational Fluid Dynamics. *Progress in Aerospace Sciences*.
- Obiedat, M. (1994). Robust Semi-Quantitative Fuzzy Cognitive Map Model for Complex Systems and Case Study : Mitigating the Water Scarcity Problem in Jordan. *Lincoln University Digital Thesis*.
- Okonya, J. S., & Kroschel, J. (2013). Indigenous knowledge of seasonal weather forecasting : A case study in six regions of Uganda. *Agricultural Sciences*, 4(12), 641-648.
- Olaode, A., Naghdy, G., & Todd, C. (2014). Unsupervised Classification of Images : A Review. *International Journal of Image Processing*, 5(8), 325-342.
- Oliva, A. (2005). Gist of the Scene. *ELSEVIER INC., CHAPTER 41*, 251-257.
- Olubunmi, A. J., Olusayo, O. E., Bola, A. A., & Ayodeji, O. O. (2015). Performance Evaluation Of Selected Principal Component Analysis-Based Techniques For Face Image Recognition. *INTERNATIONAL JOURNAL OF SCIENTIFIC & TECHNOLOGY RESEARCH*, 4(01), 35-41.

- Oreskes, N., Shrader-frechette, K., & Belitz, K. (2010). Verification , Validation , and Confirmation of Numerical Models in the Earth Sciences. *American Association for the Advancement of Science*, 263(5147), 641-646.
- Oviedo, G., Gotheil, S., Cross, K., Boedhihartono, A., Wolfangel, C., Howell, M., et al. (2008). Indigenous and Traditional Peoples and Climate Change Issues Paper. *Diversity*, (March).
- Owiny, S. A., & Maretzki, A. N. (2014). The Use of Social Media Technologies to Create, Preserve, and Disseminate Indigenous Knowledge and Skills to Communities in East Africa. *International Journal of Communication*, 8, 234-247.
- P, B., Musolesi, M., & Mascolo, C. (2007). Opportunistic Mobile Sensor Data Collection with SCAR. *IEEE*.
- Pachouri, K. K. (2015). A Comparative Analysis & Survey of various Feature Extraction Techniques. *International Journal of Computer Science and Information Technologies*, 6(1), 377-379.
- Panchal. (2013). A Comparison of SIFT and SURF. *International Journal of Innovative Research in Computer and Communication Engineering*, 1(2), 323-327.
- Pandit, A., Kolhar, S., & Patil, P. (2015). Survey on Automatic RBC Detection and Counting. *International Journal of Advanced Research in Electrical, Electronics and Instrumentation Engineering*, 4(1), 128-131.
- Pandya, M., Chitaliya, N., & Sandip, P. (2013). Accurate Image Registration using SURF Algorithm by Increasing the Matching Points of Images. *International Journal of Computer Science and Communication Engineering*, 2(1), 14-19.
- Pang, J. (2013). Intelligent Modeling and Decision Making for Product Quality of Manufacturing System Based on Fuzzy Cognitive Map. *International Journal of Computer Science Issues*, 10(1), 501-506.
- Papageorgiou. (2008). Brain tumor characterization using the soft computing technique of fuzzy cognitive maps. *Applied Soft Computing*, 8, 820-828. doi: 10.1016/j.asoc.2007.06.006.
- Papageorgiou, E. I., & Salmeron, J. L. (2014). Methods and Algorithms for Fuzzy Cognitive Map-based Modeling. *Intelligent Systems Reference Library*, 54. doi: 10.1007/978-3-642-39739-4.
- Paresh, R. (2011). Efficient CBIR Using Color Histogram Processing. *Signal & Image Processing : An International Journal(SIPIJ)*, 2(1), 94-112.
- Pasztor, E. (2010). The significance of the Sun , Moon and celestial bodies to societies in the Carpathian basin during the Bronze Age. *Proceedings IAU Symposium*, (260), 657-663. doi: 00.0000/X0000000000000000X.

- Perić, N. (2015). Fuzzy Logic and Fuzzy Set Theory Based Edge Detection Algorithm. *SERBIAN JOURNAL OF ELECTRICAL ENGINEERING*, 12(1), 109-116. doi: 10.2298/SJEE1501109P.
- Perumal, K., & Bhaskaran, R. (2010). SUPERVISED CLASSIFICATION PERFORMANCE OF MULTISPECTRAL IMAGES. *JOURNAL OF COMPUTING*, 2(2), 124-129.
- Piera, J., Baradad, V., García-LadonaParisi-, E., Lombarte, A., Recasens, L., & Cabestany, J. (2005). Otolith shape feature extraction oriented to automatic classification with open distributed data. *Marine And Freshwater Research*, 805-814.
- Pinson, P. (2013). Wind Energy : Forecasting Challenges for Its Operational Management. *Statistical Science*, 28(4), 564-585. doi: 10.1214/13-STS445.
- Pipek, V., Landgren, J., & Palen, L. (2012). Collaboration and Crisis Informatics. *Proceedings of the CSCW 2012 Workshop on Collaboration and Crisis Informatics*, 9(2).
- Ponuchamy, M. V. K. P. T. (2012). Feature Extraction and Classification of Blood Cells Using Artificial Neural Network. *American Journal of Applied Sciences*, 9(5), 615-619.
- Pradeep. (2011). DIAGONAL BASED FEATURE EXTRACTION FOR HANDWRITTEN ALPHABETS RECOGNITION. *International Journal of Computer Science & Information Technology*, 3(1), 27-38.
- Pramod, S., & Abhishek, N. (2013). CLIMATE CHANGE VULNERABILITY ASSESSMENT FOR SUSTAINABLE LIVELIHOODS USING FUZZY COGNITIVE MAPPING APPROACH. Anand, Gujarat. Retrieved from www.irma.ac.in.
- Prates, R. F., Schwartz, W. R., & Menotti, D. (2013). Brazilian License Plate Detection Using Histogram of Oriented Gradients and Sliding Windows. *International Journal of Computer Science & Information Technology*, 5(6).
- Praveena, N. J. P., with Devadoss, Victor, A., A.Rajkumar. (2012). A Study on Miracles through Holy Bible using Induced Fuzzy Cognitive Maps. *International Journal of Computer Applications*, 57(5), 22-26.
- Preist, C., Massung, E., & Coyle, D. (2014). Normification as a means of engaging digital volunteers. *In Proc. 17th ACM Conference on Computer Supported Cooperative Work and Social Computing*, 1222-1233.
- Prigent, M., Fontenelle, G., Rochet, M.-joëlle, & Trenkel, V. M. (2008). Using cognitive maps to investigate fishers ecosystem objectives and knowledge. *Ocean & Coastal Management*, 51(6), 450-462.

- Quinn, A. J., & Bederson, B. B. (2010). Human Computation : Charting The Growth Of A Burgeoning Field. *University of Maryland Department of Computer Science Human-Computer Interaction Lab*.
- R, L., & S, A. A. (2014). Facial Feature Extraction in Colour Images Based on Local Binary Pattern. *International Journal of Science and Research*, 3(3), 545-547.
- Rad, M. R., Akbari, S., & Taher, S. A. (2012). Using ANFIS , PSO , FCN in Cooperation with Fuzzy Controller for MPPT of Photovoltaic Arrays. *Advances in Digital Multimedia*, 1(1), 37-45.
- Rahat, K., Cécile, B., Damien, M., & Ducottet, C. (2015). Spatial histograms of soft pairwise similar patches to improve the bag-of-visual-words model. *Computer Vision and Image Understanding*, 132, 102-112. Elsevier Inc. doi: 10.1016/j.cviu.2014.09.005.
- Rahul, G. K., & Khurana, M. (2012). A Comparative Study Review of Soft Computing Approach in Weather Forecasting. *International Journal of Soft Computing and Engineering*, 2(5), 295-299.
- Rajan, D., & Mole, S. (2015). ACTION RECOGNITION BY ANALYSING HUMAN SILHOUETTE VIDEO – A SURVEY. *International Journal of Engineering Research*, 3(1), 47-51.
- Rajendran, P., & Madheswaran, M. (2010). Hybrid Medical Image Classification Using Association Rule Mining with Decision Tree Algorithm. *JOURNAL OF COMPUTING*, 2(1), 127-136.
- Ramana, R., Mani, R., & Kumar, V. (2009). Classification of Textures Based on Features Extracted from Preprocessing Images on Random Windows. *International Journal of Advanced Science and Technology*, 9, 9-18.
- Ramesh, B., Xiang, C., & Lee, T. H. (2015). Shape classification using invariant features and contextual information in the bag-of-words model. *Pattern Recognition Society. Published by Elsevier Science Ltd.*, 48(3), 894-906. Elsevier. doi: 10.1016/j.patcog.2014.09.019.
- Randall, D. A., & Wood, R. A. (2007). Climate Models and Their Evaluation. *The Physical Science Basis. Contribution of Working Group I to the Fourth Assessment Report of the Intergovernmental Panel on Climate Change*.
- Rangarajan, K., with Jayasudha, S., K. Ramanathan. (2012). Fuzzy Petri Nets and Fuzzy Cognitive Maps. *International Journal of Computer Applications*, 46(11), 5-9.
- Rey-otero, I., & Delbracio, M. (2014). Anatomy of the SIFT Method. *Image Processing On Line*, 4, 370-396.

- Ricci, E., Subramanian, R., & Liu, G. (2014). Multitask Linear Discriminant Analysis for View Invariant Action Recognition. *IEEE TRANSACTIONS ON IMAGE PROCESSING*, 23(12), 5599-5611.
- Richard, T. (2013). Drones in Domestic Surveillance Operations : Fourth Amendment Implications and Legislative Responses. *Congressional Research Service*.
- Risiro, J., Mashoko, D., Tshuma, T., & Rurinda, E. (2012). Weather Forecasting and Indigenous Knowledge Systems in Chimanimani District of Manicaland , Zimbabwe. *Journal of Emerging Trends in Educational Research and Policy Studies*, 3(4), 561-566.
- Roncoli, C., Ingram, K., & Kirshen, P. (2002). Society & Natural Resources Reading the Rains : Local Knowledge and Rainfall Forecasting in Burkina Faso. *Society & Natural Resources*, 15(5), 409-427.
- Rouhi, R., Amiri, M., & Irannejad, B. (2012). A R EVIEW ON F EATURE E XTRACTION. *Signal & Image Processing : An International Journal*, 3(6), 1-14.
- Ruiz, L. A., Recio, J. A., Fernández-Sarria, A., & Hermosilla, T. (2009). A TOOL FOR OBJECT DESCRIPTIVE FEATURE EXTRACTION : APPLICATION TO IMAGE CLASSIFICATION AND MAP UPDATING. *The International Archives of the Photogrammetry, Remote Sensing and Spatial Information Sciences*, XXXVIII-4/.
- Saritha, R., & Parthasarathy, C. (2014). An Efficient Information - driven Framework for Image Mining. *International Journal of Current research and Academic Review*, 2(1), 171-178.
- Savvidou, K., Lagouvardos, K., Michaelides, S., Kotroni, V., & Constantinides, P. (2010). Verification of the BOLAM weather prediction model over the area of Cyprus. *Advances In Geosciences*, 23, 93-100. doi: 10.5194/adgeo-23-93-2010.
- Setayesh, M., Zhang, M., & Johnston, M. (2008). Feature Extraction and Detection of Simple Objects Using Particle Swarm Optimisation.
- Shavlik, J. W. (1991). Finding Genes by Case-Based Reasoning in the Presence of Noisy Case Boundaries. *Proceedings of the 1991 DARPA Workshop on Case-Based Reasoning*,.
- Shoko, K. (2012). INDIGENOUS WEATHER FORECASTING SYSTEMS: A CASE STUDY OF THE BIOTIC WEATHER FORECASTING INDICATORS FOR WARDS 12 AND 13 IN MBERENGWA DISTRICT ZIMBABWE. *Journal of Sustainable Development in Africa*, 14(2), 92-114.
- Shrestha, D. L., Robertson, D. E., J.Wang, Q., Pagano, T. C., & Hapuarachchi, H. A. P. (2013). Evaluation of numerical weather prediction model precipitation forecasts for short-term streamflow forecasting purpose. *Hydrol. Earth Syst. Sci.*, 17, 1913-1931. doi: 10.5194/hess-17-1913-2013.

- Shuang, W. (2015). Texture Feature Extraction of Hyper-spectral Image with Gray-level Co-occurrence Matrix. *Journal of Information & Computational Science*, 12(4), 1439-1448. doi: 10.12733/jics20105472.
- Siddiqi, M. H., Ali, R., Rana, M. S., Hong, E.-K., Kim, E. S., & Lee, S. (2014). Video-Based Human Activity Recognition Using Multilevel Wavelet Decomposition and Stepwise Linear Discriminant Analysis. *Sensors*, 14, 6370-6392. doi: 10.3390/s140406370.
- Sikiric, I., & Brkic, K. (2013). Classifying traffic scenes using the GIST image descriptor. *Proceedings of the Croatian Computer Vision Workshop*, 19-24.
- Simeonov, I., Kilifarev, H., & Ilarionov, R. (2006). Embedded system for short-term weather forecasting. *International Conference on Computer Systems and Technologies*, 1-6.
- Sindhu. (2015). A Survey on Detecting Brain Tumor in MRI. *International Journal of Innovative Research in Computer and Communication Engineering*, 3(1), 123-129.
- Singh, H., Singh, G., & Bhatia, N. (2013). Fuzzy Cognitive Maps Based Election Results Prediction System. *International Journal of Computers & Technology*, 7(1), 483-492.
- Singhala. (2014). Temperature Control using Fuzzy Logic. *International Journal of Instrumentation and Control Systems*, 4(1), 1-10.
- Smith, J. R., & Chang, S.-fu. (1995). Single Color Extraction and Image Query. *International Conference on Image Processing*, 1-4.
- Solli, M. (2011). Color Emotions in Large Scale Content Based Image Indexing. *Linköping Studies in Science and Technology. Dissertations, No. 1362*, (1362).
- Soma, S., & Dhandra, B. V. (2015). Automatic Logo Recognition System from The Complex Document Using Shape and Moment Invariant Features. *International Journal of Advances in Computer Science and Technology*, 4(2), 06 - 13.
- Sperry, R., & Jetter, A. (2012). Fuzzy Cognitive Maps to Implement Corporate Social Responsibility in Product Planning : A Novel Approach. *Proceedings of PICMET'12* (pp. 2536 - 2541).
- Sridhar, G. (2012). Color and Texture Based Image Retrieval. *ARPJ Journal of Systems and Software*, 2(1), 1-6.
- Stach, W., Kurgan, L., & Pedrycz, W. (2007). A Framework for a Novel Scalable FCM Learning Method. *Proceedings of the 2007 Symposium on Human-Centric Computing and Data Processing* (pp. 13-14). Banff, Alberta.
- Stanchev, P. (2003). Using image mining for image retrieval. *IASTED conference of Computer Science and Technology* (pp. 214-218). Cancun, Mexico.

- Stanski, H., Wilson, L., & Burrows, W. (1871). *SURVEY OF COMMON VERIFICATION METHODS IN METEOROLOGY* (pp. 1-12).
- Stern, P. C., & Easterling, W. E. (1999). Making Climate Forecasts Matter. *Panel on the Human Dimensions of Seasonal-to-Interannual Climate Variability; Committee on the Human Dimensions of Global Change, National Research Council*.
- Steven, G., Kok, J. L. D., Helfgott, A., Dwyer, B., Jordan, R., & Nyaki, A. (2015). Using fuzzy cognitive mapping as a participatory approach to analyze change , preferred states , and perceived resilience of social-ecological systems. *Ecology And Society*, 20(2).
- Strickert, G. E., Samarasinghe, S., & Davies, T. (2009). Resilience models for New Zealand ' s Alpine Skiers based on people ' s knowledge and experience : a mixed method and multi-step fuzzy cognitive mapping approach. *18th World IMACS / MODSIM Congress* (pp. 817-823). Cairns.
- Stylios, C., Georgopoulos, V., & Manis, G. (2013). A study on Fuzzy Cognitive Map structures for Medical Decision Support Systems. *8th Conference of the European Society for Fuzzy Logic and Technology* (pp. 744-751).
- Suard, F., Rakotomamonjy, A., & Benschrair, A. (2006). Pedestrian Detection using Infrared images and Histograms of Oriented Gradients. *Intelligent Vehicles Symposium*, 206-212.
- Subba, K., & Naga, R. (2011). Feature Extraction for Image Classification and Analysis with Ant Colony Optimization Using Fuzzy Logic Approach. *Signal & Image Processing : An International Journal*, 2(4), 137-143.
- Subbulakshmi, K. (2014). Antilock-Braking System Using Fuzzy Logic. *Middle-East Journal of Scientific Research*, 20(10), 1306-1310. doi: 10.5829/idosi.mejsr.2014.20.10.232.
- Sukhpreet, S. (2013). Optical Character Recognition Techniques : A survey. *International Journal of Advanced Research in Computer Engineering & Technology*, 2(6), 2009-2015.
- Sunny, L., Mike, P., Bing, R., & Daying, Y. (2012). A comparative ownership advantage framework for cross-border M & As : The rise of Chinese and Indian MNEs. *Journal of World Business*, 47(1), 4-16. Elsevier Inc. doi: 10.1016/j.jwb.2010.10.015.
- Suter, E. (2013). An Assessment of Preliminary Issues on the Implementation of Kiswahili Oral Literature Syllabus for Secondary Schools in Marakwet District , Kenya. *International Journal of Humanities and Social Science*, 3(6), 225-233.
- Thacker, B. H., Doebeling, S. W., Hemez, F. M., Anderson, M. C., Pepin, J. E., & Rodriguez, E. A. (2004). Concepts of Model Verification and Validation. *Los Alamos National Laboratory*.

- Thakur, A., & Dhole, A. (2013). OBJECT RECOGNITION FROM IMAGE USING GRID BASED COLOR MOMENTS FEATURE EXTRACTION METHOD. *International Journal of Research in Engineering and Technology*, 333-336.
- Thepade, S., Das, R., & Ghosh, S. (2015). Content Based Image Classification with Thepade 's Static and Dynamic Ternary Block Truncation Coding. *International Journal of Engineering*, 4(1), 13 - 17.
- Thornes, J. E., & Stephenson, David B. (2001). How to judge the quality and value of weather forecast products. *Meteorol. Appl.*, 314, 307-314.
- Tian, D. P. (2013). A Review on Image Feature Extraction and Representation Techniques. *International Journal of Multimedia and Ubiquitous Engineering*, 8(4), 385-396.
- Tirilly, P., Claveau, V., & Gros, P. (2009). A review of weighting schemes for bag of visual words image retrieval. *Publications Internes de l'IRISA*.
- Toldo, R., Castellani, U., & Fusiello, A. (2009). A Bag of Words Approach for 3D Object Categorization. *Springer-Verlag Berlin Heidelberg*, 116-127.
- Tressa, F., Tara, J., & Barbara, B. (2012). Introduction to Forecast Verification. *National Center for Atmospheric Research*.
- TROY, R. (n.d.). AIRSPACE IN AN AGE OF DRONES. *Boston University Law Review*.
- Uddin, J., Islam, R., & Kim, J.-myon. (2014). Texture Feature Extraction Techniques for Fault Diagnosis of Induction Motors. *Journal of Convergence*, 5(2), 15-20.
- UNEP. (2013). A new eye in the sky : Eco-drones. *UNEP Global Environmental Alert Services*, (May), 1-13.
- United-Nations. (2004). PROTECTING AND PROMOTING TRADITIONAL KNOWLEDGE: SYSTEMS, NATIONAL EXPERIENCES AND INTERNATIONAL DIMENSIONS. In S. Twarog & P. Kapoor (Eds.), *United Nations Conference on Trade and Development*. New York.
- UNIVERSITESSI-BOBAZICI. (2010). A Survey of Mobile Phone Sensing". *IEEE Communications Magazine*, September.
- Uygar, O., & Stacy, O. (2004). Ecological models based on people 's knowledge : a multi-step fuzzy cognitive mapping approach. *Ecological Modelling*, 176, 43-64. doi: 10.1016/j.ecolmodel.2003.10.027.
- Vamvakas, G., Gatos, B., & Perantonis, S. J. (2009). A Novel Feature Extraction and Classification Methodology for the Recognition of Historical Documents. *10th*

- International Conference on Document Analysis and Recognition* (pp. 491-495). IEEE. doi: 10.1109/ICDAR.2009.223.
- Venkat, R., Jayaraman. (2015). Adaptive neuro-fuzzy inference system for temperature and humidity profile retrieval from microwave radiometer observations. *Atmos. Meas. Tech*, 8, 369-384. doi: 10.5194/amt-8-369-2015.
- Verhoeven, G., Karel, W., Doneus, M., Trinks, I., & Pfeifer, N. (2015). MIND YOUR GREY TONES – EXAMINING THE INFLUENCE OF DECOLOURIZATION METHODS ON INTEREST POINT EXTRACTION AND MATCHING FOR ARCHITECTURAL IMAGE-BASED MODELLING. *The International Archives of the Photogrammetry, Remote Sensing and Spatial Information Sciences, XL*(February), 25-27. doi: 10.5194/isprsarchives-XL-5-W4-307-2015.
- Viazzi, S., Ismayilova, G., Oczak, M., Sonoda, L. T., Fels, M., Guarino, M., et al. (2014). Image feature extraction for classification of aggressive interactions among pigs. *COMPUTERS AND ELECTRONICS IN AGRICULTURE*, 104, 57-62. Elsevier B.V. doi: 10.1016/j.compag.2014.03.010.
- Vijayarani, S., & Priyatharsini, S. (2015). Comparative Analysis of Facial Image Feature Extraction Algorithms. *Journal of Multidisciplinary Engineering Science and Technology*, 2(2), 107-112.
- Vipul, P. (2014). A single natural image denoising based on independent component analysis. *International Journal of Advanced Research in Computer and Communication Engineering*, 3(12), 8700-8702. doi: 10.17148/IJARCCCE.
- Vondrick, C., Khosla, A., Pirsiavash, H., Malisiewicz, T., & Torralba, A. (2015). Visualizing Object Detection Features. *International Journal of Computer Vision*.
- Văidianu, M.-natașa. (2013). Fuzzy cognitive maps : diagnosis and scenarios for a better management process of visitors flows in Romanian Danube Delta Biosphere Reserve. *Journal of Coastal Research, Special Is*(65), 1063-1068. doi: 10.2112/SI65-180.1.
- Wadhe, N. S., Mohod, S. W., & Khalsa, N. N. (2015). An Overview – Artificial Neural Network Based Advanced Face and Non-Face Recognition. *International Journal of Engineering Studies and Technical Approach*, 01(1), 1-10.
- Wang, Chong, & Huang, K. (2014). HOW To Use Bag-of-Words Model Better for AC SC. Elsevier B.V. doi: 10.1016/j.imavis.2014.10.013.
- Wang, J., Member, S., Li, Y., Zhang, Ying, Wang, Chao, Xie, H., et al. (2007). Bag-of-Features Based Medical Image Retrieval via Multiple Assignment and Visual Words Weighting. *IEEE TRANSACTIONS ON MEDICAL IMAGING*, 6(1), 1-18.

- Wang, Xiaojun, Pan, F., & Weihong, W. (2015). TRACKING OF MOVING TARGET BASED ON VIDEO MOTION NUCLEARALGORITHM. *INTERNATIONAL JOURNAL ON SMART SENSING AND INTELLIGENT SYSTEMS*, 8(1), 181-198.
- Wang, Xinggang, Feng, B., Bai, X., Liu, W., & Jan, L. (2014). Bag of Contour Fragments for Robust Shape Classification. *Pattern Recognition Society. Published by Elsevier Science Ltd.*
- Wangmeng, Z., David, Z., Jian, Y., & Kuanquan, W. (2006). BDPCA Plus LDA : A Novel Fast Feature Extraction Technique for Face Recognition. *IEEE TRANSACTIONS ON SYSTEMS, MAN, AND CYBERNETICS*, 36(4), 946-953.
- Warren, D. M. (1998). Information and Communication Technologies, Knowledge Management and Indigenous Knowledge: Implications to Livelihood of Communities in Ethiopia. *World Bank Discussion Paper 127, Washington, 1991*, 1-12.
- Wasim, K., Shiv, K., Neetesh, G., & Nilofar, K. (2011). A Proposed Method for Image Retrieval using Histogram values and Texture Descriptor Analysis. *International Journal of Soft Computing and Engineering*, 1(2), 33-36.
- Wei, L., & Linzhi, G. (2014). Recommendation System Based on Fuzzy Cognitive Map. *JOURNAL OF MULTIMEDIA*, 9(7), 970-976. doi: 10.4304/jmm.9.7.970-976.
- Weisheimer, A., & Palmer, T. (2014). On the Reliability of Seasonal Climate Forecasts. *J. R. Soc. Interface*, 11(96). doi: 10.1098/ rsif.2013.1162.
- Wengert, C., Douze, M., & Herve, J. (2011). Bag-of-colors for improved image search. *19th ACM International Conference on Multimedia* (pp. 1437-1440). Scottsdale, United States.
- Wetterhall, F., Winsemius, H. C., Dutra, E., Werner, M., & Pappenberger, F. (2014). Seasonal predictions of agro-meteorological drought indicators for the Limpopo basin. *Hydrology and Earth System Sciences*, 11, 861-888. doi: 10.5194/hessd-11-861-2014.
- Wong, K.-wai, Lam, K.-man, & Siu, W.-chi. (2004). An efficient algorithm for human face detection and facial feature extraction under different conditions. *Pattern Recognition Society. Published by Elsevier Science Ltd.*, 34(2001), 1993-2004.
- World-Meteorological-Organization. (2000). ON PERFORMANCE ASSESSMENT OF PUBLIC WEATHER SERVICES ON PERFORMANCE ASSESSMENT. *WMO/TD*, (1023).
- Xiaolan, L., & Afzal, G. (2010). Investigating the Bag-of-Words Method for 3D Shape Retrieval. *EURASIP Journal on Advances in Signal Processing*. doi: 10.1155/2010/108130.
- Xiaolan, L., Afzal, G., & Asim, W. (2008). Spatially Enhanced Bags of Words for 3D Shape Retrieval. *Springer-Verlag Berlin Heidelberg*, 349-358.

- Xiaoli, Y., Jing, Y., Zengchang, Q., & Tao, W. (2011). A SIFT-LBP IMAGE RETRIEVAL MODEL BASED ON BAG-OF-FEATURES. *Ieee International Conference On Image Processing* (pp. 1061-1064).
- Xirogiannis, G., & Glykas, M. (2004). Fuzzy Cognitive Maps in Business Analysis and Performance-Driven Change. *IEEE TRANSACTIONS ON ENGINEERING MANAGEMENT*, 51(3), 334-351.
- Xiuchao, W., Kenneth, B., & Cormac, S. (2014). Data Pre-Forwarding for Opportunistic Data Collection in Wireless Sensor Networks. *ACM Transactions on Sensor Networks*, 11(1).
- Xu, L., Li, Jonathan, Shu, Y., & Peng, J. (2014). SAR Image Denoising via Clustering-Based Principal Component Analysis. *IEEE TRANSACTIONS ON GEOSCIENCE AND REMOTE SENSING*, 52(11), 6858-6869.
- Xudong, J., Bappaditya, M., & Alex, K. (2009). Complete discriminant evaluation and feature extraction in kernel space for face recognition. *Machine Vision and Applications*, 20, 35-46. doi: 10.1007/s00138-007-0103-1.
- Xue, S. (2014). Neural Fuzzy Inference System-Based Weather Prediction Model and Its Precipitation Predicting Experiment. *Atmosphere*, 5, 788-805. doi: 10.3390/atmos5040788.
- Yang. (2009). INFORMATION MINING FROM REMOTE SENSING IMAGERY BASED ON MULTI-SCALE AND MULTI-FEATURE PROCESSING TECHNIQUES. *The International Archives of the Photogrammetry, Remote Sensing and Spatial Information Sciences*, 38(II), 158-161.
- Yang, S. (2013). Discriminative Data Transform for Image Feature Extraction and Classification. *Springer-Verlag Berlin Heidelberg*, 452-459.
- Yaxin, Z., Zhihua, C., & Yubo, Y. (2015). Representation of image content based on RoI-BoW. *J. Vis. Commun. Image R.*, 26, 37-49. doi: 10.1016/j.jvcir.2014.10.007.
- Yousef, O.-motlagh S. (2014). Causality analysis of the technology strategy maps using the fuzzy cognitive strategy map. *African Journal of Business Management*, 8(6), 191-210. doi: 10.5897/AJBM2014.7345.
- Yuan, Y., Minjing, M., & Menglu, Z. (2013). CLOUD DETECTION METHOD BASED ON FEATURE EXTRACTION IN REMOTE SENSING IMAGES ABSTRACT :. *International Archives of the Photogrammetry, Remote Sensing and Spatial Information Sciences*, XL-2/W1(June), 173-177.
- Yuen, M.-ching, King, I., & Leung, K.-sak. (2011). A Survey of Crowdsourcing Systems. *IEEE International Conference on Privacy, Security, Risk, and Trust, and IEEE International Conference on Social Computing*, 766-773.

- Zaghdoud, M., & Al-kahtani, M. S. (2013). Contextual Fuzzy Cognitive Map for Intrusion Response System. *International Journal of Computer and Information Technology (ISSN: 02(3)*, 471-478.
- Zhang J. (2006). Local Features and Kernels for Classification of Texture and Object Categories : A Comprehensive Study. *International Journal of Computer Vision*. doi: 10.1007/s11263-006-9794-4.
- Zhang, N., & Zhu, J. (2015). A STUDY OF X-RAY MACHINE IMAGE LOCAL SEMANTIC FEATURES EXTRACTION MODEL BASED ON BAG-OF-WORDS FOR AIRPORT SECURITY. *INTERNATIONAL JOURNAL ON SMART SENSING AND INTELLIGENT SYSTEMS*, 8(1), 45-64.
- Zhang, Yi, & Hanby, V. I. (2007). SHORT-TERM PREDICTION OF WEATHER PARAMETERS USING ONLINE WEATHER FORECASTS. *Building Simulation*, 1411-1416.
- Zhao, Y., & Zhai, X., with Rongrong. (2015). Recaptured Images Forensics Based On Color Moments and DCT Coefficients Features. *Journal of Information Hiding and Multimedia Signal Processing*, 6(2), 323-333.
- Ziervogel, G., & Downing, T. E. (2004). Stakeholder networks: improving seasonal climate forecasts. *Climate Change*, 65, 73-101.
- Ziervogel, G., New, M., Garderen, E. A. V., Midgley, G., Taylor, A., Hamann, R., et al. (2014). Climate change impacts and adaptation in South Africa. *WIREs Climate Change*, 5, 605-620. doi: 10.1002/wcc.295.
- Zuma-netshiukhwi, G., Stigter, K., & Walker, S. (2013). Use of Traditional Weather/Climate Knowledge by Farmers in the South-Western Free State of South Africa: Agrometeorological Learning by Scientists. *Atmosphere*, 4, 383-410. doi: 10.3390/atmos4040383.

A. Appendix of Tables

Table A—1: Summary of Causal effects on Weather Outcomes

WEATHER OUTCOMES	CAUSAL EFFECTS				
	STRONG POSITIVE (1)	POSITIVE (0.5)	NONE (0)	NEGATIVE (-0.5)	STRONG NEGATIVE (-1)
RAIN	Nimbostratus	Altostratus		Tower clouds	Altostratus
	Stratus	Cumulonimbus		Moon	cirrocumulus
	Stratocumulus	Cumulus		Rainbow	Cirrostratus
	Grey clouds	Cauliflower			Cirrus
	Brown clouds	Layered clouds			White clouds
	Rippled clouds	Dull stars			Blue clouds
	Uniform clouds	Ring around			Red clouds
	Few stars	Partial/dark			Feathery clouds
	New moon	Moon decreasing			Filaments clouds
	Dark sky				Ring around sun
	Lightning				Twinkling stars
					Many stars
					Full moon
					Blue moon
					Clear sky
					Red sky
					Blue sky
				Fog	
HOT	Fog	Rainbow		Dark sky	Uniform clouds
	Red sky	Lightning		Moon	Rippled clouds
	Blue sky	Clear sky		Dark moon	Layered clouds
	Blue moon	Moon increasing		New moon	Brown clouds
	Full moon	Ring around		Few stars	Grey clouds
	Many stars	Filaments clouds		Cumulus	Stratocumulus
	Twinkling stars	Feathery clouds		Nimbus	Stratus
	Dull stars	Tower clouds			Cumulonimbus
	Ring around sun	Cauliflower			
	Red clouds	Blue clouds			
	White clouds	Cirrus clouds			
	Altostratus	Cirrostratus			
		Cirrocumulus			
	Altostratus				
CLOUDY	Lightning	Red sky		Fog	Rainbow
	Dark sky	Dark moon		Clear sky	Blue sky
	Few stars	New moon		Moon larger	Full moon
	Dull stars	Filaments clouds		Ring around	Blue moon
	Uniform clouds	Rippled clouds		Altostratus	Many stars
	Layered clouds	Feathery clouds			Twinkling stars
	Blue clouds	Tower clouds			Ring around sun

	Brown clouds	Cauliflower			
	Grey clouds	Red clouds			
	Cumulus	White clouds			
	Stratocumulus	Cumulonimbus			
	Stratus	Cirrus			
	Cirrocumulus	Cirrostratus			
	Nimbus				
	Altostratus				
WINDY	Blue sky	Lightning		Rainbow	Fog
	Dark moon	Moon decreasing		Red sky	Blue moon
	Dull stars	New moon		Dark sky	Full moon
		Ring around		Clear sky	Many stars
		Few stars		Moon	Red clouds
		Uniform clouds		Twinkling stars	White clouds
		Filaments clouds		Ring around	
		Rippled clouds		Cumulus	
		Layered clouds			
		Feathery clouds			
		Tower clouds			
		Cauliflower			
		Blue clouds			
		Brown clouds			
		Grey clouds			
		Stratocumulus			
		Stratus			
		Cumulonimbus			
		Cirrus			
		Cirrostratus			
		Cirrocumulus			
		Nimbus			
	Altostratus				
	Altostratus				
DRY	Rainbow	Red sky		Fog	Lightning
	Blue sky	Clear sky		Dark moon	Moon decreasing
	Moon increasing	Full moon		New moon	Uniform clouds
		Ring around		Few stars	Filaments clouds
		Many stars		Dull stars	Rippled clouds
		Ring around sun		Layered clouds	Grey clouds
		Red clouds		Feathery clouds	Brown clouds
		Blue clouds		Tower clouds	Cauliflower clouds
		White clouds		Cumulus	Cirrocumulus
		Cirrostratus		Stratocumulus	
		Altostratus		Stratus	
				Cumulonimbus	

				Cirrus	
				Nimbus	
				altocumulus	
				dark sky	
COLD		Lightning		fog	blue sky
		Dark sky		rainbow	clear sky
		Dark moon		Red sky	Blue moon
		New moon		Moon	Full moon
		Few stars		Moon	Many stars
		Dull stars		Ring around	Twinkling stars
		Uniform clouds		Tower clouds	Ring around sun
		Rippled clouds		Cirrus	Filaments clouds
		Layered clouds		Cirrocumulus	Feathery clouds
		Blue clouds		Nimbus	Cauliflower clouds
		Brown clouds		Altostratus	Red clouds
		Grey clouds			White clouds
		Cumulus			Cirrostratus
		Stratocumulus			
		Stratus			
		Cumulonimbus			
	Altocumulus				
CALM	Cumulus	Altocumulus		Stratus	Layered clouds
	Blue clouds	Altostratus		Grey clouds	Rippled clouds
	Red clouds	Nimbus		Brown clouds	Lightning
	Tower clouds	Cirrocumulus		Ring around	
	Many stars	Cirrostratus			
	New moon	Cirrus			
	Full moon	Cumulonimbus			
	Dark moon	Stratocumulus			
		White clouds			
		Cauliflower			
		Feathery clouds			
		Filaments clouds			
		Uniform clouds			
		Dull stars			
		Twinkling stars			
		Few stars			
		Ring around			
		Moon increasing			
		Moon decreasing			
		Blue moon			
	Clear sky				
	Dark sky				
	Red sky				

		Blue sky			
		Rainbow			
		Fog			

Table A—2: Relations between Visual Weather Concepts

Concept to Concept	Causal Effect						
	Strong negative (-1.)	Negative (-0.5)	None (0)	Positive (0.5)	Strong positive (1)	mode -1 to 1	mean -1 to 1
High clouds to low clouds	3.3%	40.0%	56.7%			.0	-.2
High clouds to medium clouds	8.3%	36.7%	55.0%			.0	-.3
High clouds to clear sky			11.7%	76.7%	11.7%	.5	.5
High clouds to many stars	1.7%	8.3%	90.0%			.0	-.1
High clouds to rainbow		6.7%	93.3%			.0	.0
High clouds to lightning	86.7%	8.3%	5.0%			-1.0	-.9
High clouds to partial/dark moon	1.7%	1.7%	86.7%	6.7%	3.3%	.0	.0
High clouds to full/visible moon			86.7%	11.7%	1.7%	.0	.1
Medium clouds to low clouds		6.7%	88.3%	5.0%		.0	.0
Medium clouds to clear sky	10.0%	85.0%	5.0%			-.5	-.5
Medium clouds to many stars	11.7%	10.0%	78.3%			.0	-.2
Medium clouds to rainbow	45.0%	13.3%	41.7%			-1.0	-.5
Medium clouds to lightning			85.0%	15.0%		.0	.1
Medium clouds to partial/dark moon			80.0%	20.0%		.0	.1
Medium clouds to full/visible moon	45.0%	11.7%	43.3%			-1.0	-.5
Low clouds to clear sky	80.0%	16.7%	3.3%			-1.0	-.9
Low clouds to many stars	3.3%	8.3%	88.3%			.0	-.1
Low clouds to rainbow		8.3%	91.7%			.0	.0
Low clouds to lightning			91.7%	8.3%		.0	.0
Low clouds to partial/dark moon			91.7%	8.3%		.0	.0
Low clouds to full/visible moon	8.3%	1.7%	90.0%			.0	-.1
Clear sky to many stars			81.7%	11.7%	6.7%	.0	.1
Clear sky to rainbow		1.7%	88.3%	1.7%	8.3%	.0	.1
Clear sky to lightning	73.3%	15.0%	11.7%			-1.0	-.8
Clear sky to partial/dark moon	41.7%	6.7%	51.7%			.0	-.5
Clear sky to full/visible moon			78.3%	8.3%	13.3%	.0	.2
Many stars to rainbow			85.0%	8.3%	6.7%	.0	.1
Many stars to lightning	5.0%	11.7%	83.3%			.0	-.1
Many stars to partial/dark moon	8.3%	48.3%	41.7%	1.7%		-.5	-.3
Many stars to full/visible moon			70.0%	10.0%	20.0%	.0	.3
Rainbow to lightning	11.7%	6.7%	81.7%			.0	-.2
Rainbow to partial/dark moon	S	6.7%	75.0%	5.0%	5.0%	.0	.0
Rainbow to full/visible moon	8.3%		78.3%		13.3%	.0	.1
lightning to partial/dark moon			83.3%	5.0%	11.7%	.0	.1
lightning to full/visible moon	11.7%		88.3%			.0	-.1
Partial/dark moon to full/visible	13.3%		86.7%			.0	-.1

Table A—3: Causal Effects of Weather Concepts to Weather Outcomes during Winter Season

Concept to Outcome	Causal Effect						
	Strong negative (-1.)	Negative (-0.5)	None (0)	Positive (0.5)	Strong positive (1)	mode -1 to 1	Mean -1 to 1
Winter high clouds to rain			100.0%			.0	.0
Winter low clouds to rain			15.0%	70.0%	15.0%	.5	.5
Winter medium clouds to rain			23.3%	61.7%	15.0%	.5	.5
Winter clear sky to rain			100.0%			.0	.0
Winter many stars to rain			100.0%			.0	.0
Winter rainbow to rain	21.7%	68.3%	10.0%			-.5	-.6
Winter lightning to rain			15.0%	66.7%	18.3%	.5	.5
Winter partial/dark moon rain			98.3%	1.7%		.0	.0
Winter full/visible moon rain			100.0%			.0	.0
Winter high clouds to dry			10.0%	15.0%	75.0%	1.0	.8
Winter low clouds to dry			13.3%	18.3%	68.3%	1.0	.8
Winter medium clouds dry			10.0%	15.0%	75.0%	1.0	.8
Winter clear sky to dry			11.7%	16.7%	71.7%	1.0	.8
Winter many stars to dry			8.3%	21.7%	70.0%	1.0	.8
Winter rainbow to dry			11.7%	21.7%	66.7%	1.0	.8
Winter lightning to dry	66.7%	18.3%	15.0%			-1.0	-.8
Winter partial/dark moon dry	13.3%	73.3%	13.3%			-.5	-.5
Winter full/visible moon dry			15.0%	73.3%	11.7%	.5	.5
Winter high clouds to hot	5.0%	78.3%	16.7%			-.5	-.4
Winter low clouds to hot	8.3%	78.3%	13.3%			-.5	-.5
Winter medium clouds to hot	11.7%	78.3%	10.0%			-.5	-.5
Winter clear sky to hot			13.3%	75.0%	11.7%	.5	.5
Winter many stars to hot			5.0%	78.3%	16.7%	.5	.6
Winter rainbow to hot			3.3%	80.0%	16.7%	.5	.6
Winter lightning to hot	76.7%	13.3%	10.0%			-1.0	-.8
Winter partial/dark moon hot			100.0%			.0	.0
Winter full/visible moon hot			3.3%	83.3%	13.3%	.5	.6
Winter high clouds to cold			5.0%	15.0%	80.0%	1.0	.9
Winter low clouds to cold			3.3%	18.3%	78.3%	1.0	.9
Winter medium clouds to cold			10.0%	15.0%	75.0%	1.0	.8
Winter clear sky to cold			11.7%	76.7%	11.7%	.5	.5
Winter many stars to cold			18.3%	70.0%	11.7%	.5	.5
Winter rainbow to cold			11.7%	75.0%	13.3%	.5	.5
Winter lightning to cold			15.0%	15.0%	70.0%	1.0	.8
Winter partial/dark moon Cold			16.7%	16.7%	66.7%	1.0	.8
Winter full/visible moon Cold			11.7%	11.7%	76.7%	1.0	.8

Table A—4: Causal Effects of Weather Concepts to Weather Outcomes during Summer Season

Concept to Outcome	Causal Effect						
	Strong negative (-1)	Negative (-0.5)	No Effect (0)	Positive (0.5)	Strong positive (1)	mode -1 to 1	Mean -1 to 1
Summer high clouds to rain	78.3%	10.0%	11.7%			-1.0	-.8
Summer low clouds to rain			5.0%	16.7%	78.3%	1.0	.9
Summer medium clouds to rain			16.7%	71.7%	11.7%	.5	.5
Summer clear sky to rain	13.3%	73.3%	13.3%			-.5	-.5
Summer many stars to rain	76.7%	15.0%	8.3%			-1.0	-.8
Summer rainbow to rain	15.0%	76.7%	8.3%			-.5	-.5
Summer lightning to rain			6.7%	16.7%	76.7%	1.0	.9
Summer partial/dark moon to rain			13.3%	70.0%	16.7%	.5	.5
Summer full/visible moon to rain	78.3%	10.0%	11.7%			-1.0	-.8
Summer high clouds to dry			10.0%	13.3%	76.7%	1.0	.8
Summer low clouds to dry	73.3%	13.3%	13.3%			-1.0	-.8
Summer medium clouds to dry	13.3%	75.0%	11.7%			-.5	-.5
Summer clear sky to dry			6.7%	15.0%	78.3%	1.0	.9
Summer many stars to dry			18.3%	11.7%	70.0%	1.0	.8
Summer rainbow to dry			16.7%	70.0%	13.3%	.5	.5
Summer lightning to dry	68.3%	10.0%	21.7%			-1.0	-.7
Summer partial/dark moon to dry	63.3%	15.0%	21.7%			-1.0	-.7
Summer full/visible moon to dry			8.3%	16.7%	75.0%	1.0	.8
Summer high clouds to hot			8.3%	10.0%	81.7%	1.0	.9
Summer low clouds to hot	83.3%	11.7%	5.0%			-1.0	-.9
Summer medium clouds to hot		1.7	8.3%	5.0%	85.0%	1.0	.9
Summer clear sky to hot			11.7%	3.3%	85.0%	1.0	.9
Summer many stars to hot			6.7%	6.7%	86.7%	1.0	.9
Summer rainbow to hot			10.0%	76.7%	13.3%	.5	.5
Summer lightning to hot	10.0%	76.7%	13.3%			-.5	-.5
Summer partial/dark moon to hot	78.3%	13.3%	8.3%			-1.0	-.9
Summer full/visible moon to hot			10.0%	10.0%	80.0%	1.0	.9
Summer high clouds to cold	81.7%	8.3%	10.0%			-1.0	-.9
Summer low clouds to cold			10.0%	76.7%	13.3%	.5	.5
Summer medium clouds to cold	78.3%	8.3%	13.3%			-1.0	-.8
Summer clear sky to cold	80.0%	6.7%	13.3%			-1.0	-.8
Summer many stars to cold	75.0%	11.7%	13.3%			-1.0	-.8
Summer rainbow to cold	75.0%	10.0%	15.0%			-1.0	-.8
Summer lightning to cold			13.3%	70.0%	16.7%	.5	.5
Summer partial/darkmoon to cold			10.0%	76.7%	13.3%	.5	.5
Summer full/visible moon to cold	81.7%	10.0%	8.3%			-1.0	-.9

Table A—5: Causal Effects of Weather Concepts to Weather Outcomes during Autumn Season

Concept to Outcome	Causal Effect						
	Strong negative (-1.)	Negative (-0.5)	No Effect (0)	Positive (0.5)	Strong positive (1)	mode -1 to 1	Mean -1 to 1
Autumn high clouds to rain		91.7%	8.3%			-.5	-.5
Autumn low clouds to RAIN			10.0%	11.7%	78.3%	1.0	.8
Autumn medium clouds to rain			6.7%	70.0%	23.3%	.5	.6
Autumn clear sky to rain	80.0%	6.7%	13.3%			-1.0	-.8
Autumn many stars to rain	88.3%	5.0%	6.7%			-1.0	-.9
Autumn rainbow to rain	76.7%	13.3%	10.0%			-1.0	-.8
Autumn lightning to rain			5.0%	78.3%	16.7%	.5	.6
Autumn partial/dark moon to rain			3.3%	80.0%	16.7%	.5	.6
Autumn full/visible moon to	8.3%	83.3%	8.3%			-.5	-.5
Autumn high clouds to dry			5.0%	80.0%	15.0%	.5	.6
Autumn low clouds to dry	85.0%	10.0%	5.0%			-1.0	-.9
Autumn medium clouds to dry	85.0%	11.7%	3.3%			-1.0	-.9
Autumn clear sky to dry			5.0%	76.7%	18.3%	.5	.6
Autumn many stars to dry	80.0%	10.0%	10.0%			-1.0	-.9
Autumn rainbow to dry			13.3%	71.7%	15.0%	.5	.5
Autumn lightning to dry	15.0%	71.7%	13.3%			-.5	-.5
Autumn partial/dark moon to dry	6.7%	83.3%	10.0%			-.5	-.5
Autumn full/visible moon to dry			15.0%	70.0%	15.0%	.5	.5
Autumn high clouds to hot			6.7%	81.7%	11.7%	.5	.5
Autumn low clouds to hot	15.0%	73.3%	10.0%		1.7%	-.5	-.5
Autumn medium clouds to hot	76.7%	11.7%	11.7%			-1.0	-.8
Autumn clear sky to hot			8.3%	81.7%	10.0%	.5	.5
Autumn many stars to hot	85.0%	3.3%	11.7%			-1.0	-.9
Autumn rainbow to hot			8.3%	71.7%	20.0%	.5	.6
Autumn lightning to hot	13.3%	76.7%	10.0%			-.5	-.5
Autumn partial/dark moon to hot	13.3%	71.7%	15.0%			-.5	-.5
Autumn full/visible moon to hot			6.7%	86.7%	6.7%	.5	.5
Autumn high clouds to cold			6.7%	83.3%	10.0%	.5	.5
Autumn low clouds to cold			6.7%	81.7%	11.7%	.5	.5
Autumn medium clouds to cold			16.7%	73.3%	10.0%	.5	.5
Autumn clear sky to cold			10.0%	78.3%	11.7%	.5	.5
Autumn many stars to cold			20.0%	68.3%	11.7%	.5	.5
Autumn rainbow to cold			8.3%	83.3%	8.3%	.5	.5
Autumn lightning to cold			18.3%	68.3%	13.3%	.5	.5
Autumn partial/dark moon to			6.7%	76.7%	16.7%	.5	.6
Autumn full/visible moon to			6.7%	76.7%	16.7%	.5	.6

Table A—6: Causal Effects of Weather Concepts to Weather Outcomes during Spring Season

Concept to Outcome	Causal Effect						
	Strong negative (-1.)	Negative (-0.5)	No Effect (0)	Positive (0.5)	Strong positive (1)	mode -1 to 1	mean -1 to 1
Spring high clouds to rain	15.0%	81.7%	3.3%			-.5	-.6
Spring low clouds to rain			8.3%		76.7%	.5	.5
Spring medium clouds to rain			10.0%		73.3%	.5	.5
Spring clear sky to rain	15.0%	80.0%	5.0%			-.5	-.6
Spring many stars to rain	75.0%	20.0%	5.0%			-1.0	-.9
Spring rainbow to rain	15.0%	75.0%	10.0%			-.5	-.5
Spring lightning to rain			3.3%		15.0%	1.0	.9
Spring partial/dark moon to rain			5.0%		71.7%	.5	.6
Spring full/visible moon to rain	80.0%	15.0%	5.0%			-1.0	-.9
Spring high clouds to dry			6.7%		76.7%	.5	.6
Spring low clouds to dry			1.7%		76.7%	.5	.6
Spring medium clouds to dry	13.3%	78.3%	8.3%			-.5	-.5
Spring clear sky to dry			6.7%		73.3%	.5	.6
Spring many stars to dry			8.3%	1.7%	76.7%	.5	.5
Spring rainbow to dry	13.3%	81.7%	5.0%			-.5	-.5
Spring lightning to dry	73.3%	15.0%	11.7%			-1.0	-.8
Spring partial/dark moon to dry	71.7%	16.7%	11.7%			-1.0	-.8
Spring full/visible moon to dry	61.7%	16.7%	21.7%			-1.0	-.7
Spring high clouds to hot			5.0%		81.7%	.5	.5
Spring low clouds to hot	15.0%	71.7%	13.3%			-.5	-.5
Spring medium clouds to hot	11.7%	83.3%	5.0%			-.5	-.5
Spring clear sky to hot			3.3%		11.7%	1.0	.9
Spring many stars to hot			6.7%		81.7%	.5	.5
Spring rainbow to hot			6.7%		75.0%	.5	.6
Spring lightning to hot	11.7%	78.3%	10.0%			-.5	-.5
Spring partial/dark moon to hot	10.0%	83.3%	6.7%			-.5	-.5
Spring full/visible moon to hot			1.7%		6.7%	1.0	1.0
Spring high clouds to cold	75.0%	10.0%	15.0%			-1.0	-.8
Spring low clouds to cold					83.3%	.5	.6
Spring medium clouds to cold			8.3%		76.7%	.5	.5
Spring clear sky to cold	81.7%	10.0%	8.3%			-1.0	-.9
Spring many stars to cold	85.0%	6.7%	8.3%			-1.0	-.9
Spring rainbow to cold	10.0%	85.0%	5.0%			-.5	-.5
Spring lightning to cold			10.0%	75.0%	15.0%	.5	.5
Spring partial/darkmoon to cold			5.0%	80.0%	15.0%	.5	.6
Spring full/visible moon to cold	75.0%	13.3%	11.7%			-1.0	-.8

Table A—7: Relations between Weather Concepts

Concept to Outcome	Causal Effect						
	Strong negative (-1.)	Negative (-0.5)	No Effect (0)	Positive (0.5)	Strong positive (1)	mode -1 to 1	Mean -1 to 1
High clouds to low clouds	5.0%	11.7%	83.3%			.0	-1
High clouds to medium clouds	6.7%	8.3%	85.0%			.0	-1
High clouds to clear sky			11.7%	70.0%	18.3%	.5	.5
High clouds to many stars	1.7%	13.3%	85.0%			.0	-1
High clouds to rainbow		11.	88.3%			.0	-1
High clouds to lightning	78.3%	10.0%	11.7%			-1.0	-8
High clouds to partial/dark moon	3.3%	3.3%	83.3%	6.7%	3.3%	.0	.0
High clouds to full/visible moon			85.0%	13.3%	1.7%	.0	.1
Medium clouds to low clouds	1.7%	8.3%	81.7%	8.3%		.0	.0
Medium clouds to clear sky	11.7%	78.3%	10.0%			-.5	-5
Medium clouds to many stars	13.3%	15.0%	71.7%			.0	-2
Medium clouds to rainbow	15.0%	20.0%	65.0%			.0	-3
Medium clouds to lightning			80.0%	20.0%		.0	.1
Medium clouds to partial/dark			73.3%	26.7%		.0	.1
Medium clouds to full/visible	16.7%	13.3%	70.0%			.0	-2
Low clouds to clear sky	71.7%	25.0%	3.3%			-1.0	-8
Low clouds to many stars	5.0%	13.3%	81.7%			.0	-1
Low clouds to rainbow		11.7%	88.3%			.0	-1
Low clouds to lightning			86.7%	11.7%	1.7%	.0	.1
Low clouds to partial/dark moon			85.0%	15.0%		.0	.1
Low clouds to full/visible moon	13.3%	3.3%	83.3%			.0	-2
Clear sky to many stars			78.3%	11.7%	10.0%	.0	.2
Clear sky to rainbow		1.7%	81.7%	5.0%	11.7%	.0	.1
Clear sky to lightning	68.3%	18.3%	13.3%			-1.0	-8
Clear sky to partial/dark moon	10.0%	13.3%	76.7%			.0	-2
Clear sky to full/visible moon			73.3%	10.0%	16.7%	.0	.2
Many stars to rainbow			78.3%	13.3%	8.3%	.0	.2
Many stars to lightning	8.3%	18.3%	73.3%			.0	-2
Many stars to partial/dark moon	11.7%	21.7%	65.0%	1.7%		.0	-2
Many stars to full/visible moon			63.3%	10.0%	26.7%	.0	.3
Rainbow to lightning	21.7%	10.0%	68.3%			.0	-3
Rainbow to partial/dark moon	8.3%	10.0%	63.3%	10.0%	8.3%	.0	.0
Rainbow to full/visible moon	13.3%		68.3%		18.3%	.0	.1
Lightning to partial/dark moon			75.0%	11.7%	13.3%	.0	.2
Lightning to full/visible moon	15.0%		85.0%			.0	-2
Partial/dark moon to full/visible	20.0%		80.0%			.0	-2

Table A—8: Causal Effects of Weather Concepts during the Winter Season

Concept to Outcome	Causal Effect						
	Strong negative (-1)	Negative (-0.5)	No Effect (0)	Positive (0.5)	Strong positive (1)	mode -1 to 1	Mean -1 to 1
Winter high clouds to rain	76.7%	8.3%	15.0%			-1.0	-.8
Winter low clouds to rain			23.3%	71.7%	5.0%	.5	.4
Winter medium clouds to rain		10.0	83.3%	6.7%		.0	.0
Winter clear sky to rain	86.7%	13.3%				-1.0	-.9
Winter many stars to rain	71.7%	10.0%	18.3%			-1.0	-.8
Winter rainbow to rain	11.7%	80.0%	8.3%			-.5	-.5
Winter lightning to rain			16.7%	73.3%	10.0%	.5	.5
Winter partial/dark moon to			30.0%	65.0%	5.0%	.5	.4
Winter full/visible moon to			78.3%	15.0%	6.7%	.0	.1
Winter high clouds to dry			8.3%	15.0%	76.7%	1.0	.8
Winter low clouds to dry			10.0%	66.7%	23.3%	.5	.6
Winter medium clouds to dry	11.7%	76.7%	11.7%			-.5	-.5
Winter clear sky to dry			15.0%	20.0%	65.0%	1.0	.8
Winter many stars to dry			15.0%	65.0%	20.0%	.5	.5
Winter rainbow to dry			83.3%	11.7%	5.0%	.0	.1
Winter lightning to dry	16.7%	76.7%	6.7%			-.5	-.6
Winter partial/darkmoon to dry	13.3%	73.3%	13.3%			-.5	-.5
Winter full/visiblemoon to dry			18.3%	71.7%	10.0%	.5	.5
Winter high clouds to hot			8.3%	71.7%	20.0%	.5	.6
Winter low clouds to hot	66.7%	16.7%	16.7%			-1.0	-.8
Winter medium clouds to hot	10.0%	73.3%	16.7%			-.5	-.5
Winter clear sky to hot			6.7%	65.0%	28.3%	.5	.6
Winter many stars to hot			28.3%	63.3%	8.3%	.5	.4
Winter rainbow to hot			26.7%	70.0%	3.3%	.5	.4
Winter lightning to hot	18.3%	66.7%	15.0%			-.5	-.5
Winter partial/dark moon to hot	11.7%	61.7%	26.7%			-.5	-.4
Winter full/visible moon to hot			23.3%	65.0%	11.7%	.5	.4
Winter high clouds to cold	23.3%	58.3%	18.3%			-.5	-.5
Winter low clouds to cold			13.3%	30.0%	56.7%	1.0	.7
Winter medium clouds to cold			10.0%	71.7%	18.3%	.5	.5
Winter clear sky to cold	13.3%	71.7%	15.0%			-.5	-.5
Winter many stars to cold	13.3%	61.7%	25.0%			-.5	-.4
Winter rainbow to cold	15.0%	78.3%	6.7%			-.5	-.5
Winter lightning to cold			18.3%	70.0%	11.7%	.5	.5
Winter partial/dark moon to			23.3%	53.3%	23.3%	.5	.5
Winter full/visible moon to cold	26.7%	53.3%	20.0%			-.5	-.5

Table A—9: Causal Effects of Weather Concepts during the Summer Season

Concept to Outcome	Causal Effect						
	Strong negative (-1)	Negative (-0.5)	No Effect (0)	Positive (0.5)	Strong positive (1)	mode -1 to 1	Mean -1 to 1
Summer high clouds to rain	73.3%		16.7%	10.0%		-1.0	-.7
Summer low clouds to rain	16.7%		48.3%	16.7%	18.3%	.0	.1
Summer medium clouds to rain	18.3%		33.3%	40.0%	8.3%	.5	.1
Summer clear sky to rain	68.3%	21.7%	10.0%			-1.0	-.8
Summer many stars to rain	18.3%	78.3%	3.3%			-.5	-.6
Summer rainbow to rain	16.7%	78.3%	5.0%			-.5	-.6
Summer lightning to rain	8.3%		56.7%	11.7%	23.3%	.0	.2
Summer partial/dark moon to rain	8.3%		40.0%	46.7%	5.0%	.5	.2
Summer full/visible moon to	13.3%	80.0%	6.7%			-.5	-.5
Summer high clouds to dry			10.0%	10.0%	80.0%	1.0	.9
Summer low clouds to dry	73.3%	16.7%	10.0%			-1.0	-.8
Summer medium clouds to dry	10.0%	81.7%	8.3%			-.5	-.5
Summer clear sky to dry			13.3%	15.0%	71.7%	1.0	.8
Summer many stars to dry			13.3%	18.3%	68.3%	1.0	.8
Summer rainbow to dry			13.3%	65.0%	21.7%	.5	.5
Summer lightning to dry	76.7%	15.0%	8.3%			-1.0	-.8
Summer partial/dark moon to dry	8.3%	76.7%	15.0%			-.5	-.5
Summer full/visible moon to dry			21.7%	18.3%	60.0%	1.0	.7
Summer high clouds to hot			6.7%	26.7%	66.7%	1.0	.8
Summer low clouds to hot	73.3%	20.0%	6.7%			-1.0	-.8
Summer medium clouds to hot	25.0%	68.3%	6.7%			-.5	-.6
Summer clear sky to hot			8.3%	20.0%	71.7%	1.0	.8
Summer many stars to hot			6.7%	23.3%	70.0%	1.0	.8
Summer rainbow to hot			15.0%	16.7%	68.3%	1.0	.8
Summer lightning to hot	71.7%	16.7%	11.7%			-1.0	-.8
Summer partial/dark moon to hot	18.3%	70.0%	11.7%			-.5	-.5
Summer full/visible moon to hot			8.3%	18.3%	73.3%	1.0	.8
Summer high clouds to cold	71.7%	15.0%	13.3%			-1.0	-.8
Summer low clouds to cold			26.7%	61.7%	11.7%	.5	.4
Summer medium clouds to cold			20.0%	61.7%	18.3%	.5	.5
Summer clear sky to cold	68.3%	16.7%	15.0%			-1.0	-.8
Summer many stars to cold	18.3%	71.7%	10.0%			-.5	-.5
Summer rainbow to cold	25.0%	61.7%	13.3%			-.5	-.6
Summer lightning to cold			5.0%	73.3%	21.7%	.5	.6
Summer partial/darkmoon to cold	6.7%	75.0%	18.3%			-.5	-.4
Summer full/visible moon to cold	71.7%	18.3%	10.0%			-1.0	-.8

Table A—10: Causal Effects of Weather Concepts during the Autumn Season

Concept to Outcome	Causal Effect						
	Strong negative (-1)	Negative (-0.5)	No Effect (0)	Positive (0.5)	Strong positive (1)	mode -1 to 1	Mean -1 to 1
Autumn high clouds to rain	76.7%	15.0%	8.3%			-1.0	-.8
Autumn low clouds to rain			13.3%	20.0%	66.7%	1.0	.8
Autumn medium clouds to rain			8.3%	73.3%	18.3%	.5	.6
Autumn clear sky to rain	71.7%	21.7%	6.7%			-1.0	-.8
Autumn many stars to rain	71.7%	18.3%	10.0%			-1.0	-.8
Autumn rainbow to rain	20.0%	73.3%	6.7%			-.5	-.6
Autumn lightning to rain			3.3%	28.3%	68.3%	1.0	.8
Autumn partial/dark moon to			8.3%	73.3%	18.3%	.5	.6
Autumn full/visible moon to	18.3%	75.0%	6.7%			-.5	-.6
Autumn high clouds to dry			8.3%	21.7%	70.0%	1.0	.8
Autumn low clouds to dry	68.3%	23.3%	8.3%			-1.0	-.8
Autumn medium clouds to dry	16.7%	76.7%	6.7%			-.5	-.6
Autumn clear sky to dry			5.0%	20.0%	75.0%	1.0	.9
Autumn many stars to dry			6.7%	16.7%	76.7%	1.0	.9
Autumn rainbow to dry			6.7%	71.7%	21.7%	.5	.6
Autumn lightning to dry	65.0%	25.0%	10.0%			-1.0	-.8
Autumn partial/dark moon to dry	21.7%	73.3%	5.0%			-.5	-.6
Autumn full/visible moon to dry			8.3%	73.3%	18.3%	.5	.6
Autumn high clouds to hot			25.0%	61.7%	13.3%	.5	.4
Autumn low clouds to hot	8.3%	80.0%	11.7%			-.5	-.5
Autumn medium clouds to hot			8.3%	73.3%	16.7%	.5	.7
Autumn clear sky to hot			5.0%	31.7%	63.3%	1.0	.8
Autumn many stars to hot			5.0%	25.0%	70.0%	1.0	.8
Autumn rainbow to hot			10.0%	73.3%	15.0%	.5	.7
Autumn lightning to hot	23.3%	75.0%	1.7%			-.5	-.6
Autumn partial/dark moon to hot	21.7%	65.0%	13.3%			-.5	-.5
Autumn full/visible moon to hot			10.0%	23.3%	66.7%	1.0	.8
Autumn high clouds to cold	70.0%	21.7%	8.3%			-1.0	-.8
Autumn low clouds to cold			10.0%	66.7%	23.3%	.5	.6
Autumn medium clouds to cold			6.7%	70.0%	23.3%	.5	.6
Autumn clear sky to cold	61.7%	18.3%	20.0%			-1.0	-.7
Autumn many stars to cold	18.3%	71.7%	10.0%			-.5	-.5
Autumn rainbow to cold	18.3%	71.7%	10.0%			-.5	-.5
Autumn lightning to cold			5.0%	28.3%	66.7%	1.0	.8
Autumn partial/darkmoon to cold			10.0%	66.7%	23.3%	.5	.6
Autumn full/visible moon to cold	26.7%	58.3%	15.0%			-.5	-.6

Table A—11: Causal Effects of Weather Concepts during the Spring Season

Concept to Outcome	Causal Effect						
	Strong negative (-1)	Negative (-0.5)	No Effect (0)	Positive (0.5)	Strong positive (1)	mode -1 to 1	mean -1 to 1
Spring high clouds to rain	65.0%	11.7%	15.0%	8.3%		-1.0	-.7
Spring low clouds to rain			5.0%	75.0%	20.0%	.5	.6
Spring medium clouds to rain	21.7%	76.7%	1.7%			-.5	-.6
Spring clear sky to rain	73.3%	23.3%	3.3%			-1.0	-.9
Spring many stars to rain	76.7%	15.0%	8.3%			-1.0	-.8
Spring rainbow to rain	16.7%	78.3%	5.0%			-.5	-.6
Spring lightning to rain			15.0%	25.0%	60.0%	1.0	.7
Spring partial/dark moon to rain			13.3%	73.3%	13.3%	.5	.5
Spring full/visible moon to	16.7%	70.0%	13.3%			-.5	-.5
Spring high clouds to dry			10.0%	25.0%	65.0%	1.0	.8
Spring low clouds to dry	16.7%	65.0%	18.3%			-.5	-.5
Spring medium clouds to dry			10.0%	68.3%	21.7%	.5	.6
Spring clear sky to dry			18.3%	18.3%	63.3%	1.0	.7
Spring many stars to dry			20.0%	21.7%	58.3%	1.0	.7
Spring rainbow to dry			11.7%	66.7%	21.7%	.5	.6
Spring lightning to dry	70.0%	15.0%	15.0%			-1.0	-.8
Spring partial/dark moon to dry	23.3%	70.0%	6.7%			-.5	-.6
Spring full/visible moon to dry			10.0%	65.0%	25.0%	.5	.6
Spring high clouds to hot			15.0%	21.7%	63.3%	1.0	.7
Spring low clouds to hot	15.0%	71.7%	13.3%			-.5	-.5
Spring medium clouds to hot	20.0%	16.7%	3.3%	45.0%	15.0%	.5	.1
Spring clear sky to hot			11.7%	21.7%	66.7%	1.0	.8
Spring many stars to hot			10.0%	15.0%	75.0%	1.0	.8
Spring rainbow to hot			16.7%	66.7%	16.7%	.5	.5
Spring lightning to hot	71.7%	15.0%	13.3%			-1.0	-.8
Spring partial/dark moon to hot	20.0%	66.7%	13.3%			-.5	-.5
Spring full/visible moon to hot			15.0%	61.7%	23.3%	.5	.5
Spring high clouds to cold	81.7%	10.0%	8.3%			-1.0	-.9
Spring low clouds to cold			18.3%	65.0%	16.7%	.5	.5
Spring medium clouds to cold			6.7%	70.0%	23.3%	.5	.6
Spring clear sky to cold	63.3%	20.0%	16.7%			-1.0	-.7
Spring many stars to cold	60.0%	20.0%	20.0%			-1.0	-.7
Spring rainbow to cold			18.3%	63.3%	18.3%	.5	.5
Spring lightning to cold			5.0%	18.3%	76.7%	1.0	.9
Spring partial/darkmoon to cold			33.3%	61.7%	5.0%	.5	.4
Spring full/visible moon to cold	6.7%	60.0%	33.3%			-.5	-.4

Table A—12: Representation of Knowledge for Kenya Winter

Concepts	High clouds	Low clouds	Medium clouds	Clear sky	Many stars	Rainbow	Lightning	Dark moon	Full/visible moon	Rain	Dry	Hot	cold
High clouds	0.00	0.00	0.00	0.50	0.00	0.00	-1.00	0.00	0.00	-1.00	1.00	0.50	-0.50
Low clouds	0.00	0.00	0.00	-1.00	0.00	0.00	0.00	0.00	0.00	0.50	0.50	-1.00	1.00
Medium clouds	0.00	0.00	0.00	-0.50	0.00	0.00	0.00	0.00	-0.50	0.00	-0.50	-0.50	0.50
Clear sky	0.00	0.00	0.00	0.00	0.00	0.00	-1.00	0.00	0.00	-1.00	1.00	0.50	-0.50
Many stars	0.00	0.00	0.00	0.00	0.00	0.00	0.00	0.00	0.00	-1.00	0.50	0.50	-0.50
Rainbow	0.00	0.00	0.00	0.00	0.00	0.00	0.00	0.00	0.00	-0.50	0.00	0.50	-0.50
Lightning	0.00	0.00	0.00	0.00	0.00	0.00	0.00	0.00	0.00	0.50	-0.50	-0.50	0.50
Dark moon	0.00	0.00	0.00	0.00	0.00	0.00	0.00	0.00	0.00	0.50	-0.50	-0.50	0.50
Full/visible moon	0.00	0.00	0.00	0.00	0.00	0.00	0.00	0.00	0.00	0.00	0.50	0.50	-0.50
Rain	0.00	0.00	0.00	0.00	0.00	0.00	0.00	0.00	0.00	0.00	0.00	0.00	0.00
Dry	0.00	0.00	0.00	0.00	0.00	0.00	0.00	0.00	0.00	0.00	0.00	0.00	0.00
Hot	0.00	0.00	0.00	0.00	0.00	0.00	0.00	0.00	0.00	0.00	0.00	0.00	0.00
Cold	0.00	0.00	0.00	0.00	0.00	0.00	0.00	0.00	0.00	0.00	0.00	0.00	0.00

Table A—13: Representation of Knowledge for South Africa Winter

Concepts	High clouds	Low clouds	Medium clouds	Clear sky	Many stars	Rainbow	Lightning	Dark moon	Full/visible moon	Rain	Dry	Hot	Cold
High clouds	0.00	0.00	0.00	0.50	0.00	0.00	-1.00	0.00	0.00	0.00	1.00	-0.50	1.00
Low clouds	0.00	0.00	0.00	-1.00	0.00	0.00	0.00	0.00	0.00	0.50	1.00	-0.50	1.00
Medium clouds	0.00	0.00	0.00	-0.50	0.00	-1.00	0.00	0.00	-1.00	0.50	1.00	-0.50	1.00
Clear sky	0.00	0.00	0.00	0.00	0.00	0.00	-1.00	0.00	0.00	0.00	1.00	0.50	0.50
Many stars	0.00	0.00	0.00	0.00	0.00	0.00	0.00	-0.50	0.00	0.00	1.00	0.50	0.50
Rainbow	0.00	0.00	0.00	0.00	0.00	0.00	0.00	0.00	0.00	-0.50	1.00	0.50	0.50
Lightning	0.00	0.00	0.00	0.00	0.00	0.00	0.00	0.00	0.00	0.50	-1.00	-1.00	1.00
Dark moon	0.00	0.00	0.00	0.00	0.00	0.00	0.00	0.00	0.00	0.00	-0.50	0.00	1.00
Full/visible moon	0.00	0.00	0.00	0.00	0.00	0.00	0.00	0.00	0.00	0.00	0.50	0.50	1.00
Rain	0.00	0.00	0.00	0.00	0.00	0.00	0.00	0.00	0.00	0.00	0.00	0.00	0.00
Dry	0.00	0.00	0.00	0.00	0.00	0.00	0.00	0.00	0.00	0.00	0.00	0.00	0.00
Hot	0.00	0.00	0.00	0.00	0.00	0.00	0.00	0.00	0.00	0.00	0.00	0.00	0.00
Cold	0.00	0.00	0.00	0.00	0.00	0.00	0.00	0.00	0.00	0.00	0.00	0.00	0.00

Table A—14: Representation of Knowledge for Kenya Summer

Concepts	High clouds	Low clouds	Medium clouds	Clear sky	Many stars	Rainbow	Lightning	Dark moon	Full/visible moon	Rain	Dry	Hot	Cold
High clouds	0.00	0.00	0.00	0.50	0.00	0.00	-1.00	0.00	0.00	-1.00	1.00	1.00	-1.00
Low clouds	0.00	0.00	0.00	-1.00	0.00	0.00	0.00	0.00	0.00	0.00	-1.00	-1.00	0.50
Medium	0.00	0.00	0.00	-0.50	0.00	0.00	0.00	0.00	-0.50	0.50	-0.50	-0.50	0.50
Clear sky	0.00	0.00	0.00	0.00	0.00	0.00	-1.00	0.00	0.00	-1.00	1.00	1.00	-1.00
Many stars	0.00	0.00	0.00	0.00	0.00	0.00	0.00	0.00	0.00	-0.50	1.00	1.00	-0.50
Rainbow	0.00	0.00	0.00	0.00	0.00	0.00	0.00	0.00	0.00	-0.50	0.50	1.00	-0.50
Lightning	0.00	0.00	0.00	0.00	0.00	0.00	0.00	0.00	0.00	0.00	-1.00	-1.00	0.50
Dark moon	0.00	0.00	0.00	0.00	0.00	0.00	0.00	0.00	0.00	0.50	-0.50	-0.50	-0.50
Full/visible moon	0.00	0.00	0.00	0.00	0.00	0.00	0.00	0.00	0.00	-0.50	1.00	1.00	-1.00
Rain	0.00	0.00	0.00	0.00	0.00	0.00	0.00	0.00	0.00	0.00	0.00	0.00	0.00
Dry	0.00	0.00	0.00	0.00	0.00	0.00	0.00	0.00	0.00	0.00	0.00	0.00	0.00
Hot	0.00	0.00	0.00	0.00	0.00	0.00	0.00	0.00	0.00	0.00	0.00	0.00	0.00
Cold	0.00	0.00	0.00	0.00	0.00	0.00	0.00	0.00	0.00	0.00	0.00	0.00	0.00

Table A—15: representation of knowledge for south africa winter

Concepts	High clouds	Low clouds	Medium clouds	Clear sky	Many stars	Rainbow	Lightning	Dark moon	Full/visible moon	Rain	Dry	Hot	Cold
High clouds	0.00	0.00	0.00	0.50	0.00	0.00	-1.00	0.00	0.00	-1.00	1.00	1.00	-1.00
Low Clouds	0.00	0.00	0.00	-1.00	0.00	0.00	0.00	0.00	0.00	1.00	-1.00	-1.00	0.50
Medium Clouds	0.00	0.00	0.00	-0.50	0.00	-1.00	0.00	0.00	-1.00	0.50	-0.50	1.00	-1.00
Clear sky	0.00	0.00	0.00	0.00	0.00	0.00	-1.00	0.00	0.00	-0.50	1.00	1.00	-1.00
Many stars	0.00	0.00	0.00	0.00	0.00	0.00	0.00	-0.50	0.00	-1.00	1.00	1.00	-1.00
Rainbow	0.00	0.00	0.00	0.00	0.00	0.00	0.00	0.00	0.00	-0.50	0.50	0.50	-1.00
Lightning	0.00	0.00	0.00	0.00	0.00	0.00	0.00	0.00	0.00	1.00	-1.00	-0.50	0.50
Dark moon	0.00	0.00	0.00	0.00	0.00	0.00	0.00	0.00	0.00	0.50	-1.00	-1.00	0.50
Full/visible moon	0.00	0.00	0.00	0.00	0.00	0.00	0.00	0.00	0.00	-1.00	1.00	1.00	-1.00
Rain	0.00	0.00	0.00	0.00	0.00	0.00	0.00	0.00	0.00	0.00	0.00	0.00	0.00
Dry	0.00	0.00	0.00	0.00	0.00	0.00	0.00	0.00	0.00	0.00	0.00	0.00	0.00
Hot	0.00	0.00	0.00	0.00	0.00	0.00	0.00	0.00	0.00	0.00	0.00	0.00	0.00
Cold	0.00	0.00	0.00	0.00	0.00	0.00	0.00	0.00	0.00	0.00	0.00	0.00	0.00

Table A—16: Representation of Knowledge for Kenya Autumn

Concepts	High clouds	Low clouds	Medium clouds	Clear sky	Many stars	Rainbow	Lightning	Dark moon	Full/visible moon	Rain	Dry	Hot	Cold
High clouds	0.00	0.00	0.00	0.50	0.00	0.00	-1.00	0.00	0.00	-1.00	1.00	0.50	-1.00
Low clouds	0.00	0.00	0.00	-1.00	0.00	0.00	0.00	0.00	0.00	1.00	-1.00	-0.50	0.50
Medium clouds	0.00	0.00	0.00	-0.50	0.00	0.00	0.00	0.00	-0.50	0.50	-0.50	0.50	0.50
Clear sky	0.00	0.00	0.00	0.00	0.00	0.00	-1.00	0.00	0.00	-1.00	1.00	1.00	-1.00
Many stars	0.00	0.00	0.00	0.00	0.00	0.00	0.00	0.00	0.00	-1.00	1.00	1.00	-0.50
Rainbow	0.00	0.00	0.00	0.00	0.00	0.00	0.00	0.00	0.00	-0.50	0.50	0.50	-0.50
Lightning	0.00	0.00	0.00	0.00	0.00	0.00	0.00	0.00	0.00	1.00	-1.00	-0.50	1.00
Dark moon	0.00	0.00	0.00	0.00	0.00	0.00	0.00	0.00	0.00	0.50	-0.50	-0.50	0.50
Full/ Visible moon	0.00	0.00	0.00	0.00	0.00	0.00	0.00	0.00	0.00	-0.50	0.50	1.00	-0.50
Rain	0.00	0.00	0.00	0.00	0.00	0.00	0.00	0.00	0.00	0.00	0.00	0.00	0.00
Dry	0.00	0.00	0.00	0.00	0.00	0.00	0.00	0.00	0.00	0.00	0.00	0.00	0.00
Hot	0.00	0.00	0.00	0.00	0.00	0.00	0.00	0.00	0.00	0.00	0.00	0.00	0.00
Cold	0.00	0.00	0.00	0.00	0.00	0.00	0.00	0.00	0.00	0.00	0.00	0.00	0.00

Table A—17: Representation of Knowledge for South African Autumn

Concepts	High clouds	Low clouds	Medium clouds	Clear sky	Many stars	Rainbow	Lightning	Dark moon	Full/visible moon	Rain	Dry	Hot	Cold
High clouds	0.00	0.00	0.00	0.50	0.00	0.00	-1.00	0.00	0.00	-0.50	0.50	0.50	0.50
Low clouds	0.00	0.00	0.00	-1.00	0.00	0.00	0.00	0.00	0.00	1.00	-1.00	-0.50	0.50
Medium clouds	0.00	0.00	0.00	-0.50	0.00	-1.00	0.00	0.00	-1.00	0.50	-1.00	-1.00	0.50
Clear sky	0.00	0.00	0.00	0.00	0.00	0.00	-1.00	0.00	0.00	-1.00	0.50	0.50	0.50
Many stars	0.00	0.00	0.00	0.00	0.00	0.00	0.00	-0.50	0.00	-1.00	-1.00	-1.00	0.50
Rainbow	0.00	0.00	0.00	0.00	0.00	0.00	0.00	0.00	0.00	-1.00	0.50	0.50	0.50
Lightning	0.00	0.00	0.00	0.00	0.00	0.00	0.00	0.00	0.00	0.50	-0.50	-0.50	0.50
Dark moon	0.00	0.00	0.00	0.00	0.00	0.00	0.00	0.00	0.00	0.50	-0.50	-0.50	0.50
Full/visible moon	0.00	0.00	0.00	0.00	0.00	0.00	0.00	0.00	0.00	-0.50	0.50	0.50	0.50
Rain	0.00	0.00	0.00	0.00	0.00	0.00	0.00	0.00	0.00	0.00	0.00	0.00	0.00
Dry	0.00	0.00	0.00	0.00	0.00	0.00	0.00	0.00	0.00	0.00	0.00	0.00	0.00
Hot	0.00	0.00	0.00	0.00	0.00	0.00	0.00	0.00	0.00	0.00	0.00	0.00	0.00
Cold	0.00	0.00	0.00	0.00	0.00	0.00	0.00	0.00	0.00	0.00	0.00	0.00	0.00

Table A—18: Representation of Knowledge for Kenya Spring

Concepts	High clouds	Low clouds	Medium clouds	Clear sky	Many stars	Rainbow	Lightning	Dark moon	Full/visible moon	Rain	Dry	Hot	Cold
High clouds	0.00	0.	0.00	0.50	0.00	0.00	-1.00	0.00	0.00	-1.00	1.00	1.00	-1.00
Low clouds	0.00	0.	0.00	-1.00	0.00	0.00	0.00	0.00	0.00	0.50	-0.50	-0.50	0.50
Medium clouds	0.00	0.	0.00	-0.50	0.00	0.00	0.00	0.00	-0.50	-0.50	0.50	0.50	0.50
Clear sky	0.00	0.	0.00	0.00	0.00	0.00	-1.00	0.00	0.00	-1.00	1.00	1.00	-1.00
Many stars	0.00	0.	0.00	0.00	0.00	0.00	0.00	0.00	0.00	-1.00	1.00	1.00	-1.00
Rainbow	0.00	0.	0.00	0.00	0.00	0.00	0.00	0.00	0.00	-0.50	0.50	0.50	0.50
Lightning	0.00	0.	0.00	0.00	0.00	0.00	0.00	0.00	0.00	1.00	-1.00	-1.00	1.00
Dark moon	0.00	0.	0.00	0.00	0.00	0.00	0.00	0.00	0.00	0.50	-0.50	-0.50	0.50
Full/visible moon	0.00	0.	0.00	0.00	0.00	0.00	0.00	0.00	0.00	-0.50	0.50	0.50	-0.50
Rain	0.00	0.	0.00	0.00	0.00	0.00	0.00	0.00	0.00	0.00	0.00	0.00	0.00
Dry	0.00	0.	0.00	0.00	0.00	0.00	0.00	0.00	0.00	0.00	0.00	0.00	0.00
Hot	0.00	0.	0.00	0.00	0.00	0.00	0.00	0.00	0.00	0.00	0.00	0.00	0.00
Cold	0.00	0.	0.00	0.00	0.00	0.00	0.00	0.00	0.00	0.00	0.00	0.00	0.00

Table A—19: Representation of Knowledge for South Africa Spring

Concepts	High clouds	Low clouds	Medium clouds	Clear sky	Many stars	Rainbow	Lightning	Dark moon	Full/visible moon	Rain	Dry	Hot	Cold
High clouds	0.00	0.00	0.00	0.50	0.00	0.00	-1.00	0.00	0.00	-0.50	0.50	0.50	-1.00
Low clouds	0.00	0.00	0.00	-1.00	0.00	0.00	0.00	0.00	0.00	0.50	0.50	-0.50	0.50
Medium	0.00	0.00	0.00	-0.50	0.00	-1.00	0.00	0.00	-1.00	0.50	-0.50	-0.50	0.50
Clear sky	0.00	0.00	0.00	0.00	0.00	0.00	-1.00	0.00	0.00	-0.50	0.50	1.00	-1.00
Many stars	0.00	0.00	0.00	0.00	0.00	0.00	0.00	-0.50	0.00	-1.00	0.50	0.50	-1.00
Rainbow	0.00	0.00	0.00	0.00	0.00	0.00	0.00	0.00	0.00	-0.50	-0.50	0.50	-0.50
Lightning	0.00	0.00	0.00	0.00	0.00	0.00	0.00	0.00	0.00	1.00	-1.00	-0.50	0.50
Dark moon	0.00	0.00	0.00	0.00	0.00	0.00	0.00	0.00	0.00	0.50	-1.00	-0.50	0.50
Full/visible	0.00	0.00	0.00	0.00	0.00	0.00	0.00	0.00	0.00	-1.00	-1.00	1.00	-1.00
Rain	0.00	0.00	0.00	0.00	0.00	0.00	0.00	0.00	0.00	0.00	0.00	0.00	0.00
Dry	0.00	0.00	0.00	0.00	0.00	0.00	0.00	0.00	0.00	0.00	0.00	0.00	0.00
Hot	0.00	0.00	0.00	0.00	0.00	0.00	0.00	0.00	0.00	0.00	0.00	0.00	0.00
Cold	0.00	0.00	0.00	0.00	0.00	0.00	0.00	0.00	0.00	0.00	0.00	0.00	0.00

Table A—20 Summary of Mean Seasonal Causal effects in Kenya and South Africa

Concept to Outcome	Seasonal Causal Effects (mean Values)							
	Winter		Summer		Autumn		Spring	
	Kenya	South Africa	Kenya	South Africa	Kenya	South Africa	Kenya	South Africa
High clouds to rain	-.8	.0	-.7	-.8	-.8	-.5	-.7	-.6
Low clouds to rain	.4	.5	.1	.9	.8	.8	.6	.5
Medium clouds to rain	.0	.5	.1	.5	.6	.6	-.6	.5
Clear sky to rain	-.9	.0	-.8	-.5	-.8	-.8	-.9	-.6
Many stars to rain	-.8	.0	-.6	-.8	-.8	-.9	-.8	-.9
Rainbow to rain	-.5	-.6	-.6	-.5	-.6	-.8	-.6	-.5
Lightning to rain	.5	.5	.2	.9	.8	.6	.7	.9
Partial/dark moon to rain	.4	.0	.2	.5	.6	.6	.5	.6
Full/visible moon to rain	.1	.0	-.5	-.8	-.6	-.5	-.5	-.9
High clouds to dry	.8	.8	.9	.8	.8	.6	.8	.6
Low clouds to dry	.6	.8	-.8	-.8	-.8	-.9	-.5	.6
Medium clouds to dry	-.5	.8	-.5	-.5	-.6	-.9	.6	-.5
Clear sky to dry	.8	.8	.8	.9	.9	.6	.7	.6
Many stars to dry	.5	.8	.8	.8	.9	-.9	.7	.5
Rainbow to dry	.1	.8	.5	.5	.6	.5	.6	-.5
Lightning to dry	-.6	-.8	-.8	-.7	-.8	-.5	-.8	-.8
Partial/dark moon to dry	-.5	-.5	-.5	-.7	-.6	-.5	-.6	-.8
Full/visible moon to dry	.5	.5	.7	.8	.6	.5	.6	-.7
High clouds to hot	.6	-.4	.8	.9	.4	.5	.7	.5
Low clouds to hot	-.8	-.5	-.8	-.9	-.5	-.5	-.5	-.5
Medium clouds to hot	-.5	-.5	-.6	.9	.7	-.8	.1	-.5
Clear sky to hot	.6	.5	.8	.9	.8	.5	.8	.9
Many stars to hot	.4	.6	.8	.9	.8	-.9	.8	.5
Rainbow to hot	.4	.6	.8	.5	.7	.6	.5	.6
Lightning to hot	-.5	-.8	-.8	-.5	-.6	-.5	-.8	-.5
Partial/dark moon to hot	-.4	.0	-.5	-.9	-.5	-.5	-.5	-.5
Full/visible moon to hot	.4	.6	.8	.9	.8	.5	.5	1.0
High clouds to cold	-.5	.9	-.8	-.9	-.8	.5	-.9	-.8
Low clouds to cold	.7	.9	.4	.5	.6	.5	.5	.6
Medium clouds to cold	.5	.8	.5	-.8	.6	.5	.6	.5
Clear sky to cold	-.5	.5	-.8	-.8	-.7	.5	-.7	-.9
Many stars to cold	-.4	.5	-.5	-.8	-.5	.5	-.7	-.9
Rainbow to cold	-.5	.5	-.6	-.8	-.5	.5	.5	-.5
Lightning to cold	.5	.8	.6	.5	.8	.5	.9	.5
Partial/dark moon to cold	.5	.8	-.4	.5	.6	.6	.4	.6
Full/visible moon to cold	-.5	.8	-.8	-.9	-.6	.6	-.4	-.8

Table A—21: Final Fuzzy Cognitive Map for Autumn Season

Concepts	High clouds	Low clouds	Medium clouds	Clear sky	Many stars	Rainbow	Lightning	Partial/dark moon	Full/visible moon	Rain	Dry	Hot	Cold
High clouds	0.00	0.00	0.00	0.50	0.00	0.00	-1.00	0.00	0.00	-0.75	0.75	0.50	-0.25
Low clouds	0.00	0.00	0.00	-1.00	0.00	0.00	0.00	0.00	0.00	1.00	-1.00	-0.50	0.50
Medium clouds	0.00	0.00	0.00	-0.50	0.00	0.00	0.00	0.00	-0.50	0.50	-0.75	-0.25	0.50
Clear sky	0.00	0.00	0.00	0.00	0.00	0.00	-1.00	0.00	0.00	-1.00	0.75	0.75	-0.25
Many stars	0.00	0.00	0.00	0.00	0.00	0.00	0.00	0.00	0.00	-1.00	0.00	0.00	0.00
Rainbow	0.00	0.00	0.00	0.00	0.00	0.00	0.00	0.00	0.00	-0.75	0.50	0.50	0.00
Lightning	0.00	0.00	0.00	0.00	0.00	0.00	0.00	0.00	0.00	0.75	-0.75	-0.50	0.75
Partial/dark moon	0.00	0.00	0.00	0.00	0.00	0.00	0.00	0.00	0.00	0.50	-0.50	-0.50	0.50
Full/visible moon	0.00	0.00	0.00	0.00	0.00	0.00	0.00	0.00	0.00	-0.50	0.50	0.75	0.00
Rain	0.00	0.00	0.00	0.00	0.00	0.00	0.00	0.00	0.00	0.00	0.00	0.00	0.00
Dry	0.00	0.00	0.00	0.00	0.00	0.00	0.00	0.00	0.00	0.00	0.00	0.00	0.00
Hot	0.00	0.00	0.00	0.00	0.00	0.00	0.00	0.00	0.00	0.00	0.00	0.00	0.00
Cold	0.00	0.00	0.00	0.00	0.00	0.00	0.00	0.00	0.00	0.00	0.00	0.00	0.00

Table A—22: Final Fuzzy Cognitive Map for Spring Season

Concepts	High clouds	Low clouds	Medium clouds	Clear sky	Many stars	Rainbow	Lightning	Partial/dark moon	Full/visible moon	Rain	Dry	Hot	Cold
High clouds	0.00	0.00	0.00	0.50	0.00	0.00	-1.00	0.00	0.00	-0.75	0.75	0.75	-1.00
Low clouds	0.00	0.00	0.00	-1.00	0.00	0.00	0.00	0.00	0.00	0.50	0.00	-0.50	0.50
Medium clouds	0.00	0.00	0.00	-0.50	0.00	0.00	0.00	0.00	-0.50	0.00	0.00	0.00	0.50
Clear sky	0.00	0.00	0.00	0.00	0.00	0.00	-1.00	0.00	0.00	-0.75	0.75	1.00	-1.00
Many stars	0.00	0.00	0.00	0.00	0.00	0.00	0.00	0.00	0.00	-1.00	0.75	0.75	-1.00
Rainbow	0.00	0.00	0.00	0.00	0.00	0.00	0.00	0.00	0.00	-0.50	0.00	0.50	0.00
Lightning	0.00	0.00	0.00	0.00	0.00	0.00	0.00	0.00	0.00	1.00	-1.00	-0.75	0.75
Partial/dark moon	0.00	0.00	0.00	0.00	0.00	0.00	0.00	0.00	0.00	0.50	-0.75	-0.50	0.50
Full/visible moon	0.00	0.00	0.00	0.00	0.00	0.00	0.00	0.00	0.00	-0.75	-0.25	0.75	-0.75
Rain	0.00	0.00	0.00	0.00	0.00	0.00	0.00	0.00	0.00	0.00	0.00	0.00	0.00
Dry	0.00	0.00	0.00	0.00	0.00	0.00	0.00	0.00	0.00	0.00	0.00	0.00	0.00
Hot	0.00	0.00	0.00	0.00	0.00	0.00	0.00	0.00	0.00	0.00	0.00	0.00	0.00
Cold	0.00	0.00	0.00	0.00	0.00	0.00	0.00	0.00	0.00	0.00	0.00	0.00	0.00

C. Appendix of Figures

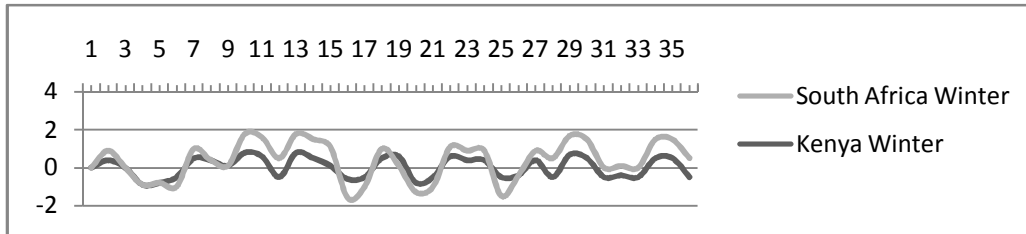


Figure C-1: Mean Causal Effect in Kenya and South Africa Winter

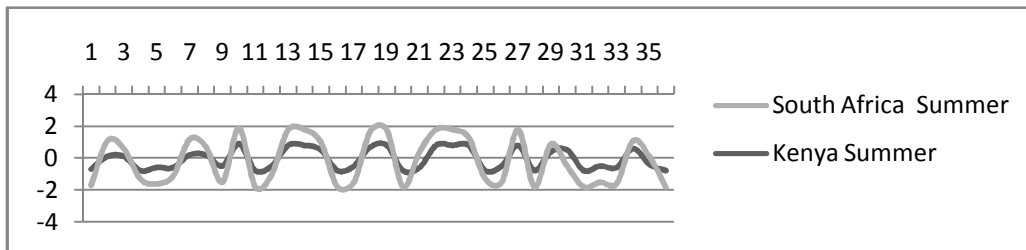


Figure C-2: Mean Causal Effect in Kenya and South Africa Summer

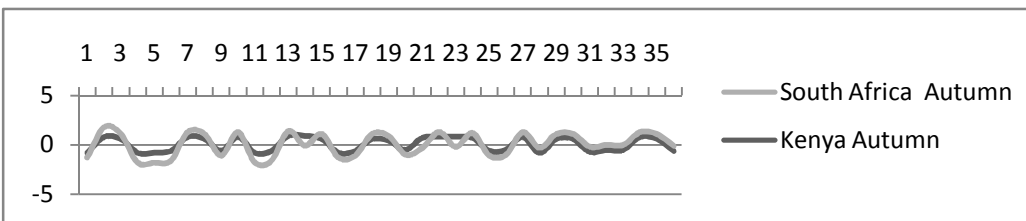


Figure C-3: Mean Causal Effect in Kenya and South Africa Autumn

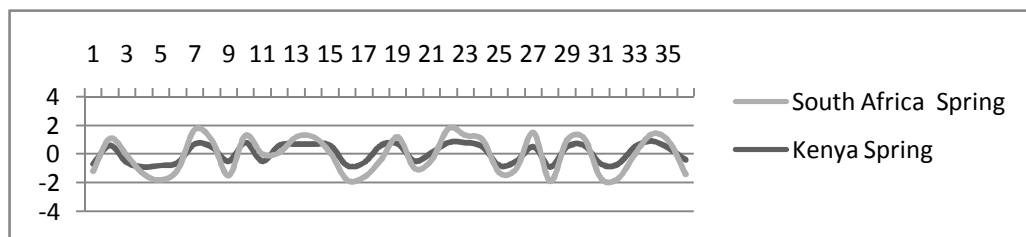


Figure C-4: Mean Causal Effect in Kenya and South Africa Spring

Appendix: Phase I Data Collection Instruments

RESEARCH INVITATION LETTER

Dear _____,

I am pleased to invite you to participate in an interview to identify traditional astronomical and meteorological aspects that are used to forecast weather. No more than thirty minutes would be required to complete the interview.

Be assured that any information you provide will be treated in the strictest confidence and your participation will not be identifiable in the resulting report. You are entirely free to discontinue your participation at any time or to decline to answer particular questions.

I will seek your consent, on the attached form, to record the interview and to use the recording in preparing the report, on condition that your name or identity is not revealed, and to make the recording available to other researchers on the same conditions.

Mrs Sizakele Ngidi will guide you through the interview process. Please give her the necessary support.

Please direct any enquiries concerning this study to the Researcher.

Thank you for your assistance.



SM Mwagha

Tel: +27 724 161 884 / +27 051 507 3092

E-mail: soprold@gmail.com || smwagha@cut.ac.za

Central University of Technology, Free State, South Africa

INTERVIEW/QUESTIONNAIRE GUIDE

The purpose of the interview is to identify aspects of astronomical and meteorological knowledge that are used in traditional weather forecast.

The researcher/research assistant will:

1. Introduce the interview session by explaining the purpose of the interview, welcome the respondent(s) and make clear why they were chosen.
2. Explain the presence and purpose of any recording equipment and give the option for respondent(s) to opt out of recording.
3. Outline ground rules and interview guidelines such as participants can end the interview at any time or refuse to answer any questions.
4. Inform the respondent(s) that a break will be provided if time goes beyond 45 minutes.
5. Address the issue of privacy and confidentiality and inform the respondent(s) that information gathered will be analyzed aggregately and respondent's personal details will not be used in any report. The researcher will also make it clear that respondents' answers and any information identifying the respondent(s) as a participant of this research will be kept confidential.
6. Inform the respondent(s) that they must sign consent forms before the interview begins.
7. Inform the respondent(s) that the interview consists of 18 questions, some with sub sections.
8. Inform the respondent(s) how to provide answers to questions by putting a mark on a check box for optional questions and giving a short answer for open ended questions.
9. Inform the respondent(s) that during or after the interview additional questions can be asked to clarify respondent(s') answer.
10. Inform respondent(s) that they may choose not to answer a particular question; in that event, he will need to inform the researcher or research assistant.
11. Inform the respondent(s) that oral interview will be recorded to ensure

responses are captured and transcribed accurately.

12. Inform the respondent(s) that they are allowed to ask questions before, during and after the interview.
13. Go through the process of completing a questionnaire with the respondent(s) as an example
14. Inform the respondent(s) of follow-up activities and that they should provide their contact details at the end of the questionnaire if they may wish to be involved in the implementation phase of the research.
15. Assist the respondent(s) to properly fill the questionnaires to completion.
16. Collect the questionnaire from the respondent(s).
17. Close the interview by thanking the respondent(s), maintaining on privacy and confidentiality considerations.

CONSENT FORM

I, the undersigned, confirm that (please tick box as appropriate):

I have read and understood the information about the research.

I have been given the opportunity to ask questions about the research and my participation.

I voluntarily agree to participate in the research.

I understand I can withdraw at any time without giving reasons and that I will not be penalized for withdrawing.

The procedures regarding confidentiality have been clearly explained to me.

If applicable, separate terms of consent for forms of data collection have been explained and provided to me.

The use of the data in research, publications, sharing and archiving has been explained to me.

I understand that other researchers will have access to this data only if they agree to preserve the confidentiality of the data and if they agree to the terms I have specified in this form.

Select only **ONE** of the following:

I would like my name used and understand what I have said or written as part of this research will be used in reports, publications and other research outputs so that anything I have contributed to this project can be recognised.

I do not want my name used in this research.

I agree to sign and date this informed consent, along with the Researcher.

Name of Respondent

Signature

Date

Name of Researcher

Signature

Date

QUESTIONNAIRE FOR DATA AND REQUIREMENTS GATHERING IN THE DESIGN OF DATA REPRESENTATION TOOLS

SCHEDULED FOR MARCH/APRIL 2015

PART A: INTRODUCTION

As a result of many years of experience in observation of weather conditions, many communities have been using weather lore observations in predicting weather and its effect on their livelihoods. With the need to make longer lead-times (over a season) weather predictions, weather lore is most considered to be uncertain.

The Department of Information Technology at the Central University of Technology (Free State, South Africa) is conducting research to identify causal effect of traditional astronomical and meteorological weather indicators to weather outcomes.

Phase I of this research seeks to gather knowledge from natives, local farmers and livestock keepers at KwaZulu-Natal province of South Africa. The results of this research will be used to design a scientific tool for weather lore validation. With the validation process, traditional knowledge on weather will become useful in enhancing modern weather prediction systems.

You are requested to participate in this valuable research by completing this questionnaire. You will to put a mark ($\sqrt{\quad}$ or X) in the check box to select an appropriate option or write down a response for open ended questions.

PART B: DEMOGRAPHIC INFORMATION

Q 1 Your Names: _____ (OPTIONAL)

Q 2 Gender? Male Female

Q 3 Your Age bracket?

Under 18 18-35 36-45 46-55 56-65 above 66

Q 4 What is your Highest Education Level:

None Primary Secondary Post-Secondary

Q 5 What is the name of your village?

Q 6 What is the main economic activity in your village?

Q 7 How long have you stayed in this village?

5- 10 years 10-20 years over 20 years

Q 8 What do you do for a living?

Peasant farming (crop or livestock farming for family use)

Small-scale farming (crop or livestock farming generating up to R 500,000 per year)

Large-scale farming- (crop or livestock farming generating over R 1,000,000 per year)

Not indicated here? Please specify.

PART C: WEATHER FORECAST KNOWLEDGE

- Q 9 Does weather affect your daily activities? Yes No
- Q 10 Do you regularly check for the weather forecast? Yes No
- Q 11 Which type of weather forecast do you have most interest in?
 Seasonal The next two days The next week Other? Specify _____
- Q 12 Where do you usually get your weather forecast from? (You may tick more than one box)
 Radio/TV Newspaper Internet Traditional observations
 Other? Please specify _____
- Q 13 Do you have confidence in the accuracy of these weather forecasts?
 Yes No
- Q 14 Do you know any astronomical and meteorological indicators associated to some kind of expected weather?
 Yes No
- If yes, which ones? (You may tick more than one box)
- Sun Moon Stars Rainbow
 Clouds Lighting Sky Other? _____
- Q 15 Do the indicators you specified above help you predict what the weather will be like?
 Yes No
- Q 16 State an instance (positive or negative) in which weather predictions based on astronomical and meteorological indicators guided your 'decisions. (NB: Please state the astronomical and/or meteorological observation and how it guided your activity)

PART D: IDENTIFICATION OF ASTRONOMICAL AND METEOROLOGICAL WEATHER INDICATORS AND CAUSAL EFFECTS

Q 17 As per your village traditional beliefs, provide knowledge of expected weather outcomes for the following astronomical and meteorological indicators.

(NB: please state the effect of the indicators to the expected weather outcomes).

You should use the following phrases to specify the effect

Increases much



Increases








No effect








Decreases







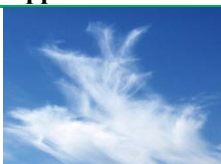

Decreases much








The following two examples will guide you in filling the table. The images are provided to guide you in visualizing the characteristic of the indicators.






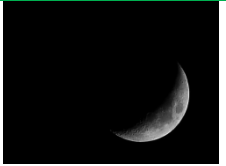

Indicator Characteristic	Expected outcomes:						
	Rain	Temp	Cloudy	Wind	Snow	Humidity	Other?
 evening sun hot	decreases	decreases much	decreases	no effect	no effect	decreases	lightning decreases
 morning sun hot	increases	increases	decreases	increases	decreases	increases	decreases lake water








Indicator Characteristic	Expected outcomes: (Give a causal effect, for example decreases/no effect/ increases)						
	Rain	Temp	Cloudy	Wind	Snow	Humid	Other?
 Altocumulus clouds							
 Altostratus clouds							
 Nimbus clouds							
 Cirrocumulus clouds							
 Cirrostratus clouds							
 Cirrus clouds							
 Cumulonimbus clouds							







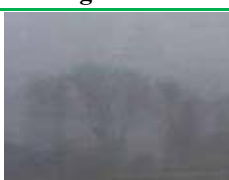
Indicator Characteristic	Expected outcomes: (Give a causal effect ,for example decreases/no effect/ increases)						
	Rain	Temp	Cloudy	Wind	Snow	Humid	Other?
 Stratus clouds							
 Stratocumulus clouds							
 Cumulus clouds							
 White clouds							
 Grey clouds							
 Brown clouds							
 Blue clouds							

Indicator Characteristic	Expected outcomes: (give a causal effect, for example decreases/no effect/ increases)						
	Rain	Temp	Cloudy	Wind	Snow	Humid	Other?
 Red clouds							
 Cauliflower clouds							
 Towers clouds							
 Feathery clouds							
 Layered clouds							
 Rippled clouds							
 Filaments clouds							
 Uniform clouds							

Indicator Characteristic	Expected outcomes: (Give a causal effect, for example decreases/no effect/ increases)						
	Rain	Temp	Cloudy	Wind	Snow	Humid	Other?
 Low clouds							
 High clouds							
 Medium clouds							
 Ring around sun							
 Dull stars							
 Twinkle stars							
 Many stars							

Indicator Characteristic	Expected outcomes: (give a causal effect for example decreases/no effect/ increases/						
	Rain	Temp	Cloudy	Wind	Snow	Humid	Other?
 Few stars							
 Ring around moon							
 New moon							
 Full moon							
 Dark moon							
 Moon getting larger							
 Moon getting smaller							

Indicator Characteristic	Expected outcomes: (Give a causal effect, for example decreases/no effect/ increases)						
	Rain	Temp	Cloudy	Wind	Snow	Humid	Other?
 Blue moon							
 Clear Night Sky							
 Dark Night Sky							
 Red Night Sky							
 Blue Sky							
 Clear Morning Sky							
 Dark Morning Sky							

Indicator Characteristic	Expected outcomes: (Give a causal effect ,for example decreases/no effect/ increases)						
	Rain	Temp	Cloudy	Wind	Snow	Humid	Other?
 Red Morning Sky							
 Red Evening Sky							
 Much Lightning							
 Less Lightning							
 Morning Rainbow							
 Evening Rainbow							
 fog							

Provide for other astronomical and meteorological indicators that you know but are not mentioned in this questionnaire							
Indicator Characteristics	Expected outcomes						

**PART E: REQUEST FOR RESPONDENT'S FURTHER INVOLVEMENT
(OPTIONAL)**

Phase II of this research, will involve capturing of weather images (astronomical and meteorological) and debrief meetings to fill knowledge gaps. If you will be interested to participate, please provide us your contact details.

Full Name:

ID Number:

Email:

Your


















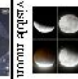

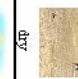
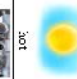


Phone Number:

Thank you very much for your participation

Researcher Sign: _____ **Date:** ____/____/2015

Appendix: Phase II Data Collection Instruments

PART B: DEMOGRAPHIC INFORMATION	PART C: WEATHER FORECAST KNOWLEDGE
<p>Q1. Your Names: _____ (OPTIONAL)</p> <p>Q2. Gender? Male <input type="checkbox"/> Female <input type="checkbox"/></p> <p>Q3. Your Age bracket? Under 18 <input type="checkbox"/> 18-35 <input type="checkbox"/> 36-45 <input type="checkbox"/> 46-55 <input type="checkbox"/> 56-65 <input type="checkbox"/> above 66 <input type="checkbox"/></p> <p>Q4. What is your Highest Education Level None <input type="checkbox"/> Primary <input type="checkbox"/> Secondary <input type="checkbox"/> Post-Secondary <input type="checkbox"/></p> <p>Q5. What is the name of your village _____</p> <p>Q6. What is the main economic activity in your village _____</p> <p>Q7. How long have you stayed in this village? Less than 5 years <input type="checkbox"/> 5-10 years <input type="checkbox"/> 10-20 years <input type="checkbox"/> over 20 years <input type="checkbox"/></p> <p>Q8. What do you do for a living? <input type="checkbox"/> Formal employment. Specify _____ <input type="checkbox"/> Self employment. Specify _____ <input type="checkbox"/> Student. Specify _____ <input type="checkbox"/> Other? Please specify _____</p>	<p>Q9. Does weather affect your daily activities? Often <input type="checkbox"/> Sometimes <input type="checkbox"/> Rarely <input type="checkbox"/> Not at all <input type="checkbox"/></p> <p>Q10. Do you check for the weather forecast? Often <input type="checkbox"/> Sometimes <input type="checkbox"/> Rarely <input type="checkbox"/> Not at all <input type="checkbox"/></p> <p>Q11. Which type of weather forecast are you most interest in? Seasonal <input type="checkbox"/> The next two days <input type="checkbox"/> The next week <input type="checkbox"/> Other? <input type="checkbox"/> specify _____</p> <p>Q12. Do you check weather by observing the environment? Yes <input type="checkbox"/> No <input type="checkbox"/></p> <p>Q13. Do you know any astronomical and meteorological indicators associated to some kind of expected weather? Substantial <input type="checkbox"/> Some <input type="checkbox"/> Few <input type="checkbox"/> None <input type="checkbox"/></p> <p>Q14. If yes, which one do you check most? Sun <input type="checkbox"/> Moon <input type="checkbox"/> Stars <input type="checkbox"/> Rainbow <input type="checkbox"/> Clouds <input type="checkbox"/> Lightning <input type="checkbox"/> Sky <input type="checkbox"/> Others? <input type="checkbox"/> specify _____</p> <p>Q15. Does the indicator you specified above help you predict what the weather will be like Very Often <input type="checkbox"/> Sometimes <input type="checkbox"/> Rarely <input type="checkbox"/> not at all <input type="checkbox"/></p>
PART D: IDENTIFICATION OF ASTRONOMICAL AND METEOROLOGICAL WEATHER INDICATORS AND THEIR CAUSAL EFFECTS	
<p>Q16. (a) How do you call the season? Local Name _____ English Name _____</p> <p>(b) What signifies the start of this season? _____</p> <p>(c) What signifies the end of this season? _____</p> <p>(d) How long is this season _____ from _____ to _____</p> <p>(e) Does this season have interrupts during progress? _____</p> <p>Q17. As per your traditional beliefs, in the next table provide your knowledge of short-term expected weather outcomes for the following astronomical and meteorological visual characteristics using the following symbols or phrases: + (very high expectation); + (some expectation); 0 (does not affect); - (not expecting); -- (very much not expecting);.</p>	

Concepts verval Olyefte	high clouds	low clouds	medium clouds	clear sky	rainy stars	rainbow	lightning	darknew moon	visible moon	rain	dry	hot	cold
 high clouds													
 low clouds													
 medium clouds													
 clear sky													
 rainy stars													
 rainbow													
 lightning													
 darknew moon													
 visible moon													
 rain													
 dry													
 hot													
 cold													